

Extending Applications of Magnesium Amide Bases  
in Asymmetric Synthesis  
and  
A Mild and Selective *N*-Debenzylation Method

Thesis submitted to the University of Strathclyde in partial fulfilment of the  
requirements for the degree of Doctor of Philosophy

By

Natalie R. Monks

2013

Department of Pure and Applied Chemistry  
University of Strathclyde  
Thomas Graham Building  
295 Cathedral Street  
Glasgow  
G1 1XL

## **Declaration of Copyright**

This thesis is the result of the author's original research. It has been composed by the author and has not been previously submitted for examination which has led to the award of a degree.

The copyright of this thesis belongs to the author under the terms of the United Kingdom Copyright Acts as qualified by University of Strathclyde Regulation 3.50. Due acknowledgement must always be made of the use of any material contained in, or derived from, this thesis.

Signed:

Date:

## Acknowledgements

First of all I would like to thank my supervisor Prof. Billy Kerr for his support and training throughout my PhD studies. I'm also grateful for his guidance and encouragement during this time and, in addition, his assistance with job hunting towards the end of my time in the Kerr group.

I must also thank the EPSRC for funding and the JCEMolChem programme for facilitating my placement at Université de Montréal. In this regard I am thankful to Prof. André Charette for hosting me during this time and for the experience of working abroad during my studies.

This work could not have been completed without my fellow lab mates, so to the Kerr group past and present I am extremely grateful for your discussions, suggestions, cakes, banter, and bombs of the Skittle variety! Thank you Vanitha, Chief, Laura, Linsey, Alison, Tina, Sara, Calum, Malcolm, R-Bo, Goldie, Marc, Murali, Kirsten, Richard, and Andy. A second thank you must go to Dr Laura Paterson (L-Patz) for your new role in the Kerr group. I'm grateful for your discussions and guidance for writing up my thesis.

I would also like to thank the Charette group for making me feel so welcome during my time in Montréal. In particular, thanks to Lab. B (Guillaume, William, and Gérald) for the discussions and laughs in your lab and to Léa for making me feel at home in Montréal.

In addition, I would like to thank my new friends in Liverpool for bearing with me whilst writing up during my first few months at Redx. Thank you to my housemates, Craig and Jonno, for keeping me sane and fed during those last few weeks of writing!

A special thank you goes to Iain, for always believing in me and being my rock throughout this time. Thank you for keeping me going and making me smile, even during the tough times; you've helped Scotland become a special place for me.

Finally, I would especially like to thank my family for all your endless love and support. In particular, thank you to Mum and Dad for always being there to keep me going and to Jo for all the cups of tea and chats in Glasgow; it was great to share my experience of this wonderful city with you.

## Abstract

Expansion of the application of readily available chiral magnesium-bisamides was the overall focus of the majority of this study. Comparing a structurally simple  $C_2$ -symmetric magnesium bisamide and a chelating magnesium bisamide, a range of cyclobutanone substrates have been desymmetrised. Early studies employed the chlorotriethylsilane electrophile, however, efficiency of the processes with the chosen base system with cyclobutanone substrates was low. When the alternative electrophile, diphenylphosphoryl chloride, was utilised, however, a drastic improvement in both reactivity and selectivity was achieved. Optimisation of the reaction conditions with both a  $C_2$ -symmetric magnesium bisamide and a chelating magnesium bisamide revealed selectivities of up to 99:1 er for the enantioenriched enol phosphate products. Furthermore, it was found that no additives are required within this novel base system and the deprotonation can be performed at a more elevated temperature of  $-40\text{ }^\circ\text{C}$  whilst maintaining high selectivity. This efficient desymmetrisation was applied to a range of cyclobutanone substrates and seven novel enol phosphate products were formed in enantioselectivities between 76:24 and 99:1er, with the majority producing ratios greater than 89:11 er.

Further application of a  $C_2$ -symmetric magnesium bisamide was also sought by employing this base reagent within the synthetic route towards the natural product (+)-(*S*)-Sporochnol A. To this end, a scalable pathway towards a novel 4,4-disubstituted cyclohexanone was devised. The asymmetric deprotonation of this intermediate, utilising a  $C_2$ -symmetric magnesium bisamide, subsequently embedded the all carbon quaternary stereocentre required within the natural product. Trapping the resulting chiral enolate with diphenylphosphoryl chloride furnished the desired enol phosphate in 88:12 er, which is an excellent level of enantioselectivity for a substrate of this type at a reaction temperature of  $-78\text{ }^\circ\text{C}$ . Furthermore, the utility of the enol phosphate product was highlighted through a palladium-catalysed cross-coupling reaction with a Grignard reagent. Although completion of the synthesis of (+)-(*S*)-Sporochnol A was not achieved, the key asymmetric deprotonation and subsequent cross-coupling step were successful and high yielding.

An additional study was the development of an improved method for the oxidation of secondary *N*-benzylamines. The application of DIAD as a means to oxidise secondary *N*-benzylamines, followed by a subsequent hydrolysis step has been employed to afford debenzylated free amines. This oxidation methodology has thus been applied to a range of amine substrates as an improved, mild, and selective method for benzyl deprotection. High yields of the free amines were obtained and the reaction proved to be tolerant of other functional groups and heteroatoms. Moreover, when an enantiopure secondary *N*-benzylamine was deprotected, the free primary amine remained optically pure, proving that these mild conditions do not interfere with other functionality within the molecule.

## Abbreviations

Ac	acetyl
acac	acetylacetone
AcOH	acetic acid
Ar	aryl
atm	atmosphere
aq.	aqueous
Bn	benzyl
Boc	<i>tert</i> -butoxycarbonyl
<i>n</i> -Bu	<i>n</i> -butyl
<i>n</i> -Bu <sub>2</sub> Mg	<i>n</i> -dibutylmagnesium
<i>t</i> -Bu	<i>tert</i> -butyl
calc.	calculated
cat.	catalytic amount
CDI	1,1'-carbonyldiimidazole
conc.	concentrated
DABCO	1,4-diazabicyclo[2.2.2]octane
dba	dibenzylideneacetone
DBU	1,8-Diazabicyclo[5.4.0]undec-7-ene
DCM	dichloromethane
DEAD	diethyl azodicarboxylate
DIAD	diisopropyl azodicarboxylate
DIHD	diisopropyl hydrazinodicarboxylate
DIPEA	diisopropylethylamine
DMAP	4,4- <i>N</i> -dimethylamminopyridine
DMF	<i>N,N</i> -dimethylformamide
DMP	Dess-Martin periodinane
DMPU	1,3-dimethyl-3,4,5,6-tetrahydro-2(1H)-pyrimidinone
DMSO	dimethylsulfoxide
DPPF	1,1'-bis(diphenylphosphino)ferrocene
dr	diastereomeric ratio

ee	enantiomeric excess
EI	electron impact (mass spectrometry)
eq	equivalent
er	enantiomeric ratio
ESI	electrospray ionization
ESR	electron spin resonance
Et	ethyl
Et <sub>3</sub> N	triethylamine
Et <sub>2</sub> O	diethyl ether
EtOAc	ethyl acetate
EtOH	ethanol
EQ	external quench
ET	electron transfer
FTIR	fourier transform infra-red
g	gram
GC	gas chromatography
HCl	hydrochloric acid
HMPA	hexamethylphosphoramide
HPLC	high-performance liquid chromatography
h	hour
HRMS	high resolution mass spectrum
Hz	Hertz
IPA	diisopropyl alcohol
IQ	internal quench
IR	infra-red
LDA	lithium diisopropylamide
LED	light emitting diode
Me	methyl
MeOH	methanol
mg	milligram
min	minute
ml	milliliter



mp	melting point
mmol	millimoles
MCPBA	<i>meta</i> -chloroperoxybenzoic acid
Ms	methanesulfonyl, mesyl
MS	mass spectroscopy
MsCl	methanesulfonyl chloride
NMO	<i>N</i> -methylmorpholine <i>N</i> -oxide
NMR	nuclear magnetic resonance
	s      single
	d      doublet
	t      triplet
	q      quartet
	pent   pentet
	m      multiplet
	br     broad
NOE	nuclear Overhauser effect
NOESY	nuclear Overhauser effect spectroscopy
PE	petroleum ether
Ph	phenyl
Pr	propyl
<i>i</i> -Pr	<i>iso</i> -propyl
PTSA	<i>para</i> -toluenesulfonic acid
Py	pyridine
RFT	riboflavin tetraacetate
rt	room temperature
sept	septet
TBAB	tetra- <i>n</i> -butylammonium bromide
temp.	temperature
TEMPO	(2,2,6,6-tetramethylpiperidin-1-yl)oxy
TESCl	triethylsilyl
TFA	trifluoroacetic acid
THF	tetrahydrofuran

TLC	thin layer chromatography
TMEDA	<i>N,N,N',N'</i> -tetramethylethylenediamine
TMS	trimethylsilyl
TPAP	tetrapropylammonium perruthenate
Ts	tosyl
UV	ultraviolet
18-c-6	1,4,7,10,13,16-hexaoxacyclooctadecane
9-BBN	9-borabicyclo[3.3.1]nonane

# Contents

*Each Chapter is self-contained and comprises separate Experimental and Reference sections.*

<b>Abstract</b>		<b>i</b>
<b>Abbreviations</b>		<b>iii</b>
<b>Contents</b>		<b>vii</b>
<b>Chapter 1</b>	Extending the Application of Magnesium Bisamides in Asymmetric Synthesis	<b>1</b>
<b>Chapter 2</b>	Towards the Total Synthesis of (+)-( <i>S</i> )-Sporochnol A	<b>176</b>
<b>Chapter 3</b>	Development of a Mild and Selective Amine Oxidation for an Improved <i>N</i> -Debenzylation Method	<b>244</b>

# **Chapter 1**

Extending the Application of Magnesium

Bisamides in Asymmetric Synthesis

# Contents

<b>1 Introduction</b> .....	5
1.1 Chiral lithium amides.....	5
1.1.1 Enantioselective rearrangement of epoxides to allylic alcohols.....	6
1.1.2 Enantioselective reactions of tricarbonyl ( $\eta^6$ -arene)chromium complexes	7
1.1.3 Deprotonation of prochiral ketones.....	8
1.2 Chiral magnesium amide complexes.....	26
1.2.1 Magnesium bisamides.....	28
1.2.2 Structural developments of magnesium bisamides.....	30
1.2.3 Heteroleptic magnesium amides.....	37
1.2.4 Developing a recycling protocol.....	43
1.2.5 Substrate scope with magnesium bisamides.....	46
<b>2 Proposed Work</b> .....	51
<b>3 Results and Discussion</b> .....	53
3.1 Benchmark deprotonations with $C_2$ -symmetric magnesium bisamide ( <i>R,R</i> )- <b>70</b> .....	53
3.1.1 $C_2$ -Symmetric amine synthesis.....	54
3.1.2 Asymmetric deprotonations of 4- <i>tert</i> -butylcyclohexanone <b>12</b> .....	55
3.2 Synthesis of 3-substituted and 3,3-disubstituted cyclobutanones.....	56
3.2.1 Synthesis of styrene derivatives.....	56
3.2.2 Optimisation of the [2+2] cycloaddition to access 3-substituted and 3,3- disubstituted cyclobutanones.....	59
3.3 Asymmetric deprotonations to afford enantioenriched silyl enol ethers.....	66
3.3.1 Optimisation of reaction conditions.....	66
3.3.2 Comparison with a chelating magnesium bisamide.....	73
3.4 Asymmetric deprotonations to afford enantioenriched enol phosphates.....	82

3.4.1 Introduction of an alternative electrophile .....	82
3.4.2 Additive studies.....	84
3.4.3 Substrate scope.....	89
3.4.4 Formation of racemic enol phosphates .....	92
3.4.5 Asymmetric deprotonations to form enantioenriched enol phosphates ....	93
3.5 Avenues for future work .....	103
<b>4 Conclusions</b> .....	<b>107</b>
<b>5 Experimental</b> .....	<b>109</b>
5.1 General Considerations .....	109
5.2 General Experimental Procedures.....	111
5.3 Benchmark deprotonations with <i>C</i> <sub>2</sub> -symmetric magnesium bisamide ( <i>R,R</i> )- <b>70</b> .....	115
5.3.1 Preparation of ( <i>R</i> )-bis(( <i>R</i> )-1-phenylethyl)amine <b>34</b> .....	115
5.3.2 Asymmetric deprotonations of 4- <i>tert</i> -butylcyclohexanone <b>12</b> .....	116
5.4 Synthesis of 3-substituted and 3,3-disubstituted cyclobutanones .....	118
5.4.1 Preparation of styrene derivatives.....	118
5.4.2 Preparation of 3-substituted and 3,3-disubstituted cyclobutanones.....	121
5.5 Asymmetric deprotonations to afford enantioenriched silyl enol ethers .....	126
5.5.1 Optimisation of reaction conditions .....	126
5.5.2 Comparison with a chelating magnesium bisamide.....	134
5.6 Asymmetric deprotonations to afford enantioenriched enol phosphates .....	142
5.6.1 Introduction of an alternative electrophile .....	143
5.6.2 Additive studies.....	143
5.6.3 Substrate scope.....	148
5.6.4 Preparation of racemic enol phosphates.....	156
5.6.5 Asymmetric deprotonations to form enantioenriched enol phosphates ..	160

5.7 Avenues for future work .....	168
<b>6 References</b> .....	170

# 1 Introduction

The introduction of asymmetry within a compound is one of the most challenging endeavours faced by modern synthetic organic chemists. Enantiomerically pure compounds have become increasingly important in the synthesis and application of biologically active molecules and potential drug candidates and, as such, the development of efficient syntheses of optically-enriched species has become a vast area of research in organic synthesis.<sup>1</sup> Over the years, a number of routes into optically active compounds have been developed. Initially, the resolution of racemic compounds was used to generate target molecules, although the major drawback of this method is the loss of half the material in the form of the unwanted enantiomer. The use of naturally occurring compounds from the available chiral pool became a more attractive method, however the choice of starting materials is somewhat limited and not all transformations can be achieved as the original stereogenic centre must remain intact throughout the entire synthesis of the desired target. An alternative approach is to use chiral auxiliaries to impart chirality to an achiral compound, although this involves additional synthetic steps to introduce and remove the auxiliary. A more efficient process is to use chiral reagents to introduce a stereogenic centre in a single synthetic step. This technique uses fewer synthetic steps and produces less waste. Furthermore, this process has the potential to be catalytic with the recycling of the chiral reagent. The chiral reagent could also be recovered and reused, making such methods more economically advantageous.

## 1.1 Chiral lithium amides

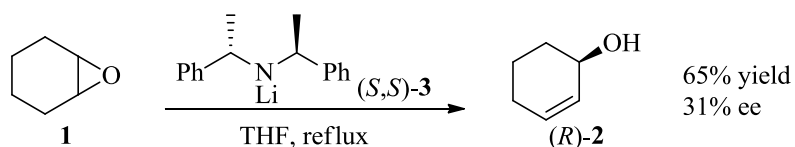
The use of organometallic reagents to impart chirality in an achiral substrate has become a popular method for the induction of asymmetry in a molecule. In particular, chiral lithium reagents have emerged in the field of asymmetric deprotonations as bases that are able to distinguish between two enantiotopic protons of a prochiral substrate.<sup>2</sup> Through enantioselective deprotonations, chiral lithium amides have been used with epoxides, tricarbonyl ( $\eta^6$ -arene)chromium complexes



and conformationally-locked prochiral ketones to form optically-enriched products. These methods are discussed herein.

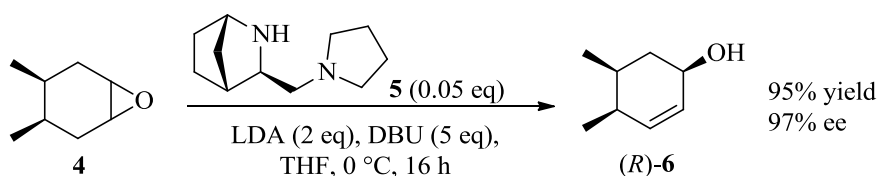
### 1.1.1 Enantioselective rearrangement of epoxides to allylic alcohols

The rearrangement of epoxides into allylic alcohols, mediated by non-chiral lithium amides has been well documented. This rearrangement proceeds *via* a *syn*  $\beta$ -elimination of a *pseudo*-axial proton.<sup>3</sup> In 1980, Whitesell first realised that a chiral base could distinguish between the two *syn*  $\beta$ -protons and therefore produce the allylic alcohol in enantiomerically-enriched form. In a more specific sense, using the chiral lithium amide base (*S,S*)-**3**, the optically active allylic alcohol was formed with 31% ee (**Scheme 1**).<sup>4</sup> Although the enantiomeric excess was only moderate for this transformation, the concept that a chiral lithium amide base can discriminate between a pair of enantiotopic protons had been proved for the first time.



**Scheme 1**

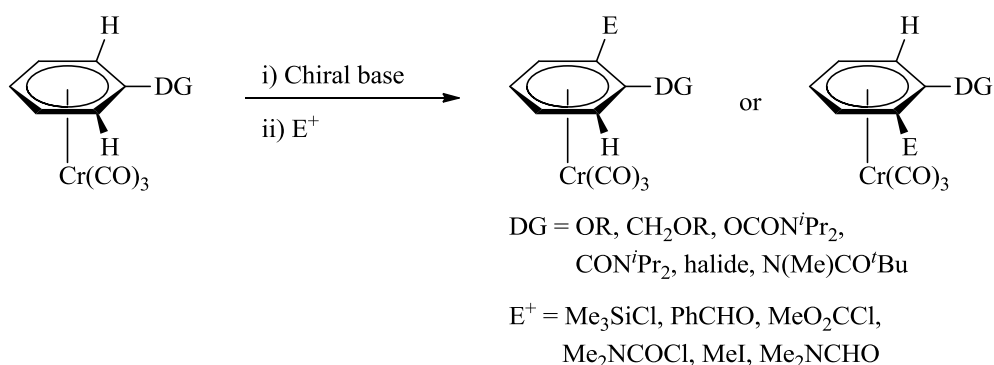
A variety of different chiral lithium amide bases have since been used for this asymmetric rearrangement, leading to enhanced levels of enantioselectivity and allowing access to both enantiomers of the desired allylic alcohol.<sup>5,6</sup> Catalytic protocols have also been developed,<sup>7</sup> including the non-substrate specific and highly enantioselective deprotonation developed by Andersson (**Scheme 2**).<sup>8</sup>



**Scheme 2**

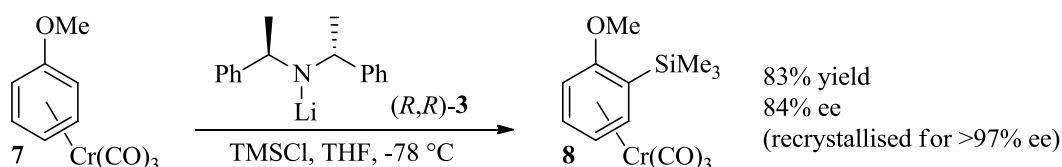
### 1.1.2 Enantioselective reactions of tricarbonyl ( $\eta^6$ -arene)chromium complexes

Research into the asymmetric metallation of tricarbonyl ( $\eta^6$ -arene)chromium complexes has revealed that the two *ortho* protons in these prochiral complexes can be distinguished by a chiral base. Such aromatic systems are set up for deprotonation by a lithium amide base due to the strongly electron-withdrawing chromium tricarbonyl moiety, combined with an electron-donating group to direct the *ortho*-lithiation.<sup>2c,2d</sup> A chiral lithium amide base therefore allows distinction between these two *ortho*-protons, providing access to a chiral non-racemic *ortho*-lithiated complex which can be subsequently trapped by a variety of electrophiles (**Scheme 3**).



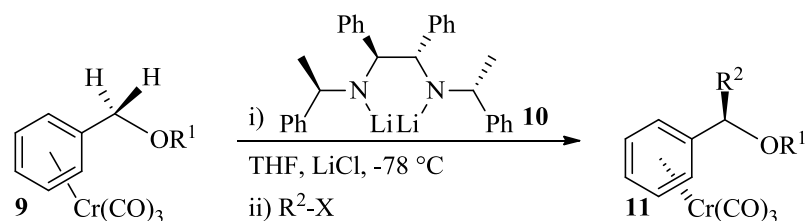
**Scheme 3**

The first preparation of an enantiomerically-enriched chromium complex in this manner, as opposed to using traditional resolution or chiral auxiliary techniques, was achieved by Simpkins and co-workers in 1994 (**Scheme 4**).<sup>9</sup> The chromium complex **7** was *ortho*-lithiated using chiral lithium amide (*R,R*)-**3** and quenched with  $\text{TMSCl}$  to afford the *ortho*-silylated complex **8** in an 83% yield with an optical purity of 84% ee. Recrystallisation of this complex enhanced this optical purity to an outstanding ee of greater than 97%.<sup>9,10</sup>



**Scheme 4**

As shown by Gibson, in addition to quenching the lithiated arene complex with an electrophile, if the electron-donating group contains two enantiotopic benzylic protons, asymmetric lithiation and subsequent electrophilic trapping can occur at this site within the molecule, leading to asymmetric benzylic functionalisation (**Scheme 5**).<sup>11</sup>



**Scheme 5**

Both Gibson<sup>11,12</sup> and Simpkins<sup>10</sup> have shown that the benzylic substitution and lithiation of tricarbonyl ( $\eta^6$ -arene)chromium complexes occurs with high enantioselectivity with the dilithiated chiral base **10**. It should be noted that, due to the steric influence of the chromium tricarbonyl moiety, the electrophile is introduced *trans* to this large group. The findings by Gibson are illustrated below (**Table 1**).<sup>12</sup>

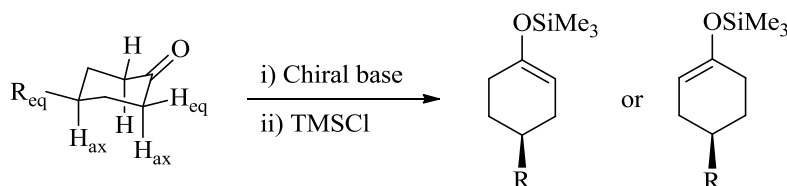
Entry	R <sup>1</sup>	R <sup>2</sup>	Yield (%)	ee (%)
1	Me	SPh	86	97
2	Me	Me	96	97
3	Bn	SPh	95	99
4	Bn	Me	89	≥99

**Table 1**

### 1.1.3 Deprotonation of prochiral ketones

Aside from the enantioselective processes described previously, the most extensively studied aspect of chiral lithium amide chemistry is the asymmetric deprotonation of conformationally-locked prochiral ketones.<sup>2</sup> Within such systems, it is believed that

there is a stereoelectronic preference that favours the removal of one of the axial protons over either of the equatorial protons  $\alpha$  to the carbonyl group (**Scheme 6**). A chiral base can thus distinguish between these two axial protons and produce an enantiomerically-enriched enolate on deprotonation. Electrophilic trapping of the chiral enolate on the carbon or oxygen leads to optically-enriched products.



**Scheme 6**

In this domain, pioneering results were published in 1986 by Koga and Simpkins, independently, who used different chiral lithium amides to effect the deprotonation of 4-*tert*-butylcyclohexanone **12**.<sup>13</sup> Koga used structurally more complex bases, which contain an additional ligating nitrogen atom (**Figure 1**).<sup>13a</sup> This second ligation site allows for the formation of a 5-membered chelate structure with the lithium, which is thought to confer rigidity onto the chiral base system and thus lead to higher enantioinduction in the formation of the resulting silyl enol ether.

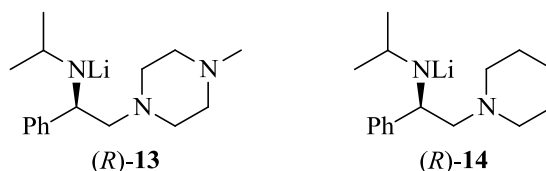
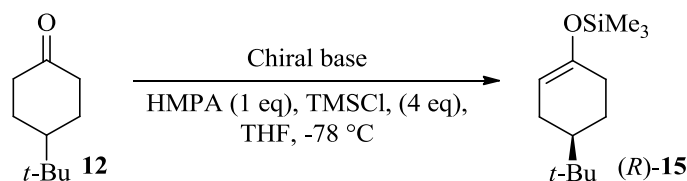


**Figure 1**

The enantioselectivity of such chiral lithium amides was demonstrated in the deprotonation of 4-*tert*-butylcyclohexanone (**12**) (**Scheme 7, Table 2**). These initial results showed that the highest enantioselectivity (89% ee) was achieved with the *N*-methylpiperazine moiety ((*R*)-**13**) and the presence of HMPA at low temperatures (**Entry 1, Table 2**). Increasing the temperature to -78 °C unfortunately resulted in a drop in enantioselectivity to 77% ee (**Entry 2, Table 2**). The use of piperidinyl base ((*R*)-**14**) led to similar yield and selectivity (**Entry 3, Table 2**). In relation to these

seminal endeavours, it should be noted that the asymmetric deprotonation of 4-*tert*-butylcyclohexanone has become the benchmark reaction against which all subsequent enantioselective deprotonations using novel chiral bases are measured.



**Scheme 7**

Entry	Chiral base	Temperature (°C)	Yield (%)	ee (%)
1	( <i>R</i> )- <b>13</b>	-105	52	89
2	( <i>R</i> )- <b>13</b>	-78	87	77
3	( <i>R</i> )- <b>14</b>	-78	82	82

**Table 2**

In contrast to the investigations of Koga, Simpkins used more structurally simple chiral lithium amides (**Figure 2**).<sup>13b</sup>

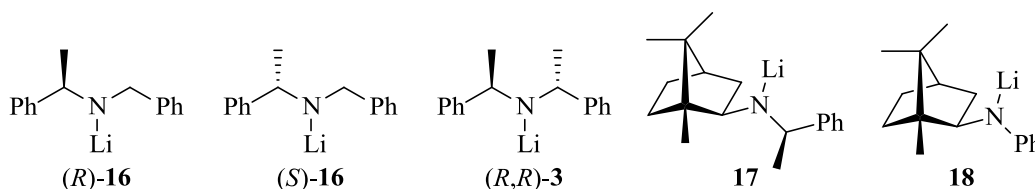
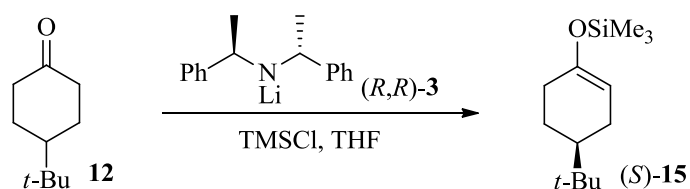


**Figure 2**

Comparing the  $C_2$ -symmetric lithium amide (*R,R*)-**3** in the benchmark deprotonation, good levels of enantioselectivity were achieved using this structurally simple base (**Scheme 8**),<sup>14</sup> albeit at the low temperature of -90 °C (**Entry 2, Table 3**). It should also be noted that, in contrast to the work of Koga, Simpkins did not use the Lewis basic additive HMPA in this asymmetric deprotonation system.



**Scheme 8**

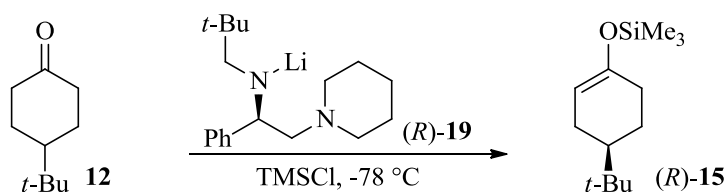
Entry	Temperature (°C)	Yield (%)	ee (%)
1	-78	73	69
2	-90	66	88

**Table 3**

After these initial asymmetric deprotonations by both research groups, further studies towards the effect of additives, quench conditions, solution aggregates, and the structure of the chiral lithium amides were carried out to gain a deeper understanding of these base systems.

#### *The use of additives*

For Koga's chiral lithium amide-mediated asymmetric deprotonation protocol, it was found that coordinating solvents, with the additive HMPA, at low temperatures, and a large excess of the electrophilic quench gave the highest enantioselectivities. Studies were carried out in order to assess the amount of HMPA required and elucidate the role of this Lewis basic additive.<sup>15</sup> This solvent study is summarised in **Scheme 9, Table 4**. The results clearly show that without the presence of a coordinating solvent the enantioselectivity is significantly decreased as the use of toluene afforded only a 12% yield and more moderate enantioinduction (58% ee, **Entry 1, Table 4**). When toluene was used in the presence of HMPA, however, the yield increased dramatically to 87% and the enantioselectivity increased to 82% ee (**Entry 2, Table 4**). Using THF, on the other hand, gave a high yield of 86% and an ee of 84%, which remained relatively unchanged with the addition of HMPA (**Entries 3 and 4, respectively, Table 4**).



**Scheme 9**

Entry	Solvent	Additive	Yield (%)	ee (%)
1	Toluene	None	12	58
2	Toluene	HMPA	87	82
3	THF	None	86	84
4	THF	HMPA	82	82

**Table 4**

These large variations in both enantioselectivity and yield were believed to be due to different aggregation states of the lithium amides in solution (**Figure 3**).<sup>16</sup> Subsequent NMR studies have supported this theory, as it was shown that the chiral lithium amide (*R*)-**19** exists as a chelated monomer (**20**) in THF but in toluene it exists as the chelated dimer (**21**). With the addition of two equivalents of HMPA to either solution, a chelated monomer was formed, which implied that the nature of the solvent is irrelevant in the presence of HMPA. It was also concluded that the chelated monomer (**20**) was the more reactive aggregate, as the lithium amide (*R*)-**19** produced higher conversion to the silyl enol ether ((*R*)-**15**) with greater enantiomeric excess in THF than in toluene, and in the presence of HMPA in toluene. The addition of HMPA in asymmetric deprotonations with similar lithium amides has also shown enhanced levels of enantioinduction.

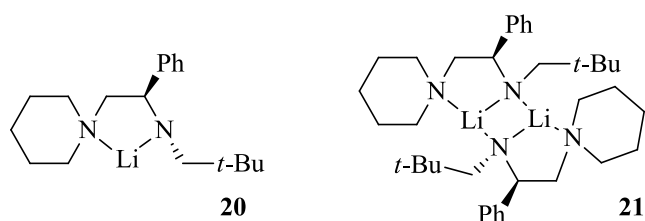


**Figure 3**

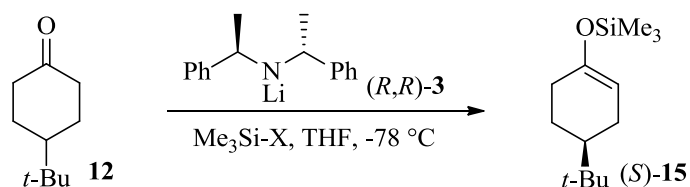
*Internal quench vs. external quench conditions*

It had been shown by both Koga<sup>13a</sup> and Simpkins<sup>14</sup> that using internal quench (IQ) conditions, developed by Corey,<sup>17</sup> results in higher levels of enantioselectivity. This internal quench protocol involves addition of the ketone substrate to a solution of the lithium amide base and the electrophilic quench reagent (TMSCl). As the reaction progresses, a build up of lithium chloride occurs *via* reaction of the lithium amide with the TMSCl directly, or by electrophilic trapping of the lithium enolate to form the silyl enol ether. An external quench (EQ) protocol, however, involves the addition of the TMSCl electrophile to a preformed solution of the lithium enolate. The EQ protocol has been shown to yield lower levels of enantioinduction. Moreover, there is a lack of lithium chloride in the reaction mixture when using an external quench procedure. Accordingly, the effect of the addition of LiCl into the system for the asymmetric deprotonation of 4-*tert*-butylcyclohexanone was investigated by Koga<sup>13a,18</sup> and Simpkins.<sup>19</sup>

Simpkins' study revealed that, when LiCl was introduced as part of the external quench protocol, much higher ees could be achieved for the formation of silyl enol ether (*S*)-**15** using the chiral lithium amide (*R,R*)-**3** (Scheme 10, Table 5).<sup>19</sup> Interestingly, although the enantioselectivity was initially higher using an IQ protocol (Entry 1, Table 5), the addition of LiCl to the EQ conditions resulted in an increase in enantioselectivity from 23% ee without LiCl to 83% ee with 0.5 equivalents of LiCl (with respect to the lithium amide base, Entries 2 and 3, Table 5). In addition, when changing the halide from chloride to bromide under IQ conditions, a drop in enantioselectivity from 69% ee to 20% ee, respectively, was



observed (**Entries 1 and 4, Table 5**). Similar effects were shown by Simpkins with alternative chiral lithium amides and substrates.

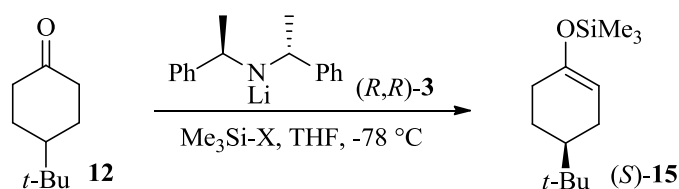


**Scheme 10**

Entry	X	Quench	LiCl (eq.)	ee (%)
1	Cl	IQ	-	69
2	Cl	EQ	-	23
3	Cl	EQ	0.5	83
4	Br	IQ	-	20

**Table 5**

This diminished asymmetric induction observed when using larger halides on the electrophilic quench was also studied by Koga during his investigations into the IQ and EQ procedures for this deprotonation using the same base (*R,R*)-**3** (**Scheme 11, Table 6**).<sup>20</sup> Several findings were made in this study. Firstly, and in line with Simpkins' results,<sup>19</sup> changing from chloride to bromide then iodide under IQ conditions lowers the enantioselectivity of this deprotonation (**Entries 1, 2, and 3, Table 6**). In addition, the IQ protocol was more selective than the EQ protocol (**Entry 1 cf. Entry 4, Table 6**). Koga also found that the addition of LiCl to this EQ protocol results in a dramatic increase in enantioselectivity from 44% ee, with no additive, to 87% ee with 0.5 equivalents of LiCl, with respect to the lithium amide base (**Entries 4 and 5, Table 6**). Increasing the number of equivalents of LiCl, did not show any further improvements to this level of selectivity (**Entries 5 to 7, Table 6**).

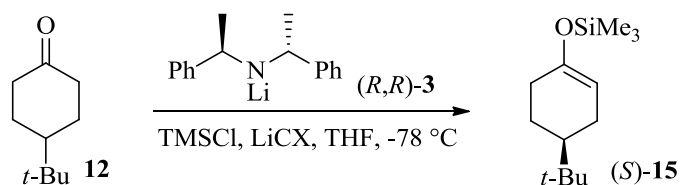


**Scheme 11**

Entry	X	Quench	Additive (eq.)	ee (%)
1	Cl	IQ	-	90
2	Br	IQ	-	65
3	I	IQ	-	31
4	Cl	EQ	-	44
5	Cl	EQ	LiCl (0.5)	87
6	Cl	EQ	LiCl (1.0)	88
7	Cl	EQ	LiCl (3.0)	88

**Table 6**

Having shown that the size of the halide from the electrophilic quench is an important factor under IQ conditions, the salt additives for the EQ protocol were studied in a similar manner, by using LiBr and LiI to compare the effects to those of LiCl (**Scheme 12, Table 7**).<sup>20</sup> Under EQ conditions, it was found that increasing the size of the halide in the LiX additive is detrimental to both the reaction yield and the enantioselectivity. These findings support the theory that under IQ conditions, it is the *in situ* formation of LiCl that affords higher enantioselectivities in the formation of the resulting silyl enol ethers, as the addition of LiBr or LiI has no distinct benefit under these conditions (**Entries 3 and 4, Table 7**). The addition of LiCl to an EQ protocol is therefore beneficial, which implies that a more reactive and selective aggregate of the lithium amide is formed under both conditions in the presence of LiCl.



**Scheme 12**

Entry	LiX (1.2 eq)	Yield (%)	ee (%)
1	-	84	44
2	LiCl	97	88
3	LiBr	89	63
4	LiI	85	44

**Table 7**

#### *NMR studies*

In order to rationalise these findings, Koga proposed that under IQ conditions, with no LiCl present, the chiral lithium amide base (*R,R*)-**3** is likely to exist in its monomeric form or as the homo dimer (**22**). By carrying out detailed  $^6\text{Li}$  and  $^{15}\text{N}$  NMR studies in THF- $d_8$ , it was revealed that the homo dimer (**22**) was in fact the major structural component of a solution of lithium amide base (*S,S*)-**3** (**Figure 4**).<sup>20</sup> Koga proposed that dimer **22** must be unable to impart high levels of enantioselectivity under EQ conditions, with no LiCl present. By including  $^6\text{LiCl}$  in the deuterated THF solution with chiral base (*S,S*)-**3** two new species which incorporated the  $^6\text{LiCl}$  were observed; these were the mixed dimer **23** and mixed trimer **24**. When more than 0.5 equivalents of LiCl were present, the major solution component was found to be the mixed dimer **23**. It was therefore suggested that this dimer was responsible for the high levels of enantioselectivity imparted.<sup>20</sup>

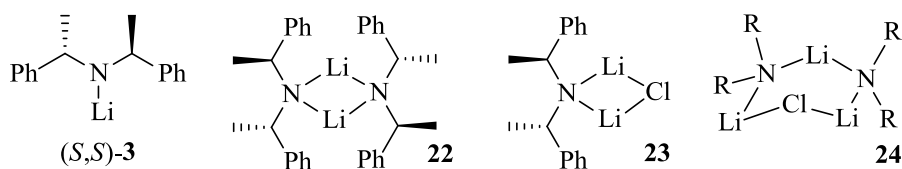


**Figure 4**

Having elucidated the structure of these various aggregates which form in solution for the  $C_2$ -symmetric lithium amide (*S,S*)-**3**, Koga then went on to determine the solution structures of the chelating lithium amides (**Figure 5**).<sup>21</sup> In the same manner, a solution of (*R*)-**19** in THF- $d_8$  revealed that this lithium amide exists as the chelated monomer (*R*)-**25**. In the presence of  $^6\text{LiCl}$ , however, the mixed dimer, **26**, was formed. It is believed that the mixed dimer is the more selective species in the asymmetric deprotonation of 4-*tert*-butylcyclohexanone.

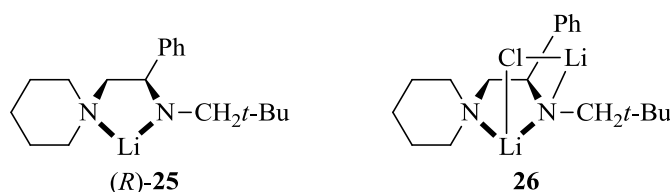


**Figure 5**

#### *Structural variations of chiral lithium amide bases*

Several other chiral lithium amides have been developed and proved to induce high levels of enantioselectivity for the deprotonation of prochiral ketones. The most successful of these were a trifluoromethyl-containing lithium amide ((*R*)-**27**) developed by Koga<sup>22</sup> and some alternative amide ligands utilised by Corey ((*R*)-**28**),<sup>23</sup> Aggarwal ((*S*)-**29**),<sup>24</sup> and Knochel ((*R,R,R,R*)-**30**, **Figure 6**).<sup>25</sup> When applied to the benchmark deprotonation of 4-*tert*-butylcyclohexanone all four of these bases showed similarly high levels of enantioselectivity and reaction yield (**Scheme 13**, **Table 8**). Having stated this and whilst these bases were, indeed, selective, overall they did not offer any greater advantage over the original bases used. In this respect, it should be noted that the conditions required to attain these levels of enantioselectivity involved the less practically convenient temperature of  $-100\text{ }^\circ\text{C}$ ,

which is also less economically viable, along with key reaction additives in two cases (**Entries 2 and 3, Table 8**).

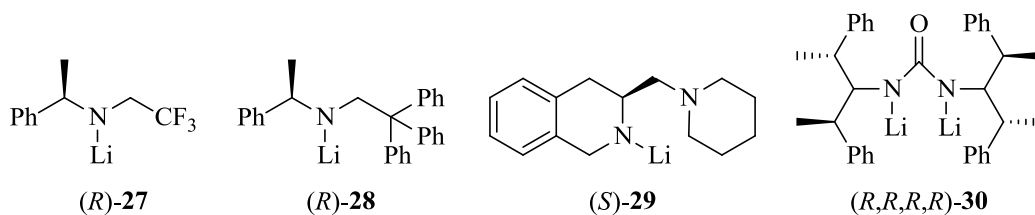
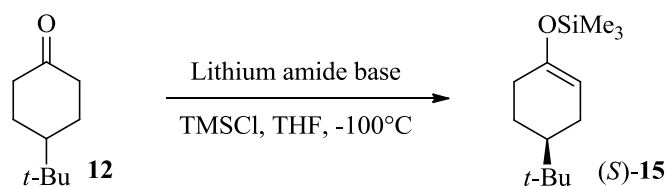


**Figure 6**



**Scheme 13**

Entry	Base	Yield (%)	ee (%)	Additive
1	(R)-27	86	89	-
2	(R)-28	89	91	LiBr
3	(R)-29	89	81	HMPA
4	(R,R,R,R)-30	85	87	-

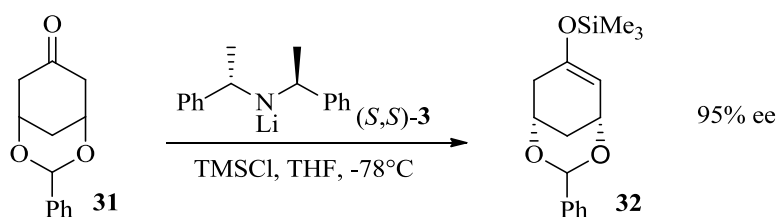
**Table 8**

### Substrate scope

After the initial development of chiral lithium amides, several research groups have probed the utility of these bases for the application in natural product syntheses which involve deprotonations of conformationally-locked prochiral ketones. The more varied substrates are discussed herein.

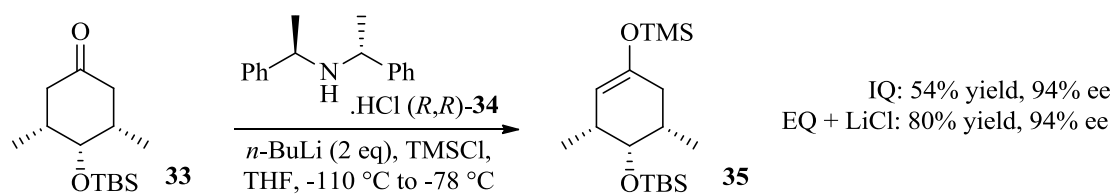
In 2001, Honda and co-workers employed the  $C_2$ -symmetric lithium amide ((*S,S*)-**3**) in the asymmetric deprotonation of cyclohexanone **31**, which is a common building

block for the synthesis of various biologically active compounds (**Scheme 14**).<sup>26</sup> Using internal quench conditions with TMSCl, the silyl enol ether (**32**) was obtained with excellent levels of selectivity (95% ee).



**Scheme 14**

As well as this rigid bicyclic ketone, 3,4,5-trisubstituted cyclohexanones (such as **33**) have been transformed into their equivalent silyl enol ethers using the lithium amide  $(R,R)$ -**3** by Prunet and Férézou (**Scheme 15**).<sup>27</sup> The amine salt  $(R,R)$ -**34** was treated with two equivalents of *n*-BuLi under IQ and EQ conditions, with the inclusion of LiCl under EQ conditions. It was found that similarly impressive stereoselection was obtained for both sets of conditions, however, the yield was significantly lower under the IQ protocol (54%) and resulted in a 30% yield of returned starting ketone at the end of the reaction.



**Scheme 15**

These high levels of optical enrichment were rationalised using molecular calculations to provide conformational analysis of this particular substrate (**Figure 7**).<sup>27</sup> It was revealed that the bulky *tert*-butyldimethylsilyloxy group adopts an axial position in which the methyl groups are in close proximity to the acidic axial protons. This hindrance could result in enhanced distinction between the two axial protons and, thus, may be leading to the elevated enantioselectivities on their removal.

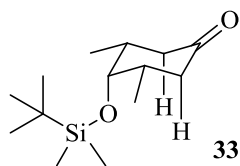
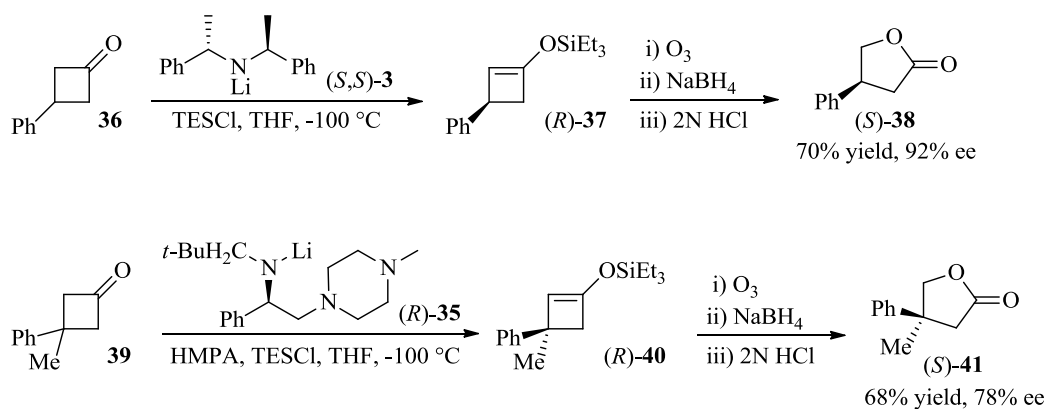


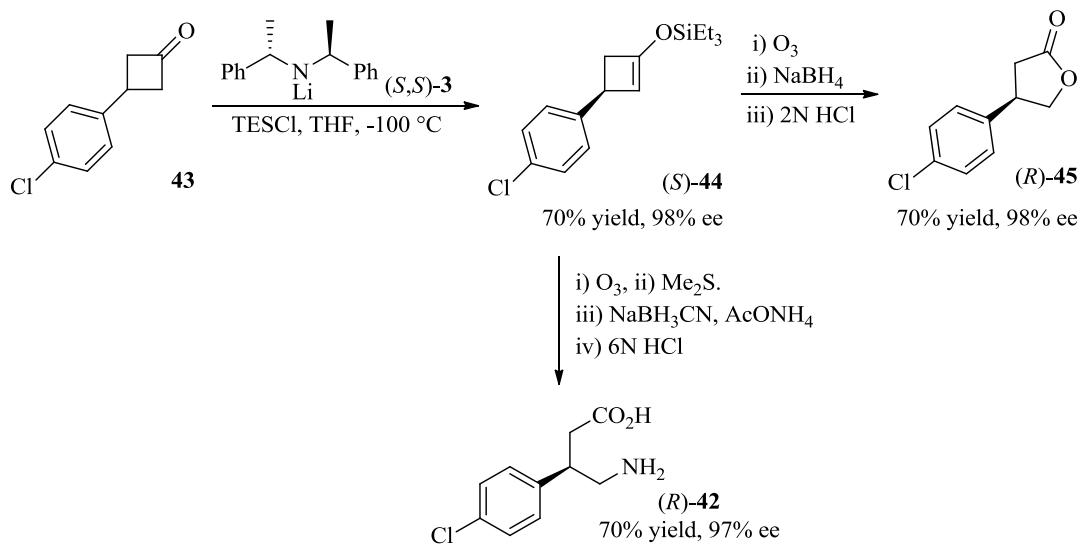
**Figure 7**

Aside from differing substitution around cyclohexanone substrates, chiral lithium amide bases have been used to deprotonate both smaller and larger sizes of cyclic ketones. It has been shown by Honda<sup>28</sup> and Coelho<sup>29</sup> that 3-substituted and 3,3-disubstituted cyclobutanones can be transformed into their enantioenriched silyl enol ethers, and subsequently their  $\gamma$ -butyrolactones, using the  $C_2$ -symmetric lithium amide (*S,S*)-**3**. Honda and co-workers first attempted this enantioselective deprotonation on 3-phenylcyclobutanone **36**, trapping the resulting enolate with TESCl (**Scheme 16**).<sup>28a</sup> The resulting silyl enol ether **37** was subsequently converted into the known lactone **38** by ozonolysis followed by reductive work-up with sodium borohydride to establish the enantioselectivity of the transformation. With an ee of 92% for the lactone **38** it was inferred that this selectivity had been imparted in the initial silyl enol ether during the desymmetrisation of the starting cyclobutanone. This strategy was then applied to the enantioselective deprotonation of 3,3-disubstituted cyclobutanone **39**.<sup>28</sup> For this 3,3-disubstituted cyclobutanone, the structurally more complex chelating base (*R*)-**35** was employed. In order to attain appreciable levels of enantioselectivity for the 3,3-disubstituted cyclobutanone **39**, HMPA was also required as an additive for this deprotonation. Although the induction asymmetrically established within the lactone **41** was lower than that of the singly substituted lactone **38**, at 78% ee, the deprotonation was successful in the formation of a quaternary chiral centre. It should be noted that for the two lithium amide bases ((*S,S*)-**3** and (*R*)-**35**) an extremely low reaction temperature of -100 °C was employed. When the deprotonations of cyclobutanone substrates **36** and **39** were carried out at more elevated temperatures, a significant drop in enantioselectivity of lactones (*S*)-**38** and (*S*)-**41** was observed.



**Scheme 16**

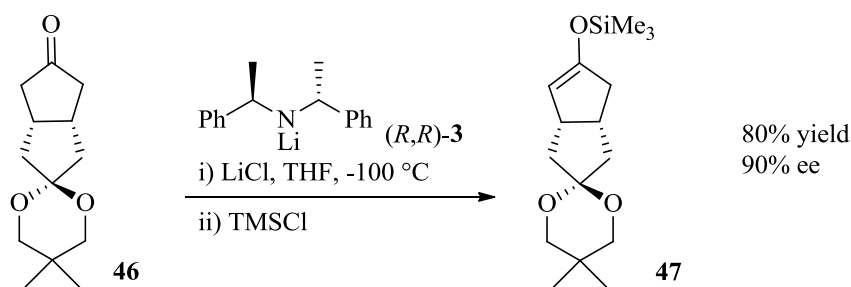
Coelho has, more recently, employed this approach in the synthesis of the natural product Baclofen (**42**, **Scheme 17**), using the same  $C_2$ -symmetric lithium amide ( $S,S$ )-**3** to desymmetrise 3-(4'-chlorophenyl)cyclobutanone **43**.<sup>29</sup> The resulting silyl enol ether **44** was thus derivatised to both the  $\gamma$ -butyrolactone ( $R$ )-**45** and the natural product ( $R$ )-**42** to assess the enantioselectivity of the deprotonation (**Scheme 17**). Once again, the asymmetric deprotonation was carried out at  $-100\text{ }^\circ\text{C}$  to achieve this level of enantioinduction within silyl enol ether ( $S$ )-**44**.



**Scheme 17**

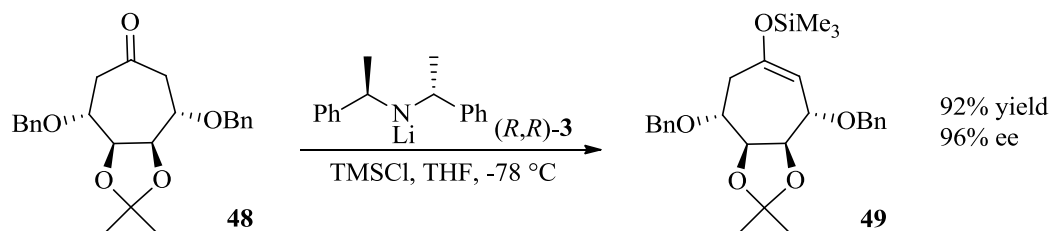


In addition to these cyclobutanone substrates, the asymmetric deprotonations of bicyclic ketones containing a cyclopentanone ring (including **46**) have been successfully employed by van Gergen and Gais.<sup>30</sup> Using an external quench protocol with the LiCl additive, the lithium enolate was trapped with TMSCl to form the desired silyl enol ether (**47**) in both high yield and ee (**Scheme 18**). Again, a reaction temperature of -100 °C is required to provide optimal selectivity. This study also illustrated the further synthetic utility of the lithium amide-mediated deprotonation as silyl enol ether **47** was synthesised as a key intermediate in the enantioselective synthesis of carba-prostacyclin analogues.<sup>30</sup>



**Scheme 18**

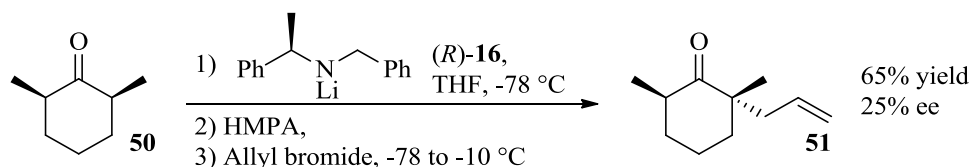
Whilst chiral lithium amide bases have proved to be widely applicable in the enantioselective deprotonation of smaller ringed cyclic ketones, these reagents have not been as widely used for the desymmetrisation of 7- and 8-membered cyclic ketones. Having stated this, the first example of such an application was demonstrated by Honda in the deprotonation of the *meso*-cycloheptanone **48** (**Scheme 19**).<sup>31</sup> The  $C_2$ -symmetric lithium amide  $((R,R)$ -**3**) was used, with TMSCl, to form the silyl enol ether **49** with an excellent ee of 96%.



**Scheme 19**

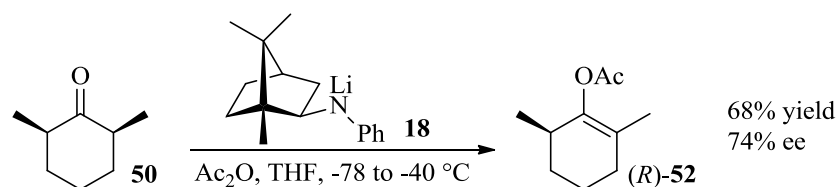
### Alternative electrophiles

In addition to a wide range of ketone substrates that have been desymmetrised in an asymmetric deprotonation process, a range of electrophiles have also been used to trap the enantioenriched enolate, with varying degrees of success. Early studies by Simpkins, revealed that electrophilic trapping on carbon rather than oxygen was only moderately yielding and did not show high levels of enantioselectivity.<sup>14,32</sup> Specifically, deprotonation of 2,6-dimethylcyclohexanone **50** with the  $C_2$ -symmetric lithium amide (*R*)-**16** and trapping the chiral enolate with allyl bromide gave the alkylated product **51** in a 65% yield but only showing 25% ee (**Scheme 20**).<sup>32</sup> Efforts to improve this ee were made, but it was found that the conditions shown below were the most effective for this alkylation. The addition of HMPA prior to the allyl bromide addition was key, followed by a slight warming of the reaction mixture in order to gain appreciable yields. Irreproducibility was observed, however, with this electrophile, and no further examples were trialled by Simpkins and co-workers.



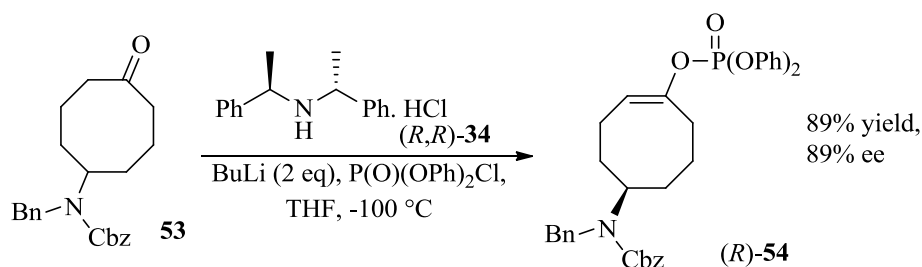
**Scheme 20**

After having achieved only low selectivity using allyl bromide as the electrophile, Simpkins turned to acetic anhydride as an alternative quench.<sup>14,32</sup> A range of base structures were compatible with this electrophile for the deprotonation of 2,6-dimethylcyclohexanone. The highest selectivity for this alternative electrophile was 74% ee using the camphor-derived base **18** (**Scheme 21**).<sup>14</sup> A good yield of enol acetate (*R*)-**52** was obtained with all bases trialled in this study, with 68% being the highest possible for this particular example.



**Scheme 21**

In addition to the anhydride quench, Aggarwal has used diphenylphosphoryl chloride successfully within the asymmetric deprotonation of eight-membered cyclic ketone **53** (Scheme 22).<sup>33</sup> Using the  $C_2$ -symmetric amine salt ( $R,R$ )-**34** with two equivalents of  $n$ -BuLi, the lithium amide ( $R,R$ )-**3** was formed *in situ* with an equivalent of LiCl also being generated in order to gain high enantioselectivity. Pleasingly, the enol phosphate ( $R$ )-**54** was formed in high 89% yield and 89% ee. In this publication, the utility of the enol phosphate produced was also demonstrated by coupling this enantioenriched product with a vinyl stannane, using palladium(0), as the subsequent step in the total synthesis of (+)-Anatoxin a.<sup>33</sup>



**Scheme 22**

### Catalytic systems

The use of chiral lithium amides for the asymmetric deprotonation of prochiral and *meso*-ketones has proved to be highly reproducible and widely applicable. All of the examples discussed thus far, however, have required stoichiometric quantities of the chiral base. In order to improve the efficiency of this process and make it more economically viable, the development of a catalytic protocol was clearly advantageous. Initial investigations towards a recycling process were carried out by Koga, who suggested that the following cycle could be possible (Figure 8).<sup>34</sup> It was

proposed that a sub-stoichiometric amount of the chiral amine (*R*)-**55** could be deprotonated by a stock, non-chiral lithium amide reagent to generate the chiral lithium amide (*R*)-**56**. The chiral lithium amide (*R*)-**56** would then effect the deprotonation of the prochiral ketone to form the chiral lithium enolate and, in doing so, liberating free chiral amine ((*R*)-**55**) back into solution. In order for this sequence of deprotonations to occur, Koga selected the tridentate lithium amide (**57**), as this base had previously shown to be ineffective towards the deprotonation of ketones and would therefore provide less competition for the deprotonation of the cyclohexanone substrate. Furthermore, the trifluoromethyl group within the chiral amine was believed to help aid rapid lithium-hydrogen exchange with the achiral lithium amide, due to the electron-withdrawing ability of this functional unit.

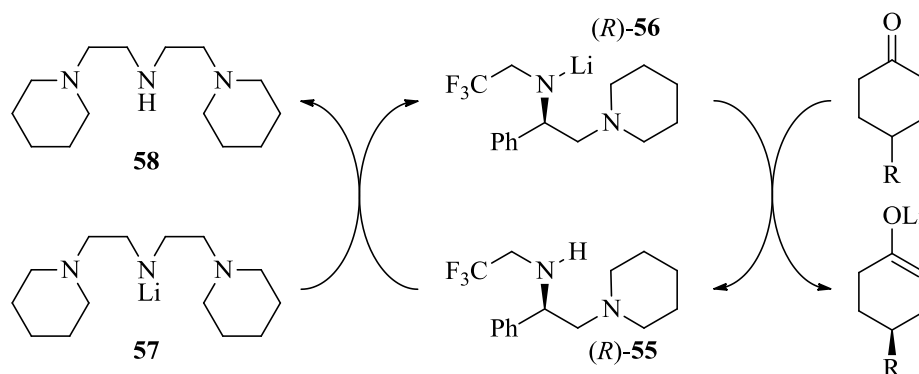
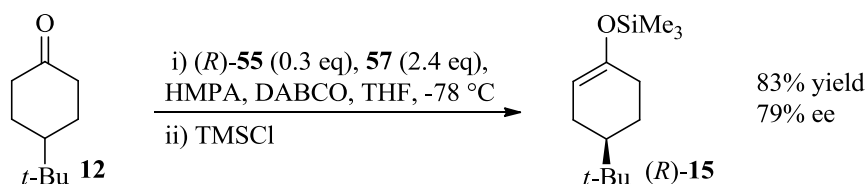


**Figure 8**

Based on all of this, just 0.3 equivalents of the trifluoromethyl chelating amine (*R*)-**55** were employed with 2.4 equivalents of the lithium base **57**, for the deprotonation of the benchmark substrate **12** (Scheme 23).<sup>34</sup> Trapping the chiral lithium enolate with TMSCl under external quench conditions afforded the silyl enol ether ((*R*)-**15**) in a high yield of 83% and an equally impressive ee of 79%.



**Scheme 23**

Overall, chiral lithium amide bases have proved to be effective tools for the formation of enantioenriched silyl enol ethers, and the development of a catalytic variant of this asymmetric deprotonation is a significant advancement to this field of organic synthesis. A number of drawbacks still remain, however. Specifically, the low temperature requirements and the instability of these base systems prevents such lithium amides being completely economical and more widely effective. Furthermore, a number of differing additives are required when non-conventional substrates are employed, which complicates these systems and requires optimisation whenever utilised. It is with this in mind that alternative reagents are being investigated to improve upon these asymmetric deprotonations.

## 1.2 Chiral magnesium amide complexes

Compared with their lithium counterparts, magnesium amide reagents have seen less use in asymmetric transformations. Although chiral lithium amides have shown high levels of enantioselectivity in asymmetric deprotonations, there are several drawbacks to using such bases. These include the complex solution aggregations formed, the structural complexity required to achieve high selectivity, and the requirements for low reaction temperatures. Chiral magnesium amide bases have similar properties to those of lithium, but offer a number of advantages to overcome the limitations of the chiral lithium amides and the subsequent potential to broaden the scope of this field of chemistry.

### *Solution aggregation*

Lithium amides have been shown to exist as a range of aggregates which are changed by the addition of additives such as HMPA and LiCl.<sup>20</sup> Koga has shown that only certain aggregates lead to high enantioselectivity and, thus, problems with reproducibility can occur when using these base systems. Magnesium bisamides, however, have been shown to exist as either monomers or dimers in solution, leading to more predictable and reproducible solution aggregation states. For example, it has been shown that in toluene, bis(dibenzylamido)magnesium exists in equilibrium

between its monomer (**59**) and dimer (**60**, **Figure 9**).<sup>35</sup> In a similar manner to lithium, the addition of HMPA simplifies this aggregation further. With two equivalents of HMPA, the bis-solvated dimer **61** is formed in equilibrium with its bis-solvated and non-solvated monomers (**62** and **59**, respectively). This solvated dimer degrades on the addition of two further equivalents of HMPA to the solvated monomer (**62**). This control of solution structures of magnesium bisamides offers the possibility of more consistent and reproducible results when using such complexes within sensitive organic processes.

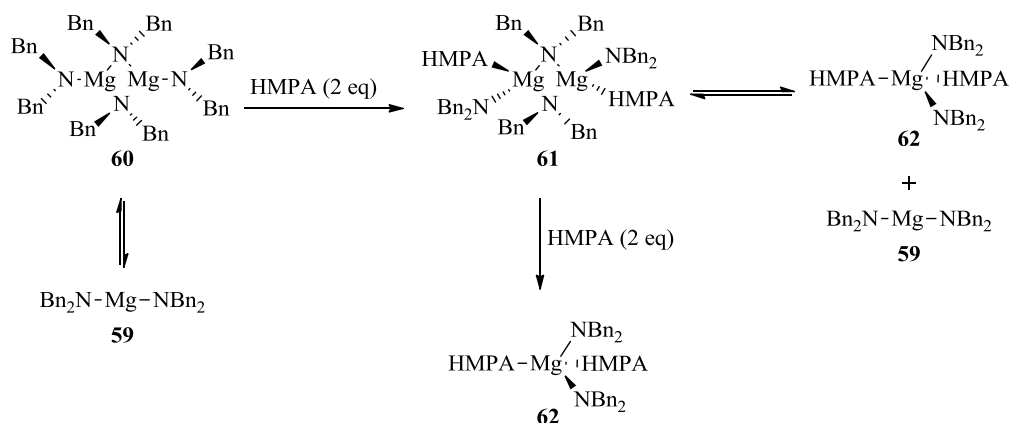


**Figure 9**

### *Thermal stability*

Lithium amides have poor thermal stability as well as high reactivity, requiring reaction temperatures as low as  $-100\text{ }^\circ\text{C}$  for the use of these reagents. In contrast, magnesium amide species are more thermally stable and less reactive,<sup>36</sup> which could be advantageous in asymmetric deprotonations, as this is normally kinetically controlled.<sup>37</sup> By using magnesium amides at more elevated temperatures a wider range of transformations and access to less reactive substrates could be available, providing an inherent economic and broader preparative advantage.

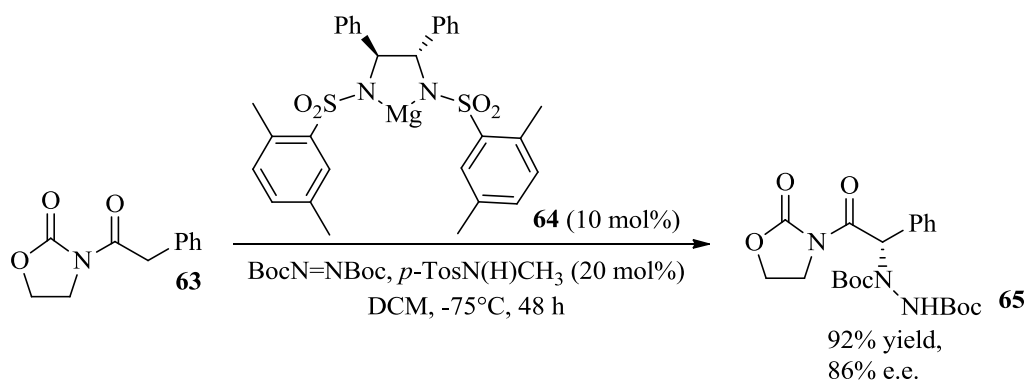
### *Divalency of magnesium*

Magnesium amide bases possess a further advantage over their lithium analogues, as their divalent nature introduces the possibility of forming both homo- and

heteroleptic complexes. Given this characteristic, the use of one chiral ligand to affect the asymmetric deprotonation could be used alongside a different spectator ligand which could influence subsequent reactions.

### 1.2.1 Magnesium bisamides

As mentioned previously, magnesium bases have had far less use in asymmetric transformations compared with lithium amides. A chiral magnesium bis(sulfonamide) was the first example to be used, catalytically, for the enantioselective amination of *N*-acyloxalidinone (**63**), by Evans and Nelson in 1989 (Scheme 24).<sup>38</sup> Whilst not an enantioselective deprotonation protocol, in this process, the resulting chiral magnesium enolate directs an asymmetric quench with a nitrogen-based electrophile.

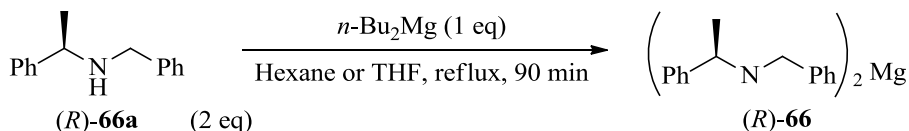


Scheme 24

Until 2000, chiral magnesium base chemistry had not seen any use in asymmetric deprotonation processes. The recent advances in this area have come from Kerr and Henderson, and their work on the enantioselective deprotonation of prochiral ketones using chiral magnesium bases is discussed below.

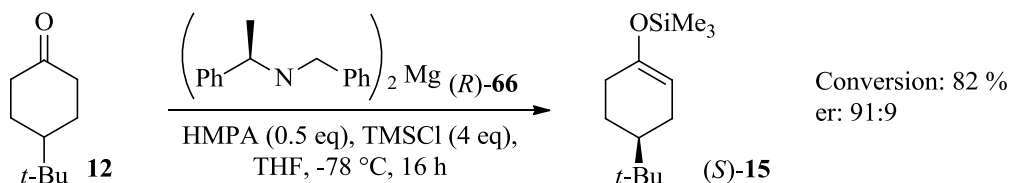
### Asymmetric deprotonations of prochiral ketones

Studies to establish the efficacy of chiral magnesium bisamides within enantioselective deprotonations of prochiral ketones began with the novel magnesium bisamide ((*R*)-**66**). This base was prepared by reacting two equivalents of the commercially available chiral amine ((*R*)-**66a**) with di-*n*-butylmagnesium by refluxing the mixture in hexane or THF (**Scheme 25**).<sup>39</sup>



**Scheme 25**

Pleasingly and following careful optimisation, when applied to the benchmark deprotonation of 4-*tert*-butylcyclohexanone (**12**), this novel and very simple chiral base ((*R*)-**66**) showed excellent conversion to the corresponding silyl enol ether (**15**) with high levels of enantioselectivity (**Scheme 26**).<sup>39</sup>

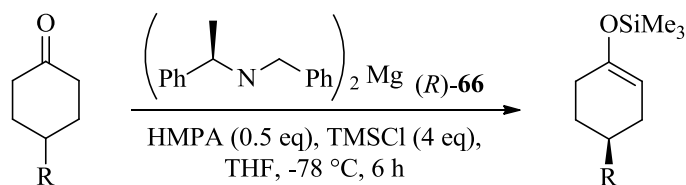


**Scheme 26**

The optimised reaction conditions applied to this deprotonation utilised an internal quench protocol, whereby a solution of 4-*tert*-butylcyclohexanone (**12**) in THF was added over the period of one hour to a solution of the chiral base ((*R*)-**66**), HMPA and TMSCl in THF at -78 °C. With this positive result and optimised reaction conditions in hand, a range of 4-substituted cyclohexanones were studied. Comparable conversions and enantioselectivities were achieved for each of these substrates, illustrating the scope and robustness of this new chiral induction method (**Scheme 27, Table 9**).<sup>39</sup> The asymmetric efficiencies observed are remarkable given the simplicity of the base reagent. Moreover, when these results are compared to the



equivalent lithium base species, an er of 75.5:25.5 is achieved at this temperature, for the *tert*-butyl analogue, whereas a significantly higher er is observed with the magnesium bisamide (*R*)-**66** (91:9 er, **Entry 1, Table 9**).



**Scheme 27**

Entry	R	Conversion (%)	Yield (%)	er (( <i>S</i> ):( <i>R</i> ))
1	<i>t</i> -Bu	82	64	91:9
2	Ph	79	48	87:13
3	Me	81	68	91:9
4	<i>i</i> -Pr	77	39	95:5
5	<i>n</i> -Pr	88	58	88:12

**Table 9**

Further optimisation of these reaction conditions revealed that DMPU could be used in place of HMPA, with no drop in conversion or selectivity.<sup>39</sup> This offered an advantage over the use of the toxic HMPA additive.

### 1.2.2 Structural developments of magnesium bisamides

Having employed the novel magnesium bisamide ((*R*)-**66**) for the desymmetrisation of a range of prochiral cyclohexanones, it was envisaged that some structural elaboration of the magnesium bisamide could result in higher enantioselectivities in the asymmetric deprotonation protocol. Accordingly, a range of novel magnesium bisamides was synthesised and the reactivity of these bases against the benchmark deprotonation of 4-*tert*-butylcyclohexanone was probed.<sup>40</sup>

Early alterations to the amide ligand structure were made by altering the achiral sidearm.<sup>40</sup> None of the alkyl or aryl substituents incorporated, however, provided any improvement over the original structure (*R*)-**66**. Elaboration of the chiral sidearm did, however, show enhanced enantioselectivity of the benchmark deprotonation.<sup>40</sup> Despite this slight improvement, it was deemed, that the original base (*R*)-**66** was the offered the most appropriate levels of conversion and selectivity employing such a structurally simple and commercially available ligand.

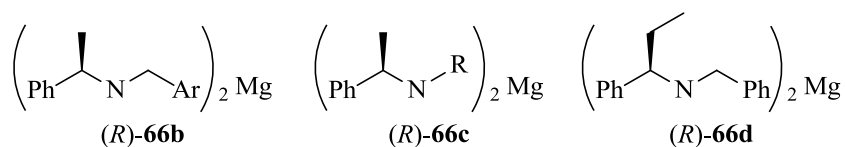


**Figure 10**

#### *Chelating magnesium bisamides*

More significant structural developments were made when a chelating amide ligand was considered. As discussed previously (**Section 1.1.3**), Koga and co-workers had shown that structurally more complex lithium amides afforded high enantioselectivity in the asymmetric deprotonation of 4-*tert*-butylcyclohexanone. It was envisaged that such complexity with the amide moiety of the chiral base could be employed as part of the emerging magnesium bisamides. A series of polydentate magnesium bisamides was thus prepared in order to test this hypothesis (**Figure 11**).<sup>41</sup>

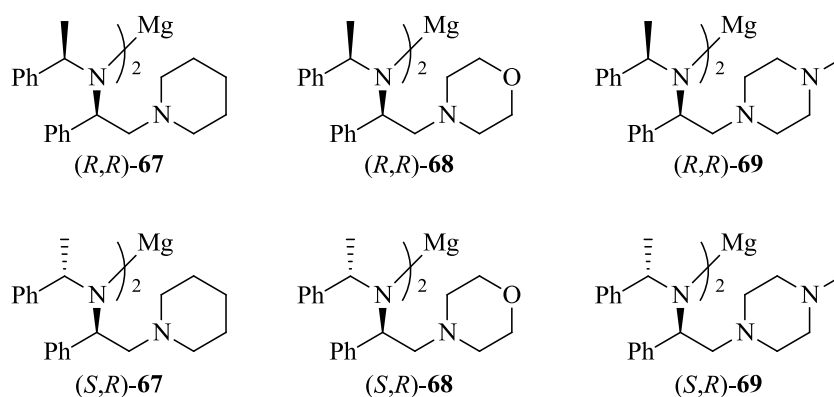
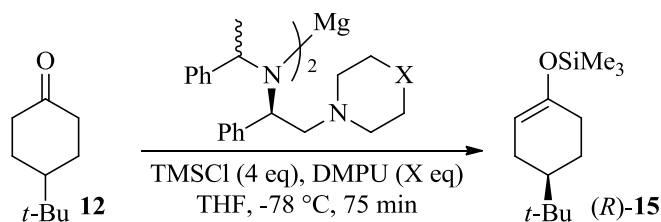


**Figure 11**

It was proposed, and later proved by X-ray crystallography, that a 5-membered chelate forms with magnesium in these bases which is believed to induce the high levels of enantioselectivity observed.<sup>41b</sup> The results of these deprotonations are illustrated below (**Scheme 28, Table 10**).<sup>41</sup> Firstly, it should be noted that inversion of the stereocentre which would sit outside any chelating ring form results in formation of the same product enantiomer (for example changing from *(R,R)*-**67** to *(S,R)*-**67**, **Entries 1 and 3, Table 10**). Furthermore, there is no appreciable drop in the enantioselectivity when using the diastereomeric base. Indeed, high levels of enantioinduction were obtained across the board. These two observations imply that the chiral information is being transferred mostly through the stereocentre closest to the chelating moiety. This trend is observed for all six of the chelating magnesium bisamides employed below. Secondly, the inclusion of DMPU as an additive within the benchmark asymmetric deprotonation showed enhanced levels of conversion to silyl enol ether (*R*)-**15**. For each base illustrated in **Table 10**, a marked increase in conversion to silyl enol ether (*R*)-**15** was observed when 0.5 equivalents was employed. Moreover, the enantioselectivity remained high with the inclusion of the Lewis basic additive.



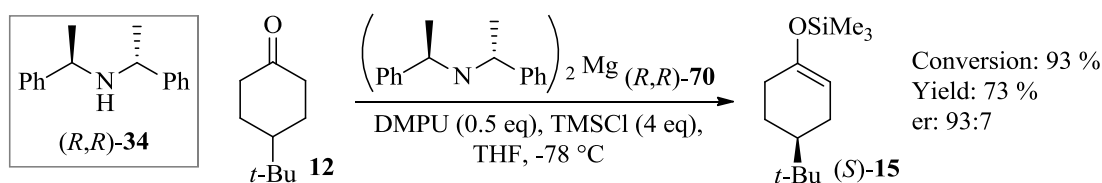
**Scheme 28**

Entry	Base	X	DMPU eq.	Conv. (%)	er ((R):(S))
1	(R,R)- <b>67</b>	CH <sub>2</sub>	0	58	93:7
2	(R,R)- <b>67</b>	CH <sub>2</sub>	0.5	90	93:7
3	(S,R)- <b>67</b>	CH <sub>2</sub>	0	87	88:12
4	(S,R)- <b>67</b>	CH <sub>2</sub>	0.5	88	88:12
5	(R,R)- <b>68</b>	O	0	89	91:10
6	(R,R)- <b>68</b>	O	0.5	96	88:12
7	(S,R)- <b>68</b>	O	0	55	89:11
8	(S,R)- <b>68</b>	O	0.5	83	89:11
9	(R,R)- <b>69</b>	NMe	0	88	91:9
10	(R,R)- <b>69</b>	NMe	0.5	94	92:8
11	(S,R)- <b>69</b>	NMe	0	59	87:13
12	(S,R)- <b>69</b>	NMe	0.5	92	92:8

**Table 10**

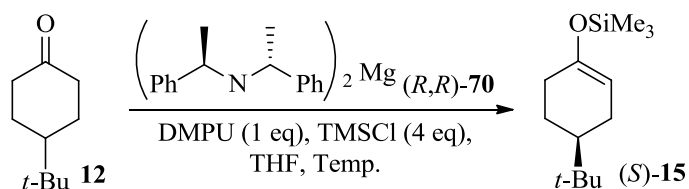
#### *C*<sub>2</sub>-Symmetric magnesium bisamides

Another programme of study within the Kerr group focused on the development of novel *C*<sub>2</sub>-symmetric magnesium bisamides. As shown by Simpkins,<sup>13b</sup> the simple yet elegantly structured *C*<sub>2</sub>-symmetric amine (*R,R*)-**34** was used as its lithium base in the enantioselective deprotonation of 4-*tert*-butylcyclohexanone. Given the less sterically crowded nature of this base it was envisaged that the corresponding magnesium bisamide would maintain the high enantioselectivity shown by the chelating bases, but would allow higher conversions to be achieved alongside this. Thus, the *C*<sub>2</sub>-symmetric magnesium bisamide (*R,R*)-**70** was synthesised and used within deprotonations of the benchmark ketone (**Scheme 29**).<sup>42</sup> This new base did, indeed, show high selectivity with excellent levels of conversion. Furthermore, the selectivity displayed surpassed that of the corresponding results for the lithium amide.



**Scheme 29**

To confirm the efficacy of base  $(R,R)$ -70, a temperature study was carried out (**Scheme 30, Table 11**) with the expectation being that even higher conversions could be achieved at more elevated temperatures and with the selectivities also being assessed under these more accessible conditions.<sup>42a</sup> Pleasingly, the  $C_2$ -symmetric bisamide ( $(R,R)$ -70) maintains excellent levels of conversion and good enantioselectivities across a range of temperatures. Of particular note to this system is that the enantioselectivity achieved at 0 °C with the magnesium bisamide (**Entry 5, Table 11**) requires a temperature of -78 °C with the equivalent lithium amide.<sup>14</sup> This exploits the greater thermal stability of magnesium amides, compared with lithium amides, and offers energetic advantages in relation to how these processes are performed. It is also worth noting that a selectivity of 75:25 er can be achieved even at room temperature with magnesium bisamide  $(R,R)$ -70 (**Entry 6, Table 11**).



**Scheme 30**

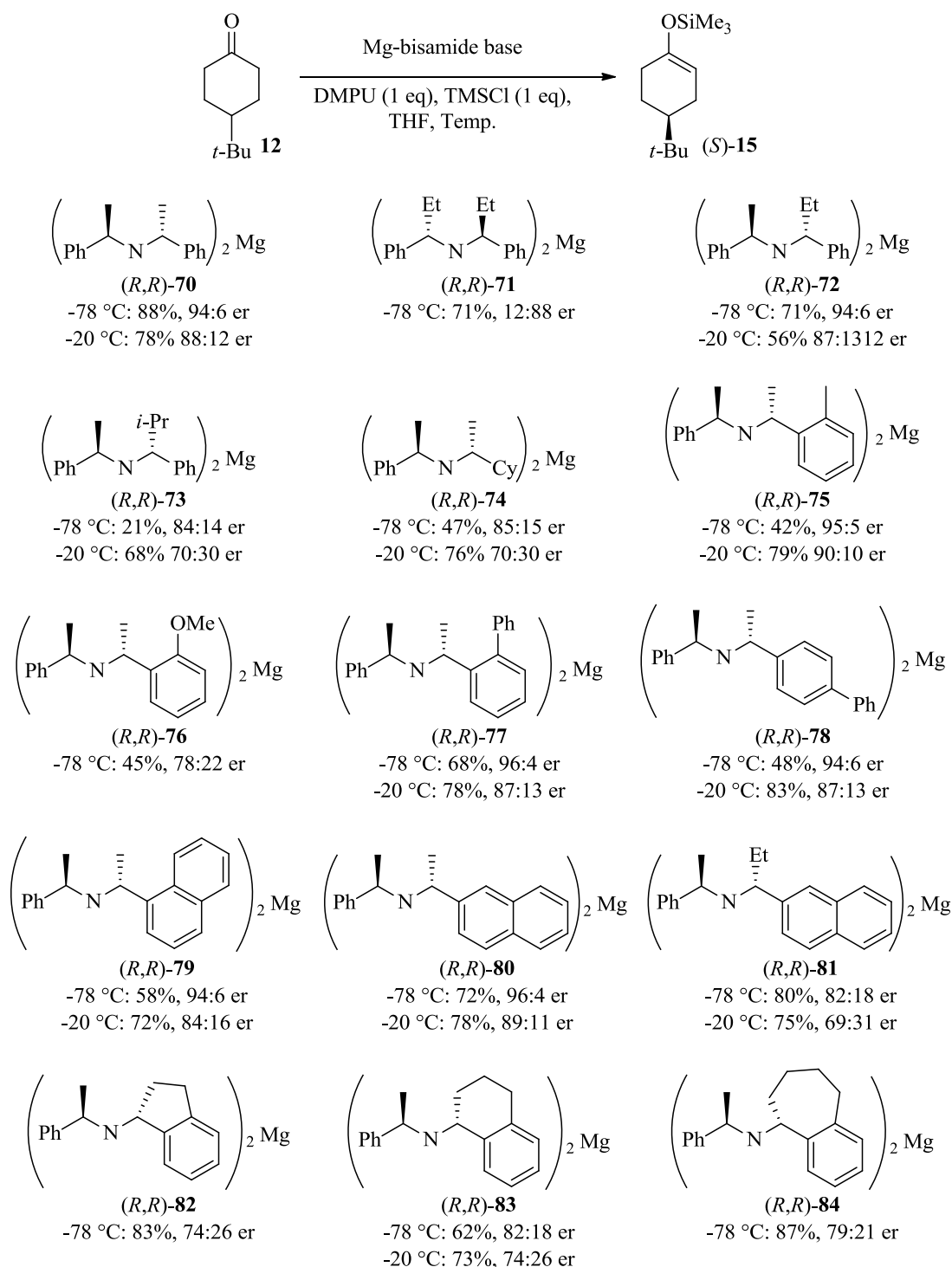
Entry	Temperature (°C)	Conversion (%)	Yield (%)	er (( <i>S</i> ):( <i>R</i> ))
1	-78	96	88	94:6
2	-60	93	69	92:8
3	-40	95	74	90:10
4	-20	97	78	88:12
5	0	93	66	86:14
6	25	89	66	75:25

**Table 11**

Given the success of the  $C_2$ -symmetric bisamide, some structural modifications were made to this base in order to broaden the overall scope of this family of chiral bases.

*Other  $C_2$ - and pseudo- $C_2$ -symmetric bisamides*

A variety of novel *pseudo- $C_2$* -symmetric magnesium bisamides were synthesised and applied to the benchmark deprotonation (**Scheme 31**).<sup>42b,42c</sup>



**Scheme 31**

Overall, most *pseudo*-C<sub>2</sub>-symmetric magnesium bisamides perform well in the benchmark deprotonation at -78 °C, as well as the energetically more viable temperature of -20 °C. There are some bases that do not fit this trend, however.

Specifically, *ortho*-methoxy-substituted base (*R,R*)-**76**, which only showed 78:22 er at -78 °C. The tethered bases (*R,R*)-**82** and (*R,R*)-**84** also showed lower levels of enantioselectivity at -78 °C so were not trialled at -20 °C. Despite these selectivity dips, some of the highest levels of enantioinduction for this benchmark deprotonation have been observed with these bases. In addition to the original  $C_2$ -symmetric magnesium bisamide (*R,R*)-**70**, the 2-naphthyl- and biphenyl-substituted *pseudo*- $C_2$ -symmetric magnesium bisamides, (*R,R*)-**80** and (*R,R*)-**78**, respectively, showed outstanding levels of enantioselectivity. Indeed, these selectivities are higher than the analogous asymmetric deprotonation with  $C_2$ -symmetric lithium amides. As an aid to elucidate the reason for this high selectivity, computational studies now have confirmed that the reaction pathway of these magnesium bisamides is theoretically lower in energy than the same reaction with the lithium amide (*R,R*)-**3**.<sup>42b</sup>

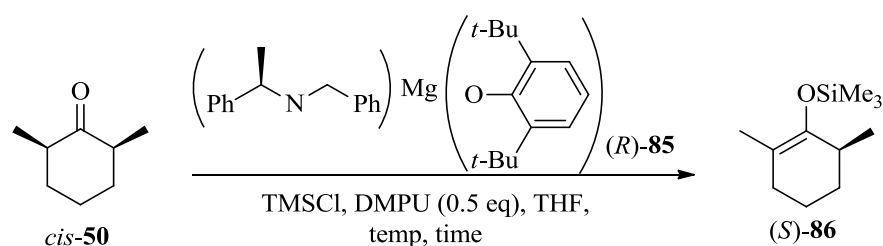
### 1.2.3 Heteroleptic magnesium amides

#### *Aryloxymagnesium amides*

As mentioned previously, the divalent nature of magnesium allows for the possibility of forming a heteroleptic magnesium complex possessing a reactive anion and a spectator anion, therefore only requiring half the amount of chiral amine. To this end, an aryloxymagnesium bisamide (*R*)-**85** was developed within our laboratory. In the benchmark deprotonation of 4-*tert*-butylcyclohexanone **12**, this base did not induce any enantioselectivity. With 2,6-dimethylcyclohexanone **50**, however, some interesting results were observed. (Scheme 32, Table 12).<sup>43</sup> A temperature study with this base system revealed that the highest selectivities were achieved at more elevated temperatures. This is an unusual observation for such deprotonations as low temperatures are normally required to obtain high enantioselectivity, *cf.* the lithium and magnesium systems discussed to this stage. In addition, it should be noted that the opposite enantiomer of silyl enol ether **86** was formed using the aryloxymagnesium amide (*R*)-**85**, compared to the equivalent magnesium bisamide ((*R*)-**66**) (see Section 1.2.5), which possesses the chiral amide unit of identical stereogenicity. Thus, by using the same chiral amine but a different magnesium complex thereof, access to both enantiomers of the silyl enol ether is possible. This



implies that the chiral information transferred from the magnesium base is not solely controlled by the chirality of the amide ligand. In contrast, it is the overall chiral environment within these complexes that impart their chirality into the product.



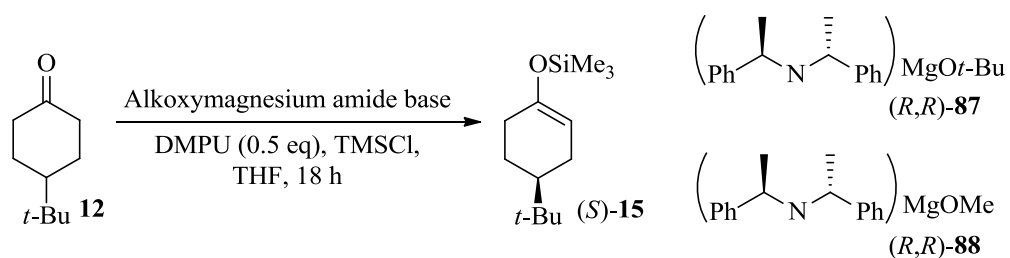
Entry	Temp. (°C)	Time (h)	Conversion (%)	er. (S:R)
1	-78	68	78	46:54
2	-40	68	54	76:24
3	r.t.	19	62	78:22
4	40	1	33	83:17
5	50	1	46	76:24
6	66	1	11	67:33

**Table 12**

### *Alkoxy magnesium amides*

Given the success and interesting results of the aryloxymagnesium amide ((*R*)-**85**) a series of structurally simpler alkoxy magnesium amides was studied. For this novel system, the  $C_2$ -symmetric amine (**34**) was used as the chiral ligand alongside either a methoxide anion or *tert*-butoxide anion as the spectator ligand. The efficacy of these complexes was studied against the benchmark deprotonation (**Scheme 33**, **Table 13**).<sup>42d</sup> Although the alkoxy magnesium amide (*R,R*)-**87** exhibited very high enantioselectivity, only moderate conversion was achieved at -78 °C (**Entry 1**, **Table 13**). Conversely, (*R,R*)-**88** showed much better conversion at this temperature, as well as at room temperature, but only a moderate selectivity in comparison (**Entries**

**2** and **3**, **Table 13**). Having stated this, the enantioselectivities of both alkoxy magnesium amides were generally higher than that of the aryloxy magnesium amide (*R*)-**85**.



**Scheme 33**

Entry	Base	Temp. (°C)	Conversion (%)	Yield (%)	er. ( <i>S</i> : <i>R</i> )
1	( <i>R,R</i> )- <b>87</b>	-78	56	53	95:5
2	( <i>R,R</i> )- <b>88</b>	-78	87	83	75:25
3	( <i>R,R</i> )- <b>88</b>	r.t.	90	87	78:22

**Table 13**

### Aminonaphthols

Subsequent to the studies with alkoxy magnesium amides, chiral aminonaphthols were reacted with di-*n*-butylmagnesium to form a 6-membered complex (**Figure 12**).<sup>44</sup> It was envisaged that such complexes could be highly enantioselective in asymmetric deprotonations.

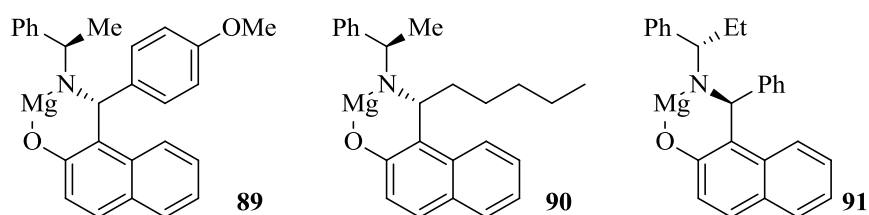
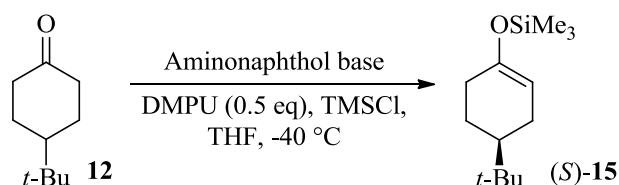


**Figure 12**

When studied in the benchmark deprotonation, the aminonaphthol complexes **89**, **90** and **91** showed reasonably high levels of enantioselectivity and good levels of conversion at -40 °C (**Scheme 34**, **Table 14**).<sup>44</sup> At this stage in the development of chiral magnesium base-mediated systems for the deprotonation of conformationally locked prochiral ketones, it was clear that the magnesium bisamides are still consistently the most efficient.



**Scheme 34**

Entry	Base	Conversion (%)	Yield (%)	er. ( <i>S</i> : <i>R</i> )
1	<b>89</b>	84	69	85:15
2	<b>90</b>	74	64	86:16
3	<b>91</b>	91	83	15:85

**Table 14**

#### *Hauser bases*

Hauser bases are a form of magnesium bases containing an amide and a halide ligand. They exist in an equilibrium with their magnesium bisamide and magnesium halide, which is dependent on temperature, solvent, concentration, and the nature of the halide (**Figure 13**).

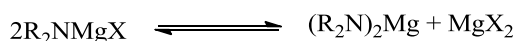
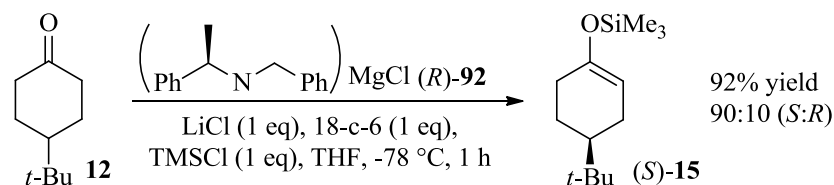


**Figure 13**

Employing a chiral amide component in the Hauser base initially showed a lack of any enantioselectivity in the asymmetric deprotonation of prochiral ketones.<sup>39b</sup> Using

alternative additives, specifically LiCl and 18-crown-6, did, however, result in high selectivities and yields for the benchmark deprotonation (**Scheme 35**).<sup>42d</sup>

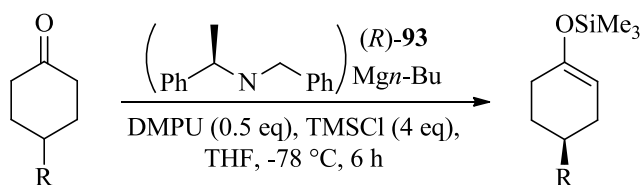


**Scheme 35**

It is believed that these additives work to keep the equilibrium in favour of the magnesium bisamide species. Furthermore, the LiCl could form an aggregate with the magnesium bisamide, as occurs with the analogous lithium amide species.<sup>20</sup> Additionally, crown ethers are known to coordinate to dialkyl magnesium species. This too may favour a shift in the equilibrium towards the magnesium bisamide or an alternative complex is both highly active and selective in the asymmetric deprotonation.<sup>45</sup>

#### *Alkylmagnesium amides*

To further extend the scope of heteroleptic magnesium complexes, a series of alkylmagnesium amides was synthesised and applied to the asymmetric deprotonation of a range of conformationally-locked ketones (**Scheme 36, Table 15**).<sup>43</sup> The *n*-butylmagnesium amide (*R*)-**93** showed high levels of reactivity and stereoselection in this asymmetric transformation, illustrating the possibility of using only half the quantity of chiral amine, whilst retaining enantioselectivity (*cf.* 86:14 – 91:10 with the equivalent magnesium bisamide species (*R*)-**66**, for R = *t*-Bu).



**Scheme 36**

Entry	R	Conversion (%)	er (S:R)
1	<i>t</i> -Bu	80	86:14
2	Ph	83	86:14
3	Me	84	83:17
4	<i>i</i> -Pr	84	86:14
5	<i>n</i> -Pr	85	87:13

**Table 15**

Studies to understand the reactivity of the alkylmagnesium amide ((*R*)-**93**) were undertaken, as well as optimisation of this new system, in order to effect further enhancements to the enantioselectivity observed.

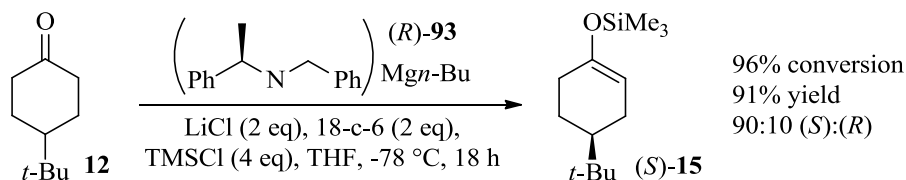
### NMR studies

Formation of the alkylmagnesium amide (*R*)-**93** from (*R*)-*N*-benzyl- $\alpha$ -methylbenzylamine ((*R*)-**67**) and dibutylmagnesium, and its reaction with 4-*tert*-butylcyclohexanone, was monitored using <sup>1</sup>H NMR spectroscopy.<sup>43,44a</sup> Analysis showed that the base had been formed after 15 minutes and after a further 35 minutes of reaction with the cyclic ketone the deprotonation had occurred. This was elucidated from the initial disappearance of the amine NH resonance to form the alkylmagnesium amide, and its subsequent reappearance upon deprotonation of the substrate. It was thus concluded that deprotonation of the ketone occurs through the amide ligand of the magnesium base, with the butyl anion acting as the spectator ligand. This study also confirmed that because the butyl group remains bound to the metal centre, no alkylation or reduction products are observed within this novel system.

### Improvements to the additive conditions

After a thorough study of alternative additives, including a variety of lithium salts and coordinating co-solvents, it was found that two equivalents of both LiCl and 18-

crown-6 yielded the highest enantioselectivities without compromising the reactivity of the system.<sup>42d</sup> Application of (*R*)-**93** under these conditions with the benchmark substrate revealed high stereinduction and conversion (**Scheme 37**),<sup>42d</sup> notably using only half the amount of chiral amine, compared to the magnesium bisamide (*R*)-**66**.



**Scheme 37**

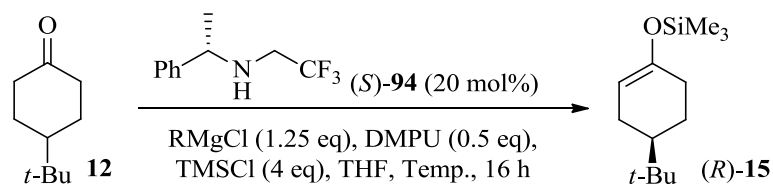
### 1.2.4 Developing a recycling protocol

In addition to the above stoichiometric reaction, successful efforts to use a reduced amount of chiral amine have been achieved through the formation of heteroleptic magnesium amide species. Polymer-supported magnesium bisamide and alkylmagnesium amides have also been developed.<sup>44b,46</sup> These bases showed high levels of conversion and enantioselectivity but, perhaps more importantly, the polymer-supported bases could be re-used without significant loss of selectivity. To try and establish an even more economical system in terms of the amount of chiral amine required, studies towards the development of a catalytic system have been carried out. Two strategies have been employed to this end and their outcomes are summarised below.

#### *Recycling reactions employing an amide transfer protocol*

Hauser bases have shown some of the highest levels of both conversion and enantioselectivity in stoichiometric asymmetric deprotonations. Thus, it was proposed that such species may be used in an amide transfer protocol as a method to reduce the amount of chiral amine required to affect an asymmetric deprotonation. More specifically, a less reactive, non-chiral Hauser base could be used as a stock reagent with a sub-stoichiometric quantity of chiral amine. It was hoped that the

stock reagent would not react directly with the prochiral ketone, but would instead form a chiral Hauser base which would carry out this deprotonation. A number of studies were performed using three different Hauser bases as the stock reagent, the final results of which are outlined below (**Scheme 38, Table 16**).<sup>42b,42d</sup> Initially, magnesium chloride diisopropylamide was used as the stock reagent, providing a moderate 47% yield of silyl enol ether (**Entry 1, Table 16**).<sup>42d</sup> Attempts to improve upon this yield by using bulkier Hauser bases (TMP and HMDS amide components) were unsuccessful (**Entries 2 to 4, Table 16**).<sup>42b</sup> It was hoped that higher conversions would be achieved at elevated temperatures and that the stock reagent would be too sterically-encumbered to deprotonate the ketone itself. Unfortunately this was not the case (**Entry 5, Table 16**) and an alternative recycling protocol was sought.



Entry	Stock reagent	Temperature (°C)	Yield (%)	er ( <i>R</i> : <i>S</i> )
1	<i>i</i> -Pr <sub>2</sub> NMgCl	-78	47	17:83 <sup>a</sup>
2	TMPMgCl	-78	0	-
3	TMPMgCl	-60	20	50:50
4	HMDSMgCl	-78	0	-
5	HMDSMgCl	-60	18	50:50

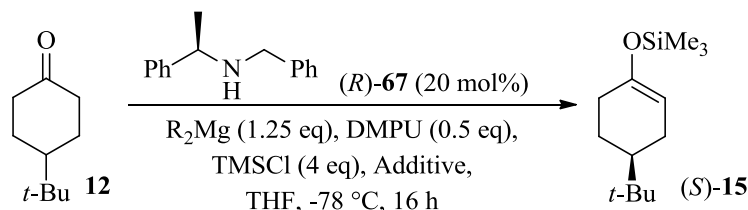
<sup>a</sup>Using (*R*)-**94**

**Table 16**

#### *Recycling reactions employing di-tert-butylmagnesium*

Originally, it was proposed that magnesium (*R*)-benzyl(1-phenylethyl)amide ((*R*)-**66**) derived from the structurally simple chiral amine (*R*)-**66a** could be formed *in situ* from this amine and a dialkyl magnesium stock reagent. The stock reagent and

different additives have been studied, with the best results highlighted in **Scheme 39** and **Table 17**.<sup>42b,42d,44a</sup> A promising result was initially obtained with di-*n/s*-butylmagnesium, yielding 30% of the silyl enol ether in a moderate 79:21 er (**Entry 1, Table 17**).<sup>44a</sup> Moving to di-*tert*-butylmagnesium under the same additive conditions did not offer any improvements in terms of conversion or enantioselectivity (**Entry 2, Table 17**).<sup>42b,42d</sup> When the additive was changed to LiCl, however, a more acceptable er of 83:17 was obtained, albeit in a 33% yield (**Entry 3, Table 17**).<sup>42b</sup>



**Scheme 39**

Entry	Stock reagent	Additive (Eq.)	Yield (%)	er (S:R)
1	<i>n/s</i> -Bu <sub>2</sub> Mg	None	30	79:21
2	<i>t</i> -Bu <sub>2</sub> Mg	1,4-Dioxane (2.5 eq)	15	79:21
3	<i>t</i> -Bu <sub>2</sub> Mg	LiCl (2 eq)	33	83:17

**Table 17**

In an attempt to enhance the yield of this catalytic deprotonation, the *C*<sub>2</sub>-symmetric amine (*R*)-bis(*R*)-1-phenylethylamine ((*R,R*)-**34**) was trialled under the same reaction conditions. Unfortunately no conversion to the silyl enol ether was achieved, thus, a more acidic amide was turned to in order to facilitate formation of the desired alkylmagnesium amide during the reaction. To this end, (*S*)-**94** was employed under a range of conditions at 20 mol% (**Scheme 40**).<sup>42b</sup> At a low temperature (-78 °C, **Entry 1, a Using** (*R*)-**34**.

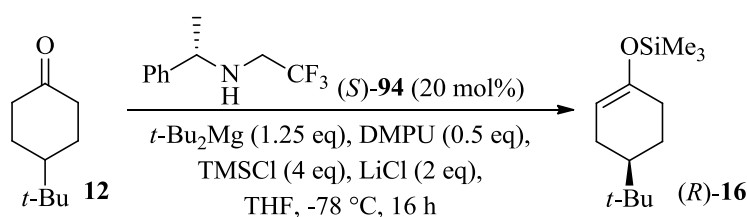
Table 18), good selectivity was achieved but a poor yield of silyl enol ether was obtained. On warming the reaction mixture, in the hope that more of the desired



chiral base species would be readily formed, a higher conversion was obtained (66%) but a drop in enantioselectivity came with this (**Entry 2, a Using (R)-34**).

Table 18). Unfortunately, this implied that the stock reagent itself was potentially carrying out some of the deprotonation. Keeping the reaction temperature low but leaving the reaction to run for a longer time did not yield more of the product (**Entry 3, a Using (R)-34**).

Table 18), leading to the conclusion that the alkylmagnesium amide was unable to form at -78 °C. Indeed, <sup>1</sup>H NMR studies have revealed this to be true and it is regretful that an efficient recycling protocol has not yet been developed within our laboratory.



Entry	Temp. (°C)	Time (h)	Conversion (%)	Yield (%)	er (R:S)
1	-78	16	30	25	87:13
2	-50	16	66	58	66:34
3	-78	48	25	18	17:83 <sup>a</sup>

<sup>a</sup> Using (R)-34.

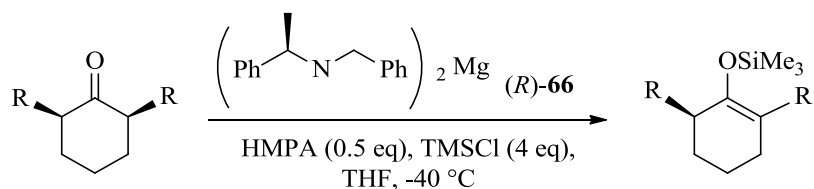
**Table 18**

### 1.2.5 Substrate scope with magnesium bisamides

#### 2,6-Disubstituted cyclohexanones

Having established an excellent asymmetric deprotonation protocol using magnesium bisamides, expansion of the substrate scope with these emerging base systems was initiated. Specifically, the desymmetrisation of a small selection of *cis*-

2,6-disubstituted cyclohexanones was explored (**Scheme 41, Table 19**).<sup>47</sup> Extremely high levels of enantioselectivity were achieved across this range of substrates with the simple amide (*R*)-**66**. In addition, these deprotonations were carried out at the elevated temperature of -40 °C, illustrating the greater thermal stability of the magnesium bisamide (*R*)-**66** compared with lithium amide bases which require lower reaction temperatures.

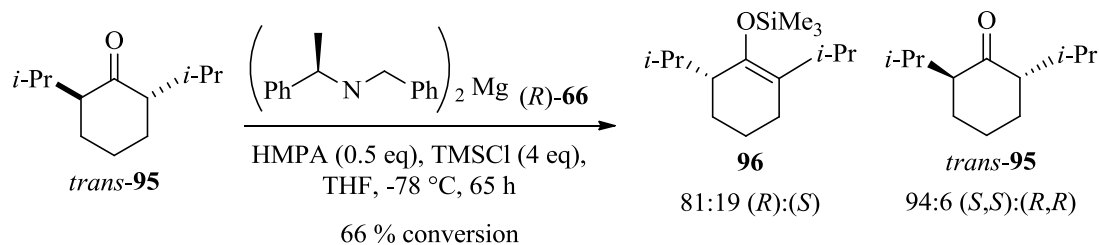


**Scheme 41**

Entry	R	Time (h)	Conversion (%)	Yield (%)	er
1	Me	6	99	92	93:7 ( <i>R</i> ):( <i>S</i> )
2	<i>i</i> -Pr	6	99	90	98.8:1.2 ( <i>S</i> ):( <i>R</i> )
3	Ph	8	-	86	82:18 ( <i>S</i> ):( <i>R</i> )

**Table 19**

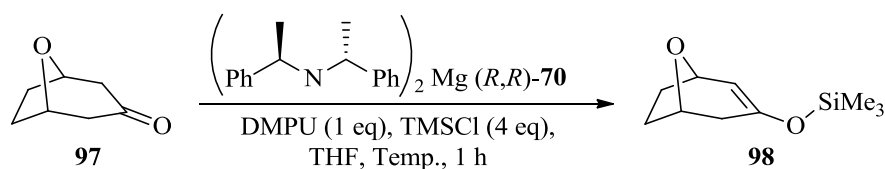
When comparing the asymmetric deprotonation of 2,6-*trans*-di-*iso*-propylcyclohexanone (*trans*-**95**, **Scheme 42**) with its *cis*-isomer, it was revealed that a kinetic resolution process was also taking place.<sup>47</sup> In the reaction of the racemic mixture of 2,6-*trans*-di-*iso*-propylcyclohexanone (**95**), the silyl enol ether (**96**) was obtained in 81:19 er, whilst also returning the starting ketone (**95**) in an enantiomerically enriched form of 94:6 er.



**Scheme 42**

### Bridged-bicyclic ketone substrates

Additional substrates that have undergone asymmetric deprotonations more recently are bridged-bicyclic ketones. For these substrates, the now favoured  $C_2$ -symmetric magnesium bisamide ( $R,R$ )-**70** was used for the desymmetrisation with some of the highest enantioselectivities observed to date. More specifically, the oxabicyclic substrate **97** was subjected to the asymmetric deprotonation over a range of temperatures (**Scheme 43**, **Table 20**).<sup>42b</sup> After a one hour reaction time, excellent levels of both conversion and selectivity were observed. In particular, at 0 °C an enantioselectivity of 83:17 was achieved (**Entry 5**, **Table 20**). It should also be highlighted that these levels of enantioselectivity surpass those obtained with the analogous lithium amide (( $R,R$ )-**3**).<sup>19a</sup>



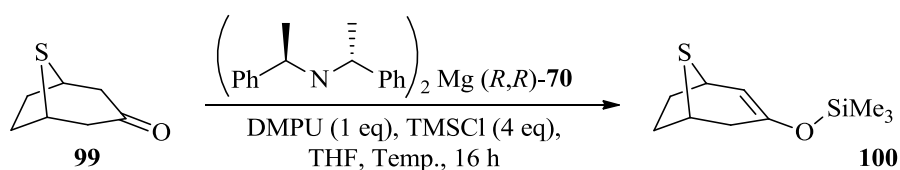
**Scheme 43**

Entry	Temp. (°C)	Conversion (%)	Yield (%)	er
1	-78	94	85	92:8
2	-60	78	60	87:13
3	-40	55	54	82:18
4	-20	80	63	84:16
5	0	97	84	83:17

**Table 20**

As well as the oxabicyclic substrate (**97**), a thiabicyclic substrate (**99**) was also studied with  $C_2$ -symmetric magnesium bisamide ( $R,R$ )-**70**.<sup>42b</sup> Although this substrate required a longer reaction time of 16 hours, the highest levels of enantioinduction observed to date were achieved for this substrate (**Scheme 44**, **Table 21**).<sup>42b</sup> At -78 °C (**Entry 1**, **Table 21**) almost complete enantioselectivity was observed for silyl

enol ether **100**, and an outstanding 94:6 er was obtained at room temperature (**Entry 2, Table 21**). This level of enantioselectivity at such an elevated temperature is unprecedented for this type of asymmetric deprotonation.

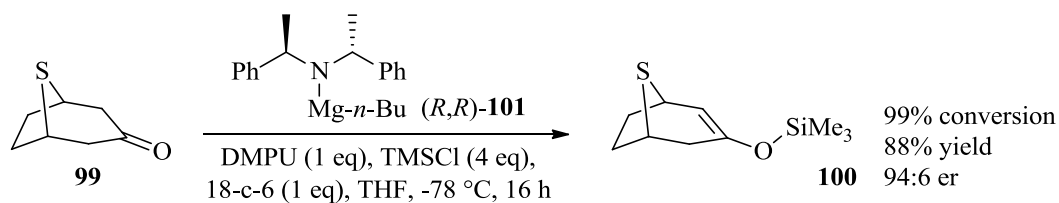


**Scheme 44**

Entry	Temp.	Conversion (%)	Yield (%)	er
1	-78 °C	97	70	99:1
2	rt	99	85	94:6

**Table 21**

Having obtained such impressive results for the desymmetrisation of **99** with a magnesium bisamide, an attempt to implement the same levels of conversion and selectivity using less of the chiral amine was carried out. Thus, using alkylmagnesium amide (*R,R*)-**101**, under previously optimised reaction conditions for this base, thiabicyclic ketone **99** was subjected to the deprotonation conditions (**Scheme 45**).<sup>42b</sup> Pleasingly, outstanding conversion was maintained and only a slight drop in enantioselectivity was observed, providing further evidence that such base species are a valuable alternative to magnesium bisamides and, indeed, lithium amides for such substrates.



**Scheme 45**

The desymmetrisation of bicyclic ketones has shown that magnesium bisamides are not limited to the desymmetrisation of 6-membered cyclic ketone substrates. Furthermore, such base species have proven to be robust across a range of temperatures. With more elaborate substrates being desymmetrised this has opened up avenues for further application of our base systems within the arena of asymmetric synthesis.

## 2 Proposed Work

As discussed, a range of magnesium amide species have been developed within our laboratory and applied successfully in a number of asymmetric deprotonation reactions. To date, the majority of this work has focused on the base species itself. With a broad range of base systems now in place, attention has turned to expanding the application of these species in a broader sense. Initial efforts have shown that the application of the magnesium bases to the asymmetric deprotonation of conformationally-locked ketones occurs with high degrees of success. After trialling some of the early base systems with a range of 4-substituted and 2,6-disubstituted cyclohexanone substrates, focus has turned to the more recently established  $C_2$ -symmetric magnesium bisamide (*R,R*)-**70** for the further application of this emerging chemistry. More specifically, the desymmetrisation of bridged-bicyclic ketones has been achieved with outstanding levels of enantioselectivity which far surpass those attained with analogous chiral lithium amide bases. Thus, to strive towards comprehensive use of our  $C_2$ -symmetric magnesium bisamide (*R,R*)-**70**, application in the asymmetric deprotonation of strained cyclic ketones was chosen as an avenue to expand upon this work.

Honda has shown that chiral lithium amides can effect the deprotonation of 3-substituted and 3,3-disubstituted cyclobutanone substrates with varying degrees of enantioselectivity, depending on the base structure and additives used (*vide supra*). Coelho has also demonstrated the use of  $C_2$ -symmetric lithium amide (*R,R*)-**3** in the asymmetric deprotonation of 3-(4'-chlorophenyl)cyclobutanone with high enantioselectivity but with the requirement for an extremely low reaction temperature of -100 °C. This less predictable outcome, depending on base structure and additives, as well as the low temperatures required to achieve appreciable levels of selectivity, highlights the limitations of lithium amide species. Having shown that magnesium bisamides offer higher thermal stability, whilst maintaining high enantioselectivity, and require predictable amounts of additives, it was proposed that effective outcomes could be achieved for the desymmetrisation of 3-substituted cyclobutanone substrates.

A range of 3-substituted and 3,3-disubstituted cyclobutanones were selected as substrates to be desymmetrised using  $C_2$ -symmetric magnesium bisamide ( $R,R$ )-**70**, starting with 3-(4'-chlorophenyl)cyclobutanone and 3-methyl-3-phenylcyclobutanone **39** as a direct comparison with the analogous lithium amides (**Figure 14**).

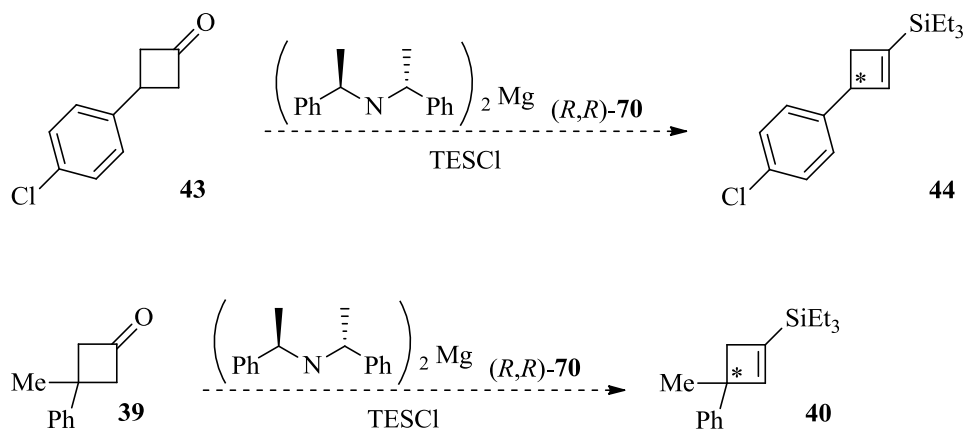


**Figure 14**

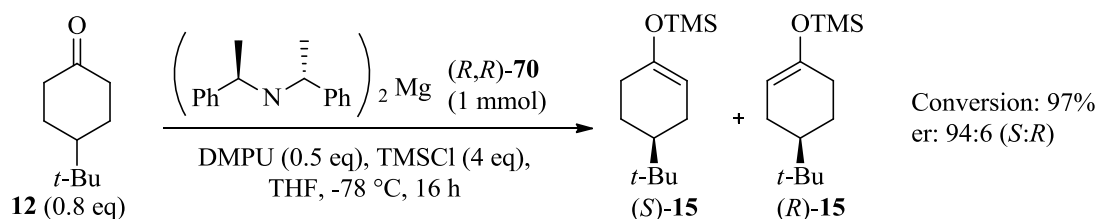
As these substrates are not commercially available, a scalable synthesis to access these prochiral ketones was also required.

### 3 Results and Discussion

Within the field of asymmetric deprotonations, chiral lithium amides have been used to desymmetrise a range of prochiral ketone substrates. With a view to expanding the scope of the emerging magnesium bisamide species, studies towards the asymmetric deprotonations of a selection of these substrates have begun. More specifically, the deprotonations of cyclobutanones have been investigated within this programme of research. As discussed in the previous section, the structurally simple  $C_2$ -symmetric magnesium bisamide ( $R,R$ )-**70** has revealed the highest levels of enantioselectivity for the deprotonation of 4-*tert*-butylcyclohexanone **12** to date.<sup>42</sup> This reaction has therefore become a benchmark with which to compare subsequent results. More importantly, this benchmark reaction was used to acquire the requisite practical skills for these air-sensitive transformations.

#### 3.1 Benchmark deprotonations with $C_2$ -symmetric magnesium bisamide ( $R,R$ )-**70**

Employing the  $C_2$ -symmetric magnesium bisamide ( $R,R$ )-**70** for the deprotonation of prochiral ketone **12**, the resultant silyl enol ether ( $S$ )-**15** is formed in excellent conversion with outstanding enantioselectivity (**Scheme 46**).<sup>42a</sup> An excess of the TMSCl electrophile is used, along with half an equivalent of the DMPU additive, under an internal quench protocol in order to achieve this result.

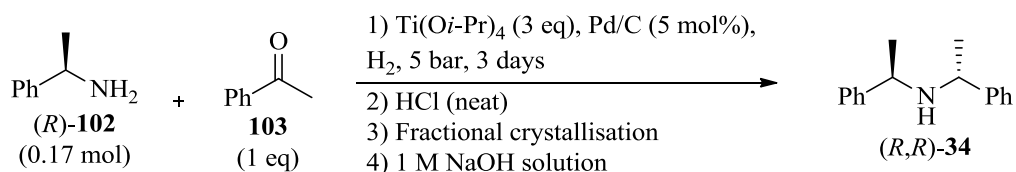


**Scheme 46**



### 3.1.1 C<sub>2</sub>-Symmetric amine synthesis

In order to perform the benchmark asymmetric deprotonation of 4-*tert*-butylcyclohexanone **12**, and indeed for use in subsequent asymmetric deprotonations, the parent chiral amine (*R,R*)-**34** first had to be synthesised. Using scalable, efficient conditions developed by Alexakis and co-workers,<sup>48</sup> (*R,R*)-**34** was prepared from (*R*)- $\alpha$ -methylbenzylamine **102** and acetophenone **103** (Scheme 47). This diastereoselective reductive amination was carried out using titanium(IV) *iso*-propoxide and palladium on charcoal and hydrogen gas under a pressure of 5 bar over three days. After work-up, the diastereomeric ratio was calculated from the <sup>1</sup>H NMR spectrum of the crude mixture of products (Table 22). This diastereomeric mixture was then salted with concentrated HCl and the salt recrystallised from IPA to afford the single (*R,R*)-diastereoisomer HCl salt of **34**. After neutralisation of the salt with 1 M sodium hydroxide solution and extraction with ethyl acetate, the single diastereoisomer was obtained as a colourless oil, which was distilled over calcium hydride under vacuum prior to use in asymmetric deprotonations.



Scheme 47

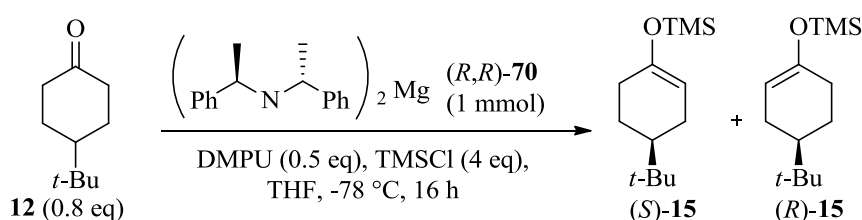
Entry	dr (( <i>R,R</i> ):( <i>R,S</i> )) <sup>a</sup>	Yield (%)
1	6:1	72
2	7:1	65
3	8:1	73
4	6:1	63

<sup>a</sup> Determined from the crude <sup>1</sup>H NMR spectrum.

Table 22

### 3.1.2 Asymmetric deprotonations of 4-*tert*-butylcyclohexanone **12**

With a batch of chiral amine (*R,R*)-**34** in hand, practice using Schlenk techniques was performed using the benchmark deprotonation reaction as a tool to this end. To ensure the exclusion of air and moisture from all asymmetric deprotonations the amine (*R,R*)-**34**, TMSCl, and DMPU were all distilled prior to use and stored under argon; the ketone **12** was recrystallised from dry hexane, dried under high vacuum, and stored under argon prior to use. The benchmark reaction was thus performed several times in order to provide confidence in the required techniques for this field of synthetic chemistry (**Scheme 48**, **Table 23**). Initial results were a little lower than acceptable in terms of selectivity, however, repeats of this reaction were performed until consistently high levels of yield and selectivity were achieved.



**Scheme 48**

Entry	Conversion (%)	Yield (%)	er ( <i>S</i> : <i>R</i> )
1	95	92	84:16
2	96	90	96:4
3	90	74	94:6
4	96	76	93:7

**Table 23**

Confident that the required skill for the manipulation of sensitive organometallic species had been gained, the application of magnesium bisamides with alternative substrates was focused on.

## 3.2 Synthesis of 3-substituted and 3,3-disubstituted cyclobutanones

To broaden the application of our magnesium bisamide bases, a wider range of conformationally-locked ketone substrates have been desymmetrised *via* an enantioselective deprotonation procedure. While previous examples have included the asymmetric deprotonation of bridged-bicyclic ketones,<sup>42b</sup> this work has focused on the deprotonation of smaller cyclic systems. More specifically, cyclobutanone substrates have been studied for direct comparison with some of the lithium amide deprotonations carried out by the groups of Honda<sup>28</sup> and Coelho.<sup>29</sup> In order to carry out this investigation, the prochiral cyclobutanone substrates were synthesised. It was proposed that, in order to access these 4-membered ring ketones with substitution in the 3-position, a [2+2] cycloaddition of dichloroketene and the requisite substituted styrenes could be performed to yield a range of 3-substituted and 3,3-disubstituted cyclobutanones (**Figure 15**).<sup>49</sup>

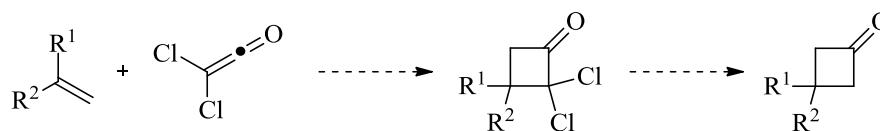
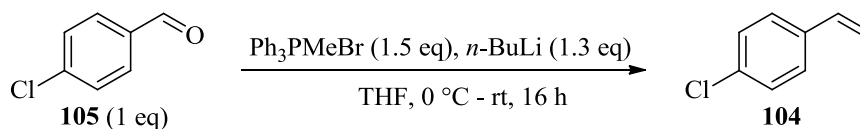


**Figure 15**

### 3.2.1 Synthesis of styrene derivatives

Due to the expense and instability of substituted styrene derivatives (these starting materials are usually sold containing a stabiliser which may not be compatible with reaction conditions subsequently employed) these starting materials were synthesised *via* a Wittig reaction from the parent carbonyl compound. All aldehyde and ketone starting materials were commercially available and literature conditions were applied to form the desired substituted styrene analogues for the [2+2] cycloaddition reactions.<sup>50</sup> 2-Chlorostyrene **104** was therefore synthesised from 2-chlorobenzaldehyde **105** and methyltriphenylphosphonium bromide, forming the ylide *in situ* with *n*-butyllithium (**Scheme 49, Table 24**). Initially on a small scale (**Entry 1, Table 3**) and as described in the literature, the reaction proceeded in a good 74% yield. Pleasingly, scale up of this reaction to access larger amounts of this

starting material provided even higher quantities of **104** in up to 90% yield. Forming the ylide *in situ* at 0 °C, with a slight excess of the Wittig salt, allowed full consumption of the organometallic base which prevented any dechlorination of the aromatic ring (*via* lithium-halogen exchange) on addition of the aldehyde **105**.



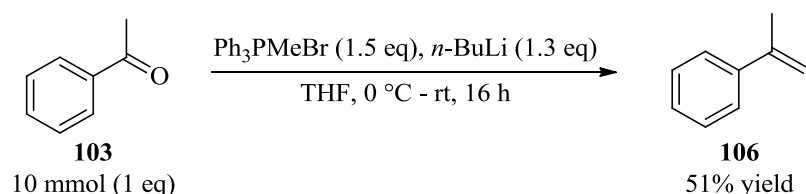
**Scheme 49**

Entry	Scale (mmol)	Yield (%)
1	20	74
2	100	90
3	100	86

**Table 24**

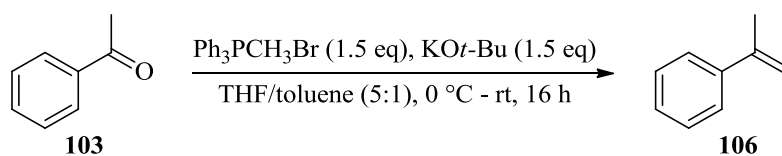
All entries in **Table 24** provided high yields on a large scale for the synthesis of 4-chlorostyrene **104**. This provided 11 – 12 gram batches of pure starting material for the synthesis of 3-(4'-chlorophenyl)cyclobutanone **43** (*vide supra*).

Additionally,  $\alpha$ -methylstyrene **106** was required for the synthesis of 3-methyl-3-phenylcyclobutanone **39**. This starting material was also synthesised from the parent ketone in a Wittig reaction. Since the conditions using methyltriphenylphosphonium bromide and *n*-butyllithium had worked so successfully for the synthesis of 4-chlorostyrene **104**, these were applied to the reaction of acetophenone **103** and methyltriphenylphosphonium bromide (**Scheme 50**). Unfortunately, these conditions were not effective for this substrate as only 51% yield of **106** was obtained after column chromatography.



**Scheme 50**

Having obtained this lower than anticipated yield, alternative conditions were investigated and found to be far more effective for this particular substrate. By using an excess of potassium *tert*-butoxide and running the reaction in a mixed solvent system of THF and toluene, the yield was improved to 88% on a trial scale (**Scheme 51** and **Table 25, Entry 1**). With this excellent enhancement in yield, the reaction was scaled up to 100 mmol. Pleasingly, these alternative conditions were reproducible for the synthesis of  $\alpha$ -methylstyrene **106** and provided ample amounts of this starting material for the synthesis of 3-methyl-3-phenylcyclobutanone **39** in excellent yields (**Table 25, Entries 2 and 3**).



**Scheme 51**

Entry	Scale (mmol)	Yield (%)
1	10	88
2	100	100
3	100	99

**Table 25**

With the required starting styrenes in hand, the synthesis of two key cyclobutanones commenced. 3-(4'-Chlorophenyl)cyclobutanone **43** and 3-methyl-3-phenylcyclobutanone **39** were chosen to enable a direct comparison of the selectivity

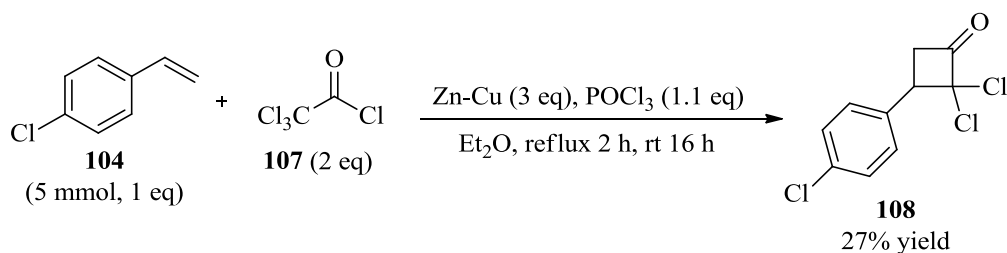
achieved in the resulting silyl enol ethers with our magnesium bisamide bases and the lithium amide bases used previously by the groups of Coelho and Honda.<sup>28,29</sup>

### 3.2.2 Optimisation of the [2+2] cycloaddition to access 3-substituted and 3,3-disubstituted cyclobutanones

Preparations of 3-substituted and 3,3-disubstituted cyclobutanones are well preceded within the literature.<sup>51</sup> It was noted that all experimental procedures described in these references follow the same basic set up; dichloroketene is generated *in situ* from trichloroacetyl chloride **107** and activated zinc. More specifically, the styrene derivative is stirred with a zinc-copper couple in diethyl ether. To generate the dichloroketene slowly, and to avoid any side-reactions, a solution of trichloroacetyl chloride **107** and phosphorus(V) oxychloride is added slowly to the styrene and zinc suspension. Having stated this, discrepancies among procedures arise between the excesses of zinc-copper couple, trichloroacetyl chloride, and phosphorus(V) oxychloride required, as well as the reaction temperature.<sup>51</sup> Furthermore, activation of the zinc (to form the zinc-copper couple) is not described in every procedure. Taking all this information into account, a procedure described by Malkov, Kočovský, and co-workers was selected,<sup>52</sup> as the specifically desired cyclobutanone substrates had been synthesised according to this detailed experimental procedure, which also outlined the preparation of the activated zinc-copper couple and its storage.

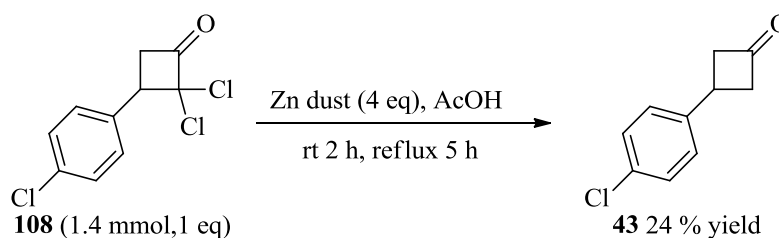
This literature procedure was applied to the synthesis of 2,2-dichloro-3-(4'-chloro)phenylcyclobutanone **108** (Scheme 52).<sup>52</sup> All liquids and oils were distilled prior to use and the zinc-copper couple was heated under vacuum and stored under argon before use. After work-up, analysis of the crude reaction mixture by <sup>1</sup>H NMR spectroscopy revealed that a significant amount of styrene **104** starting material was still present. At this stage, the crude mixture was a cream waxy solid, so trituration in petroleum ether was carried out in order to remove the excess styrene (column chromatography was not advised for such an intermediate). After trituration, a white solid was obtained, but only in 27% yield. It should be noted that traces of styrene

**104** still remained in this solid so full characterisation of **108** was not possible at this stage.



**Scheme 52**

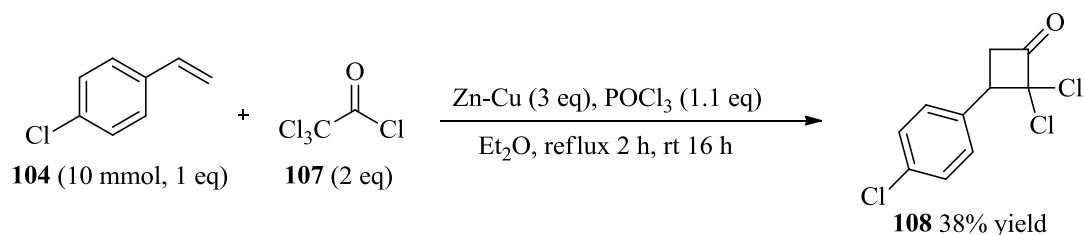
Although only a small amount of product had been obtained in the above reaction, **108** was taken on to the dechlorination step in an effort to form cyclobutanone **43** (**Scheme 53**). After column chromatography, the remaining styrene **104** (from **Scheme 52**) was effectively removed; however, only a low 24% yield of the desired cyclobutanone **43** was obtained.



**Scheme 53**

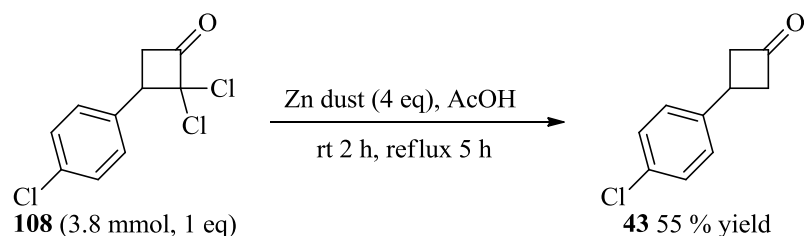
It was speculated that the low yields obtained at this early stage were due to the small scale of the above reactions. The literature describes these reactions being carried out on a 10 mmol scale, therefore with freshly prepared starting materials in hand, a scaled up reaction was performed in an attempt to access larger quantities of the cyclobutanone required for the asymmetric deprotonation studies. In the same manner as above, the intermediate cyclobutanone **108** was prepared (**Scheme 54**). As before, the waxy solid obtained after work-up was triturated to remove some of the excess starting material **104**. Although a slight improvement in the yield of **108** was

observed (38%), this was still disappointing when compared with the literature yield of 90% for this particular substrate.



**Scheme 54**

Subjecting the crude cyclobutanone **108** to the dechlorination step under the same conditions as previously used yielded 55% of the desired cyclobutanone **43** (after column chromatography, **Scheme 55**).

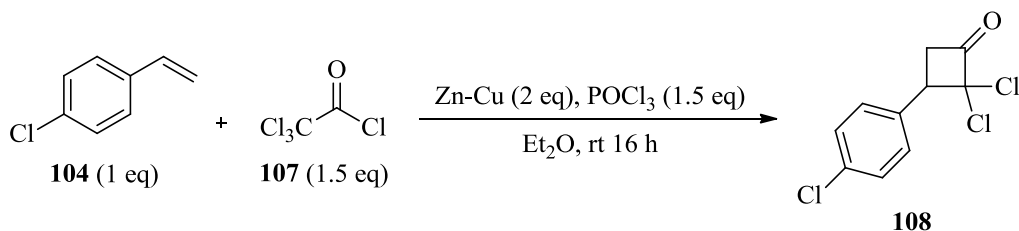


**Scheme 55**

After having struggled to obtain sufficient amounts of prochiral cyclobutanone **43** using reflux conditions for the [2+2] cycloaddition followed by refluxing conditions for the subsequent de-chlorination step, alternative reaction conditions were sought. In the total synthesis of (*R*)-(-)-baclofen **42**, Coelho described the preparation of 3-(4'-chlorophenyl)cyclobutanone **43** using milder reaction conditions, along with a more rigorous reaction work-up.<sup>29</sup> Pleasingly, applying these conditions within our laboratory, improved yields were observed in all cases (**Scheme 56, Table 26**). On a larger scale than previously trialled, **108** was formed in an excellent 83% yield (**Entry 1, Table 26**). This proved to be a more promising procedure for the formation of our desired cyclobutanones. When repeating this reaction on larger scales to access new batches of the required ketone for our asymmetric deprotonation studies, poorer yields were obtained (**Entries 2 and 3, Table 26**). Unfortunately,



styrene starting material **104** remained in these samples, yielding only 46% and 56% of cyclobutanone **108**, respectively. These yields were therefore calculated from the crude  $^1\text{H}$  NMR spectra. As trituration had resulted in a significant reduction in the mass balance of the crude cyclobutanone intermediate **108** in previous preparations of this substrate, it was decided that no purification would be carried out at this stage.



**Scheme 56**

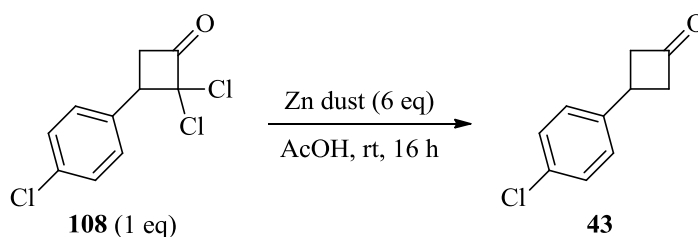
Entry	Scale (mmol)	Yield (%)
1	30	83
2	50	46 <sup>a</sup>
3	72	56 <sup>a</sup>

<sup>a</sup>  $^1\text{H}$  NMR yield.

**Table 26**

Crude **108** (containing remaining starting material **104**) was subsequently subjected to the de-chlorination step in the hope of obtaining larger amounts of the desired ketone **43** at the end of this short synthetic sequence. Continuing to use the procedure outlined by Coelho, milder reduction conditions were used for the following transformations. Stirring the crude 2,2-dichloro-3-(4'-chlorophenyl)cyclobutanone **108** batches with six equivalents of zinc dust in acetic acid at room temperature showed improved yields of the final ketone **43** after stirring overnight (**Scheme 57**, **Table 27**). Initially, for the cyclobutanone **108** containing no remaining starting material, a high 79% yield of the desired product **43** was obtained after column chromatography (**Entry 1**, **Table 27**). For the subsequent batches, which did contain significant amounts of unreacted styrene **104** from the previous step (in **Scheme 56**), moderated yields of **43** were obtained. Although these yields are lower than those

quoted in the literature, large quantities of the required ketone substrate were obtained in pure form for use in asymmetric deprotonations (**Entries 2 and 3, Table 27**).

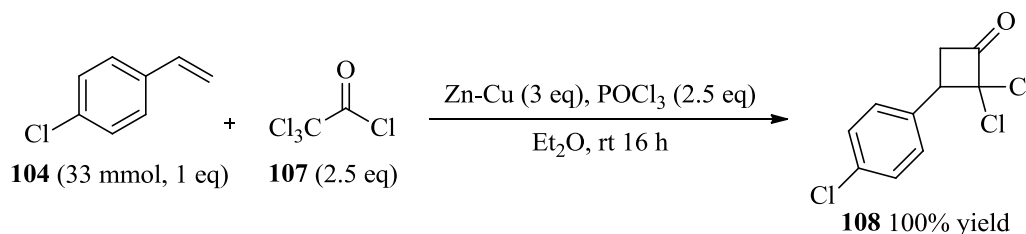


**Scheme 57**

Entry	Scale (mmol)	Yield (%)
1	24	79
2	72	39
3	56	46

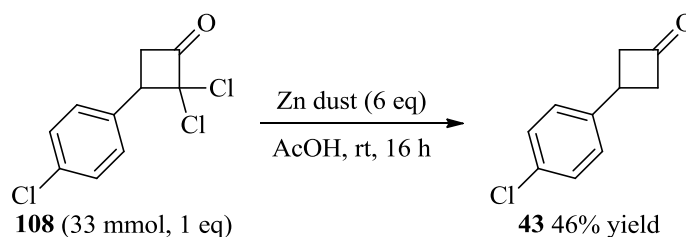
**Table 27**

Having improved upon previous yields for the [2+2] cycloaddition reaction and subsequent de-chlorination step to access cyclobutanone the desired **43**, it was envisaged that the reaction could be pushed further towards completion by using a greater excess of the trichloroacetyl chloride, phosphorus(V) oxychloride, and zinc-copper couple. To this end, the reaction was repeated with 2.5 equivalents of trichloroacetyl chloride and phosphorus(V) oxychloride, and 3 equivalents of zinc-copper couple (**Scheme 58**). Delightedly, a quantitative recovery was obtained, which contained only a trace amount of unreacted styrene.



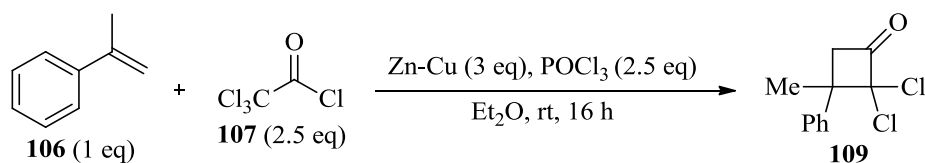
**Scheme 58**

Subjecting **108** to the previously employed chloride reduction conditions yielded 46% of the desired cyclobutanone **43** (**Scheme 59**). Although this was disappointing after achieving success for the first step of this synthesis, adequate amounts of material were obtained so it was decided that these conditions would not be altered further. It was noted, however, that this procedure must be capricious in relation to any styrene being present within the reaction mixture.



**Scheme 59**

An additional substrate under investigation in the asymmetric deprotonation studies was 3-methyl-3-phenylcyclobutanone **39**, as studied by Honda and co-workers during their studies of its desymmetrisation with chiral lithium amide bases. The synthesis of this substrate for our study was carried out by applying the conditions optimised above. The previously synthesised  $\alpha$ -methylstyrene **106** was subjected to the [2+2] cycloaddition conditions (**Scheme 60**, **Table 28**). Gratifyingly, a moderate 50% yield of intermediate cyclobutanone **109** was formed in the first attempt (**Entry 1**, **Table 28**). On scale up of this reaction, an improved yield of 82% was obtained (**Entry 2**, **Table 28**), providing acceptable quantities of material to access the prochiral cyclobutanone **39** required in our study. Once again, it should be noted that the yields obtained were calculated from the  $^1\text{H}$  NMR spectra as unreacted styrene **106** remained in the product.



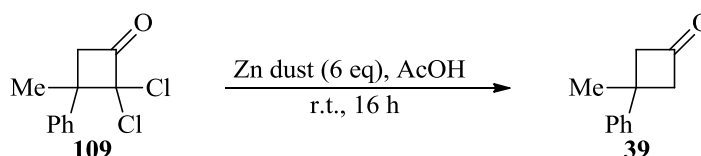
**Scheme 60**

Entry	Scale (mmol)	Yield (%) <sup>a</sup>
1	33	50
2	50	82

<sup>a</sup><sup>1</sup>H NMR yield.

**Table 28**

With the intermediate **109** now in hand, the de-chlorination step was performed to obtain the desired cyclobutanone **39**. Using the previously employed mild reaction conditions at room temperature, **109** was stirred in acetic acid with zinc dust for 16 hours to provide **39** (Scheme 61, Table 29). A good 79% yield was obtained on the smaller scale attempt at this synthesis (Entry 1, Table 29). On scale up of this reaction, however, a reduction in yield was observed (Entry 2, Table 29). Nonetheless, a satisfactory amount of cyclobutanone **39** had been synthesised, due to the larger reaction scale, and was distilled over calcium chloride under reduced pressure prior to use in asymmetric deprotonations.



**Scheme 61**

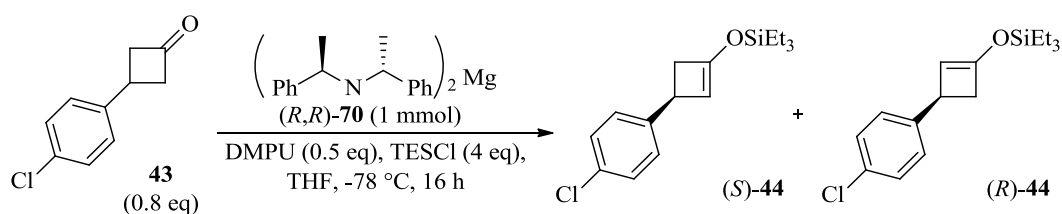
Entry	Scale (mmol)	Yield (%)
1	16	79
2	41	49

**Table 29**

### 3.3 Asymmetric deprotonations to afford enantioenriched silyl enol ethers

#### 3.3.1 Optimisation of reaction conditions

Having synthesised the requisite cyclobutanone substrates, efforts to apply the emerging chiral magnesium bisamides in the asymmetric deprotonation of these substrates began. Earlier studies of these bases have shown that the Lewis basic additive DMPU is required in order to form the reactive aggregate of the organometallic base.<sup>35,39-44,46-47</sup> Although it should be noted that just half an equivalent (with respect to the magnesium bisamide) is sufficient for this purpose. Additionally, the electrophile is used in excess and generally an internal quench protocol is successful in trapping the enantioenriched enolate in high yield and enantiopurity. TMSCl has been the electrophile of choice in the past for 4-substituted cyclohexanone and bridged-bicyclic substrates, however, Honda showed that the resulting silyl enol ethers of 4-membered ketones are unstable with this small silane.<sup>28a</sup> The bulkier TESCl electrophile has therefore been used for 3-substituted cyclobutanone substrates. To begin an assessment of the reactivity of our prepared substrates towards the highly selective  $C_2$ -symmetric magnesium bisamide (*R,R*)-**70**, our initial experiments focused on the optimisation of reaction conditions<sup>42a</sup> for the deprotonation of cyclobutanone **43**. TESCl was employed as the electrophile under IQ conditions (**Scheme 62**, **Table 30**). Unfortunately, under an IQ protocol none of the desired silyl enol ether **44** was formed at -78 °C (**Entry 1**, **Table 30**). As described previously, this (*R,R*)-**70** has proved to be highly thermally stable without significant loss in selectivity up to room temperature.<sup>42a,42b</sup> Having observed no reactivity for **43** at -78 °C, therefore, the reaction was repeated at room temperature in an effort to form the desired silyl enol ether **44** with some degree of enantioselectivity (**Entry 2**, **Table 30**). Disappointingly, under these reaction conditions, no product was observed and the starting cyclobutanone **43** was recovered. Finally, an EQ protocol was employed in an effort to observe some reactivity with this particular substrate (**Entry 3**, **Table 30**). Regrettably, this protocol was unfruitful for the formation of silyl enol ether **44**.

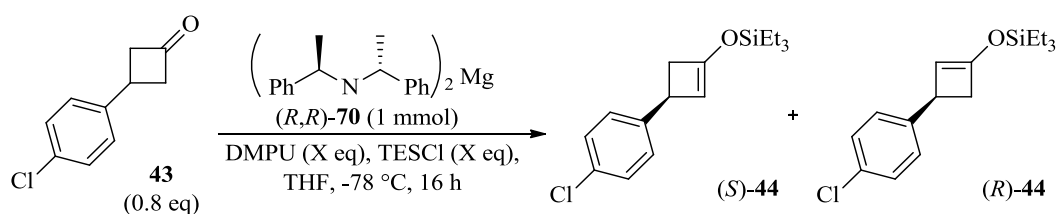


**Scheme 62**

Entry	Quench conditions	Temp. (°C)	Yield (%)
1	IQ	-78	0
2	IQ	rt	0
3	EQ	-78	0

**Table 30**

Although all variables of this general deprotonation system had remained unchanged, apart from the electrophile, it was suspected that this bulkier electrophile may be interacting with the various reaction components in a different manner from the previously used TMSCl. To overcome the lack of reactivity observed, the amount of TESCl and DMPU were varied in an attempt to enhance the reactivity of this system (**Scheme 63**, **Table 31**). Initially, fewer equivalents of TESCl were used, keeping half an equivalent of DMPU (**Entry 1**, **Table 31**), but only a trace amount of silyl enol ether **44** was obtained. The quantity of DMPU was then increased to one equivalent, whilst keeping the amount of TESCl high, to ensure the reactive aggregate of the base was forming (**Entry 2**, **Table 31**). Again, only a trace amount of product was obtained. With such a small amount of silyl enol ether **44**, optical purity could not be determined at this stage, as optical rotation values were the only method for such analysis and required more, and purer, material.

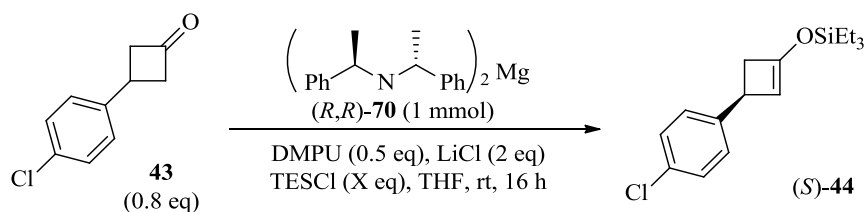


**Scheme 63**

Entry	Eq. DMPU	Eq. TESCl	Yield (%)
1	0.5	2	Trace
2	1	4	Trace

**Table 31**

Having not observed any reactivity with the magnesium bisamide  $(R,R)$ -**70** towards cyclobutanone **43** thus far, it was proposed that this base was not reactive enough for the strained cyclobutanone substrate. Previous studies have shown that LiCl can enhance the reactivity of magnesium base systems through the formation of an ate-complex.<sup>42d</sup> With this in mind, the addition of two equivalents of LiCl was made to this reaction protocol (**Scheme 64**, **Table 32**). The reaction was performed at room temperature, in an effort to achieve the maximum yield possible, and the amount of electrophile was varied to determine its compatibility with the new LiCl additive. Pleasingly, an increase in the yield of silyl enol ether **44** was obtained with 0.9, two, and four equivalents of TESCl (**Entries 1, 2, and 3**, **Table 32**), with four equivalents providing the highest yield. Analysis of the enantioselectivity of **44**, however, was somewhat disappointing. In all cases, only a slight excess of *(S)*-**44** was present over *(R)*-**44**, as established by optical rotation and comparison with the literature maximum  $[\alpha]_D$  value for this silyl enol ether (see Experimental section **5.1 General Considerations** for further details).



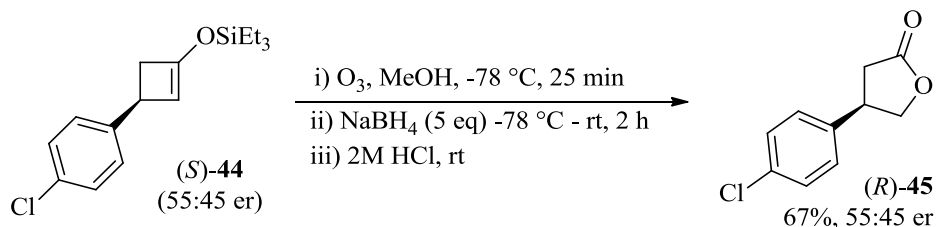
**Scheme 64**

Entry	Eq. TESCl	Yield (%)	er*
1	0.9	56	53.5:46.5
2	2	54	57:43
3	4	76	55:45

\* Calculated from the optical rotation,  $[\alpha]_{\text{D}}$  (lit) = -4.25 for 98% ee of (*S*)-**44**.<sup>29</sup>

**Table 32**

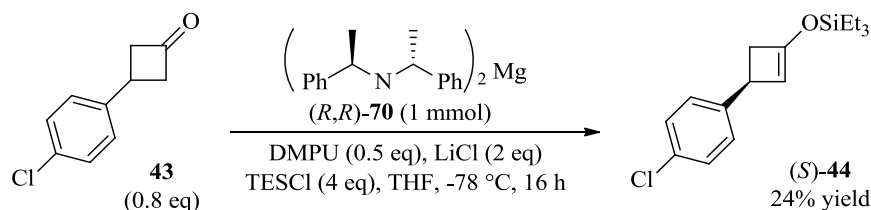
To verify whether the optical rotation values obtained in **Scheme 64** and **Table 32** were accurate measurements to determine the level of enantioselectivity for our preparation of (*S*)-**44**, derivatisation of this silyl enol ether was carried out. Such silyl enol ethers have been subjected to ozonolysis conditions, followed by a reductive work-up, to form  $\gamma$ -lactones.<sup>28</sup> Using literature conditions,<sup>28b</sup> ozonolysis was performed on a sample of silyl enol ether **44** calculated as having a 55:45 er (*S*:*R*) from **Scheme 64**, **Table 32**, **Entry 3**. After the reductive work-up and acid quench, the lactone (*R*)-**45** was formed in 67% yield. Analysis by chiral HPLC revealed 55:45 er, as possessed by the starting silyl enol ether, revealing the optical rotation measurements to be accurate (**Scheme 65**).



**Scheme 65**

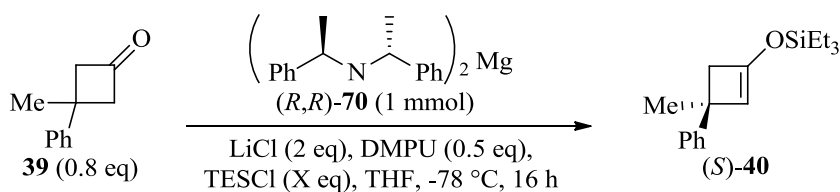


Having observed a marked improvement in the reaction yield of (*S*)-**44**, an attempt to enhance the enantioselectivity was made by performing this reaction at -78 °C (**Scheme 66**). Although the presence of LiCl did increase the efficiency of this reaction when compared with the same conditions in the absence of LiCl (**Scheme 62**), the silyl enol ether formed in this reaction was not pure by <sup>1</sup>H NMR analysis, and, as such, optical purity could not be measured.



**Scheme 66**

Despite the poor results obtained for the desymmetrisation of **43**, we were keen to ascertain whether magnesium bisamide (*R,R*)-**70** was reactive towards other cyclobutanone substrates. The best conditions obtained thus far were applied to the asymmetric deprotonation of 3-methyl-3-phenylcyclobutanone **39** (**Scheme 67**). Keeping the amount of each additive (LiCl and DMPU) consistent, the amount of electrophile was investigated (**Scheme 67**, **Table 33**). It was revealed that two equivalents of TESCl was sufficient for achieving a high 78% yield of (*S*)-**40** (**Entry 2**, **Table 33**). Unfortunately, very little enantioinduction was observed for this substrate in all cases, even at this -78 °C reaction temperature.



**Scheme 67**

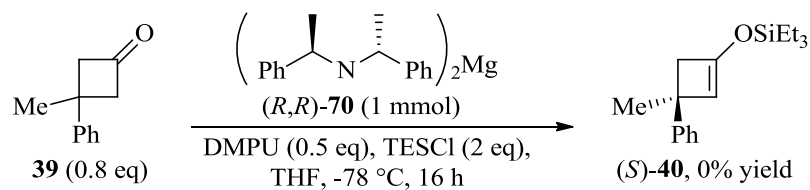
Entry	Eq. TESC1	Yield (%)	$[\alpha]_D^{20}$	er*
1	0.9	54	-5.7 °	55:45
2	2	78	-8.8 °	57:43
3	4	64	-9.1 °	58:42

\*  $[\alpha]_D$  (max) = -59.4 (calculated from  $[\alpha]_D$  (obs) = -46.3 for a sample of 78% ee).<sup>28a</sup>

**Table 33**

Although the level of enantioinduction observed was low at this stage, it should be noted that this result is comparable to the results obtained by Honda and co-workers when employing lithium amide (*S,S*)-**3** to furnish (*R*)-**40** and -78 °C.<sup>28a</sup> In order to attain appreciable levels of optical purity of (*R*)-**40**, more structurally complex chelating lithium amides were required at -100 °C.

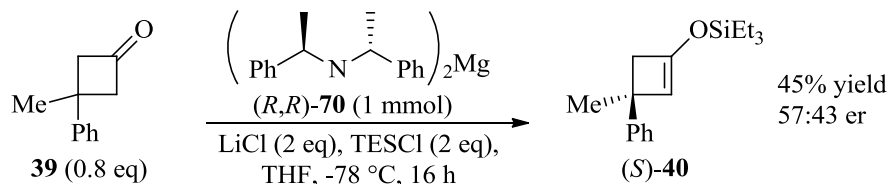
Pleased that the deprotonation of **39** was showing promising, albeit, low selectivity, efforts to enhance this enantioselectivity were made. A more thorough additive study for this substrate was therefore undertaken. Firstly, to determine if LiCl is, indeed, required to enhance the reactivity of this novel system, this additive was eliminated from the reaction (**Scheme 68**). After work-up and purification of this reaction, it was clear that the LiCl additive is imperative within these systems as none of the desired silyl enol ether **40** was obtained from this reaction and only the starting ketone **39** was recovered after column chromatography.



**Scheme 68**

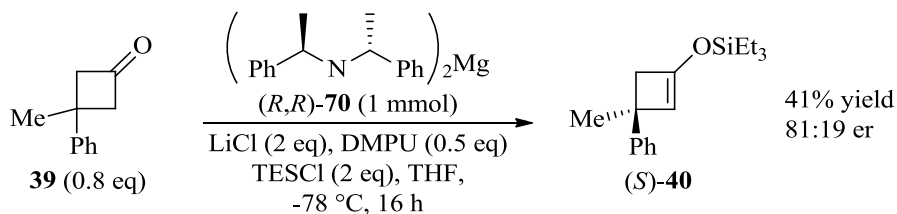
Having shown that LiCl is required to enhance the reactivity of the magnesium bisamide (*R,R*)-**70**, the requirement for DMPU was subsequently investigated. With two equivalents of LiCl, DMPU was excluded from the reaction mixture to establish if both of these additives were required for reactivity and enantioselectivity (**Scheme**

**69**). Although only a slight drop in er was observed (1% decrease compared with previous results, **Table 33**), a significant decrease in the yield was observed when no DMPU was added (45%, **Scheme 69**). Clearly, both DMPU and LiCl are required for this novel asymmetric deprotonation.



**Scheme 69**

At this stage within the research project some discrepancies and irreproducibility of the above described results were encountered. On repetition of the best conditions to date, employing two equivalents of both TESCl and LiCl (see **Scheme 67, Entry 2, Table 33**), a significant reduction in the yield was observed (**Scheme 70**). On the contrary, an elevated enantioselectivity of 81:19 (*S*):(*R*) was observed for this reaction, as determined by chiral HPLC analysis. This enantioselectivity, however, was also irreproducible when repetitions of this reaction were carried out.



**Scheme 70**

Given the less than desirable levels of stereochemical induction at this stage of the study, attention was turned to an alternative base system. As discussed in **Section 1.1.3**, the structurally more elaborate chelating lithium amide (*R*)-**35** showed superior levels of enantioselectivity for some cyclobutanone substrates, as shown by Honda and co-workers.<sup>28a</sup> Furthermore, and of significance to this study, previous results from our laboratory have shown that a range of chelating magnesium bisamides can effect the deprotonation of 4-substituted cyclohexanone substrates in higher levels

than those obtained with the more simple  $C_2$ -symmetric magnesium bisamide (*R,R*)-**70**.<sup>41</sup> A more rigid base complex appears to be required for the enhanced levels of enantioselectivity observed for the 3-substituted cyclobutanone substrates in the lithium amide system and it is feasible that this may also be the case for our magnesium bisamide-mediated deprotonation.

### 3.3.2 Comparison with a chelating magnesium bisamide

To address the possibility that a structurally more elaborate magnesium bisamide may enhance the yield and enantioselectivity for the asymmetric deprotonation of cyclobutanone substrates the chiral amine ligand (*R,R*)-**115** was synthesised. Although Honda and co-workers used the chelating lithium amide developed by Koga, we wished to investigate the activity of a similar amide ligand used to form magnesium bisamides previously within our research group.<sup>41</sup> This would allow for a more direct comparison of new substrate scope with emerging magnesium bisamides from our laboratory and would also circumvent the long-winded synthesis used by Koga to access the analogous lithium amides.<sup>53</sup> It should be noted that loss in enantiopurity is also observed during the amide coupling step of Koga's synthesis, which is less than desirable for such amines that are to be used as chiral ligands. A more general synthesis has, however, been developed by O'Brien and co-workers,<sup>54</sup> and used previously within our laboratory.<sup>41b</sup> This improved route facilitates access to a range of chiral, chelating amines *via* a 'one-pot' strategy and has been used with high degrees of success in the past so it was turned to once again to acquire the desired amine for this study (**Figure 16**). Starting from enantiopure (*R*)-styrene oxide **110**, ring opening using piperidine (**111**) affords the regioisomeric amino alcohols **112** and **113**, which can then be mesylated to form the same aziridinium ion **114**. This aziridinium ion is subsequently opened with the commercially available  $\alpha$ -methylbenzylamine (*R*)-**102** to access the desired chelating amine (*R,R*)-**115**.

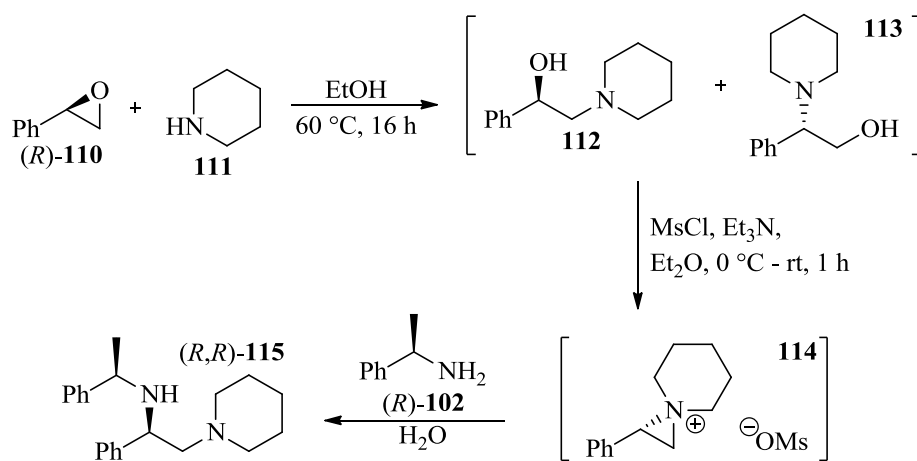
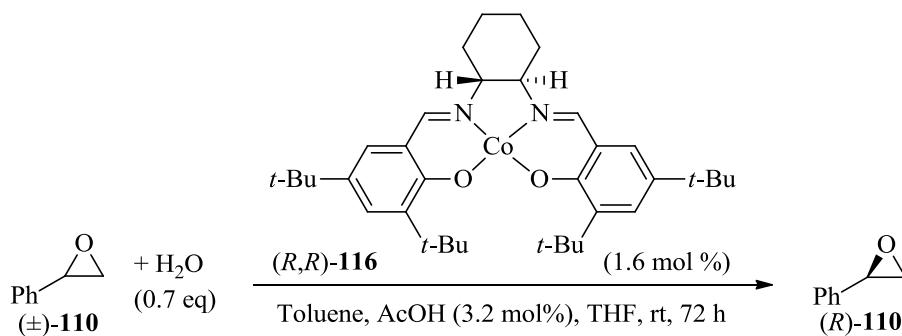


**Figure 16**

Although optically pure (*R*)-styrene oxide **110** is commercially available, the racemic form is a fraction of the price and can be efficiently accessed using a catalytic Hydrolytic Kinetic Resolution (HKR) developed by Jacobsen and co-workers using the cobalt-salen catalyst (*R,R*)-**116**.<sup>55</sup> Although the literature conditions for this HKR are general and reproducible, achieving high enantiopurity can be somewhat substrate-dependent. As shown previously within our laboratory, unacceptable levels of ee were observed for the initial attempts at this HKR with racemic styrene oxide **110**.<sup>41b</sup> A short study to optimise this reaction, however, has revealed reproducible results providing high yield and optical purity of the desired (*R*)-styrene oxide **110**. With this insight to hand, the synthesis of chelating chiral amine (*R,R*)-**115** could commence.

Under conditions developed previously within our laboratory, the HKR of racemic styrene oxide **110** was carried out (**Scheme 71, Table 34**). Initially attempted on a small scale (**Entry 1, Table 34**), the enantioenriched (*R*)-styrene oxide **110** was obtained with 99% ee, but only in moderate yield. Upon scale up of this reaction, however, acceptably high yields for this reaction were obtained with equally impressive levels of ee (**Entries 2 and 3, Table 34**).



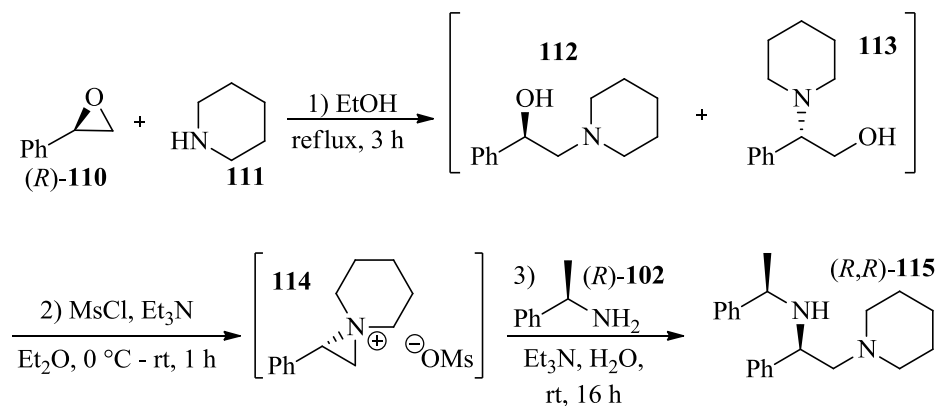
**Scheme 71**

Entry	Scale (mmol)	Yield (%)	ee (%)
1	20	18	99
2	207	44	>99
3	207	33	>99

**Table 34**

With batches of the required enantiomer in hand, the synthesis of our desired chelating amine (*R,R*)-**115** began (**Scheme 72, Table 35**). Opening the chiral epoxides (**110**) with piperidine (**111**) allowed access to the regioisomeric mixture of amino alcohols (**112** and **113**), after refluxing this mixture in ethanol for three hours. Removal of the solvent and drying the amino alcohols under high vacuum for one hour permitted this crude mixture to be subjected to the remaining synthesis. The amino alcohol mixture was subsequently dissolved in ether and triethylamine then cooled to 0 °C. Dropwise addition of mesyl chloride resulted in the formation of a thick precipitate which became difficult to stir. After stirring for 30 minutes formation of the aziridinium ion **114** was assumed and the primary chiral amine (*R*)-**102** was introduced to the reaction mixture along with a further portion of triethylamine and water; this biphasic mixture was stirred vigorously overnight. After work-up of the reaction, the crude product was initially purified using column chromatography (**Entry 1, Table 35**). Unfortunately, this proved to be an ineffective method of purification as the amine still contained impurities from the reaction mixture, preventing isolation of optically pure chiral product. All future crude

products were distilled using Kugelrohr apparatus to afford the pure chiral amine (*R,R*)-**115** (Entries 2 – 3, Table 35). The subsequent batches were synthesised in good yields, comparable to those obtained by O'Brien and co-workers,<sup>54</sup> and with high enantiomeric excess, providing sufficient quantities of the chiral amine to use as a ligand in our asymmetric deprotonation studies.



**Scheme 72**

Entry	Scale (mmol)	Yield (%)	ee (%)
1	3.4	20 <sup>a</sup>	N.D. <sup>b</sup>
2	49	65	99
3	71	79	99

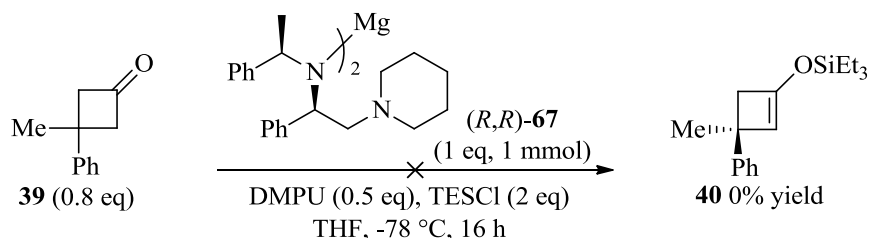
<sup>a</sup> Purified by column chromatography. <sup>b</sup> Unsuccessful purification.

**Table 35**

With the chelating chiral amine (*R,R*)-**115** now in hand, studies to determine whether a chelating magnesium bisamide would be more effective for the asymmetric deprotonation of prochiral cyclobutanone substrates commenced. Reviewing the conditions developed previously within our laboratory for the chelating magnesium bisamides, it should be noted that they differ from the conditions used in this study of cyclobutanone substrates to date. Firstly, the TESCl electrophile is bulkier (as required to stabilise the resulting highly strained silyl enol ethers), so it was anticipated that this could perhaps demonstrate differing reactivity within a chelating

magnesium bisamide system. The additives used for 3-substituted cyclobutanone **39** have also been altered in comparison with the previous studies of 4-substituted cyclohexanone substrates with the chelating magnesium bisamides. Due to these factors, a complex study was anticipated for 3-substituted cyclobutanone **39**, realising that differences between reaction conditions were already evident. With this in mind an attempt to outline the differences was made.

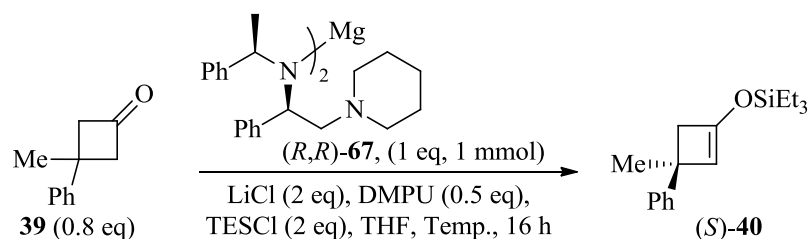
As a starting point, we applied the conditions developed previously within our laboratory for chelating magnesium bisamides, which have proved to be effective using, 0.5 equivalents of the DMPU additive and two equivalents of the electrophile.<sup>41</sup> Employing these conditions with cyclobutanone **39** we initially observed no reactivity (**Scheme 73**).



**Scheme 73**

Indeed, with the  $C_2$ -symmetric base (*R,R*)-**70**, we had also observed no reactivity under these reaction conditions either (*cf.* **Scheme 68**). As shown previously, the addition of LiCl seemed to be key to the reactivity of (*R,R*)-**70** with cyclobutanone **39**. At this point, the lack of reactivity with the chelating base (*R,R*)-**67** was believed to be due to the lack of LiCl in the reaction mixture which would, potentially, form a more reactive base complex. The reaction was therefore repeated with the addition of two equivalents of LiCl and a temperature study carried out. (**Scheme 74**, **Table 36**). Pleasingly, the addition of LiCl greatly improved the yield of this deprotonation. Good yields of silyl enol ether (*S*)-**40** were obtained, with greater yields at more elevated temperatures. In contrast, enantioselectivity was only moderate and this fell further at higher temperatures, despite the *er* at 0 °C being only 5% below that found at -78 °C (**Entry 4** compared with **Entry 1**, **Table 36**).



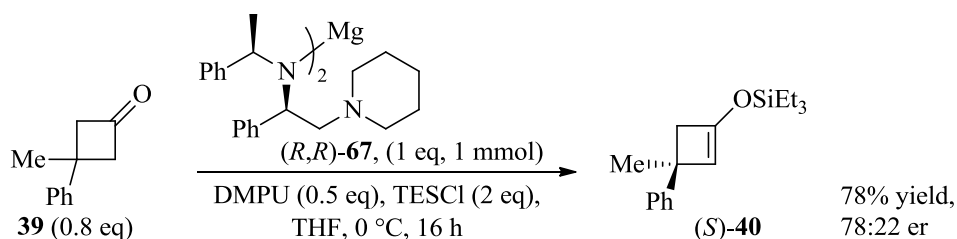


**Scheme 74**

Entry	Temp. (°C)	Yield (%)	e.r.
1	-78	58	60:40
2	-40	53	57:43
3	-20	70	55:45
4	0	75	55:45

**Table 36**

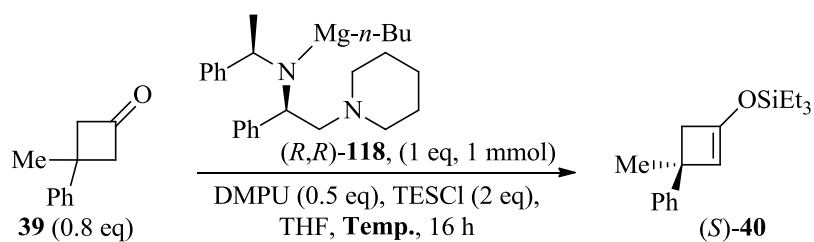
In addition to the above experiments, the reaction was also carried out in the absence of LiCl. In an effort to maintain as high a yield as possible without significant loss in enantioselectivity, the chelating magnesium bisamide  $(R,R)$ -**67** was employed for the deprotonation of **39**, using only DMPU as the additive, at 0 °C (**Scheme 75**). Pleasingly, as high yield of 78% was obtained alongside a much improved 78:22 er. Indeed, this result represents the highest enantioselectivity observed for this magnesium bisamide with cyclobutanone **39** to date.



**Scheme 75**

Although this result was one of the best results obtained at this stage in the research project, numerous repeats of this reaction did not provide as high a yield or

enantioselectivity, highlighting the capricious nature of this deprotonation process. An attempt to reach this level of enantioinduction alongside a high yield was made using an alternative base system. The chelating alkylmagnesium amide (*R,R*)-**118** has previously yielded silyl enol ethers with high levels of enantiopurity.<sup>41b</sup> With this in mind, the deprotonation of **39** was carried out at two different temperatures using conditions previously optimised for this base (**Scheme 76**, **Table 37**). Unfortunately, none of the silyl enol ether **40** was obtained at either -78 °C or 0 °C.

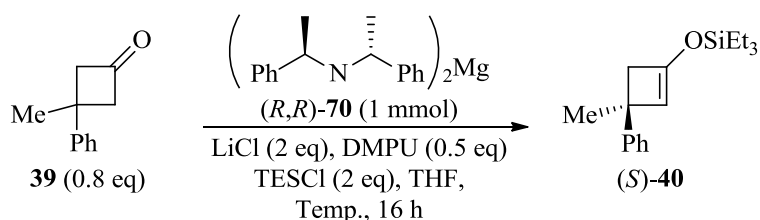


**Scheme 76**

Entry	Temp. (°C)	Yield (%)	e.r.
1	-78	0	-
2	0	0	-

**Table 37**

In a final effort to observe higher levels of enantioselectivity and yield for this substrate, a short temperature study of the  $C_2$ -symmetric magnesium bisamide (*R,R*)-**70** was attempted. Under the optimised conditions using LiCl and DMPU as additives, the deprotonation of **39** was carried out over a range of temperatures (**Scheme 77**, **Table 38**). In line with previous results, a general decrease in yield was observed as the reaction temperature was decreased (**Entries 1 to 4**, **Table 38**). Unfortunately, only moderate yields were obtained across the board. As expected, a slight increase in enantioselectivity was observed as the temperature decreased, from 56:44 at 0 °C (**Entry 1**, **Table 38**) to 67:33 at -78 °C (**Entry 4**, **Table 38**), however, the results obtained did not reach our desired levels of selectivity.



**Scheme 77**

Entry	Temp. (°C)	Yield (%)	e.r.
1	0	61	56:44
2	-20	67	57:43
3	-40	45	53:47
4 <sup>a</sup>	-78	43	67:33

<sup>a</sup> Amino-silane **119** by-product also observed.

**Table 38**

Despite these somewhat disappointing results, a curious observation was made when the deprotonation was carried out at -78 °C (**Entry 4, Table 38**). After column chromatography of this crude reaction mixture, an interesting by-product was obtained (**119, Figure 17**). This amino-silane was thought to have formed *via* attack of the magnesium bisamide (*R,R*)-**70** on the silane electrophile present in the reaction mixture under the internal quench conditions. Deprotonation of the *C*<sub>2</sub>-symmetric amino-silane to form an iminium species, followed by hydrolysis during reaction work-up could be an explanation of the formation of by-product **119**. Or, the free amine produced after deprotonation of the ketone substrate could nucleophilically attack the chlorotriethylsilane and break down, as described, to form the observed by-product **119**. Regardless of the mechanism of its production, the formation of this by-product presented potential reasons for the low yields of asymmetric deprotonation observed to date. The low yields of silyl enol ether could therefore be attributed to the consumption of the magnesium bisamide itself by the electrophile present in the reaction mixture from the start. This led us to believe that rather than the base not being active enough to perform the deprotonation of the 3,3-

disubstituted cyclobutanone it might be the electrophile that is hindering the overall reactivity of this system. Alternatively, if the electrophilic quench of the resultant magnesium enolate is slow, this could mean that free amine now present is mopping up the electrophile and the magnesium enolate is then quenched by a proton on work-up of the reaction to afford the starting ketone. Finally, if the electrophilic quench is slow, and the magnesium bisamide is being consumed by the electrophile, an alternative magnesium base species could be present in the reaction mixture. This could be a Hauser base which, for this cyclobutanone substrate, may not perform an asymmetric deprotonation with the required levels of selectivity.

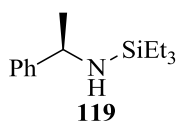
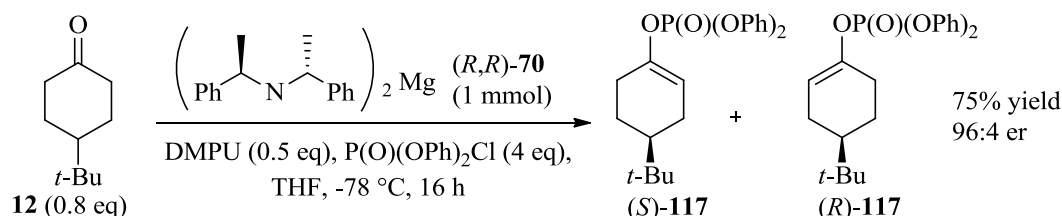


**Figure 17**

Having reached the conclusion that the electrophile under study may be impeding the reactivity and enantioselectivity of the cyclobutanone substrates, attention was turned to seeking out an alternative electrophile species. Due to their high affinity for oxygen and the resultant strength of the phosphorus-oxygen bond, diethyl- and diphenylphosphoryl chloride electrophiles have been used to trap enolates from the deprotonation of a ketone.<sup>56</sup> To the best of our knowledge, Aggarwal and co-workers have shown the only example of such an electrophile being used in an asymmetric deprotonation.<sup>33</sup> Thus, the full scope of this process for the production of enantioenriched enol phosphates was yet to be realised, especially with alternative substrates such as the substituted cyclobutanones under investigation here. Alongside the search for an alternative electrophile to use within the magnesium bisamide-mediated asymmetric deprotonation of cyclobutanones, an opportunity to capitalise on the lack of these products became apparent. It was envisaged that this could further expand the use of these emerging base systems.

### 3.4 Asymmetric deprotonations to afford enantioenriched enol phosphates

Wishing to employ the alternative diphenylphosphoryl chloride electrophile within magnesium bisamide-mediated deprotonations, a benchmark reaction for the formation of enol phosphates has undergone very recent development within our laboratory. Although work in this area is ongoing,<sup>57</sup> original conditions for this novel benchmark deprotonation reflected the previous benchmark deprotonation for the formation of silyl enol ethers.<sup>42b</sup> Thus, the DMPU additive was employed with an excess of the electrophile (diphenylphosphoryl chloride) under IQ conditions at -78 °C (**Scheme 78**). Pleasingly, the resultant enol phosphate **117** was obtained in 75% yield and with 96:4 er, as determined by chiral HPLC. It should be noted that these enol phosphate products are more stable than silyl enol ethers and can therefore survive an acid wash and slower column chromatography.



**Scheme 78**

With a new benchmark reaction for the formation of enantioenriched enol phosphates in place, attention returned to the use of this phosphorus-based electrophile in the asymmetric deprotonation of cyclobutanone substrates.

#### 3.4.1 Introduction of an alternative electrophile

After observing poor asymmetric induction with a silicon electrophile, the use of diphenylphosphoryl chloride was turned to in an effort to expand upon the applicability of our magnesium bisamide species. As the resulting enol phosphate products have been used as an alternative to a triflate coupling partner in metal-mediated cross coupling reactions,<sup>58,33</sup> it was believed that the enantioenriched enol

phosphates would be valuable additions to this field of organometallic chemistry. To this end, an investigation into the compatibility of diphenylphosphoryl chloride with a magnesium bisamide species was initiated in an effort to form the enantioenriched enol phosphate **120** (Figure 18).

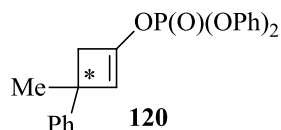
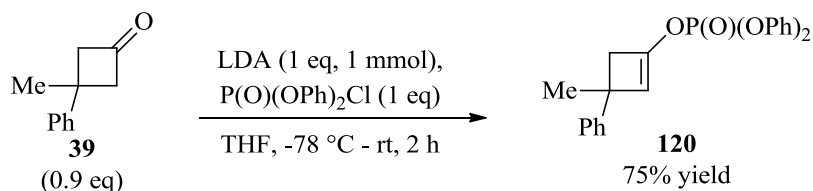


**Figure 18**

As with previous asymmetric synthesis studies, analytical techniques were established to determine the degree of enantioinduction, using chiral HPLC or GC methods. In this regard, a racemic mixture of the desired enol phosphate **120** was thus synthesised for analysis by chiral HPLC. Using literature conditions,<sup>56a,56b</sup> LDA was used to deprotonate cyclobutanone **39** (Scheme 79). Employing diphenylphosphoryl chloride as the electrophile for the first time with this ketone substrate, we were pleased to obtain the 4-membered cyclic enol phosphate **120** in high yield.

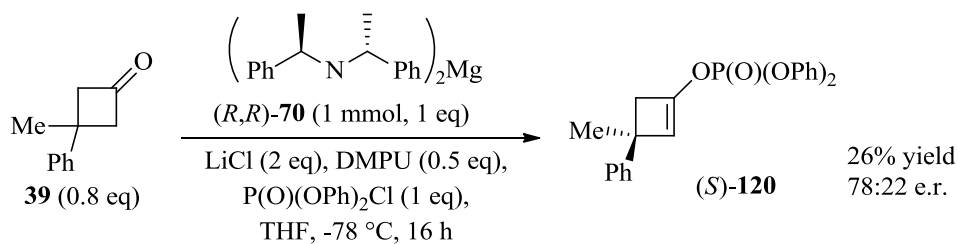


**Scheme 79**

After developing HPLC methods for the analysis of this novel enol phosphate, attention turned to discovering the compatibility of diphenylphosphoryl chloride as an electrophile within our magnesium bisamide-mediated deprotonation processes.

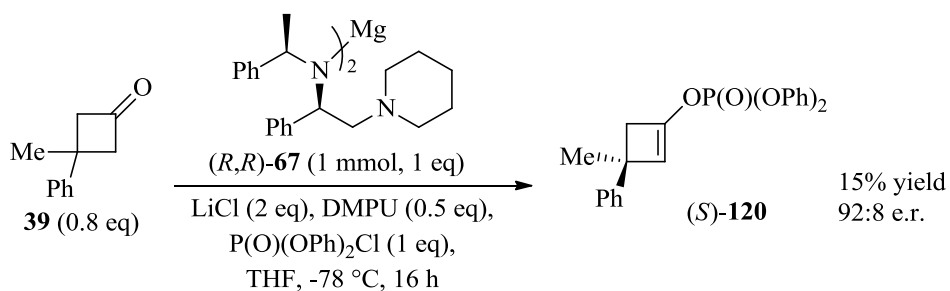
### 3.4.2 Additive studies

In the quest to access novel enol phosphate **120**, and others, in an asymmetric fashion, the  $C_2$ -symmetric magnesium bisamide ( $R,R$ )-**70** was initially investigated as a suitable base to effect the asymmetric deprotonation. Having found that LiCl was required for the deprotonation of cyclobutanone **39** when TESCl was used as an electrophile, and without wishing to alter more than one variable of the reaction at this stage, the conditions shown in **Scheme 80** were used in the initial experiment. Thus, taking cyclobutanone **39**, under internal quench conditions, the  $C_2$ -symmetric magnesium bisamide ( $R,R$ )-**70** was used with LiCl and DMPU additives along with one equivalent of diphenylphosphoryl chloride as the new electrophile (**Scheme 80**). Although a low 26% yield of enol phosphate ( $S$ )-**120** was obtained a moderately high enantioselectivity was observed. As an initial attempt to use this alternative electrophile, this was an extremely promising result.



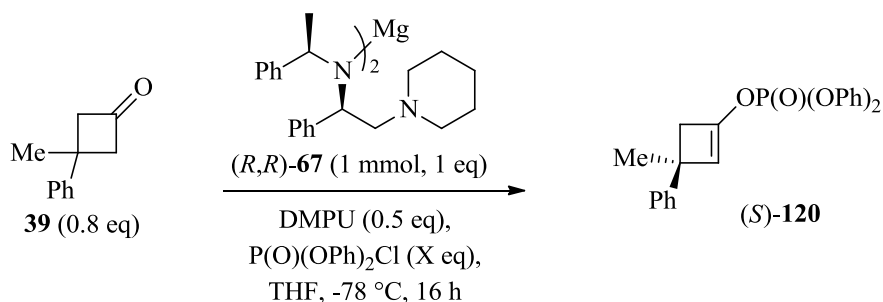
**Scheme 80**

In order to compare the chelating magnesium bisamide ( $R,R$ )-**67** throughout this study, the same reaction was carried out using this base. Pleasingly, an excellent level of enantioselectivity (92:8 e.r.) was observed, albeit in a low yield of 15% (**Scheme 81**).



**Scheme 81**

Having observed greater selectivity when employing the chelating base (*(R,R)*-**67**, attention focused on the optimisation of this novel system in order to enhance the yield of enantioenriched enol phosphate **120**. It was believed at this stage that the mixture of additives used thus far may not be compatible with the phosphorous electrophile that had been introduced. To explore this possibility, the LiCl was first removed from the reaction mixture to assess what effect this would have on the efficiency of the reaction. To this end, using only DMPU as an additive, the equivalents of electrophile were studied with the chelating base (*(R,R)*-**67**, under internal quench conditions, at -78 °C (**Scheme 82**, **Table 39**). A marked increase in yield was observed for all entries compared with the previous reaction in **Scheme 81** with the inclusion of LiCl. Although the enantioselectivities varied between 72:28 (**Entry 2**, **Table 39**) to 98:2 (**Entry 3**, **Table 39**), they had remained significantly higher than the initial results obtained in this study with the TESCl electrophile.



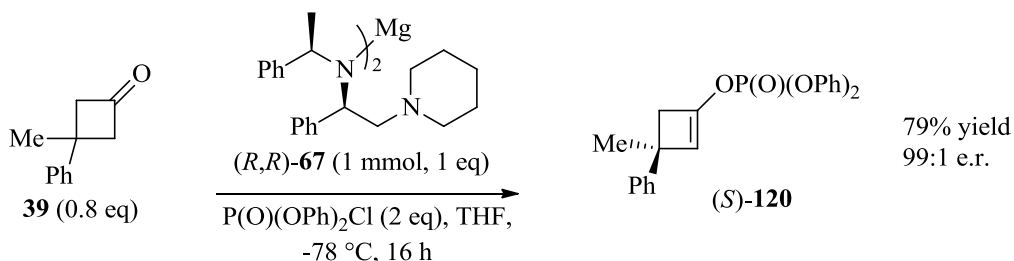
**Scheme 82**



Entry	P(O)(OPh) <sub>2</sub> Cl Eq.	Yield (%)	e.r.
1	1	40	84:16
2	2	64	72:28
3	4	37	98:2

**Table 39**

In an effort to probe the effect of additives further, it was envisaged that no additive may be required at all.<sup>41</sup> To verify this hypothesis, DMPU was also removed from the reaction mixture. From the previous reactions (**Scheme 82, Table 39**), it seemed that a large excess of the electrophile was detrimental to the reaction yield (**Entry 4, Table 39**), but one equivalent provided only a moderate result (**Entry 1, Table 39**). As such, two equivalents were used in the hope of achieving an even greater yield without the inclusion of DMPU at all. Accordingly, the asymmetric deprotonation of **39** was carried out using the chelating base (*R,R*)-**67** and quenching with just two equivalents of diphenylphosphoryl chloride (**Scheme 83**). An excellent yield of 79% was achieved under these reaction conditions and, even more impressively, an outstanding er of 99:1 was observed for enol phosphate **120**.

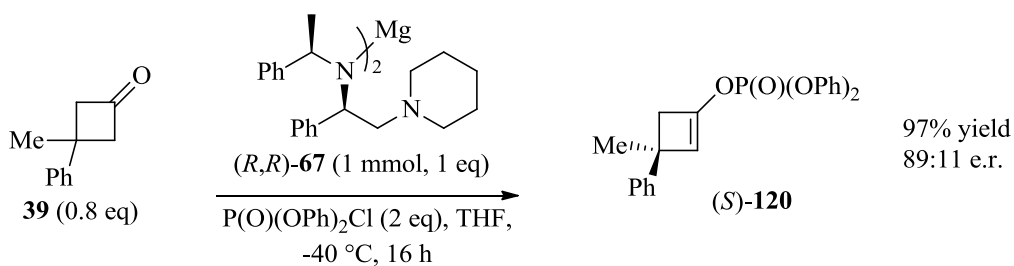


**Scheme 83**

This exceptional result highlights the efficacy of this alternative electrophile under the deprotonation conditions for cyclobutanone **39**. It has shown the highest level of enantioselectivity achieved to date for the asymmetric deprotonation of such a substrate. Moreover, the simplicity of the reaction mixture was revealed as no additives are required in order to achieve these yields of almost enantiopure enol

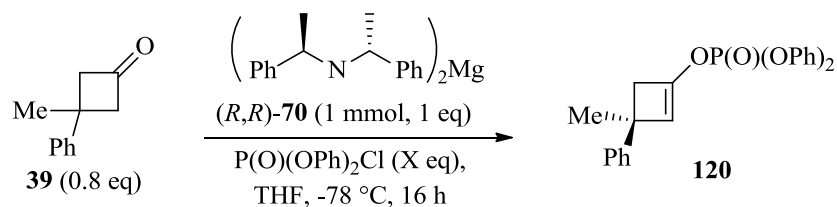
phosphate, making this an elegant and highly attractive transformation in the arena of asymmetric synthesis.

As magnesium bisamides have proved to be stable at higher temperatures, without significant loss in selectivity, the previous reaction was repeated at  $-40\text{ }^{\circ}\text{C}$  (**Scheme 84**). Delightedly, almost quantitative yield was achieved and only moderate reduction in the enantioselectivity was observed. Unfortunately, however, attempts to elevate the reaction temperature any further were detrimental to the yield in all cases.



**Scheme 84**

To determine the robustness of this electrophile, and to establish whether any other magnesium bisamides were as effective under these reaction conditions, this study was repeated using the structurally more simple  $C_2$ -symmetric magnesium bisamide  $(R,R)$ -**70**. It seemed unnecessary to repeat all the trial reactions removing one additive at a time from the reaction mixture, therefore, the newly optimised conditions (with no additive present) were applied to the deprotonation of ketone **39** with  $C_2$ -symmetric base  $(R,R)$ -**70** (**Scheme 85**, **Table 40**). In line with the results obtained using the chelating base  $(R,R)$ -**67**, this more simple base  $(R,R)$ -**70** showed excellent levels of enantioselectivity and high yields with either one or two equivalents of the phosphorus electrophile.

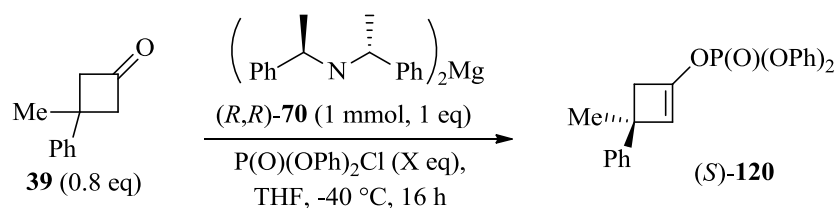


**Scheme 85**

Entry	P(O)(OPh) <sub>2</sub> Cl Eq.	Yield (%)	e.r.
1	1	63	93:7
2	2	78	96:4

**Table 40**

Pleased that the *C*<sub>2</sub>-symmetric magnesium bisamide (*R,R*)-**70** showed comparably high levels of yield and selectivity, the temperature at which this base could perform with this alternative electrophile was subsequently studied. As with the chelating base, none of the desired enol phosphate was obtained at 0 °C, but the lower temperature of -40 °C maintained moderate yields (**Scheme 86, Table 41**). Again, using either one or two equivalents of diphenylphosphoryl chloride electrophile, the enantioselectivity remained outstanding. However, in both instances, a surprising reduction in yield was observed compared with the reactions performed at -78 °C.



**Scheme 86**

Entry	P(O)(OPh) <sub>2</sub> Cl Eq.	Yield (%)	e.r.
1	1	39	97:3
2	2	61	99:1

**Table 41**

It was apparent that the *C*<sub>2</sub>-symmetric base (*R,R*)-**70** did not perform as well at elevated temperatures, but was equally as efficient at -78 °C compared with the chelating base (*R,R*)-**67**. With these results in hand, it was envisaged that the optimised conditions could be applied to a wider range of cyclobutanone substrates in order to expand the scope of this novel electrophile for such deprotonations.

Examining the results from these optimisation studies revealed that both the  $C_2$ -symmetric base (*R,R*)-**70** and the chelating base (*R,R*)-**67** could be employed for each new substrate at  $-78\text{ }^\circ\text{C}$ , and the chelating base (*R,R*)-**67** could also be employed at  $-40\text{ }^\circ\text{C}$ . To this end, a range of cyclobutanone substrates bearing different groups in the 3-position of the 4-membered ring were selected to expand the substrate scope for this asymmetric deprotonation, as well as to access a wider range of novel enol phosphates. The proposed cyclobutanone substrates are outlined in **Figure 19**.

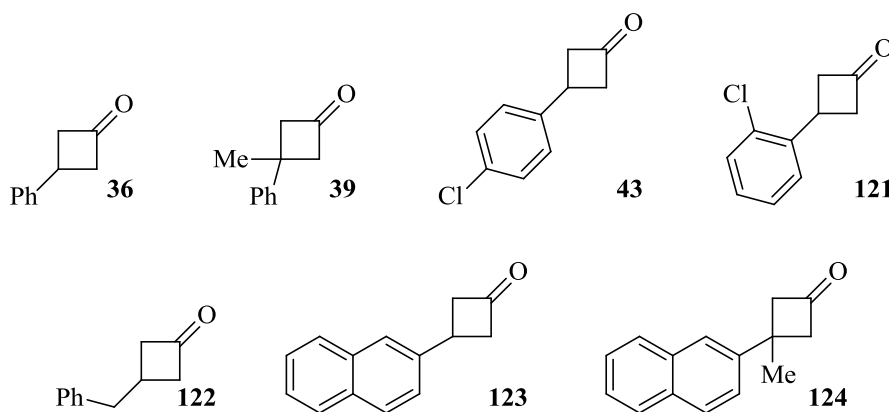


**Figure 19**

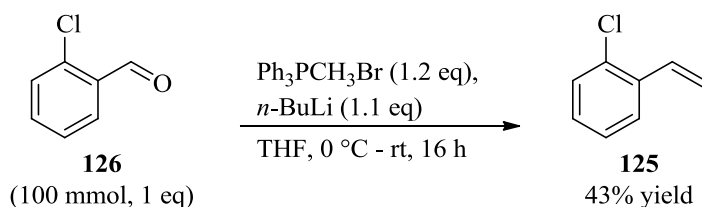
### 3.4.3 Substrate scope

With a view to synthesising a small library of novel, enantioenriched enol phosphates, exhibiting differing steric bulk around the stereogenic centre, a range of prochiral ketones were first synthesised. Having developed scalable methods to access such substrates *via* a [2+2] cycloaddition (see **Section 3.2.3**), these reaction conditions were applied to the requisite substituted styrenes. For the styrene derivatives that were expensive or not commercially available, these were formed *via* a Wittig reaction from the parent carbonyl compound, as carried out previously.

#### *Synthesis of styrene derivatives*

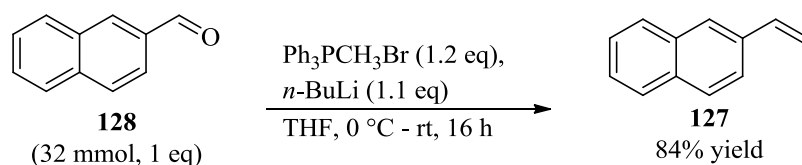
For the 4- and 2-substituted aryl rings of cyclobutanones **43** and **121**, respectively, the styrene starting materials were synthesised from the cheap and readily available aldehydes. 2-Chlorostyrene **125** was thus formed in a moderate 43% yield from 4-

chlorobenzaldehyde **105** and methyltriphenylphosphonium bromide, using *n*-BuLi as the base to form the ylide (**Scheme 87**). Due to the large scale of this reaction, further attempts to improve upon this yield were not attempted as six grams of styrene **125** had been obtained which provided sufficient material for the formation of the desired cyclobutanone **121**.



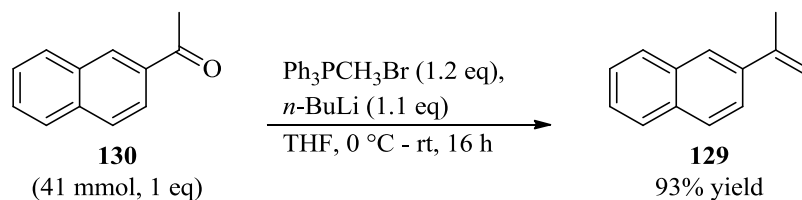
**Scheme 87**

In the same manner, 2-vinylnaphthalene **127** was formed from 2-naphthaldehyde **128** under these Wittig conditions (**Scheme 88**). The desired alkene **127** was formed a high 84% yield after purification.



**Scheme 88**

Finally the highly substituted styrene derivative **129** was synthesised under the above conditions (**Scheme 89**). For this substrate, a 93% yield was obtained after purification.

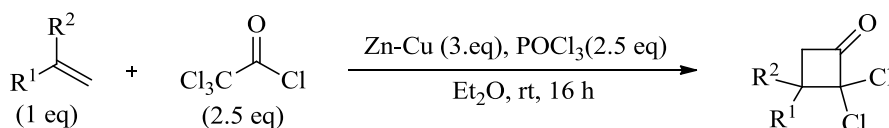


**Scheme 89**

With the necessary styrenes now prepared, along with the commercially available analogues, synthesis of the desired cyclobutanones commenced.

#### Synthesis of cyclobutanone substrates

Taking the styrene starting materials, these substrates underwent a [2+2] cycloaddition with *in situ* generated dichloroketene, as performed previously (Section 3.2.2). As described, these 2,2-dichlorocyclobutanone products were subjected to the subsequent dechlorination step as crude products. Purification was performed after the second step to access the desired cyclobutanone substrates. Thus, each styrene derivative was subjected to these reaction conditions (Scheme 90, Table 42). Moderate to high yields were obtained in all entries, providing sufficient material to progress onto the dechlorination step.

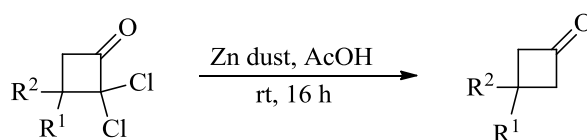


Scheme 90

Entry	Styrene	Cyclobutanone	R <sup>1</sup>	R <sup>2</sup>	<sup>1</sup> H NMR Yield (%)
1	<b>131a</b>	<b>131</b>	Ph	H	56
2	<b>106</b>	<b>109</b>	Ph	Me	61
3	<b>104</b>	<b>108</b>	4-ClC <sub>6</sub> H <sub>5</sub>	H	96
4	<b>125</b>	<b>132</b>	2- ClC <sub>6</sub> H <sub>5</sub>	H	67
5	<b>133a</b>	<b>133</b>	Benzyl	H	80
6	<b>127</b>	<b>134</b>	2-Naphthyl	H	77
7	<b>128</b>	<b>135</b>	2-Naphthyl	Me	79

Table 42

Taking each of the crude products from **Table 42** and subjecting to the zinc dust with acetic acid reduction, the desired cyclobutanones were obtained (**Scheme 91, Table 43**). After column purification to remove any remaining styrene derivative from the previous step, moderate to high yields were obtained for all cyclobutanones. For **Entries 1 to 5, Table 43**, the products obtained were colourless or pale yellow oils which could subsequently be distilled over calcium hydride to remove any traces of moisture and to allow storage under an argon atmosphere for use in asymmetric deprotonations. **Entries 6 and 7, Table 43**, were white solids which were recrystallised from dry hexane, dried under high vacuum for 16 hours, and stored under argon prior to use.



**Scheme 91**

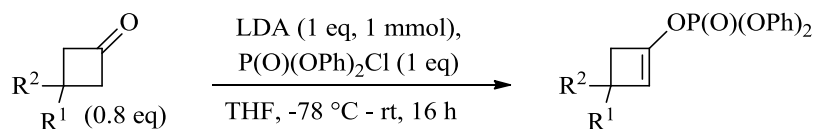
Entry	Cyclobutanone	R <sup>1</sup>	R <sup>2</sup>	Yield (%)
1	<b>36</b>	Ph	H	61
2	<b>39</b>	Ph	Me	64
3	<b>43</b>	4-Chlorophenyl	H	38
4	<b>121</b>	2-Chlorophenyl	H	58
5	<b>122</b>	Benzyl	H	60
6	<b>123</b>	2-Naphthyl	H	50
7	<b>124</b>	2-Naphthyl	Me	57

**Table 43**

#### 3.4.4 Formation of racemic enol phosphates

After synthesising and purifying the chosen cyclobutanones, their respective enol phosphates were required in racemic form for analysis by chiral stationary phase HPLC. To this end, each cyclobutanone was treated with LDA and

diphenylphosphoryl chloride, using literature conditions,<sup>57a,57b</sup> to access the desired enol phosphates (**Scheme 92**, **Table 44**). Again, a range of yields was obtained at this stage, however, in all cases the enol phosphate products were successfully purified and analysed by chiral HPLC. Optimisation of the chemical yields using LDA as the base was not the key focus, as it was felt that the asymmetric deprotonations employing chiral magnesium bisamides would allow access to these novel products in higher yields and in enantioenriched form.



**Scheme 92**

Entry	Cyclobutanone	R <sup>1</sup>	R <sup>2</sup>	Enol phosphate	Yield (%)
1	<b>36</b>	Ph	H	<b>136</b>	57
2	<b>43</b>	4-Chlorophenyl	H	<b>137</b>	37
3	<b>121</b>	2-Chlorophenyl	H	<b>138</b>	60
4	<b>122</b>	Benzyl	H	<b>139</b>	39
5	<b>123</b>	2-Naphthyl	H	<b>140</b>	65
6	<b>124</b>	2-Naphthyl	Me	<b>141</b>	93

**Table 44**

### 3.4.5 Asymmetric deprotonations to form enantioenriched enol phosphates

With a range of 3-substituted and 3,3-disubstituted cyclobutanones synthesised, the applicability of the novel asymmetric deprotonation could be established. The substrates chosen bear a range of steric bulk around the 3-position, in order to study the influence of 3-substituted cyclobutanone substrates (for example **36** and **123**) versus the more challenging 3,3-disubstituted substrates (**39** and **124**). The compatibility of other heteroatoms was incorporated into this investigation using the



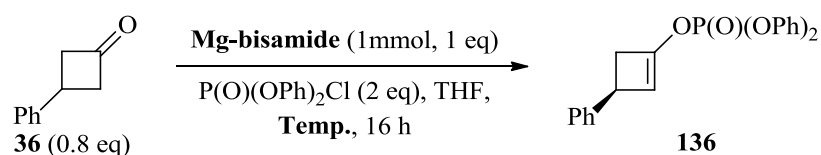
chloro-substituted aryl rings (**43** and **121**). Finally, a *pseudo*-alkyl derivative (3-benzylcyclohexanone **122**) was also studied to delineate whether non-aryl groups at this position could be used.

After analysis of the optimisation conditions (**Section 3.4.2**), it was decided that each substrate would be investigated under the following three conditions:

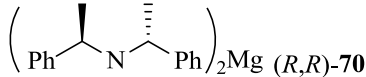
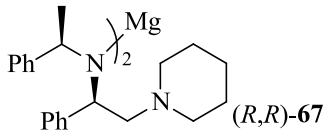
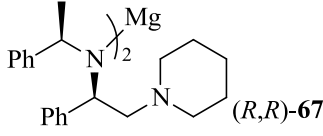
- 1) using the  $C_2$ -symmetric magnesium bisamide (*R,R*)-**70** at  $-78\text{ }^\circ\text{C}$ ;
- 2) using the chelating magnesium bisamide (*R,R*)-**67** at  $-78\text{ }^\circ\text{C}$ ;
- 3) using the chelating magnesium bisamide (*R,R*)-**67** at  $-40\text{ }^\circ\text{C}$ .

It should be noted that two equivalents of the diphenylphosphoryl chloride electrophile were used for each set of conditions under an internal quench protocol.

The study commenced with 3-phenylcyclobutanone **36** (**Scheme 93**, **Table 45**). Under the first set of reaction conditions (**Entry 1**, **Table 45**) an excellent yield of 81% was obtained with an equally excellent enantioselectivity of 97:3. A comparable yield of 77% was obtained in **Entry 2**, using the chelating base (*R,R*)-**67**, although a slightly lower enantioselectivity of 91:9 was obtained. At the slightly elevated reaction temperature (**Entry 3**, **Table 45**), this base showed a similar yield (80%) and, more pleasingly, a similarly high enantioselectivity (89:11). This illustrates both the stability of (*R,R*)-**67** at higher temperature and the robust nature of the alternative electrophile under these deprotonation conditions.

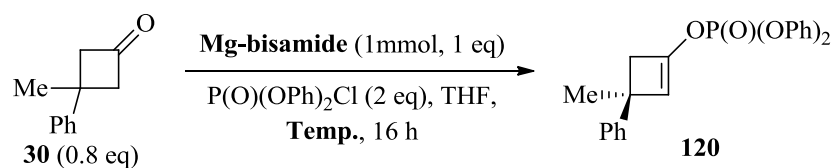


**Scheme 93**

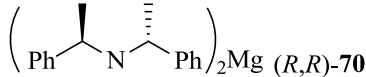
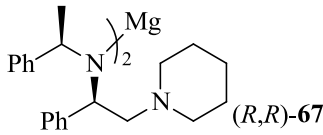
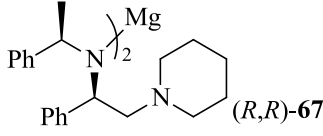
Entry	Mg-bisamide	Temp. °C	Yield (%)	e.r.
1		-78	81	97:3
2		-78	77	91:9
3		-40	80	89:11

**Table 45**

To directly compare how an increase in steric bulk affects the outcome of this asymmetric deprotonation, 3-methyl-3-phenylcyclobutanone **39** was treated with the two bases under the three reaction conditions (**Scheme 94, Table 46**). The good yield and exceptional enantioselectivity observed previously for this substrate (see the optimisation studies **Section 3.4.2**) were observed once again for the  $C_2$ -symmetric magnesium bisamide (*R,R*)-**70** (**Entry 1, Table 46**). This also proves the repeatability of these reaction conditions and outlines their superiority over using chlorotriethylsilane as the electrophile. Furthermore, the chelating base (*R,R*)-**67** showed excellent yield and selectivity at both -78 °C and -40 °C (**Entries 2 and 3, Table 46**), which was consistent with previous results under these conditions to form enol phosphate **120**.

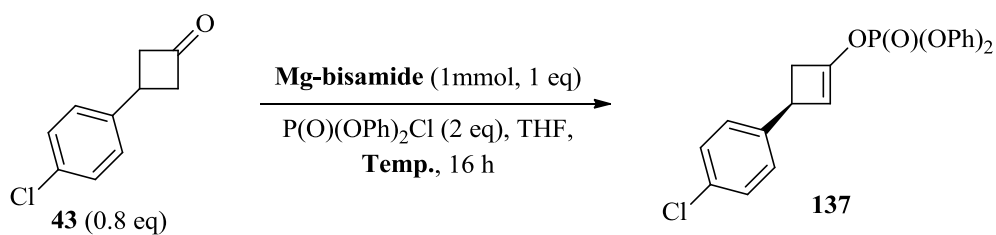


**Scheme 94**

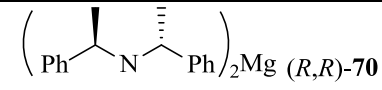
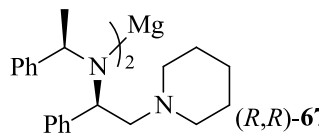
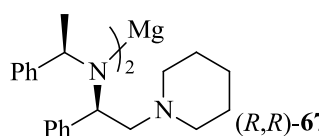
Entry	Mg-bisamide	Temp. °C	Yield (%)	e.r.
1	 $(R,R)$ -70	-78	65	99:1
2	 $(R,R)$ -67	-78	76	98:2
3	 $(R,R)$ -67	-40	68	98:2

**Table 46**

Without wanting to deviate in structure drastically, cyclobutanone **43** was chosen as the next ketone to investigate in this study. Bearing a chloride in the 4-position of the phenyl ring, **43** would provide an example for compatibility of other functional groups within the molecule, or indeed other functional handles (see Future Work **Section 3.5**). To this end, enol phosphate **137** was formed under the three different reaction conditions (**Scheme 95**, **Table 47**). Pleasingly, a good yield and high enantioselectivity were obtained with the  $C_2$ -symmetric base  $(R,R)$ -**70** (**Entry 1**, **Table 47**). An improvement in the yield was observed with chelating base  $(R,R)$ -**67** (**Entry 2**, **Table 47**), whilst maintaining good enantioinduction. Unfortunately, enol phosphate **137** was formed in poor enantioselectivity with chelating base  $(R,R)$ -**67** at  $-40$  °C (**Entry 3**, **Table 47**), albeit in a high 90% yield. Although poor results were obtained at the higher reaction temperature, the asymmetric deprotonation of **43** was effective at the more common reaction temperature of  $-78$  °C, keeping this substrate in line with previous examples. This particular ketone had also proven to show irreproducible levels of enantioselectivity when the silane quench was employed in previous studies (see **Section 3.3**), highlighting the effectiveness of this phosphorus electrophile.



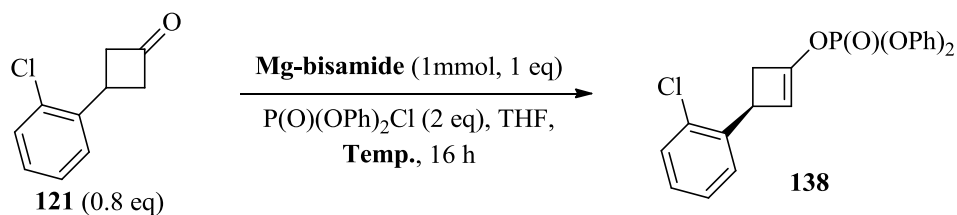
**Scheme 95**

Entry	Mg-bisamide	Temp. °C	Yield (%)	e.r.
1	 $(R,R)$ - <b>70</b>	-78	66	90:10
2	 $(R,R)$ - <b>67</b>	-78	89	87:13
3	 $(R,R)$ - <b>67</b>	-40	90	53:47

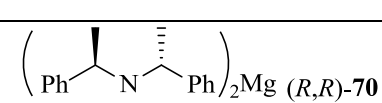
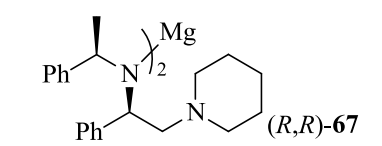
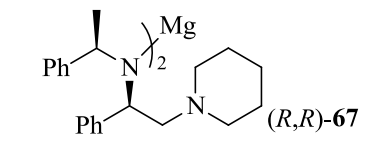
**Table 47**

As a substituent in the 4-position of the phenyl ring had proved to be compatible within this asymmetric deprotonation, the effect of this substituent in closer proximity to the stereocentre of the molecule was subsequently investigated. Thus, cyclobutanone **121** was subjected to the three sets of reaction conditions (**Scheme 96**, **Table 48**). Across the board, this substrate appeared to be high yielding and showed greater levels of enantioselectivity. With the  $C_2$ -symmetric base  $(R,R)$ -**70** (**Entry 1**, **Table 48**), an excellent 90% yield of enol phosphate **138** was obtained with 93:7 selectivity. For the chelating base  $(R,R)$ -**67** at -78 °C (**Entry 2**, **Table 48**) a slight drop in yield to 78% was obtained for **138**, but selectivity remained high at 96:4. Remarkably, at -40 °C this base showed the same enantioselectivity alongside an improvement in the yield of **138** to 88% (**Entry 3**, **Table 48**). This could be due to the substitution in the 2-position increasing the steric bulk around the 3-position of

cyclobutanone **121**, leading to a higher energy barrier for the ring flip and causing this substrate to be more conformationally locked.

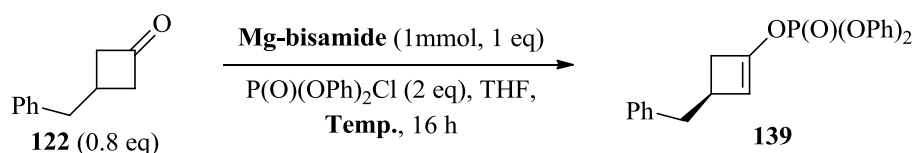


**Scheme 96**

Entry	Mg-bisamide	Temp. °C	Yield (%)	e.r.
1	 $(R,R)$ - <b>70</b>	-78	90	93:7
2	 $(R,R)$ - <b>67</b>	-78	78	96:4
3	 $(R,R)$ - <b>67</b>	-40	88	96:4

**Table 48**

Turning to an alkyl substituent, 3-benzylcyclobutanone **122** was considered (**Scheme 97, Table 49**). High levels of enantioselectivity of enol phosphate **139** were observed under all three reaction conditions. With  $C_2$ -symmetric base  $(R,R)$ -**70** and chelating base  $(R,R)$ -**67** at -78 °C, moderate yields of 60% and 55% were obtained, respectively (**Entries 1 and 2, Table 49**). An improved 79% yield of **139** was obtained employing chelating base  $(R,R)$ -**67** at -40 °C (**Entry 3, Table 49**) and, again and exceedingly pleasingly, an excellent er was observed at this more elevated temperature. These results, gratifyingly, proved that the substituent(s) in the 3-position of the cyclobutanone ring were not limited to aryl groups, which further expanded the scope of these novel asymmetric deprotonation conditions.

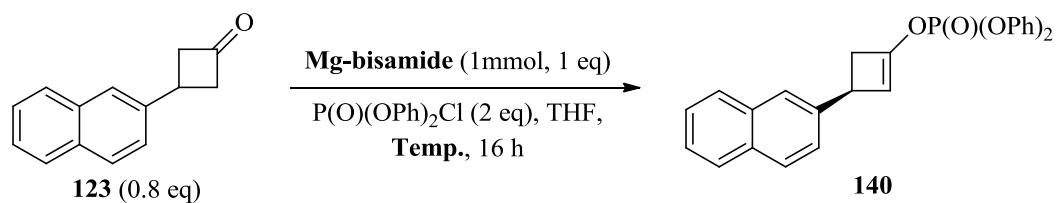


**Scheme 97**

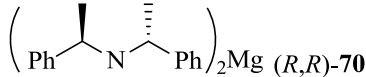
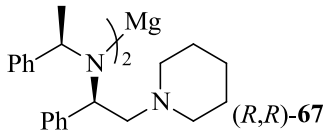
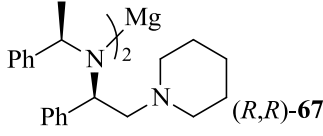
Entry	Mg-bisamide	Temp. °C	Yield (%)	e.r.
1	 ( <i>R,R</i> )- <b>70</b>	-78	60	95:5
2	 ( <i>R,R</i> )- <b>67</b>	-78	55	92:8
3	 ( <i>R,R</i> )- <b>67</b>	-40	79	95:5

**Table 49**

The final two substrates assessed were those containing a naphthyl instead of phenyl substituent in the 3-position. The 3-naphthylcyclobutanone **123** was subjected to the reaction conditions used for this study (**Scheme 98**, **Table 50**). With the  $C_2$ -symmetric magnesium bisamide (*R,R*)-**70** a moderate 53% yield of enol phosphate **140** was obtained in a good enantioselectivity of 82:12 (**Entry 1**, **Table 50**). Disappointingly, with the chelating magnesium bisamide (*R,R*)-**67**, at both -78 °C and -40 °C, very little enantioinduction occurred, although at -78 °C a higher yield of 70% was obtained (**Entry 2**, **Table 50**).

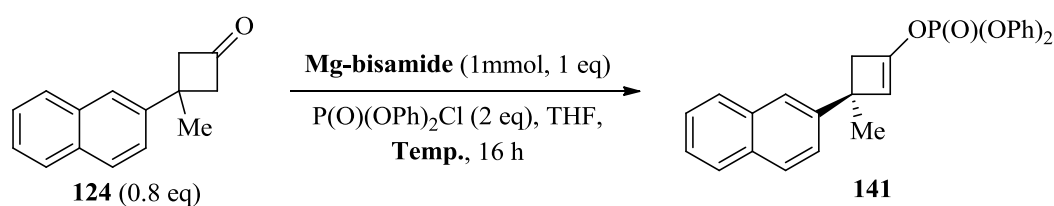


**Scheme 98**

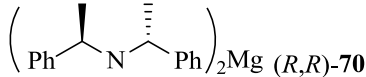
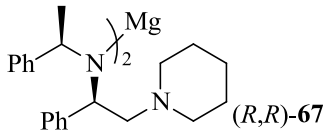
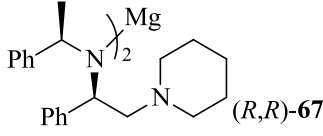
Entry	Mg-bisamide	Temp. °C	Yield (%)	e.r.
1		-78	53	82:18
2		-78	70	46:54
3		-40	44	48:52

**Table 50**

To analyse the effect of more substitution in this position, the 3-methyl-3-naphthylcyclobutanone **124** was the final substrate to be studied (**Scheme 99**, **Table 51**). In a similar manner to substrate **123**, the more heavily substituted derivative cyclobutanone **124** also led to a low level of enantioinduction. A lower level of enantioselectivity (76:24) was observed for enol phosphate **141** when the  $C_2$ -symmetric base  $(R,R)$ -**70** was employed at  $-78$  °C (**Entry 1**, **Table 51**), when compared with enol phosphate **140**. With the chelating base  $(R,R)$ -**67** at  $-78$  °C, enol phosphate **141** was formed in 61:39 e.r. (**Entry 2**, **Table 51**) which is higher than for enol phosphate **140** under these conditions. However, at  $-40$  °C, this dropped to be almost racemic (**Entry 3**, **Table 51**).



**Scheme 99**

Entry	Mg-bisamide	Temp. °C	Yield (%)	e.r.
1	 $(R,R)$ -70	-78	51	76:24
2	 $(R,R)$ -67	-78	61	61:39
3	 $(R,R)$ -67	-40	66	53:47

**Table 51**

It is apparent from these results that there is a cut-off for the amount of steric bulk around the 3-position of cyclobutanone substrates. Impressive levels of enantioselectivity have been observed for five substrates containing phenyl-, substituted phenyl-, phenyl- with methyl-, and alkyl- substituents, and in each example, a good to excellent yield of the enantioenriched enol phosphate was obtained. When the phenyl-substituent is replaced with a naphthyl-substituent, however, a significant decrease in enantioselectivity was encountered. This bulkier aromatic system is undoubtedly detrimental to the asymmetric deprotonation; however, it is unclear at this stage why this is the case. Speculation has led to the possibility that the large naphthyl substituent may distort the cyclobutanone ring, such that there is less distinction between the  $\alpha$ -axial protons for asymmetric differentiation. Alternatively, as the naphthyl ring is flat, 1,3-diaxial interactions between itself and other substituents around the ring may be minimised. This would result in a smaller difference in energy between the *pseudo*-equatorial and *pseudo*-axial position it can adopt, which would inherently result in a diminished energy barrier for the ring flip.<sup>59</sup> These two conformations would therefore become readily interchangeable so would no longer be recognisable in an asymmetric sense and would thus explain the lack of enantioinduction for such substrates.

In summary, a total of seven novel enol phosphates have been synthesised in enantioenriched form, employing two different magnesium amide bases (**Figure 20**).



With the structurally simple chiral magnesium base (*R,R*)-**70**, good yields were obtained for all enol phosphates at -78 °C and high levels of enantioselectivity were achieved. For the chelating magnesium base (*R,R*)-**67** the asymmetric deprotonation was performed at both -78 °C and -40 °C. Pleasingly, good yields were obtained at both temperatures and, in general, high enantioselectivities were also achieved. Although enol phosphates **140** and **141** showed only low levels of enantioinduction with chelating base (*R,R*)-**67**, moderate selectivities were maintained when (*R,R*)-**70** was employed as the chiral base. The range of substrates employed proves this to be a robust and general method for the desymmetrisation of strained cyclobutanone substrates and allows for the formation of interesting reaction products.

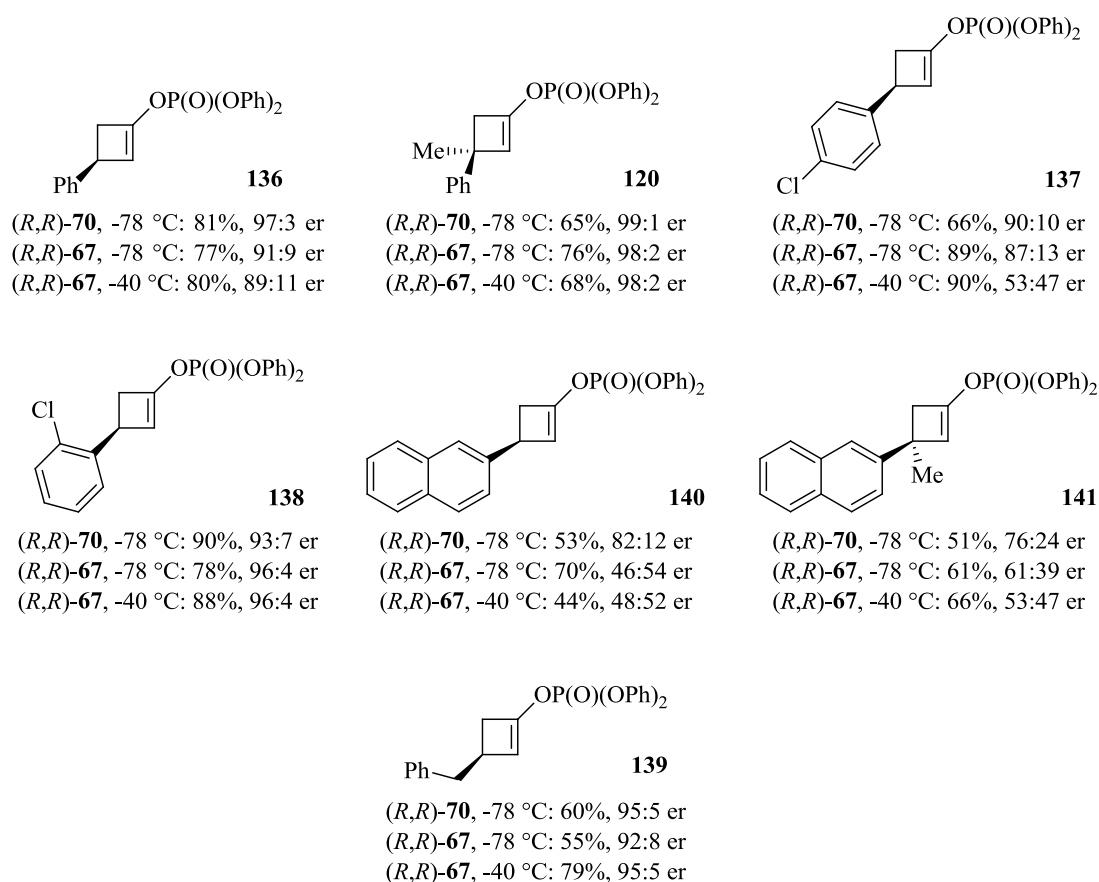
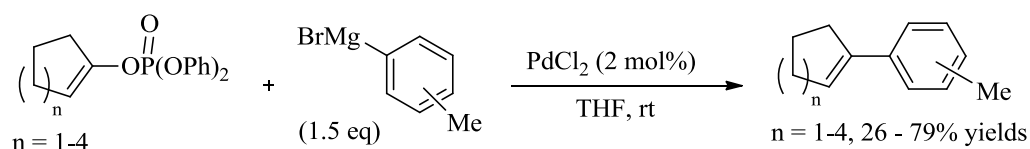


**Figure 20**

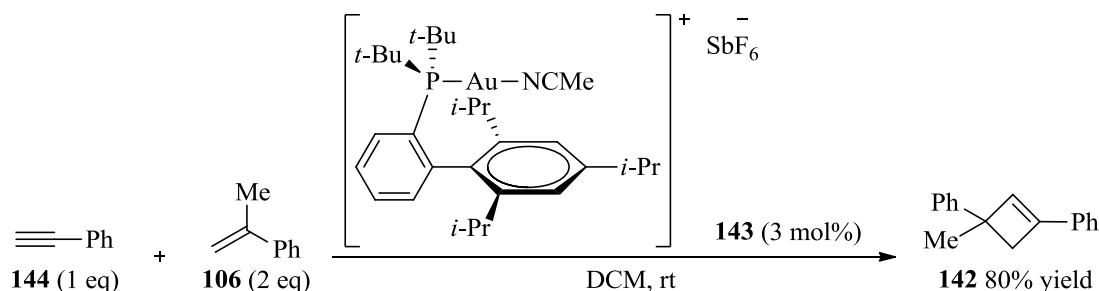
### 3.5 Avenues for future work

As alluded to previously, enol phosphates have been used as components of metal-mediated coupling reactions to form carbon-carbon bonds.<sup>58</sup> With this in mind, it is envisaged that the enantioenriched enol phosphates formed using this magnesium bisamide-mediated methodology could be used in this context. More specifically, the elegant ligand-free conditions developed by Skrydstrup appeared to be suited to the type of cross-coupling that could be possible for our novel 4-membered enol phosphates.<sup>60</sup> Using 2 mol% palladium(II) chloride, Skrydstrup coupled a range of commercially available Grignard reagents with both cyclic and acyclic enol phosphates in THF at room temperature to access highly substituted alkene products (**Scheme 100**).



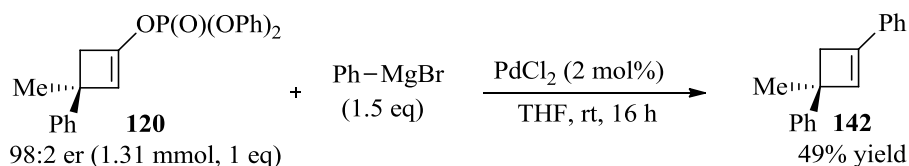
**Scheme 100**

Furthermore, highly substituted cyclobutene rings (such as **142** in **Scheme 101**) have been synthesised previously, in a racemic fashion, by Echavarren and co-workers using the gold(I) catalyst **143**.<sup>61</sup> The cyclobutene core is a useful synthetic building block and could potentially be accessed in an asymmetric fashion using an asymmetric deprotonation process.



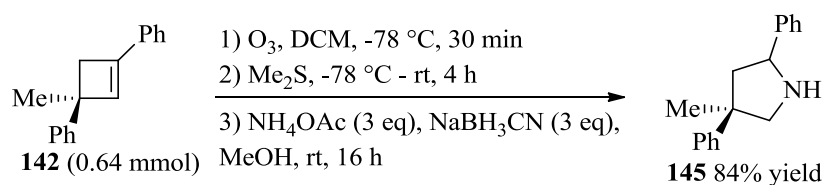
**Scheme 101**

It was believed that using our methodology to access enantioenriched 4-membered cyclic enol phosphates, we could combine the cross-coupling conditions developed by Skrydstrup in order to access cyclobutenes of this type in an asymmetric fashion and without the requirement for the expensive gold(I) catalyst **143**. As a preliminary investigation for further applications of our methodology, the reaction of enol phosphate **120** with phenylmagnesium bromide and 2 mol% palladium(II) chloride was attempted (**Scheme 102**). Although the literature procedure describes this transformation to be carried out in a glove box, it was pleasing to observe formation of cyclobutene **142** in a 49% <sup>1</sup>H NMR yield using a Schlenk line in which to perform the reaction. This 49% yield is a combination of 24% isolated yield of **142** and a further 25% yield calculated from the <sup>1</sup>H NMR spectrum of a mixture of **142** and biphenyl. The biphenyl is believed to have formed as a by-product of the reaction mixture through the homocoupling of phenylmagnesium bromide.



**Scheme 102**

Although only a moderate yield of **142** was observed in this initial cross-coupling reaction, this proves that the enantioenriched enol phosphates prepared *via* a magnesium bisamide-mediated deprotonation process can be used as effective coupling partners in carbon-carbon bond formations. To further derivatise this highly functionalised core, it was envisaged that the alkene bond could be oxidatively cleaved and treated with an ammonia source to access a substituted pyrrolidine. With this in mind, ozonolysis was performed on cyclobutene **142** (**Scheme 103**). After quenching with dimethyl sulfide, the reaction mixture was treated with ammonium acetate and sodium cyanoborohydride. To our delight, pyrrolidine **145** was formed in an 84% crude yield. Attempts to purify this pyrrolidine *via* salt formation and recrystallisation, however, were unsuccessful. Substituted pyrrolidines of this type are known, therefore efforts to synthesise similar compounds could be pursued after a suitable purification method has been established.



**Scheme 103**

Having applied our enantioenriched enol phosphates in palladium-catalysed cross-coupling reactions, this branch of methodology could be further expanded to form a wider range of cyclobutene products. These enantioenriched cyclobutenes could then be further elaborated to access a range of substituted heterocycles (**Figure 21**).

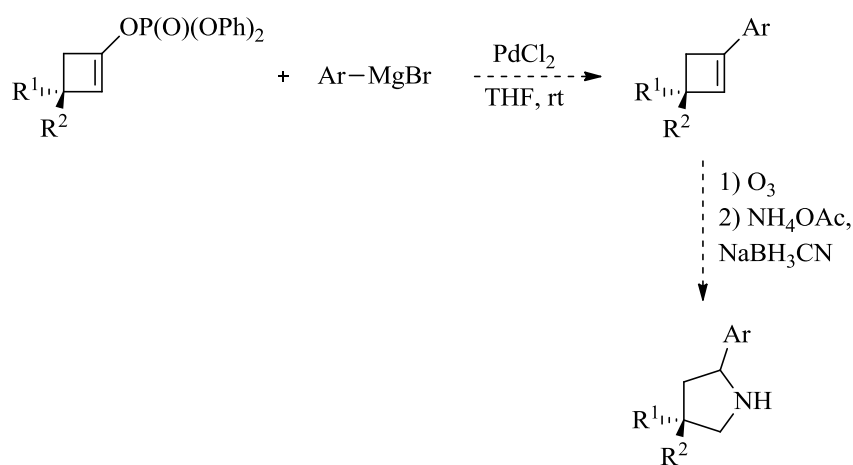


**Figure 21**

Moreover, in relation to enol phosphates **137** and **138** that contain a halogen substituent, such compounds could allow for selective cross-coupling reactions. For example, the ligand-free palladium(II) conditions with an aryl Grignard reagent could first be employed, followed by a Buchwald-Hartwig amination to install a nitrogen heteroatom into the molecule (**Figure 22**).

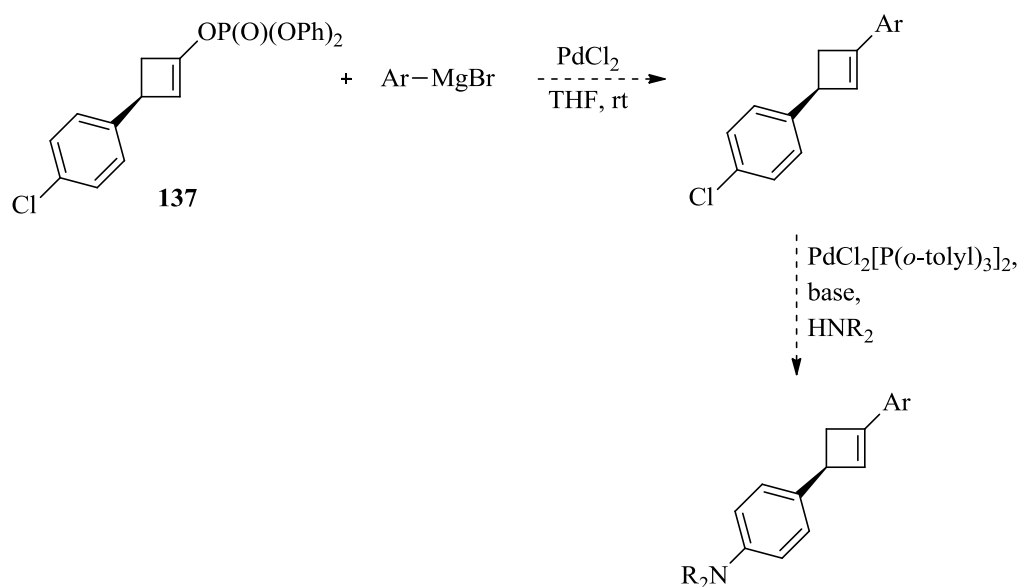


**Figure 22**

It is clear from these initial investigative reactions (**Scheme 102** and **Scheme 103**) that cross-coupling reactions are possible with our novel enol phosphates. Due to the high optical purity of the enol phosphate formed *via* the asymmetric deprotonation, the derivatisation products should retain this level of enantioenrichment. It is believed that this methodology utilising magnesium bisamides could allow access to more elaborate structures possessing high levels of enantiopurity.

The following section details a summary of the research described throughout this chapter.

## 4 Conclusions

After setting out to apply some emerging chiral magnesium bisamide species to the asymmetric deprotonation of cyclobutanone substrates, some limitations of this transformation were encountered. Having stated this, the use of an alternative electrophile and thus the formation of new and intriguing products proved that such magnesium species are viable reagents for the formation of enantioenriched phosphate cross-coupling partners.

More specifically, the structurally simple  $C_2$ -symmetric magnesium bisamide (*R,R*)-**70** has been applied to the desymmetrisation of 3-(4'-chlorophenyl)cyclobutanone **43** and 3-methyl-3-phenylcyclobutanone **39** to form silyl enol ethers **44** and **40**, respectively. As used with the analogous lithium amide bases, TESCOI was employed as the electrophilic quench in these deprotonations. Low reactivity was encountered when applying this electrophile with magnesium bisamide (*R,R*)-**70** and, furthermore, little enantioinduction was observed alongside this. Within the arena of lithium amide-mediated asymmetric deprotonations of cyclobutanone substrates structurally more elaborate chelating lithium amide bases have been shown to yield silyl enol ethers with higher optical purity. Thus, the chelating magnesium amide (*R,R*)-**67** was employed in the asymmetric deprotonations of cyclobutanone **39** in an effort to mirror these results with this base previously developed within our laboratory. Although a moderate enantioselectivity of 78:22 was achieved for the formation of (*S*)-**40**, in 78% yield, on one occasion, this result was unfortunately irreproducible. Returning to the  $C_2$ -symmetric magnesium bisamide (*R,R*)-**70**, (*S*)-**40** was formed in just 67:33 er and 43% yield. Interestingly, this low yield was attributed to the formation of an amino-silane by-product (**119**), whereby the base itself had reacted with the electrophile. It was therefore concluded that, for this novel base system, the bulky electrophile was not reactive enough to allow the effective formation of the desired silyl enol ether products. At this point, an alternative electrophile, that could exhibit higher reactivity, was sought.

The application of diphenylphosphoryl chloride has thus allowed the formation of 4-membered enol phosphate products. Pleasingly, initial results obtained using the 3-methyl-3-phenylcyclobutanone **39** substrate yielded the novel enol phosphate **120** in

high enantioselectivity. Further optimisation of reaction conditions revealed that no additives were required for this transformation, making this an attractive transformation in metal amide-mediated asymmetric deprotonations. To elaborate these promising results, a range of pro-chiral cyclobutanone substrates were synthesised and applied to our optimised reaction conditions. More specifically,  $C_2$ -symmetric magnesium bisamide (*R,R*)-**70** was employed at the reaction temperature of -78 °C and chelating magnesium bisamide (*R,R*)-**67** was employed at the reaction temperatures of -78 °C and -40 °C. Thus, seven novel enol phosphates have been formed in enantioenriched form with varying degrees of success. For phenyl and substituted phenyl groups in the 3-position, enantioselectivities were high for both bases at -78 °C (ranging from 87:13 to 99:1 er), and most remained high at -40 °C (ranging from 89:11 to 96:4 er) with chelating base (*R,R*)-**67** (excluding cyclobutanone **43** which only reacted to give enol phosphate **137** in 53:47 er at this more elevated temperature). An alkyl substituent also proved to be compatible with both bases, as enol phosphate **139** was formed in 92:8 to 95:5 er. It was, unfortunately, realised that a drop off in reactivity occurs when the phenyl group is replaced with a naphthyl group. Enol phosphates **140** and **141** were only formed in moderate yields. With the  $C_2$ -symmetric magnesium bisamide (*R,R*)-**70**, **140** and **141** were formed in good to moderate enantioselectivities of 82:18 and 76:25 er, respectively, however, with the chelating base (*R,R*)-**67** almost racemic enol phosphates were formed.

With such outstanding levels of enantioinduction for the formation of a good range of novel enol phosphates using chiral magnesium bisamides, a broader application of these organometallic species has been realised. These products are a valuable addition to the arena of organic synthesis as they can be applied in metal-mediated cross-coupling reactions as an alternative to a triflate coupling partner. Furthermore, enantioenriched carbon frameworks can be formed without the use of expensive metal catalysts using this methodology to form these enantioenriched enol phosphate coupling partners.

## 5 Experimental

### 5.1 General Considerations

All reagents were obtained from commercial suppliers and were used without further purification unless otherwise stated. Purification was carried out according to standard laboratory methods.<sup>62</sup>

- Diethyl ether, DCM, and toluene were obtained from an Innovative Technology, Pure Solv, PSP-400-5 solvent purification system.
- THF was dried by heating to reflux over sodium wire, using benzophenone ketyl as an indicator, then distilled under nitrogen.
- *n*-Bu<sub>2</sub>Mg, obtained as 1 M solution in heptane and *n*-BuLi, obtained as a 2.5 M solution in hexane or THF, were standardised using salicylaldehyde phenylhydrazone as an indicator.<sup>63</sup>
- DMPU, diphenylphosphoryl chloride, and (*R,R*)-*bis*-(1-phenylethyl)amine were dried by heating to reflux over calcium hydride and distilled under reduced pressure, then purged with and stored under argon over 4 Å molecular sieves.
- LiCl was flame-dried under high vacuum, then purged with and stored under argon.
- 4-*tert*-Butylcyclohexanone and solid cyclobutanones were purified by recrystallisation from hexane at 4 °C and stored under argon.
- TMSCl, TESCl, and trichloroacetyl chloride were distilled under argon and stored over 4 Å molecular sieves.
- 4-Chlorostyrene,  $\alpha$ -methylstyrene, and phosphorus(V) oxychloride were distilled under reduced pressure and stored over 4 Å molecular sieves.
- Liquid cyclobutanones were dried by heating to reflux over calcium chloride and distilled under reduced pressure, then purged with and stored under argon over 4 Å molecular sieves.

*Thin layer chromatography* was carried out using Camlab silica plates coated with fluorescent indicator UV<sub>254</sub>. This was analysed using a Mineralight UVGL-25 lamp and developed using potassium permanganate or vanillin solution.



*Flash chromatography* was carried out using Prolabo silica gel (230-400 mesh).

*Gas chromatography* was carried out using a Carlo Erba HRGC 5300 gas chromatograph fitted with (i) a CP SIL-19CB column or (ii) a CP-Chirasil-DEX CB column. Detection was by flame ionisation and the chromatograph was interpreted using JLC 6000 computer software.

*High pressure liquid chromatography* was carried out using a Chirasil OD-H or Chiralsil OJ column using a Waters 501 HPLC pump, a Waters 484 tuneable absorbance detector (set at 254 nm unless otherwise specified), and processed using a Waters 746 data module.

$^1\text{H}$ ,  $^{13}\text{C}$ , and  $^{31}\text{P}$  NMR spectra were obtained on a Bruker DPX 400 spectrometer at 400, 100, and 162 MHz, respectively. Chemical shifts are reported in ppm, and coupling constants are reported in Hz and refer to  $^3J_{\text{H-H}}$  interactions unless otherwise specified.

*FTIR spectra* were obtained on a Nicolet Impact 400D machine.

*High-resolution mass spectra* were obtained on a Finnigan MAT900XLT instrument at the EPSRC National Mass Spectrometry Services Centre, University of Wales, Swansea.

*Optical rotations* were obtained on Perkin Elmer 341 polarimeter using a cell with a path length of 1 dm, at 20 °C. Concentration is expressed in g/100 cm<sup>3</sup>.

ee was calculated using: %ee = ( $[\alpha]_{\text{obs}}/[\alpha]_{\text{max}}$ )x100.

Conversion to er: major isomer = (ee/2)+50.

*Ozone* was formed using a Fischer OZ 500 ozone generator.

*Air-sensitive reactions* were carried out using Schlenk apparatus, which was initially evacuated and flame-dried under vacuum (0.005 mbar), then allowed to cool under an atmosphere of argon.

## 5.2 General Experimental Procedures

### *General Procedure A for the preparation of magnesium bisamide reagents*

*n*-Bu<sub>2</sub>Mg (1 ml, 1 M solution in heptanes, 1 mmol, 1 eq) was transferred to a flame-dried Schlenk tube and the solvent removed *in vacuo* (0.005 mbar) until the appearance of a white solid. THF (10 ml) was then added followed by the amine (2 mmol, 2 eq) and the mixture was stirred at reflux for 90 min under an atmosphere of argon. After this time, quantitative formation of the chiral magnesium bisamide (1 mmol, 0.1 M in THF) was assumed.

### *General Procedure B for the preparation of magnesium bisamide reagents with the inclusion of LiCl*

A Schlenk tube was charged with LiCl (85 mg, 2 mmol, 2 eq) and flame-dried under vacuum. The tube was then purged three times with argon and allowed to cool to room temperature. *n*-Bu<sub>2</sub>Mg (1 ml, 1 M solution in heptanes, 1 mmol, 1 eq) was then added and the heptane removed *in vacuo*. The resulting white solid was dissolved in THF (10 ml) and the amine (2 mmol, 2 eq) was added. The resulting mixture was stirred at reflux for 90 min after which time quantitative formation of magnesium bisamide (1 mmol, 0.1 M in THF) was assumed.

### *General Procedure C for the asymmetric deprotonation of cyclic ketones to form silyl enol ethers*

A solution of chiral magnesium base (1 mmol, 1 eq) prepared *via General Procedure A or B* was cooled to the appropriate temperature under argon. The Schlenk flask was then charged with DMPU (if added) followed by the electrophile and the mixture was stirred for 10 min at the temperature stated. The ketone (0.8 mmol, 0.8 eq) was added to a flame-dried pear-shaped flask under argon and dissolved in freshly distilled THF (2 ml). The ketone solution was subsequently added to the reaction mixture over a period of 1 h *via* syringe pump. The resulting solution was allowed to stir at the temperature stated for 16 h before quenching with a saturated solution of

NaHCO<sub>3</sub> (10 ml) and warming to room temperature. The reaction mixture was extracted with diethyl ether (3 x 20 ml) to give a solution of the crude product which was dried over Na<sub>2</sub>SO<sub>4</sub>, filtered, and concentrated *in vacuo* to give an oil. Purification *via* flash chromatography provided the silyl enol ether as a colourless oil.

*General Procedure D for the asymmetric deprotonation of cyclic ketones to form enol phosphates*

A solution of chiral magnesium base (1 mmol, 1 eq) prepared *via* General Procedure A or B was cooled to the appropriate temperature under argon. The Schlenk flask was then charged with DMPU (if added) followed by diphenylphosphoryl chloride and the mixture was stirred for 10 min at the temperature stated. The ketone (0.8 mmol, 0.8 eq) was added to a flame-dried pear-shaped flask under argon and dissolved in freshly distilled THF (2 ml). The ketone solution was subsequently added to the reaction mixture over a period of 1 h *via* syringe pump. The resulting solution was allowed to stir at the temperature stated for 16 h before quenching with a saturated solution of NaHCO<sub>3</sub> (10 ml), warming to room temperature, and extracting with diethyl ether (3 x 20 ml). The combined organics were dried over Na<sub>2</sub>SO<sub>4</sub>, filtered, and concentrated *in vacuo*. The resulting oil was dissolved in diethyl ether (10 ml) and washed with 1 M HCl (3 x 20 ml) to remove the chiral amine. The organics were dried over Na<sub>2</sub>SO<sub>4</sub>, filtered, and concentrated *in vacuo* to give an oil which was subsequently purified *via* flash chromatography to give the enol phosphate as a colourless oil.

*General Procedure E for the preparation of zinc-copper couple*

A solution of copper sulfate pentahydrate (0.76 g, 3 mmol, 3 mol%) in water (5 ml, 20 M) was added in two portions at one minute intervals to a stirring suspension of zinc dust (6.50 g, 100 mmol, 1 eq) in water (10 ml, 10 M). After stirring for 5 minutes, the activated zinc-copper couple was filtered through a Buchner funnel and washed with water (2 x 5 ml), acetone (2 x 5 ml), and Et<sub>2</sub>O (5 ml). The resulting dark

grey powder was dried at 100 °C under vacuum for 16 h then purged with and stored under argon before use.

*General Procedure F for the preparation of 2,2-dichloro-3-substituted cyclobutanones and 2,2-dichloro-3,3-disubstituted cyclobutanones*

A flame-dried three-neck flask, equipped with a dropping funnel, under argon was charged with styrene derivative (1 eq), zinc-copper couple (prepared according to *General Procedure E*), and Et<sub>2</sub>O (2/3 of the total volume). To the dropping funnel was added Et<sub>2</sub>O (1/3 of the total volume), trichloroacetyl chloride, and phosphorus(V) oxychloride. This solution was added over a period of 1 h to the styrene and zinc-copper couple suspension at rt and the reaction mixture was stirred for 16 h. After this time, the reaction mixture was filtered through a pad of Celite and washed with hexane. The filtrate was concentrated to 1/3 of its volume *in vacuo* then hexane was added to induce precipitation of zinc chloride. The filtrate was diluted with hexane and concentrated twice more. The final concentrate was washed with water, saturated NaHCO<sub>3</sub> solution, and saturated brine solution. The now clear organic extracts were dried over Na<sub>2</sub>SO<sub>4</sub>, filtered, and concentrated to afford the crude 2,2-dichloro-3-substituted or 2,2-dichloro-3,3-disubstituted cyclobutanone which was used in the subsequent step without purification.

*General Procedure G for the preparation of 3-substituted cyclobutanones and 3,3-disubstituted cyclobutanones*

A three-neck flask fitted with a reflux condenser was charged with 2,2-dichloro-3-substituted or 2,2-dichloro-3,3-disubstituted cyclobutanone (1 eq) and acetic acid (0.16 M). This solution was stirred at room temperature until the solids fully dissolved. Zinc dust (6 eq) was added portionwise and the resulting suspension was stirred at room temperature for 16 h. The reaction mixture was filtered and diluted with Et<sub>2</sub>O. Water was added and the biphasic mixture was shaken and separated. The organic layer was washed with water (x 2) and saturated NaHCO<sub>3</sub> (x 3) taking care of the evolution of CO<sub>2</sub>. The organics were finally washed with saturated brine solution before drying over Na<sub>2</sub>SO<sub>4</sub>, filtering, and concentrating *in vacuo*. This crude

product was purified by silica gel chromatography, eluting with a gradient of 0 – 20% Et<sub>2</sub>O in PE (40 – 60 °C) to obtain the desired cyclobutanone.

*General Procedure H for the formation of racemic enol phosphates*

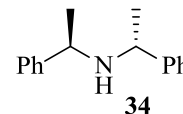
A Schlenk flask was charged with diisopropylamine (0.14 ml, 1 mmol, 1 eq) and THF (5 ml) then cooled to -78 °C. *n*-BuLi (0.40 ml, 2.5 M in hexane, 1 mmol, 1 eq) was added dropwise and the reaction mixture was warmed to rt over 30 min. The Schlenk was re-cooled to -78 °C and the ketone (0.9 mmol, 0.9 eq) in a solution of THF (5 ml) was added, dropwise, to the reaction mixture. The reaction was stirred for 30 min before the addition of diphenylphosphoryl chloride (0.21 ml, 1 mmol, 1 eq), dropwise. The reaction mixture was slowly warmed to rt and stirred for a further 90 min. After this time, the reaction mixture was quenched with saturated NH<sub>4</sub>Cl solution (10 ml) and extracted with Et<sub>2</sub>O (3 x 15 ml). The combined organics were dried over Na<sub>2</sub>SO<sub>4</sub>, filtered, and concentrated *in vacuo*. The crude residue was purified by silica gel chromatography, eluting with 5 – 50% Et<sub>2</sub>O in PE (40 – 60 °C) to afford the enol phosphate as a colourless oil.

*General Procedure I for the synthesis of styrene derivatives*

A flame-dried three-neck flask was charged with methyltriphenylphosphonium bromide (1.2 eq) and THF (0.2 M). The suspension was cooled to 0 °C and *n*-BuLi (1.1 eq, 2.5 M) was added dropwise and the now yellow reaction mixture was stirred for 20 min to allow complete formation of the ylide. The carbonyl derivative (1 eq) was added, portionwise, and the reaction mixture was stirred at 0 °C for 20 min then at rt for 16 h. The reaction mixture was quenched with saturated NH<sub>4</sub>Cl solution and the layers separated. The organic layer was washed with water, dried over Na<sub>2</sub>SO<sub>4</sub>, filtered, and concentrated *in vacuo*. The residue was purified by silica gel chromatography, eluting with PE (40 – 60 °C) to afford the styrene derivative as a yellow or colourless oil.

### 5.3 Benchmark deprotonations with $C_2$ -symmetric magnesium bisamide (*R,R*)-70

#### 5.3.1 Preparation of (*R*)-bis((*R*)-1-phenylethyl)amine **34**<sup>48</sup>



##### Scheme 47

A mixture of (*R*)- $\alpha$ -methylbenzylamine (*R*)-**102** (20 g, 0.17 mol, 1 eq), acetophenone **103** (19.8 g, 0.17 mol, 1 eq) and titanium (IV) *iso*-propoxide (141 g, 0.5 mol, 3 eq) was stirred at room temperature for 30 minutes before the addition of 10% palladium on carbon (720 mg, 8.5 mmol, 5 mol %). The mixture was then reduced under an atmosphere of hydrogen (5 bar) with stirring for three days. The reaction mixture was treated with a saturated solution of NaOH (250 ml) and filtered to remove the resultant precipitate. This precipitate was washed with EtOAc (750 ml) and the EtOAc extracts were washed with water, dried over Na<sub>2</sub>SO<sub>4</sub>, and concentrated *in vacuo* to leave a pale yellow oil. From the crude <sup>1</sup>H NMR spectrum, the (*R,R*)/(*R,S*) ratio could be established by comparison of the *CH* resonances. The oil was treated with the portionwise addition of HCl (5.80 ml, 0.19 mol), with cooling over dry ice, to immediately precipitate a white solid which was subsequently recrystallised from IPA. The diastereomerically pure salt was treated with an aqueous solution of 1 M NaOH and extracted with ethyl acetate. The combined organic washings were dried over Na<sub>2</sub>SO<sub>4</sub>, filtered, and the solvent removed *in vacuo* to leave (*R,R*)-bis(1-phenylethyl)amine (*R,R*)-**34** as a colourless oil. The amine was dried by heating to 100 °C under vacuum (0.005 mbar) over calcium hydride, then distilled (134 °C, 0.005 mbar) and stored over 4 Å molecular sieves under argon.

**Table 1:** Following the above procedure, data are reported as (a) dr (crude amine (*R,R*):(*R,S*)); (b) yield of (*R,R*)-**34**.

**Entry 1** (a) 6:1; (b) 27.5 g, 72%.

**Entry 2** (a) 7:1; (b) 24.8 g, 65%.

**Entry 3** (a) 8:1; (b) 27.9 g, 73%.

**Entry 4** (a) 6:1; (b) 24.1 g, 63%.

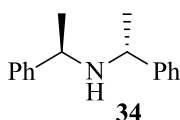
Peaks to deduce the (*R,R*)/(*R,S*) ratio of the crude amine **34**, from the <sup>1</sup>H NMR spectrum (400 MHz, CDCl<sub>3</sub>): δ 3.52 (*R,R*) (q, 1H, CH); 3.79 (*R,S*) (q, 1H, CH).

<sup>1</sup>H NMR (400 MHz, CDCl<sub>3</sub>): δ 1.29 (d, 6H, *J* = 6.7 Hz, CH<sub>3</sub>), 1.59, (s, 1H, NH), 3.52 (q, 2H, *J* = 6.7, CH), 7.23 – 7.28 (m, 4H, ArH), 7.33 – 7.36 (m, 6H, ArH)

<sup>13</sup>C NMR (100 MHz, CDCl<sub>3</sub>): δ 25.1, 55.2, 126.6, 126.8, 128.4, 145.8.

FTIR (neat): 2961 cm<sup>-1</sup>.

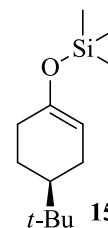
[α]<sub>D</sub> = +171.6° (c = 6.71, CHCl<sub>3</sub>). Lit: [α]<sub>D</sub> = -171.6° ((*S,S*), c = 6.71 CHCl<sub>3</sub>).<sup>48</sup>



### 5.3.2 Asymmetric deprotonations of 4-*tert*-butylcyclohexanone **12**

Preparation of (*S*)-((4-(*tert*-butyl)cyclohex-1-en-1-yl)oxy)trimethylsilane, (*S*)-**15**<sup>39b</sup>

**Scheme 48, Table 23**



Following *General Procedure A* for the preparation of Mg-bisamide (*R,R*)-**70**, data are reported as (a) amount of *n*-Bu<sub>2</sub>Mg; (b) amine used; (c) amount of amine.

Following *General Procedure C* for the asymmetric deprotonation, data are reported as (a) Mg base; (b) Lewis base additive; (c) electrophile; (d) ketone; (e) temperature; (f) conversion; (g) isolated yield; (h) er (*S*:*R*).

**Entry 1:** *General Procedure A* (a) 1.00 ml, 1 M in THF, 1 mmol, 1 eq; (b) (*R*)-bis((*R*)-1-phenylethyl)amine **34**; (c) 0.44 ml, 2 mmol, 2 eq.

*General Procedure C* (a) (*R,R*)-**70** (0.1 M in THF, 1 mmol, 1 eq); (b) DMPU, 60 μl, 0.5 mmol, 0.5 eq; (c) TMSCl, 0.5 ml, 4 mmol, 4 eq; (d) 4-*tert*-butylcyclohexanone **12**, 123 mg, 0.8 mmol, 0.8 eq; (e) -78 °C; (f) 95%; (g) 92%; (h) 84:16.

**Entry 2:** *General Procedure A* (a) 1.00 ml, 1 M in THF, 1 mmol, 1 eq; (b) (*R*)-bis((*R*)-1-phenylethyl)amine **34**; (c) 0.44 ml, 2 mmol, 2 eq.

*General Procedure C* (a) (*R,R*)-**70** (0.1 M in THF, 1 mmol, 1 eq); (b) DMPU, 60  $\mu$ l, 0.5 mmol, 0.5 eq; (c) TMSCl, 0.5 ml, 4 mmol, 4 eq; (d) 4-*tert*-butylcyclohexanone **12**, 123 mg, 0.8 mmol, 0.8 eq; (e) -78 °C; (f) 96%; (g) 90%; (h) 96:4.

**Entry 3:** *General Procedure A* (a) 1.00 ml, 1 M in THF, 1 mmol, 1 eq; (b) (*R*)-bis((*R*)-1-phenylethyl)amine **34**; (c) 0.44 ml, 2 mmol, 2 eq.

*General Procedure C* (a) (*R,R*)-**70** (0.1 M in THF, 1 mmol, 1 eq); (b) DMPU, 60  $\mu$ l, 0.5 mmol, 0.5 eq; (c) TMSCl, 0.5 ml, 4 mmol, 4 eq; (d) 4-*tert*-butylcyclohexanone **12**, 123 mg, 0.8 mmol, 0.8 eq; (e) -78 °C; (f) 90%; (g) 74%; (h) 94:6.

**Entry 4:** *General Procedure A* (a) 1.00 ml, 1 M in THF, 1 mmol, 1 eq; (b) (*R*)-bis((*R*)-1-phenylethyl)amine **34**; (c) 0.44 ml, 2 mmol, 2 eq.

*General Procedure C* (a) (*R,R*)-**70** (0.1 M in THF, 1 mmol, 1 eq); (b) DMPU, 60  $\mu$ l, 0.5 mmol, 0.5 eq; (c) TMSCl, 0.5 ml, 4 mmol, 4 eq; (d) 4-*tert*-butylcyclohexanone **12**, 123 mg, 0.8 mmol, 0.8 eq; (e) -78 °C; (f) 96%; (g) 76%; (h) 93:7.

$^1\text{H}$  NMR (400 MHz,  $\text{CDCl}_3$ ):  $\delta$  0.19 (s, 9H,  $\text{Si}(\text{CH}_3)_3$ ), 0.88 (s, 9H,  $\text{C}(\text{CH}_3)_3$ ), 1.24 – 1.32 (m, 2H,  $\text{CH}_2$ ), 1.77 – 1.85 (m, 2H,  $\text{CH}_2$ ), 1.97 – 2.13 (m, 3H,  $\text{CHC}(\text{CH}_3)_3 + \text{CH}_2$ ), 4.84 – 4.86 (m, 1H,  $\text{C}=\text{CH}$ ).

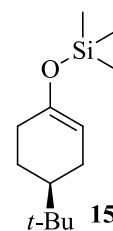
$^{13}\text{C}$  NMR (100 MHz,  $\text{CDCl}_3$ ):  $\delta$  0.3, 24.1, 26.9, 27.0, 30.7, 31.8, 43.7, 103.6, 149.9.

FTIR ( $\nu_{\text{max}}$  ( $\text{CHCl}_3$ )): 1674  $\text{cm}^{-1}$ .

Achiral GC analysis: [CP SIL-19 capillary column; carrier gas,  $\text{H}_2$  (80 kPa); injector/detector temperature, 200 °C; initial oven temperature, 45 °C; temperature gradient, 20 °C  $\text{min}^{-1}$ ; final oven temperature, 190 °C];  $t_{\text{R}}$  (**12**) = 5.27 min;  $t_{\text{R}}$  (**15**) = 5.49 min.

Chiral GC analysis: [Chirasil-DEX CB capillary column; carrier gas  $\text{H}_2$  (80 kPa); injector/detector temperature, 200 °C; initial oven temperature, 70 °C; temperature gradient, 5 °C  $\text{min}^{-1}$ ; final oven temperature, 120 °C];  $t_{\text{R}}$  ((*S*)-**15**) = 25.67 min;  $t_{\text{R}}$  ((*R*)-**15**) = 25.95 min.

$[\alpha]_{\text{D}}^{20} = -48.2^\circ$  (93:7 (*S*):(*R*),  $c = 1.5$ ,  $\text{CHCl}_3$ ). Lit:  $[\alpha]_{\text{D}}^{20} = -49.0^\circ$  (95:5 (*S*):(*R*),  $c = 1.5$ ,  $\text{CHCl}_3$ ).<sup>39c</sup>



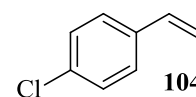


## 5.4 Synthesis of 3-substituted and 3,3-disubstituted cyclobutanones

### 5.4.1 Preparation of styrene derivatives

Preparation of 4-chlorostyrene **104**<sup>50</sup>

#### Scheme 49



To a flame dried three necked flask was added methyltriphenylphosphonium bromide (1.5 eq) and THF (0.12 M). The suspension was cooled in an ice bath and *n*-BuLi (1.3 eq) was added dropwise causing the white solid to dissolve and turn bright yellow indicating formation of the ylide. The ylide was stirred at 0 °C for a further 20 min before the addition of 4-chlorobenzaldehyde **105** (1 eq). The ice bath was removed and the reaction was warmed to room temperature and stirred for 16 h. After this time, the reaction mixture was quenched with the addition of saturated ammonium chloride solution (800 ml) and diluted with Et<sub>2</sub>O (500 ml). The biphasic mixture was shaken and the layers separated. The aqueous layer was extracted once more with Et<sub>2</sub>O (800 ml) and the combined organic layers were washed with water (800 ml) and saturated brine (800 ml). The ethereal solution was then dried with anhydrous sodium sulfate, filtered, and concentrated *in vacuo* to afford the crude product as a yellow oil. The oil was purified by silica gel chromatography, eluting with PE (40 – 60 °C) to yield the 4-chlorostyrene **104** as a pale yellow oil.

**Table 24:** The following experiments were carried out according to the above procedure. Data are reported as (a) amount of methyltriphenylphosphonium bromide; (b) amount of THF; (c) amount of *n*-BuLi; (d) amount of 4-chlorobenzaldehyde **105**; (e) yield of **104**.

**Entry 1:** (a) 10.72 g, 30 mmol, 1.5 eq; (b) 165 ml, 0.12 M; (c) 10.4 ml, 2.5 M in hexanes, 26 mmol, 1.3 eq; (d) 2.81 g, 20 mmol, 1 eq; (e) 2.05 g, 74%.

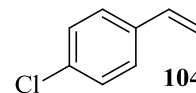
**Entry 2:** (a) 53.58 g, 150 mmol, 1.5 eq; (b) 830 ml, 0.12 M; (c) 52.0 ml, 2.5 M in hexanes, 130 mmol, 1.3 eq; (d) 14.05 g, 100 mmol, 1 eq; (e) 12.46 g, 90%.

**Entry 3:** (a) 53.58 g, 150 mmol, 1.5 eq; (b) 830 ml, 0.12 M; (c) 52.0 ml, 2.5 M in hexanes, 130 mmol, 1.3 eq; (d) 14.05 g, 100 mmol, 1 eq; (e) 11.91 g, 86%.

$^1\text{H}$  NMR (400 MHz,  $\text{CDCl}_3$ ):  $\delta$  5.28 (dd, 1H,  $^2J = 0.6, 11.0$  Hz, CH), 5.73 (dd, 1H,  $^2J = 0.7, 17.6$  Hz, CH), 6.68 (dd, 1H,  $J = 10.9, 17.6$  Hz, CH), 7.30 (d, 2H,  $J = 8.5$  Hz, 2 x ArH), 7.35 (d, 2H,  $J = 8.5$  Hz, 2 x ArH).

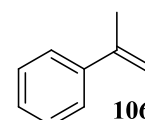
$^{13}\text{C}$  NMR (100 MHz,  $\text{CDCl}_3$ ):  $\delta$  114.0, 127.0, 128.2, 133.0, 135.2, 135.6.

FTIR ( $\nu_{\text{max}}$ ,  $\text{CHCl}_3$ ): 2961  $\text{cm}^{-1}$ .



Preparation of  $\alpha$ -methylstyrene **106**<sup>50,44a,64</sup>

### Scheme 50



To a flame-dried three-neck flask was added methyltriphenylphosphonium bromide (5.36 g, 15 mmol, 1.5 eq) and THF (83 ml). The suspension was cooled in an ice bath and *n*-BuLi (5.2 ml, 2.5 M in hexanes, 13 mmol, 1.3 eq) was added dropwise causing the white solid to dissolve and turn bright yellow indicating formation of the ylide. The ylide was stirred at 0 °C for a further 20 min before the addition of acetophenone **103** (1.20 g, 10 mmol, 1 eq). The ice bath was removed and the reaction was warmed to room temperature and stirred for 16 h. After this time, the reaction mixture was quenched with the addition of saturated ammonium chloride solution (100 ml) and diluted with  $\text{Et}_2\text{O}$  (50 ml). The biphasic mixture was shaken and the layers separated. The aqueous layer was extracted once more with  $\text{Et}_2\text{O}$  (100 ml) and the combined organic layers were washed with water (100 ml) and saturated brine (100 ml). The organics were dried over  $\text{Na}_2\text{SO}_4$ , filtered, and concentrated *in vacuo* to afford the crude product as a colourless oil. The oil was purified by silica gel chromatography, eluting with PE (40 – 60 °C) to yield  $\alpha$ -methylstyrene **106** (0.60 g, 51% yield) as a pale yellow oil.

### Scheme 51, Table 25

To a flame-dried three-neck flask was added THF (1 M), toluene (5 M), and methyltriphenylphosphonium bromide (1.5 eq) and the resulting suspension was cooled to 0 °C. Potassium *tert*-butoxide (1.5 eq) was added to this suspension,

portionwise, resulting in an instant colour change from white to yellow. The suspension was stirred for 10 minutes before the addition of acetophenone **103** (1 eq). The resulting mixture was stirred at rt for a further 16 h prior to being quenched with water and extracted with PE (40 – 60 °C) to afford crude styrene **106**. The combined organics were dried over Na<sub>2</sub>SO<sub>4</sub>, filtered, and concentrated *in vacuo*. Purification of the crude product by silica gel chromatography, eluting with PE (40 – 60 °C), yielded  $\alpha$ -methylstyrene **106** as a colourless oil.

**Table 25:** Data are reported as (a) volume of THF; (b) volume of toluene; (c) amount of methyltriphenylphosphonium bromide; (d) amount of KO*t*-Bu; (e) amount of acetophenone **103**; (f) yield of  $\alpha$ -methylstyrene **106**.

**Entry 1:** (a) 10 ml; (b) 2 ml; (c) 5.36 g, 15 mmol, (d) 1.68 g, 15 mmol; (e) 1.20 g, 10 mmol; (f) 1.04 g 88%.

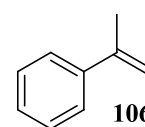
**Entry 2:** (a) 100 ml; (b) 20 ml; (c) 53.60 g, 150 mmol; (d) 16.80 g, 150 mmol; (e) 12.00 g, 100 mmol; (f) 11.8 g, 100%.

**Entry 3:** (a) 100 ml; (b) 20 ml; (c) 53.60 g, 150 mmol; (d) 16.80 g, 150 mmol; (e) 12.00 g, 100 mmol; (f) 11.7 g 99%.

<sup>1</sup>H NMR (400 MHz, CDCl<sub>3</sub>):  $\delta$  2.17 – 2.18 (m, 3H, CH<sub>3</sub>), 5.09 – 5.10 (m, 1H, CH), 5.38 – 5.39 (m, 1H, CH), 7.25 – 7.29 (m, 1H, ArH), 7.33 – 7.36 (m, 2H, 2 x ArH), 7.47 – 7.50 (m, 2H, 2 x ArH).

<sup>13</sup>C NMR (100 MHz, CDCl<sub>3</sub>):  $\delta$  21.5, 112.1, 125.1, 127.0, 127.9, 140.9, 142.9.

FTIR (CHCl<sub>3</sub>): 2838, 2962, 3087 cm<sup>-1</sup>.

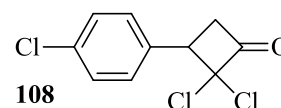


## 5.4.2 Preparation of 3-substituted and 3,3-disubstituted cyclobutanones

### Optimisation reactions

#### Preparation of

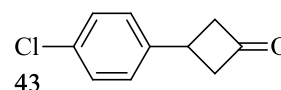
2,2-dichloro-3-(4'-chlorophenyl)cyclobutanone **108**<sup>52</sup>



#### Scheme 52

A flame-dried three-neck flask under argon, fitted with a dropping funnel and reflux condenser, was charged with 4-chlorostyrene **104** (0.60 ml, 5 mmol, 1 eq), zinc-copper couple (0.98 g, 15 mmol, 3 eq, prepared according to *General Procedure E*), and diethyl ether (10 ml, 0.5 M). The dropping funnel was charged with trichloroacetyl chloride (1.12 ml, 10 mmol, 2 eq), phosphorus(V) oxychloride (0.51 ml, 5.5 mmol, 1.1 eq), and diethyl ether (5 ml, 1 M), and this solution was added to the stirring suspension in the three-neck flask over a period of 1 h at rt. The resulting suspension was then heated to reflux for 2 h then stirred for a further 16 h at rt. The reaction mixture was filtered through a pad of Celite and washed with diethyl ether (100 ml). Hexane (50 ml) was added to the organic filtrate to induce precipitation zinc chloride salts. These combined organics were washed with water (100 ml), saturated NaHCO<sub>3</sub> solution (80 ml), and saturated brine solution (80 ml) to remove inorganic residues. The organic phase was dried over Na<sub>2</sub>SO<sub>4</sub>, filtered and concentrated *in vacuo* to afford **108** as cream waxy solid. <sup>1</sup>H NMR spectroscopy revealed a large amount of 4-chlorostyrene **104** was still present at this stage. Trituration in PE (40 – 60 °C) removed some of the remaining starting material leaving 0.35 g, 27% yield of **108**, based on the <sup>1</sup>H NMR spectrum.

Preparation of 3-(4'-chlorophenyl)cyclobutanone **43**<sup>52</sup>



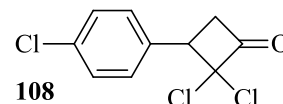
#### Scheme 53

Crude 2,2-dichloro-3-(4'-chlorophenyl)cyclobutanone **108** (0.35 g, 1.4 mmol, 1 eq, prepared in **Scheme 52**) was dissolved in acetic acid (14 ml, 0.1 M) in a round-bottom flask. Zinc dust (0.36 g, 5.6 mmol, 4 eq) was added and the reaction mixture was stirred at rt for 2 h then heated to reflux and stirred for a further 5 h. After cooling to rt, the reaction mixture was diluted with water (20 ml) and extracted with

diethyl ether (3 x 30 ml). The combined organics were washed with saturated NaHCO<sub>3</sub> solution (50 ml), water (50 ml), and saturated brine solution (50 ml), before drying over Na<sub>2</sub>SO<sub>4</sub>, filtered and concentrated *in vacuo*. The resulting yellow oil was purified by flash chromatography, eluting with a gradient of 0 – 20% Et<sub>2</sub>O in PE (40 – 60 °C) to afford cyclobutanone **43** as a colourless oil in a 24% yield (0.21 g).

*Preparation of*

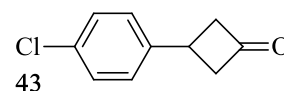
2,2-dichloro-3-(4'-chlorophenyl)cyclobutanone **108**<sup>52</sup>



#### Scheme 54

A flame-dried three-neck flask under argon, fitted with a dropping funnel and reflux condenser, was charged with 4-chlorostyrene **104** (1.20 ml, 10 mmol, 1 eq), zinc-copper couple (1.95 g, 30 mmol, 3 eq, prepared according to *General Procedure E*), and diethyl ether (20 ml, 0.5 M). The dropping funnel was charged with trichloroacetyl chloride (2.23 ml, 20 mmol, 2 eq), phosphorus(V) oxychloride (1.02 ml, 11 mmol, 1.1 eq), and diethyl ether (10 ml, 1 M). The resulting solution was added to the stirring suspension in the three-neck flask over a period of 1 h at rt. The resulting suspension was then heated to reflux for 2 h then stirred for a further 16 h at rt. The reaction mixture was filtered through a pad of Celite and washed with diethyl ether (200 ml). Hexane (100 ml) was added to the organic filtrate to induce precipitation zinc chloride salts. These combined organics were washed with water (200 ml), saturated NaHCO<sub>3</sub> solution (150 ml), and saturated brine solution (150 ml) to remove inorganic residues. The organic phase was dried over Na<sub>2</sub>SO<sub>4</sub>, filtered and concentrated *in vacuo* to afford **108** as cream waxy solid. <sup>1</sup>H NMR spectroscopy revealed a large amount of 4-chlorostyrene **104** was still present at this stage. Trituration in PE (40 – 60 °C) removed some of the remaining starting material leaving 1.12 g, 38% yield of **108**, based on the <sup>1</sup>H NMR spectrum.

Preparation of 3-(4'-chlorophenyl)cyclobutanone **43**<sup>52</sup>

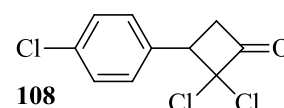


### Scheme 55

Crude 2,2-dichloro-3-(4'-chlorophenyl)cyclobutanone **108** (1.12 g, 3.8 mmol, 1 eq) was dissolved in acetic acid (38 ml, 0.1 M) in a round-bottom flask. Zinc dust (0.99 g, 15.2 mmol, 4 eq) was added and reaction mixture was stirred at rt for 2 h then heated to reflux and heated for a further 5 h. After cooling to rt, the reaction mixture was diluted with water (40 ml) and extracted with diethyl ether (3 x 60 ml). The combined organics were washed with saturated NaHCO<sub>3</sub> solution (100 ml), water (100 ml), and saturated brine solution (100 ml), dried over Na<sub>2</sub>SO<sub>4</sub>, filtered and concentrated *in vacuo*. The resulting yellow oil was purified by flash chromatography, eluting with a gradient of 0 – 20% Et<sub>2</sub>O in PE (40 – 60 °C) to afford cyclobutanone **43** as a colourless oil in a 55% yield (0.38 g).

Preparation of

2,2-dichloro-3-(4'-chlorophenyl)cyclobutanone **108**<sup>52</sup>



### Scheme 56, Table 26

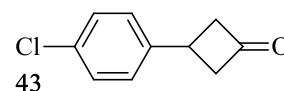
Prepared according to *General Procedure F*. Data are reported as (a) styrene derivative and amount; (b) amount of Zn-Cu couple (prepared according to *General Procedure E*); (c) total volume of Et<sub>2</sub>O; (d) amount of trichloroacetyl chloride; (e) amount of phosphorus(V) oxychloride; (f) product and yield.

**Entry 1:** (a) 4-chlorostyrene **104**, 4.16 g, 30 mmol, 1 eq; (b) 3.90 g, 60 mmol, 2 eq; (c) 90 ml, 0.33 M; (d) 8.19 g, 45 mmol, 1.5 eq; (e) 6.91 g, 45 mmol, 1.5; (f) **108**, 6.21 g, 83%.

**Entry 2:** (a) 4-chlorostyrene **104**, 6.93 g, 50 mmol, 1 eq; (b) 6.50 g, 100 mmol, 2 eq; (c) 150 ml, 0.33 M; (d) 13.65 g, 75 mmol, 1.5 eq; (e) 11.51 g, 75 mmol, 1.5 eq; (f) **108**, 5.74 g, 46% (<sup>1</sup>H NMR yield).

**Entry 3:** (a) 4-chlorostyrene **104**, 9.97 g, 72 mmol, 1 eq; (b) 9.36 g, 144 mmol, 2 eq; (c) 220 ml, 0.33 M; (d) 19.66 g, 108 mmol, 1.5 eq; (e) 16.58 g, 108 mmol, 1.5 eq; (f) **108**, 10.06 g, 56% (<sup>1</sup>H NMR yield).

Preparation of 3-(4'-chlorophenyl)cyclobutanone **43**<sup>52</sup>



**Scheme 57, Table 27**

Prepared according to *General Procedure G*. Data are reported as (a) cyclobutanone and amount; (b) amount of AcOH; (c) amount of Zn dust; (d) cyclobutanone and yield.

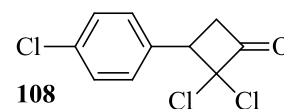
**Entry 1** (a) **108**, 5.98 g, 24 mmol; (b) 150 ml 0.16 M; (c) 9.36 g, 144 mmol, 6 eq; (d) **43**, 3.42 g, 79%.

**Entry 2** (a) **108**, 17.95 g, 72 mmol; (b) 450 ml, 0.16 M; (c) 28.08 g, 432 mmol, 6 eq; (d) **43**, 5.07 g, 39%.

**Entry 5** (a) **108**, 13.97 g, 56 mmol; (b) 350 ml, 0.16 M; (c) 21.84 g, 336 mmol, 6 eq; (d) **43**, 4.65 g, 46%.

Preparation of

2,2-dichloro-3-(4'-chlorophenyl)cyclobutanone **108**<sup>52</sup>



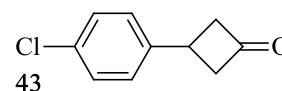
**Scheme 58**

Prepared according to *General Procedure F*. Data are reported as (a) styrene derivative and amount; (b) amount of Zn-Cu couple (prepared according to *General Procedure E*); (c) total volume of Et<sub>2</sub>O; (d) amount of trichloroacetyl chloride; (e) amount of phosphorus(V) oxychloride; (f) product and yield.

(a) 4-chlorostyrene **104**, 4.64 g, 33 mmol, 1 eq; (b) 6.44 g, 99 mmol, 3 eq, (c) 100 ml, 0.33 M; (d) 15.00 g, 82.5 mmol, 2.5 eq; (e) 12.65 g, 82.5 mmol, 2.5; (f) **108**, 8.23 g, 100%.

<sup>1</sup>H NMR (400 MHz, CDCl<sub>3</sub>): δ 3.58 (dd, 1H, *J* = 10.2 Hz, <sup>2</sup>*J*<sub>H-H</sub> = 17.6 Hz, CH<sub>2</sub>), 3.69 (dd, 1H, *J* = 10.4 Hz, <sup>2</sup>*J*<sub>H-H</sub> = 17.6 Hz, CH<sub>2</sub>), 4.23 (t, 1H, *J* = 10.3 Hz, CH), 7.25 (d, 2H, *J* = 8.4 Hz, 2 x ArH), 7.41 (d, 2H, *J* = 8.4 Hz, 2 x ArH).

Preparation of 3-(4'-chlorophenyl)cyclobutanone **43**<sup>52</sup>



**Scheme 59**

Prepared according to *General Procedure G*. Data are reported as (a) cyclobutanone and amount; (b) amount of AcOH; (c) amount of Zn dust; (d) cyclobutanone and yield.

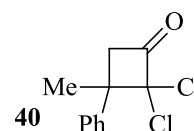
(a) **108**, 8.23 g, 33 mmol, 1 eq; (b) 206 ml 0.16 M; (c) 12.87 g, 198 mmol, 6 eq; (d) **43**, 2.74 g, 46%.

<sup>1</sup>H NMR (400 MHz, CDCl<sub>3</sub>): δ 3.18 – 3.25 (m, 2H, CH<sub>2</sub>), 3.48 – 3.55 (m, 2H, CH<sub>2</sub>), 3.67 (pent, 1H, *J* = 8.1 Hz, CH), 7.24 (d, 2H, *J* = 8.3 Hz, 2 x ArH), 7.33 (d, 2H, *J* = 8.5 Hz, 2 x ArH).

<sup>13</sup>C NMR (100 MHz, CDCl<sub>3</sub>): δ 27.7, 54.3, 127.8, 128.4, 131.9, 142.0, 205.3.

FTIR (neat): 1778 cm<sup>-1</sup>.

Preparation of 2,2-dichloro-3-methyl-3-phenylcyclobutanone **40**<sup>52</sup>



**Scheme 60, Table 28**

Prepared according to *General Procedure F*. Data are reported as (a) styrene derivative and amount; (b) amount of Zn-Cu couple (*General Procedure E*); (c) total volume of Et<sub>2</sub>O; (d) amount of trichloroacetyl chloride; (e) amount of phosphorus(V) oxychloride; (f) product and yield.

**Entry 1:** (a) **106**, 3.89g, 33 mmol; (b) 6.44 g, 99 mmol, 3 eq; (c) 100 ml, 0.33 M; (d) 15.02 g, 82.5 mmol, 2.5 eq; (e) 12.66 g, 82.5 mmol, 2.5 eq; (f) **109**, 3.78 g, 50% <sup>1</sup>H NMR yield.

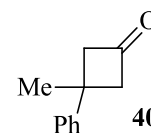
**Entry 2:** (a) **106**, 5.90 g, 50 mmol; (b) 9.75 g, 150 mmol, 3 eq; (c) 150 ml, 0.33 M; (d) 22.83 g, 125 mmol, 2.5 eq; (e) 19.17 g, 125 mmol, 2.5; (f) **109**, 9.39 g, 82% <sup>1</sup>H NMR yield.

<sup>1</sup>H NMR (400 MHz, CDCl<sub>3</sub>): δ 1.69 (s, 3H, CH<sub>3</sub>), 3.11 (d, 1H, *J* = 16.4 Hz, CH<sub>2</sub>), 4.03 (d, 1H, *J* = 16.3 Hz, CH<sub>2</sub>), 7.22 – 7.32 (m, 5H, 5 x ArH).



Preparation of 3-methyl-3-phenylcyclobutanone **40**<sup>52</sup>

**Scheme 61, Table 29**



Prepared according to *General Procedure G*. Data are reported as (a) cyclobutanone and amount; (b) amount of AcOH; (c) amount of Zn dust; (d) cyclobutanone and yield.

**Table 8, Entry 1:** (a) **109**, 3.66 g, 16 mmol, 1 eq; (b) 100 ml, 0.16 M; (c) 6.24 g, 96 mmol, 6 eq; (d) **40**, 2.02 g, 79%.

**Table 8, Entry 2:** (a) **109**, 9.39 g, 41 mmol, 1eq; (b) 256 ml, 0.16 M; (c) 15.99 g, 246 mmol, 6 eq; (d) **40**, 3.21 g, 49%.

<sup>1</sup>H NMR (400 MHz, CDCl<sub>3</sub>): δ 1.64 (s, 3H, CH<sub>3</sub>), 3.14 (d, 2H, <sup>2</sup>J<sub>H-H</sub> = 19.4 Hz, CH<sub>2</sub>), 3.50 (d, 2H, <sup>2</sup>J<sub>H-H</sub> = 19.2 Hz, CH<sub>2</sub>), 7.26 – 7.36 (m, 5H, 5 x ArH).

<sup>13</sup>C NMR (100 MHz, CDCl<sub>3</sub>): δ 30.9, 33.8, 59.1, 125.6, 126.2, 128.5, 148.2, 206.1.

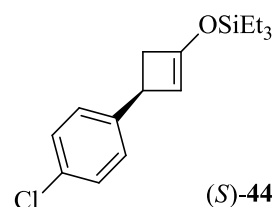
FTIR (neat): 1778 cm<sup>-1</sup>.

## 5.5 Asymmetric deprotonations to afford enantioenriched silyl enol ethers

### 5.5.1 Optimisation of reaction conditions

Preparation of (*S*)-((3-(4-chlorophenyl)cyclobut-1-en-1-yl)oxy)triethylsilane **44**<sup>29</sup>

**Scheme 62, Table 30**



Following *General Procedure A* for the formation of Mg-bisamide (*R,R*)-**70**, data are reported as: (a) amount of *n*-Bu<sub>2</sub>Mg; (b) amine used; (c) amount of amine.

Following *General Procedure C* for the asymmetric deprotonation, data are reported as: (a) Mg-base; (b) Lewis base additive; (c) electrophile; (d) ketone; (e) temperature; (f) isolated yield; (g) er.

**Entry 1:** *General Procedure A:* (a) 1.00 ml, 1 M in THF, 1 mmol, 1 eq; (b) (*R*)-bis((*R*)-1-phenylethyl)amine **34**; (c) 0.44 ml, 2 mmol, 2 eq.

*General Procedure C:* (a) (*R,R*)-**70** (0.1 M in THF, 1 mmol, 1 eq); (b) DMPU, 60  $\mu$ l, 0.5 mmol, 0.5 eq; (c) TESCl, 0.67 ml, 4 mmol, 4 eq; (d) 3-(4'-chlorophenyl)cyclobutanone **43**, 144 mg, 0.8 mmol, 0.8 eq; (e) -78 °C; (f) 0 mg, 0%; (g) -.

**Entry 2:** *General Procedure A:* (a) 1.00 ml, 1 M in THF, 1 mmol, 1 eq; (b) (*R*)-bis((*R*)-1-phenylethyl)amine **34**; (c) 0.44 ml, 2 mmol, 2 eq.

*General Procedure C:* (a) (*R,R*)-**70** (0.1 M in THF, 1 mmol, 1 eq); (b) DMPU, 60  $\mu$ l, 0.5 mmol, 0.5 eq; (c) TESCl, 0.67 ml, 4 mmol, 4 eq; (d) 3-(4'-chlorophenyl)cyclobutanone **43**, 144 mg, 0.8 mmol, 0.8 eq; (e) rt; (f) 0 mg, 0%; (g) -.

**Entry 3:** *General Procedure A:* (a) 1.00 ml, 1 M in THF, 1 mmol, 1 eq; (b) (*R*)-bis((*R*)-1-phenylethyl)amine **34**; (c) 0.44 ml, 2 mmol, 2 eq.

For the asymmetric deprotonation under EQ conditions, the Schlenk flask containing (*R,R*)-**70** (0.1 M, in THF, 1 mmol, 1 eq) was cooled to -78 °C and DMPU (60  $\mu$ l, 0.5 mmol, 0.5 eq) was added. A flame-dried pear-shaped flask under argon was charged with 3-(4'-chlorophenyl)cyclobutanone **43** (144 mg, 0.8 mmol, 0.8 eq) and freshly distilled THF (2 ml); this solution was subsequently added to the Schlenk flask over a period of 1 h *via* syringe pump. The reaction was stirred at -78 °C for 16 h before quenching with TESCl (0.67 ml, 4 mmol, 4 eq) and stirring for a further 1 h. After this time the reaction mixture was quenched with a saturated solution of NaHCO<sub>3</sub> (10 ml) and warmed to room temperature. The reaction mixture was extracted with diethyl ether (3 x 20 ml) to give a solution of the crude product which was dried over Na<sub>2</sub>SO<sub>4</sub>, filtered, and concentrated *in vacuo* to give an oil. Purification *via* flash chromatography provided only starting cyclobutanone **43**.

### Scheme 63, Table 31

Following *General Procedure A* for the formation of Mg-bisamide (*R,R*)-**70**, data are reported as: (a) amount of *n*-Bu<sub>2</sub>Mg; (b) amine used; (c) amount of amine.

Following *General Procedure C* for the asymmetric deprotonation, data are reported as: (a) Mg-base; (b) Lewis base additive; (c) electrophile; (d) ketone; (e) temperature; (f) isolated yield; (g) er.

**Entry 1:** *General Procedure A*: (a) 1.00 ml, 1 M in THF, 1 mmol, 1 eq; (b) (*R*)-bis((*R*)-1-phenylethyl)amine **34**; (c) 0.44 ml, 2 mmol, 2 eq.

*General Procedure C*: (a) (*R,R*)-**70** (0.1 M in THF, 1 mmol, 1 eq); (b) DMPU, 60  $\mu$ l, 0.5 mmol, 0.5 eq; (c) TESCl, 0.36 ml, 2 mmol, 2 eq; (d) 3-(4'-chlorophenyl)cyclobutanone **43**, 144 mg, 0.8 mmol, 0.8 eq; (e) -78 °C; (f) 6 mg, trace; (g) -.

**Entry 2:** *General Procedure A*: (a) 1.00 ml, 1 M in THF, 1 mmol, 1 eq; (b) (*R*)-bis((*R*)-1-phenylethyl)amine **34**; (c) 0.44 ml, 2 mmol, 2 eq.

*General Procedure C*: (a) (*R,R*)-**70** (0.1 M in THF, 1 mmol, 1 eq); (b) DMPU, 120  $\mu$ l, 1 mmol, 1 eq; (c) TESCl, 0.67 ml, 4 mmol, 4 eq; (d) 3-(4'-chlorophenyl)cyclobutanone **43**, 144 mg, 0.8 mmol, 0.8 eq; (e) -78 °C; (f) 5 mg, trace; (g) -.

### Scheme 64, Table 32

Following *General Procedure B* for the formation of Mg-bisamide (*R,R*)-**70**, data are reported as: (a) amount of LiCl; (b) amount of *n*-Bu<sub>2</sub>Mg; (c) amine used; (d) amount of amine.

Following *General Procedure C* for the asymmetric deprotonation, data are reported as: (a) Mg-base; (b) Lewis base additive; (c) electrophile; (d) ketone; (e) temperature; (f) isolated yield; (g) er; (h)  $[\alpha]_D$ .

**Entry 1:** *General Procedure B:* (a) 85 mg, 2 mmol, 2 eq; (b) 1.00 ml, 1 M in THF, 1 mmol, 1 eq; (c) (*R*)-bis((*R*)-1-phenylethyl)amine **34**; (d) 0.44 ml, 2 mmol, 2 eq.

*General Procedure C:* (a) (*R,R*)-**70** (0.1 M in THF, 1 mmol, 1 eq); (b) DMPU, 60  $\mu$ l, 0.5 mmol, 0.5 eq; (c) TESCl, 0.15 ml, 0.9 mmol, 0.9 eq; (d) 3-(4'-chlorophenyl)cyclobutanone **43**, 144 mg, 0.8 mmol, 0.8 eq; (e) rt; (f) 132 mg, 56%; (g) 53.5:46.5, calculated from the  $[\alpha]_D$  value for this sample; (h)  $-0.29^\circ$  ( $c = 1$ , CHCl<sub>3</sub>).

**Entry 2:** *General Procedure B:* (a) 85 mg, 2 mmol, 2 eq; (b) 1.00 ml, 1 M in THF, 1 mmol, 1 eq; (c) (*R*)-bis((*R*)-1-phenylethyl)amine **34**; (d) 0.44 ml, 2 mmol, 2 eq.

*General Procedure C:* (a) (*R,R*)-**70** (0.1 M in THF, 1 mmol, 1 eq); (b) DMPU, 60  $\mu$ l, 0.5 mmol, 0.5 eq; (c) TESCl, 0.36 ml, 2 mmol, 2 eq; (d) 3-(4'-chlorophenyl)cyclobutanone **43**, 144 mg, 0.8 mmol, 0.8 eq; (e) rt; (f) 127 mg, 54%; (g) 57:43, calculated from the  $[\alpha]_D$  value for this sample; (h)  $-0.61^\circ$  ( $c = 1$ , CHCl<sub>3</sub>).

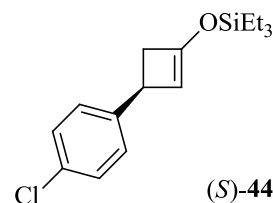
**Entry 3:** *General Procedure B:* (a) 85 mg, 2 mmol, 2 eq; (b) 1.00 ml, 1 M in THF, 1 mmol, 1 eq; (c) (*R*)-bis((*R*)-1-phenylethyl)amine **34**; (d) 0.44 ml, 2 mmol, 2 eq.

*General Procedure C:* (a) (*R,R*)-**70** (0.1 M in THF, 1 mmol, 1 eq); (b) DMPU, 60  $\mu$ l, 0.5 mmol, 0.5 eq; (c) TESCl, 0.67 ml, 4 mmol, 4 eq; (d) 3-(4'-chlorophenyl)cyclobutanone **43**, 144 mg, 0.8 mmol, 0.8 eq; (e) rt; (f) 179 mg, 76%; (g) 55:45, calculated from the  $[\alpha]_D$  value for this sample; (h)  $-0.44^\circ$  ( $c = 1$ , CHCl<sub>3</sub>).

<sup>1</sup>H NMR (400 MHz, CDCl<sub>3</sub>):  $\delta$  0.75 (q, 6H,  $J = 8.0$  Hz, SiCH<sub>2</sub>CH<sub>3</sub>), 1.03 (t, 9H,  $J = 8.0$  Hz, SiCH<sub>2</sub>CH<sub>3</sub>), 2.33 (dd, 1H,  $^2J_{\text{H-H}}, J = 1.7, 13.0$  Hz, CH<sub>2</sub>), 3.10 (dd, 1H,  $^2J_{\text{H-H}}, J = 4.6, 13.0$  Hz, CH<sub>2</sub>), 3.52 – 3.53 (m, 1H, CH), 4.84 (d, 1H,  $J = 0.8$  Hz, C=CH), 7.20 – 7.26 (m, 4H, ArH).

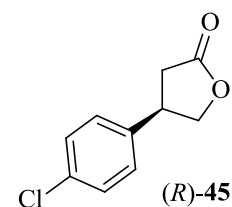
<sup>13</sup>C NMR (100 MHz, CDCl<sub>3</sub>):  $\delta$  5.9 (3C), 6.3 (3C), 27.5, 54.2, 127.4 (2C), 128.3 (2C), 128.6, 132.0, 141.5, 151.0.

FTIR (CHCl<sub>3</sub>): 845, 998, 1212, 1571, 1622, 1640, 2914, 2969, 3071 cm<sup>-1</sup>.



Preparation of (*R*)-4-(4-chlorophenyl)dihydrofuran-2(3*H*)-one  
**45**<sup>52</sup>

**Scheme 65**



A flame-dried three-neck flask was charged with (*S*)-((3-(4-chlorophenyl)cyclobut-1-en-1-yl)oxy)triethylsilane **44** (65 mg, 0.22 mmol, 1 eq, with 55:45 (*S*):(*R*)) and methanol (7 ml) and cooled to -78 °C. Ozone was bubbled through the solution until the starting material had disappeared, as shown by TLC (approximately 25 min). Oxygen was then bubbled through the reaction mixture to remove the excess ozone and the flask was transferred to an argon line. Sodium borohydride (42 mg, 1.1 mmol, 5 eq) was added at -78 °C and the reaction mixture was slowly warmed to room temperature and stirred for 2 h. After this time, the methanol was removed *in vacuo* and the residue was treated with 2 M HCl (7 ml). The now acidic reaction mixture was extracted with EtOAc (3 x 20 ml) and the combined extracts were washed with saturated brine (50 ml) before drying over Na<sub>2</sub>SO<sub>4</sub>, filtering and concentrating *in vacuo*. The crude product was purified by silica gel chromatography, eluting with 10 – 50% Et<sub>2</sub>O in PE (30 – 40 °C) to afford (*S*)-**45** as a colourless oil, 40 mg, 67% yield, and 55:45 er.

Chiral HPLC analysis: Chiracel OJ column, 1% IPA in *n*-hexane, 1.5 ml/min flow rate, 254 nm detector,  $t_R$  (*S*)-**45** = 42.5 min and  $t_R$  (*R*)-**45** = 44.2 min.

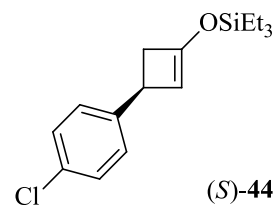
<sup>1</sup>H NMR (400 MHz, CDCl<sub>3</sub>): δ 2.62 (dd, 1H, <sup>2</sup>*J*<sub>H-H</sub>, *J* = 17.1, 8.8 Hz, CH<sub>2</sub>), 2.93 (dd, 1H, <sup>2</sup>*J*<sub>H-H</sub>, *J* = 17.1, 8.8 Hz, CH<sub>2</sub>), 3.77 (pent, 1H, *J* = 8.8 Hz, CH), 4.23 (dd, 1H, <sup>2</sup>*J*<sub>H-H</sub>, *J* = 8.8, 7.8 Hz, CH<sub>2</sub>), 4.65 (dd, 1H, <sup>2</sup>*J*<sub>H-H</sub>, *J* = 8.8, 7.8 Hz, CH<sub>2</sub>), 7.17 (d, 2H, *J* = 8.3 Hz, 2 x ArH), 7.34 (d, 2H, *J* = 8.3 Hz, 2 x ArH).

<sup>13</sup>C NMR (100 MHz, CDCl<sub>3</sub>): δ 35.6, 40.5, 73.7, 128.0 (2C), 129.2 (2C), 133.5, 137.9, 175.8.

FTIR (CHCl<sub>3</sub>): 1763 cm<sup>-1</sup>.

Preparation of (*S*)-((3-(4-chlorophenyl)cyclobut-1-en-1-yl)oxy)triethylsilane **44**<sup>29</sup>

**Scheme 66**



Following *General Procedure B* for the formation of Mg-bisamide (*R,R*)-**70**, data are reported as: (a) amount of LiCl; (b) *n*-Bu<sub>2</sub>Mg; (c) amine used; (d) amount of amine.

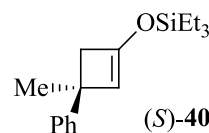
Following *General Procedure C* for the asymmetric deprotonation, data are reported as: (a) Mg-base; (b) Lewis base additive; (c) electrophile; (d) ketone; (e) temperature; (f) isolated yield; (g) er.

*General Procedure B*: (a) 85 mg, 2 mmol, 2 eq; (b) 1.00 ml, 1 M in THF, 1 mmol, 1 eq; (c) (*R*)-bis((*R*)-1-phenylethyl)amine **34**; (d) 0.44 ml, 2 mmol, 2 eq.

*General Procedure C*: (a) (*R,R*)-**70** (0.1 M in THF, 1 mmol, 1 eq); (b) DMPU, 60  $\mu$ l, 0.5 mmol, 0.5 eq; (c) TESCl, 0.67 ml, 4 mmol, 4 eq; (d) 3-(4'-chlorophenyl)cyclobutanone **43**, 144 mg, 0.8 mmol, 0.8 eq; (e) -78  $^{\circ}$ C; (f) 56 mg, 24%; (g) -.

Preparation of (*S*)-triethyl((3-methyl-3-phenylcyclobut-1-en-1-yl)oxy)silane **40**<sup>28a</sup>

**Scheme 67, Table 33**



Following *General Procedure B* for the formation of Mg-bisamide (*R,R*)-**70**, data are reported as: (a) amount of LiCl; (b) *n*-Bu<sub>2</sub>Mg; (c) amine used; (d) amount of amine.

Following *General Procedure C* for the asymmetric deprotonation, data are reported as: (a) Mg-base; (b) Lewis base additive; (c) electrophile; (d) ketone; (e) temperature; (f) isolated yield; (g)  $[\alpha]_D^{20}$ ; (h) er.

**Entry 1:** *General Procedure B*: (a) 85 mg, 2 mmol, 2 eq; (b) 1.00 ml, 1 M in THF, 1 mmol, 1 eq; (c) (*R*)-bis((*R*)-1-phenylethyl)amine **34**; (d) 0.44 ml, 2 mmol, 2 eq.

*General Procedure C:* (a) (*R,R*)-**70** (0.1 M in THF, 1 mmol, 1 eq); (b) DMPU, 60  $\mu$ l, 0.5 mmol, 0.5 eq; (c) TESC*l*, 0.15 ml, 0.9 mmol, 0.9 eq; (d) 3-methyl-3-phenylcyclobutanone **40**, 128 mg, 0.8 mmol, 0.8 eq; (e) -78  $^{\circ}$ C; (f) 118 mg, 54%; (g) -5.7  $^{\circ}$  (c = 1, CHCl<sub>3</sub>); (h) 55:45.

**Entry 2:** *General Procedure B:* (a) 85 mg, 2 mmol, 2 eq; (b) 1.00 ml, 1 M in THF, 1 mmol, 1 eq; (c) (*R*)-bis(*R*)-1-phenylethylamine **34**; (d) 0.44 ml, 2 mmol, 2 eq.

*General Procedure C:* (a) (*R,R*)-**70** (0.1 M in THF, 1 mmol, 1 eq); (b) DMPU, 60  $\mu$ l, 0.5 mmol, 0.5 eq; (c) TESC*l*, 0.34 ml, 2 mmol, 2 eq; (d) 3-methyl-3-phenylcyclobutanone **40**, 128 mg, 0.8 mmol, 0.8 eq; (e) -78  $^{\circ}$ C; (f) 171 mg, 78%; (g) -8.8  $^{\circ}$  (c = 1, CHCl<sub>3</sub>); (h) 57:43.

**Entry 3:** *General Procedure B:* (a) 85 mg, 2 mmol, 2 eq; (b) 1.00 ml, 1 M in THF, 1 mmol, 1 eq; (c) (*R*)-bis(*R*)-1-phenylethylamine **34**; (d) 0.44 ml, 2 mmol, 2 eq.

*General Procedure C:* (a) (*R,R*)-**70** (0.1 M in THF, 1 mmol, 1 eq); (b) DMPU, 60  $\mu$ l, 0.5 mmol, 0.5 eq; (c) TESC*l*, 0.67 ml, 4 mmol, 4 eq; (d) 3-methyl-3-phenylcyclobutanone **40**, 128 mg, 0.8 mmol, 0.8 eq; (e) -78  $^{\circ}$ C; (f) 140 mg, 64%; (g) -9.1  $^{\circ}$  (c = 1, CHCl<sub>3</sub>); (h) 58:42.

## Scheme 68

Following *General Procedure A* for the formation of Mg-bisamide (*R,R*)-**70**, data are reported as: (a) amount *n*-Bu<sub>2</sub>Mg; (b) amine used; (c) amount of amine.

Following *General Procedure C* for the asymmetric deprotonation, data are reported as: (a) Mg-base; (b) Lewis base additive; (c) electrophile; (d) ketone; (e) temperature; (f) isolated yield; (g) [ $\alpha$ ]<sub>D</sub><sup>20</sup>; (h) er.

*General Procedure A:* (a) 1.00 ml, 1 M in THF, 1 mmol, 1 eq; (b) (*R*)-bis(*R*)-1-phenylethylamine **34**; (c) 0.44 ml, 2 mmol, 2 eq.

*General Procedure C:* (a) (*R,R*)-**70** (0.1 M in THF, 1 mmol, 1 eq); (b) DMPU, 60  $\mu$ l, 0.5 mmol, 0.5 eq; (c) TESC*l*, 0.34 ml, 2 mmol, 2 eq; (d) 3-methyl-3-phenylcyclobutanone **40**, 128 mg, 0.8 mmol, 0.8 eq; (e) -78  $^{\circ}$ C; (f) 0 mg, 0%; (g) -; (h) -.

## Scheme 69

Following *General Procedure B* for the formation of Mg-bisamide (*R,R*)-**70**, data are reported as: (a) amount of LiCl; (b) *n*-Bu<sub>2</sub>Mg; (c) amine used; (d) amount of amine.

Following *General Procedure C* for the asymmetric deprotonation, data are reported as: (a) Mg-base; (b) Lewis base additive; (c) electrophile; (d) ketone; (e) temperature; (f) isolated yield; (g)  $[\alpha]_D^{20}$ ; (h) er.

*General Procedure B*: (a) 85 mg, 2 mmol, 2 eq; (b) 1.00 ml, 1 M in THF, 1 mmol, 1 eq; (c) (*R*)-bis((*R*)-1-phenylethyl)amine **34**; (d) 0.44 ml, 2 mmol, 2 eq.

*General Procedure C*: (a) (*R,R*)-**70** (0.1 M in THF, 1 mmol, 1 eq); (b) none; (c) TESCl, 0.34 ml, 2 mmol, 2 eq; (d) 3-methyl-3-phenylcyclobutanone **40**, 128 mg, 0.8 mmol, 0.8 eq; (e) -78 °C; (f) 99 mg, 45%; (g) -8.3 ° (c = 1, CHCl<sub>3</sub>); (h) 57:43.

## Scheme 70

Following *General Procedure B* for the formation of Mg-bisamide (*R,R*)-**70**, data are reported as: (a) amount of LiCl; (b) *n*-Bu<sub>2</sub>Mg; (c) amine used; (d) amount of amine.

Following *General Procedure C* for the asymmetric deprotonation, data are reported as: (a) Mg-base; (b) Lewis base additive; (c) electrophile; (d) ketone; (e) temperature; (f) isolated yield; (g) er (as determined by chiral HPLC).

*General Procedure B*: (a) 85 mg, 2 mmol, 2 eq; (b) 1.00 ml, 1 M in THF, 1 mmol, 1 eq; (c) (*R*)-bis((*R*)-1-phenylethyl)amine **34**; (d) 0.44 ml, 2 mmol, 2 eq.

*General Procedure C*: (a) (*R,R*)-**70** (0.1 M in THF, 1 mmol, 1 eq); (b) 60 μl, 0.5 mmol, 0.5 eq; (c) TESCl, 0.34 ml, 2 mmol, 2 eq; (d) 3-methyl-3-phenylcyclobutanone **40**, 128 mg, 0.8 mmol, 0.8 eq; (e) -78 °C; (f) 90 mg, 41%; (g) 81:19.

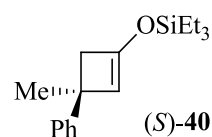
Chiral HPLC analysis: Chiracel OJ column, 100% *n*-hexane, 0.25 ml/min flow rate, 254 nm detector,  $t_R$  (minor, (*R*)-**40**) = 27.2 min and  $t_R$  (major, (*S*)-**40**) = 29.3 min.

<sup>1</sup>H NMR (400 MHz, CDCl<sub>3</sub>): δ 0.74 (q, 6H, *J* = 7.9 Hz, Si(CH<sub>2</sub>CH<sub>3</sub>)<sub>3</sub>), 1.02 (t, 9H, *J* = 7.9 Hz, Si(CH<sub>2</sub>CH<sub>3</sub>)<sub>3</sub>), 1.56 (s, 3H, CH<sub>3</sub>), 2.72 (s, 2H, CH<sub>2</sub>), 5.08 (s, 1H, C=CH), 7.18 – 7.22 (m, 1H, ArH), 7.28 – 7.34 (m, 4H, 4 x ArH).



$^{13}\text{C}$  NMR (100 MHz,  $\text{CDCl}_3$ ):  $\delta$  4.3, 6.0, 27.5, 30.6, 49.4, 58.8, 109.7, 125.0, 125.1, 125.5, 125.8, 127.4, 128.1.

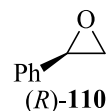
FTIR ( $\nu_{\text{max}}$ ,  $\text{CHCl}_3$ ):  $1611\text{ cm}^{-1}$ .



### 5.5.2 Comparison with a chelating magnesium bisamide

Preparation of (*R*)-styrene oxide **110**<sup>41b,55</sup>

#### Scheme 71, Table 34



A round-bottom flask was charged with Jacobsen catalyst (*R,R*)-**116**, toluene, and acetic acid. The solution was stirred for 90 min under air to activate the catalyst. After this time, the solvent was evaporated to leave a brown residue which was dried under vacuum for 30 min. ( $\pm$ )-Styrene oxide **110**, THF, and water were added and a  $\text{CaCl}_2$  drying tube was fitted to the reaction flask. The reaction mixture was stirred for 72 h at rt. After this time, the reaction vessel was fitted with a Vigreux distillation column and receiver flasks. The red reaction mixture was carefully heated under vacuum to remove the water and THF. The flask was then heated to 89 – 90 °C at 31 mbar to distil (*R*)-styrene oxide **110** away from the reaction mixture, which was obtained as a colourless oil. After cooling the reaction mixture to rt, the residue was suspended in MeOH and the catalyst was filtered then washed with MeOH for re-use.

**Table 34:** Data are presented as (a) amount of catalyst (*R,R*)-**116**; (b) amount of toluene; (c) amount of acetic acid; (d) amount of ( $\pm$ )-styrene oxide **110**; (e) amount of THF; (f) amount of water; (g) yield of (*R*)-styrene oxide **110**; (h)  $[\alpha]_{\text{D}}^{20}$ ; (i) ee (%).

**Entry 1:** (a) 193 mg, 0.32 mmol, 1.6 mol%; (b) 1.60 ml, 0.2 M (w.r.t. catalyst); (c) 38  $\mu\text{l}$ , 0.64 mmol, 3.2 mol%; (d) 2.40 g, 20 mmol, 1 eq; (e) 2.3 ml, 8.7 M (w.r.t. ( $\pm$ )-styrene oxide **110**); (f) 250  $\mu\text{l}$ , 14 mmol, 0.7 eq; (g) 441 mg, 18%; (h)  $+5.668^\circ$  ( $c = 2.47$ , acetone); (i) 99%.

**Entry 2:** (a) 2.00 g, 3.31 mmol, 1.6 mol%; (b) 16 ml, 0.2 M (w.r.t. catalyst); (c) 0.38 ml, 6.62 mmol, 3.2 mol%; (d) 24.87 g, 207 mmol, 1 eq; (e) 23.6 ml, 8.7 M (w.r.t.

(±)-styrene oxide **110**); (f) 2.61 ml, 145 mmol, 0.7 eq; (g) 10.90 g, 44%; (h) +5.656 ° (c = 2.47, acetone); (i) >99%.

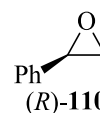
**Entry 3:** (a) 2.00 g, 3.31 mmol, 1.6 mol%; (b) 16 ml, 0.2 M (w.r.t. catalyst); (c) 0.38 ml, 6.62 mmol, 3.2 mol%; (d) 24.87 g, 207 mmol, 1 eq; (e) 23.6 ml, 8.7 M (w.r.t. (±)-styrene oxide **110**); (f) 2.61 ml, 145 mmol, 0.7 eq; (g) 7.96 g, 33%; (h) +5.847 ° (c = 2.47, acetone); (i) >99%.

$[\alpha]_{\text{D}}^{20} = +5.71$  ° (lit, c = 2.47, acetone)<sup>65</sup>

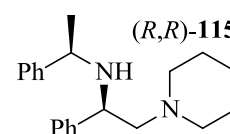
<sup>1</sup>H NMR (400 MHz, CDCl<sub>3</sub>): δ 2.80 (dd, 1H, <sup>2</sup>J<sub>H-H</sub> = 5.5 Hz, J = 2.6 Hz, CH<sub>2</sub>), 3.14 (dd, 1H, <sup>2</sup>J<sub>H-H</sub> = 5.5 Hz, J = 4.0 Hz, CH<sub>2</sub>), 3.85 (dd, 1H, J = 4.0, 2.6 Hz, CH), 7.26 – 7.37 (m, 5H, 5 x ArH).

<sup>13</sup>C NMR (100 MHz, CDCl<sub>3</sub>): δ 51.1, 52.3, 125.5, 128.3, 129.0, 137.6.

FTIR (neat): 815, 878, 2913, 2967, 3035, 3087 cm<sup>-1</sup>.



*Preparation of (R)-1-phenyl-N-((R)-1-phenylethyl)-2-(piperidin-1-yl)ethanamine **115***<sup>54,41b</sup>



### Scheme 72, Table 35

A round-bottom flask fitted with a reflux condenser was charged with (*R*)-styrene oxide **110**, piperidine **111** and EtOH. The reaction mixture was heated to reflux and stirred for 3 h. After cooling to rt, the EtOH was removed *in vacuo* to afford a mixture of regioisomeric amino alcohols **112** and **113** as a cream/white solid. The solid was dried by heating to 60 °C under vacuum for 1 h then re-cooled to rt. This regioisomeric mixture was dissolved in Et<sub>2</sub>O in a two-neck flask under argon and cooled to 0 °C. Triethylamine was added followed by the dropwise addition of methanesulfonyl chloride, resulting in the formation of a white precipitate which became difficult to stir. The reaction mixture was stirred at 0 °C for 5 min then warmed to rt and stirred for 1 h. After this time, triethylamine, (*R*)-(+)- $\alpha$ -methylbenzylamine **102**, and water were added and the reaction mixture was stirred vigorously for 16 h. The biphasic mixture was separated and the aqueous layer was extracted with Et<sub>2</sub>O (x 3). The combined organics were washed with saturated NaHCO<sub>3</sub> solution and water, then dried over Na<sub>2</sub>SO<sub>4</sub>, filtered, and concentrated *in*

*vacuo*. The orange oil obtained was distilled under Kugelrohr apparatus to remove excess (*R*)-(+)- $\alpha$ -methylbenzylamine **102** (90 °C, 0.02 mbar) and additional impurities (120 °C, 0.2 mbar). The remaining oil was subsequently heated to 180 °C at 0.2 mbar for 4 h to remove any traces of water before purging with and storing under argon.

**Table 35:** Data are presented as (a) amount of (*R*)-styrene oxide **110**; (b) amount of piperidine **111**; (c) amount of EtOH; (d) amount of Et<sub>2</sub>O; (e) amount of Et<sub>3</sub>N; (f) amount of MsCl; (g) second amount of Et<sub>3</sub>N; (h) amount of (*R*)-(+)- $\alpha$ -methylbenzylamine **102**; (i) amount of water; (j) yield of (*R,R*)-**115**; (k) ee.

**Entry 1:** (a) 409 mg, 3.4 mmol, 1 eq; (b) 477 mg, 5.6 mmol, 1.65 eq; (c) 4.5 ml, 0.8 M; (d) 12 ml, 0.29 M; (e) 0.76 ml, 5.44 mmol, 1.6 eq; (f) 0.32 ml, 4.08 mmol, 1.2 eq; (g) 0.95 ml, 6.8 mmol, 2 eq; (h) 0.49 ml, 4.08 mmol, 1.2 eq; (i) 1.94 ml, 1.75 M; (j) 209 mg, 20%; (k) -.

*NB:* Distillation was not performed for this entry. Purification of the crude product was performed by silica gel chromatography, eluting with 40:10:4 PE (40 – 60 °) : DCM : MeOH.

**Entry 2:** (a) 5.89 g, 49 mmol, 1 eq; (b) 7.98 ml, 80.9 mmol, 1.65 eq; (c) 60 ml, 0.8 M; (d) 170 ml, 0.29 M; (e) 10.93 ml, 78.4 mmol, 1.6 eq; (f) 4.55 ml, 58.8 mmol, 1.2 eq; (g) 13.65 ml, 98.0 mmol, 2 eq; (h) 7.47 ml, 58.8 mmol, 1.2 eq; (i) 28.0 ml, 1.75 M; (j) 9.90 g, 65%; (k) >99%.

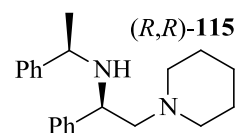
**Entry 3:** (a) 8.53 g, 71 mmol, 1 eq; (b) 4.54 ml, 46 mmol, 1.65 eq; (c) 90 ml, 0.8 M; (d) 245 ml, 0.29 M; (e) 15.80 ml, 113.6 mmol, 1.6 eq; (f) 6.60 ml, 85.2 mmol, 1.2 eq; (g) 19.80 ml, 142 mmol, 2 eq; (h) 10.80 ml, 85.2 mmol, 1.2 eq; (i) 40.60 ml, 1.75 M; (j) 17.19 g, 79%; (k) >99%.

$$[\alpha]_{\text{D}}^{20} = -47^{\circ} (c = 1, \text{CHCl}_3) (\text{lit} = -46^{\circ}, c = 1, \text{CHCl}_3)^{54}$$

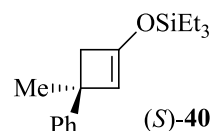
<sup>1</sup>H NMR (400 MHz, CDCl<sub>3</sub>):  $\delta$  1.37 (d, 3H, *J* = 6.6 Hz, CH<sub>3</sub>), 1.43 – 1.46 (m, 2H, CH<sub>2</sub>), 1.56 – 1.62 (m, 4H, 2 x CH<sub>2</sub>), 2.27 – 2.31 (m, 4H, 2 x CH<sub>2</sub>), 2.45 – 2.54 (m, 3H, CH<sub>2</sub> + NH), 3.78 (q, 1H, *J* = 6.6 Hz, CH), 3.97 (dd, 1H, *J* = 10.6, 3.8 Hz, CH), 7.16 – 7.27 (m, 10H, 2 x Ph).

$^{13}\text{C}$  NMR (100 MHz,  $\text{CDCl}_3$ ):  $\delta$  21.3, 24.1, 25.8, 54.1, 54.6, 57.2, 65.9, 126.0, 126.3, 126.4, 127.2, 127.7, 127.7, 127.8, 143.2, 146.0.

FTIR ( $\nu_{\text{max}}$ ,  $\text{CHCl}_3$ ): 3304  $\text{cm}^{-1}$ .



Preparation of (*S*)-triethyl((3-methyl-3-phenylcyclobut-1-en-1-yl)oxy)silane **40**



### Scheme 73

Following *General Procedure A* for the formation of Mg-bisamide (*R,R*)-**67**, data are reported as: (a) amount of  $n\text{-Bu}_2\text{Mg}$ ; (b) amine used; (c) amount of amine.

Following *General Procedure C* for the asymmetric deprotonation, data are reported as: (a) Mg-base; (b) Lewis base additive; (c) electrophile; (d) ketone; (e) temperature; (f) isolated yield; (g) er.

*General Procedure A*: (a) 1.00 ml, 1 M in THF, 1 mmol, 1 eq; (b) (*R*)-1-phenyl-*N*-((*R*)-1-phenylethyl)-2-(piperidin-1-yl)ethanamine **115**; (d) 0.62 ml, 2 mmol, 2 eq.

*General Procedure C*: (a) (*R,R*)-**67** (0.1 M in THF, 1 mmol, 1 eq); (b) DMPU, 60  $\mu\text{l}$ , 0.5 mmol, 0.5 eq; (c)  $\text{TESCl}$ , 0.34 ml, 2 mmol, 2 eq; (d) 3-methyl-3-phenylcyclobutanone **39**, 128 mg, 0.8 mmol, 0.8 eq; (e)  $-78\text{ }^\circ\text{C}$ ; (f) 0 mg, 0%; (g) -.

### Scheme 74, Table 36

Following *General Procedure B* for the formation of Mg-bisamide (*R,R*)-**67**, data are reported as: (a) amount of  $\text{LiCl}$ ; (b) amount of  $n\text{-Bu}_2\text{Mg}$ ; (c) amine used; (d) amount of amine.

Following *General Procedure C* for the asymmetric deprotonation, data are reported as: (a) Mg-base; (b) Lewis base additive; (c) electrophile; (d) ketone; (e) temperature; (f) isolated yield; (g) er (as determined by chiral HPLC).

**Entry 1:** *General Procedure B:* (a) 85 mg, 2 mmol, 2 eq; (b) 1.00 ml, 1 M in THF, 1 mmol, 1 eq; (b) (*R*)-1-phenyl-N-((*R*)-1-phenylethyl)-2-(piperidin-1-yl)ethanamine **115**; (d) 0.62 ml, 2 mmol, 2 eq.

*General Procedure C:* (a) (*R,R*)-**67** (0.1 M in THF, 1 mmol, 1 eq); (b) DMPU, 60  $\mu$ l, 0.5 mmol, 0.5 eq; (c) TESCl, 0.34 ml, 2 mmol, 2 eq; (d) 3-methyl-3-phenylcyclobutanone **39**, 128 mg, 0.8 mmol, 0.8 eq; (e) -78 °C; (f) 127 mg, 58%; (g) 60:40.

**Entry 2:** *General Procedure B:* (a) 85 mg, 2 mmol, 2 eq; (b) 1.00 ml, 1 M in THF, 1 mmol, 1 eq; (b) (*R*)-1-phenyl-N-((*R*)-1-phenylethyl)-2-(piperidin-1-yl)ethanamine **115**; (d) 0.62 ml, 2 mmol, 2 eq.

*General Procedure C:* (a) (*R,R*)-**67** (0.1 M in THF, 1 mmol, 1 eq); (b) DMPU, 60  $\mu$ l, 0.5 mmol, 0.5 eq; (c) TESCl, 0.34 ml, 2 mmol, 2 eq; (d) 3-methyl-3-phenylcyclobutanone **39**, 128 mg, 0.8 mmol, 0.8 eq; (e) -40 °C; (f) 116 mg, 53%; (g) 57:43.

**Entry 3:** *General Procedure B:* (a) 85 mg, 2 mmol, 2 eq; (b) 1.00 ml, 1 M in THF, 1 mmol, 1 eq; (b) (*R*)-1-phenyl-N-((*R*)-1-phenylethyl)-2-(piperidin-1-yl)ethanamine **115**; (d) 0.62 ml, 2 mmol, 2 eq.

*General Procedure C:* (a) (*R,R*)-**67** (0.1 M in THF, 1 mmol, 1 eq); (b) DMPU, 60  $\mu$ l, 0.5 mmol, 0.5 eq; (c) TESCl, 0.34 ml, 2 mmol, 2 eq; (d) 3-methyl-3-phenylcyclobutanone **39**, 128 mg, 0.8 mmol, 0.8 eq; (e) -20 °C; (f) 153 mg, 70%; (g) 55:45.

**Entry 4:** (a) *General Procedure B:* (a) 85 mg, 2 mmol, 2 eq; (b) 1.00 ml, 1 M in THF, 1 mmol, 1 eq; (b) (*R*)-1-phenyl-N-((*R*)-1-phenylethyl)-2-(piperidin-1-yl)ethanamine **115**; (d) 0.62 ml, 2 mmol, 2 eq.

*General Procedure C:* (a) (*R,R*)-**67** (0.1 M in THF, 1 mmol, 1 eq); (b) DMPU, 60  $\mu$ l, 0.5 mmol, 0.5 eq; (c) TESCl, 0.34 ml, 2 mmol, 2 eq; (d) 3-methyl-3-phenylcyclobutanone **39**, 128 mg, 0.8 mmol, 0.8 eq; (e) 0 °C; (f) 164 mg, 75%; (g) 55:45.

## Scheme 75

Following *General Procedure A* for the formation of Mg-bisamide (*R,R*)-**67**, data are reported as: (a) amount of *n*-Bu<sub>2</sub>Mg; (b) amine used; (c) amount of amine.

Following *General Procedure C* for the asymmetric deprotonation, data are reported as: (a) Mg-base; (b) Lewis base additive; (c) electrophile; (d) ketone; (e) temperature; (f) isolated yield; (g) er.

*General Procedure A*: (a) 1.00 ml, 1 M in THF, 1 mmol, 1 eq; (b) (*R*)-1-phenyl-*N*-((*R*)-1-phenylethyl)-2-(piperidin-1-yl)ethanamine **115**; (d) 0.62 ml, 2 mmol, 2 eq.

*General Procedure C*: (a) (*R,R*)-**67** (0.1 M in THF, 1 mmol, 1 eq); (b) DMPU, 60  $\mu$ l, 0.5 mmol, 0.5 eq; (c) TESCl, 0.34 ml, 2 mmol, 2 eq; (d) 3-methyl-3-phenylcyclobutanone **39**, 128 mg, 0.8 mmol, 0.8 eq; (e) 0 °C; (f) 171 mg, 78%; (g) 78:22.

## Scheme 76, Table 37

*n*-Bu<sub>2</sub>Mg (1 ml, 1 M solution in heptanes, 1 mmol, 1 eq) was transferred to a flame-dried Schlenk tube and the solvent removed *in vacuo* (0.005 mbar) until the appearance of a white solid. THF (10 ml) was then added followed by (*R*)-1-phenyl-*N*-((*R*)-1-phenylethyl)-2-(piperidin-1-yl)ethanamine **115** (0.62 ml, 2 mmol, 2 eq) and the mixture was stirred at rt for 90 min under an atmosphere of argon. After this time, quantitative formation of the alkylmagnesium amide (*R*)-**118** (1 mmol, 0.1 M in THF) was assumed. The solution of chiral magnesium base was cooled to the appropriate temperature under argon. The Schlenk flask was then charged with DMPU (60  $\mu$ l, 0.5 mmol, 0.5 eq) followed by TESCl (0.34 ml, 2 mmol, 2 eq) and the mixture was stirred for 10 min at the temperature stated. 3-Methyl-3-phenylcyclobutanone **39** (128 mg, 0.8 mmol, 0.8 eq) was added to a flame-dried pear-shaped flask under argon and dissolved in freshly distilled THF (2 ml). The ketone solution was subsequently added to the reaction mixture over a period of 1 h *via* syringe pump. The resulting solution was allowed to stir at the temperature stated for 16 h before quenching with a saturated solution of NaHCO<sub>3</sub> (10 ml) and warming to room temperature. The reaction mixture was extracted with diethyl ether (3 x 20

ml) to give a solution of the crude product which was dried over Na<sub>2</sub>SO<sub>4</sub>, filtered, and concentrated *in vacuo* to give an oil. Purification *via* flash chromatography provided the silyl enol ether (*S*)-**40** as a colourless oil.

Following the above procedure, data are reported as (a) temperature; (b) yield.

**Entry 1:** (a) -78 °C; (b) 0 mg, 0%; (i) -.

**Entry 2:** (a) 0 °C; (b) 0 mg, 0%; (i) -.

### Scheme 77, Table 38

Following *General Procedure B* for the formation of Mg-bisamide (*R,R*)-**70**, data are reported as: (a) amount of LiCl; (b) *n*-Bu<sub>2</sub>Mg; (c) amine used; (d) amount of amine.

Following *General Procedure C* for the asymmetric deprotonation, data are reported as: (a) Mg-base; (b) Lewis base additive; (c) electrophile; (d) ketone; (e) temperature; (f) isolated yield; (g) er (as determined by chiral HPLC).

**Entry 1:** *General Procedure B*: (a) 85 mg, 2 mmol, 2 eq; (b) 1.00 ml, 1 M in THF, 1 mmol, 1 eq; (c) (*R*)-bis((*R*)-1-phenylethyl)amine **34**; (d) 0.44 ml, 2 mmol, 2 eq.

*General Procedure C*: (a) (*R,R*)-**70** (0.1 M in THF, 1 mmol, 1 eq); (b) DMPU, 60 μl, 0.5 mmol, 0.5 eq; (c) TESCl, 0.34 ml, 2 mmol, 2 eq; (d) 3-methyl-3-phenylcyclobutanone **39**, 128 mg, 0.8 mmol, 0.8 eq; (e) 0 °C; (f) 134 mg, 61%; (g) 56:44.

**Entry 2:** *General Procedure B*: (a) 85 mg, 2 mmol, 2 eq; (b) 1.00 ml, 1 M in THF, 1 mmol, 1 eq; (c) (*R*)-bis((*R*)-1-phenylethyl)amine **34**; (d) 0.44 ml, 2 mmol, 2 eq.

*General Procedure C*: (a) (*R,R*)-**70** (0.1 M in THF, 1 mmol, 1 eq); (b) DMPU, 60 μl, 0.5 mmol, 0.5 eq; (c) TESCl, 0.34 ml, 2 mmol, 2 eq; (d) 3-methyl-3-phenylcyclobutanone **39**, 128 mg, 0.8 mmol, 0.8 eq; (e) -20 °C; (f) 147 mg, 67%; (g) 57:43.

**Entry 3:** *General Procedure B*: (a) 85 mg, 2 mmol, 2 eq; (b) 1.00 ml, 1 M in THF, 1 mmol, 1 eq; (c) (*R*)-bis((*R*)-1-phenylethyl)amine **34**; (d) 0.44 ml, 2 mmol, 2 eq.

*General Procedure C*: (a) (*R,R*)-**70** (0.1 M in THF, 1 mmol, 1 eq); (b) DMPU, 60 μl, 0.5 mmol, 0.5 eq; (c) TESCl, 0.34 ml, 2 mmol, 2 eq; (d) 3-methyl-3-

phenylcyclobutanone **39**, 128 mg, 0.8 mmol, 0.8 eq; (e) -40 °C; (f) 99 mg, 45%; (g) 53:47.

**Entry 4: General Procedure B:** (a) 85 mg, 2 mmol, 2 eq; (b) 1.00 ml, 1 M in THF, 1 mmol, 1 eq; (c) (*R,R*)-bis(*R*)-1-phenylethylamine **34**; (d) 0.44 ml, 2 mmol, 2 eq.

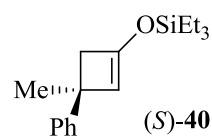
*General Procedure C:* (a) (*R,R*)-**70** (0.1 M in THF, 1 mmol, 1 eq); (b) DMPU, 60  $\mu$ l, 0.5 mmol, 0.5 eq; (c) TESCl, 0.34 ml, 2 mmol, 2 eq; (d) 3-methyl-3-phenylcyclobutanone **39**, 128 mg, 0.8 mmol, 0.8 eq; (e) -78 °C; (f) 94 mg, 43%; (g) 67:33.

Chiral HPLC analysis: Chiracel OJ column, 100% *n*-hexane, 0.25 ml/min flow rate, 254 nm detector,  $t_R$  (minor) = 27.2 min and  $t_R$  (major) = 29.3 min.

$^1\text{H}$  NMR (400 MHz,  $\text{CDCl}_3$ ):  $\delta$  0.73 (q, 6H,  $J = 7.8$  Hz,  $\text{SiCH}_2\text{CH}_3$ ), 1.01 (t, 9H,  $J = 7.9$  Hz,  $\text{SiCH}_2\text{CH}_3$ ), 1.55 (s, 3H,  $\text{CH}_3$ ), 2.71 (s, 2H,  $\text{CH}_2$ ), 5.06 (s, 1H,  $\text{C}=\text{CH}$ ), 7.17 – 7.20 (m, 1H, *Ph*), 7.28 – 7.32 (m, 2H, *Ph*), 7.35 – 7.38 (m, 2H, *Ph*).

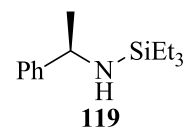
$^{13}\text{C}$  NMR (100 MHz,  $\text{CDCl}_3$ ):  $\delta$  4.3 (3C), 6.0 (3C), 27.5, 30.6, 49.4, 58.8, 109.7, 125.0, 125.1, 125.5, 125.8, 127.4, 128.1

FTIR ( $\nu_{\text{max}}$ ,  $\text{CHCl}_3$ ): 1611  $\text{cm}^{-1}$ .



*By-product isolated:*

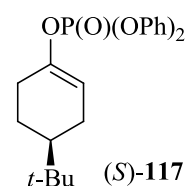
$^1\text{H}$  NMR (400 MHz,  $\text{CDCl}_3$ ):  $\delta$  0.60 (q, 6H,  $J = 8.0$  Hz,  $\text{Si}(\text{CH}_2\text{CH}_3)_3$ ), 0.98 (t, 9H,  $J = 8.0$  Hz,  $\text{Si}(\text{CH}_2\text{CH}_3)_3$ ), 1.28 (d, 3H,  $J = 6.5$  Hz,  $\text{CH}_3$ ), 3.51 (q, 1H,  $J = 6.6$  Hz,  $\text{CH}$ ), 7.22 – 7.27 (m, 3H, *Ph*), 7.32 – 7.36 (m, 2H, *Ph*).





## 5.6 Asymmetric deprotonations to afford enantioenriched enol phosphates

Preparation of (*S*)-*O,O*-diphenyl 4-*tert*-butylcyclohex-1-enylphosphonate **117**<sup>66</sup>



### Scheme 78

Following *General Procedure A* for the formation of Mg-bisamide (*R,R*)-**67**, data are reported as: (a) amount of *n*-Bu<sub>2</sub>Mg; (b) amine used; (c) amount of amine.

Following *General Procedure D* for the asymmetric deprotonation, data are reported as: (a) Mg-base; (b) Lewis base additive; (c) electrophile; (d) ketone; (e) temperature; (f) isolated yield; (g) er (as determined by chiral HPLC).

*General Procedure A*: (a) 1.00 ml, 1 M in THF, 1 mmol, 1 eq; (b) (*R*)-bis((*R*)-1-phenylethyl)amine **34**; (c) 0.44 ml, 2 mmol, 2 eq.

*General Procedure D*: (a) (*R,R*)-**70** (0.1 M in THF, 1 mmol, 1 eq); (b) DMPU, 60  $\mu$ l, 0.5 mmol, 0.5 eq; (c) diphenylphosphoryl chloride, 0.83 ml, 4 mmol, 4 eq; (d) 4-*tert*-butylcyclohexanone **12**, 123 mg, 0.8 mmol, 0.8 eq; (e) -78  $^{\circ}$ C; (f) 232 mg, 75%; (g) 96:4.

Chiral HPLC analysis: Chiralcel OD-H column, 1% IPA in *n*-hexane, 1.40 ml/min, 254 nm detector,  $t_R$  (minor) = 26.2 min,  $t_R$  (major) = 25.4 min.

$[\alpha]_D^{20} = -35^{\circ}$  (96:4 er,  $c = 1$ , CHCl<sub>3</sub>). No literature data are available for comparison.

<sup>1</sup>H NMR (400 MHz, CDCl<sub>3</sub>):  $\delta$  0.87 (s, 9H, C(CH<sub>3</sub>)<sub>3</sub>), 1.23 – 1.37 (m, 2H, CH<sub>2</sub>), 1.81 – 1.92 (m, 2H, CH<sub>2</sub>), 2.06 – 2.15 (m, 1H, CH), 2.19 – 2.34 (m, 2H, CH<sub>2</sub>), 5.53 – 5.57 (m, 1H, C=CH), 7.17 – 7.38 (m, 10H, 2 x ArH).

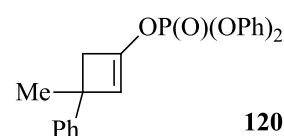
<sup>13</sup>C NMR (100 MHz, CDCl<sub>3</sub>):  $\delta$  23.6, 24.6, 26.9, 28.3, 31.7, 42.8, 111.4, 119.7, 125.0, 147.4, 150.3.

<sup>31</sup>P NMR (162 MHz, CDCl<sub>3</sub>):  $\delta$  -17.5.

FTIR ( $\nu_{\max}$ , CHCl<sub>3</sub>): 964, 1192, 1691 cm<sup>-1</sup>.

### 5.6.1 Introduction of an alternative electrophile

Preparation of 3-methyl-3-phenylcyclobut-1-en-1-yl diphenyl phosphate **120**



#### Scheme 79

Following *General Procedure H*, the data are reported as (a) ketone; (b) enol phosphate, yield.

(a) 3-Methyl-3-phenylcyclobutanone **39**, 144 mg, 0.9 mmol, 0.9 eq; (b) **120**, 237 mg, 75%.

$^1\text{H}$  NMR (400 MHz,  $\text{CDCl}_3$ ):  $\delta$  1.57 (s, 3H,  $\text{CH}_3$ ), 2.90 (s, 2H,  $\text{CH}_2$ ), 5.62 (s, 1H,  $\text{CH}=\text{C}$ ), 7.20 – 7.27 (m, 9H, 9 x  $\text{ArH}$ ), 7.26 – 7.33 (m, 6H, 6 x  $\text{ArH}$ ).

$^{13}\text{C}$  NMR (100 MHz,  $\text{CDCl}_3$ ):  $\delta$  26.7, 41.6, 48.1 (d, 1C,  $^3J_{\text{C-P}} = 5.5$  Hz), 117.3 (d, 1C,  $^3J_{\text{C-P}} = 7.6$  Hz), 119.6 (d, 2C,  $^3J_{\text{C-P}} = 4.9$  Hz), 125.2, 125.4, 125.6, 127.7, 129.2, 141.2 (d, 1C,  $^2J_{\text{C-P}} = 9.8$  Hz), 145.7, 149.8 (d, 1C,  $^2J_{\text{C-P}} = 7.1$  Hz).

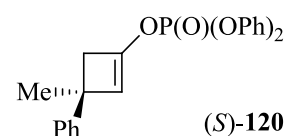
$^{31}\text{P}$  NMR (400 MHz,  $\text{CDCl}_3$ ):  $\delta$  -18.1.

FTIR (neat): 1182, 1300, 1487, 2864, 2953, 3053  $\text{cm}^{-1}$ .

HRMS (ESI)  $m/z$  calculated for  $\text{C}_{23}\text{H}_{22}\text{O}_4\text{P}$   $[\text{M}+\text{H}]^+$ : 393.1250. Found: 393.1252.

### 5.6.2 Additive studies

Preparation of 3-methyl-3-phenylcyclobut-1-en-1-yl diphenyl phosphate (*S*)-**120**



#### Scheme 80

Following *General Procedure B* for the formation of Mg-bisamide (*R,R*)-**67**, data are reported as: (a) amount of LiCl; (b) amount of *n*- $\text{Bu}_2\text{Mg}$ ; (c) amine used; (d) amount of amine.

Following *General Procedure D* for the asymmetric deprotonation, data are reported as: (a) Mg-base; (b) Lewis base additive; (c) electrophile; (d) ketone; (e) temperature; (f) isolated yield; (g) er (as determined by chiral HPLC).

*General Procedure B*: (a) 85 mg, 2 mmol, 2 eq; (b) 1.00 ml, 1 M in THF, 1 mmol, 1 eq; (c) (*R*)-bis((*R*)-1-phenylethyl)amine **34**; (d) 0.44 ml, 2 mmol, 2 eq.

*General Procedure D*: (a) (*R,R*)-**70** (0.1 M in THF, 1 mmol, 1 eq); (b) DMPU, 60  $\mu$ l, 0.5 mmol, 0.5 eq; (c) diphenylphosphoryl chloride, 0.21 ml, 1 mmol, 1 eq; (d) 3-methyl-3-phenylcyclobutanone **39**, 128 mg, 0.8 mmol, 0.8 eq; (e) -78 °C; (f) 82 mg, 26%; (g) 78:22.

### Scheme 81

Following *General Procedure B* for the formation of Mg-bisamide (*R,R*)-**67**, data are reported as: (a) amount of LiCl; (b) amount of *n*-Bu<sub>2</sub>Mg; (c) amine used; (d) amount of amine.

Following *General Procedure D* for the asymmetric deprotonation, data are reported as: (a) Mg-base; (b) Lewis base additive; (c) electrophile; (d) ketone; (e) temperature; (f) isolated yield; (g) er (as determined by chiral HPLC).

*General Procedure B*: (a) 85 mg, 2 mmol, 2 eq; (b) 1.00 ml, 1 M in THF, 1 mmol, 1 eq; (c) (*R*)-1-phenyl-*N*-((*R*)-1-phenylethyl)-2-(piperidin-1-yl)ethanamine **115**; (d) 0.62 ml, 2 mmol, 2 eq.

*General Procedure D*: (a) (*R,R*)-**67** (0.1 M in THF, 1 mmol, 1 eq); (b) DMPU, 60  $\mu$ l, 0.5 mmol, 0.5 eq; (c) diphenylphosphoryl chloride, 0.21 ml, 1 mmol, 1 eq; (d) 3-methyl-3-phenylcyclobutanone **39**, 128 mg, 0.8 mmol, 0.8 eq; (e) -78 °C, (f) 47 mg, 15%; (g) 92:8.

### Scheme 82, Table 39

Following *General Procedure A* for the formation of Mg-bisamide (*R,R*)-**67**, data are reported as: (a) amount of *n*-Bu<sub>2</sub>Mg; (b) amine used; (c) amount of amine.

Following *General Procedure D* for the asymmetric deprotonation, data are reported as: (a) Mg-base; (b) Lewis base additive; (c) electrophile; (d) ketone; (e) temperature; (f) isolated yield; (g) er (as determined by chiral HPLC).

**Entry 1:** *General Procedure A:* (a) 1.00 ml, 1 M in THF, 1 mmol, 1 eq; (b) (*R*)-1-phenyl-*N*-((*R*)-1-phenylethyl)-2-(piperidin-1-yl)ethanamine **115**; (c) 0.62 ml, 2 mmol, 2 eq.

*General Procedure D:* (a) (*R,R*)-**67** (0.1 M in THF, 1 mmol, 1 eq; (b) DMPU, 60  $\mu$ l, 0.5 mmol, 0.5 eq; (c) diphenylphosphoryl chloride, 0.21 ml, 1 mmol, 1 eq; (d) 3-methyl-3-phenylcyclobutanone **39**, 128 mg, 0.8 mmol, 0.8 eq; (e) -78  $^{\circ}$ C; (f) 125 mg, 40%; (g) 84:16.

**Entry 2:** *General Procedure A:* (a) 1.00 ml, 1 M in THF, 1 mmol, 1 eq; (b) (*R*)-1-phenyl-*N*-((*R*)-1-phenylethyl)-2-(piperidin-1-yl)ethanamine **115**; (c) 0.62 ml, 2 mmol, 2 eq.

*General Procedure D:* (a) (*R,R*)-**67** (0.1 M in THF, 1 mmol, 1 eq; (b) DMPU, 60  $\mu$ l, 0.5 mmol, 0.5 eq; (c) diphenylphosphoryl chloride, 0.42 ml, 2 mmol, 2 eq; (d) 3-methyl-3-phenylcyclobutanone **39**, 128 mg, 0.8 mmol, 0.8 eq; (e) -78  $^{\circ}$ C; (f) 201 mg, 64%; (g) 72:28.

**Entry 3:** *General Procedure A:* (a) 1.00 ml, 1 M in THF, 1 mmol, 1 eq; (b) (*R*)-1-phenyl-*N*-((*R*)-1-phenylethyl)-2-(piperidin-1-yl)ethanamine **115**; (c) 0.62 ml, 2 mmol, 2 eq.

*General Procedure D:* (a) (*R,R*)-**67** (0.1 M in THF, 1 mmol, 1 eq; (b) DMPU, 60  $\mu$ l, 0.5 mmol, 0.5 eq; (c) diphenylphosphoryl chloride, 0.83 ml, 4 mmol, 4 eq; (d) 3-methyl-3-phenylcyclobutanone **39**, 128 mg, 0.8 mmol, 0.8 eq; (e) -78  $^{\circ}$ C; (f) 116 mg, 37%; (g) 98:2.

### Scheme 83

Following *General Procedure A* for the formation of Mg-bisamide (*R,R*)-**67**, data are reported as: (a) amount of *n*-Bu<sub>2</sub>Mg; (b) amine used; (c) amount of amine.

Following *General Procedure D* for the asymmetric deprotonation, data are reported as: (a) Mg-base; (b) Lewis base additive; (c) electrophile; (d) ketone; (e) temperature; (f) isolated yield; (g) er (as determined by chiral HPLC).

*General Procedure A:* (a) 1.00 ml, 1 M in THF, 1 mmol, 1 eq; (b) (*R*)-1-phenyl-*N*-((*R*)-1-phenylethyl)-2-(piperidin-1-yl)ethanamine **115**; (c) 0.62 ml, 2 mmol, 2 eq.

*General Procedure D:* (a) (*R,R*)-**67** (0.1 M in THF, 1 mmol, 1 eq; (b) none; (c) diphenylphosphoryl chloride, 0.42 ml, 2 mmol, 2 eq; (d) 3-methyl-3-phenylcyclobutanone **39**, 128 mg, 0.8 mmol, 0.8 eq; (e) -78 °C; (f) 248 mg, 79%; (g) 99:1.

#### **Scheme 84**

Following *General Procedure A* for the formation of Mg-bisamide (*R,R*)-**67**, data are reported as: (a) amount of *n*-Bu<sub>2</sub>Mg; (b) amine used; (c) amount of amine.

Following *General Procedure D* for the asymmetric deprotonation, data are reported as: (a) Mg-base; (b) Lewis base additive; (c) electrophile; (d) ketone; (e) temperature; (f) isolated yield; (g) er (as determined by chiral HPLC).

*General Procedure A:* (a) 1.00 ml, 1 M in THF, 1 mmol, 1 eq; (b) (*R*)-1-phenyl-*N*-((*R*)-1-phenylethyl)-2-(piperidin-1-yl)ethanamine **115**; (c) 0.62 ml, 2 mmol, 2 eq.

*General Procedure D:* (a) (*R,R*)-**67** (0.1 M in THF, 1 mmol, 1 eq; (b) none; (c) diphenylphosphoryl chloride, 0.42 ml, 2 mmol, 2 eq; (d) 3-methyl-3-phenylcyclobutanone **39**, 128 mg, 0.8 mmol, 0.8 eq; (e) -40 °C; (f) 304 mg, 97%; (g) 89:11.

#### **Scheme 85, Table 40**

Following *General Procedure A* for the formation of Mg-bisamide (*R,R*)-**70**, data are reported as: (a) amount of *n*-Bu<sub>2</sub>Mg; (b) amine used; (c) amount of amine.

Following *General Procedure D* for the asymmetric deprotonation, data are reported as: (a) Mg-base; (b) Lewis base additive; (c) electrophile; (d) ketone; (e) temperature; (f) isolated yield; (g) er (as determined by chiral HPLC).

**Entry 1:** *General Procedure A:* (a) 1.00 ml, 1 M in THF, 1 mmol, 1 eq; (b) (*R*)-bis((*R*)-1-phenylethyl)amine **34**; (c) 0.44 ml, 2 mmol, 2 eq.

*General Procedure D:* (a) (*R,R*)-**70** (0.1 M in THF, 1 mmol, 1 eq; (b) none; (c) diphenylphosphoryl chloride, 0.21 ml, 1 mmol, 1 eq; (d) 3-methyl-3-phenylcyclobutanone **39**, 128 mg, 0.8 mmol, 0.8 eq; (e) -78 °C; (f) 198 mg, 63%; (g) 93:7.

**Entry 2:** *General Procedure A:* (a) 1.00 ml, 1 M in THF, 1 mmol, 1 eq; (b) (*R*)-bis((*R*)-1-phenylethyl)amine **34**; (c) 0.44 ml, 2 mmol, 2 eq.

*General Procedure D:* (a) (*R,R*)-**70** (0.1 M in THF, 1 mmol, 1 eq; (b) none; (c) diphenylphosphoryl chloride, 0.42 ml, 2 mmol, 2 eq; (d) 3-methyl-3-phenylcyclobutanone **39**, 128 mg, 0.8 mmol, 0.8 eq; (e) -78 °C; (f) 245 mg, 78%; (g) 96:4.

### **Scheme 86, Table 41**

Following *General Procedure A* for the formation of Mg-bisamide (*R,R*)-**67**, data are reported as: (a) amount of *n*-Bu<sub>2</sub>Mg; (b) amine used; (c) amount of amine.

Following *General Procedure D* for the asymmetric deprotonation, data are reported as: (a) Mg-base; (b) Lewis base additive; (c) electrophile; (d) ketone; (e) temperature; (f) isolated yield; (g) er (as determined by chiral HPLC).

**Entry 1:** *General Procedure A:* (a) 1.00 ml, 1 M in THF, 1 mmol, 1 eq; (b) (*R*)-bis((*R*)-1-phenylethyl)amine **34**; (c) 0.44 ml, 2 mmol, 2 eq.

*General Procedure D:* (a) (*R,R*)-**70** (0.1 M in THF, 1 mmol, 1 eq; (b) none; (c) diphenylphosphoryl chloride, 0.21 ml, 1 mmol, 1 eq; (d) 3-methyl-3-phenylcyclobutanone **39**, 128 mg, 0.8 mmol, 0.8 eq; (e) -40 °C; (f) 122 mg, 39%; (g) 97:3.

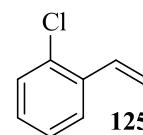
**Entry 2:** *General Procedure A:* (a) 1.00 ml, 1 M in THF, 1 mmol, 1 eq; (b) (*R*)-bis((*R*)-1-phenylethyl)amine **34**; (c) 0.44 ml, 2 mmol, 2 eq.

*General Procedure D:* (a) (*R,R*)-**70** (0.1 M in THF, 1 mmol, 1 eq; (b) none; (c) diphenylphosphoryl chloride, 0.42 ml, 2 mmol, 2 eq; (d) 3-methyl-3-phenylcyclobutanone **39**, 128 mg, 0.8 mmol, 0.8 eq; (e) -40 °C; (f) 191 mg, 61%; (g) 99:1.

### 5.6.3 Substrate scope

#### *Synthesis of styrene derivatives*

#### *Preparation of 2-chlorostyrene **125***<sup>50,67</sup>



#### **Scheme 87**

The following experiment was carried out according to *General Procedure I*. The data are reported as (a) amount of methyltriphenylphosphonium bromide; (b) amount of THF; (c) amount of *n*-BuLi; (d) carbonyl derivative, amount of carbonyl derivative; (e) styrene, yield.

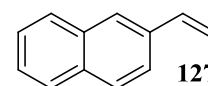
(a) 42.87 g, 120 mmol, 1.2 eq; (b) 500 ml, 0.2 M; (c) 44 ml, 2.5 M in hexanes, 110 mmol, 1.1 eq; (d) 2-chlorobenzaldehyde **126**, 11.26 ml, 100 mmol, 1 eq; (e) **125**, 6.02 g, 43%, as a yellow oil.

<sup>1</sup>H NMR (400 MHz, CDCl<sub>3</sub>): δ 5.42 (d, 1H, *J* = 11.0 Hz, C=CH<sub>2</sub>), 5.78 (d, 1H, *J* = 17.5 Hz, C=CH<sub>2</sub>), 7.15 (dd, 1H, *J* = 17.5, 11.0 Hz, CH=C), 7.21 – 7.29 (m, 2H, 2 x ArH), 7.38 – 7.41 (m, 1H, ArH), 7.59 – 7.62 (m, 1H, ArH).

<sup>13</sup>C NMR (100 MHz, CDCl<sub>3</sub>): δ 116.0, 126.1, 126.3, 128.3, 129.2, 132.74, 132.75, 135.3.

FTIR (neat): 943, 1042, 1628, 2957, 3067 cm<sup>-1</sup>.

#### *Preparation of 2-vinylnaphthalene **127***<sup>50,67</sup>



#### **Scheme 88**

The following experiment was carried out according to *General Procedure I*. The data are reported as (a) amount of methyltriphenylphosphonium bromide; (b) amount of THF; (c) amount of *n*-BuLi; (d) carbonyl derivative, amount of carbonyl derivative; (e) styrene, yield.

(a) 13.71 g, 38.4 mmol, 1.2 eq; (b) 160 ml, 0.2 M; (c) 14.08 ml, 2.5 M in hexanes, 35.2 mmol, 1.1 eq; (d) 2-naphthaldehyde **128**, 5.00 g, 32 mmol, 1 eq; (e) **127**, 4.16 g, 84%, as a white gummy solid.

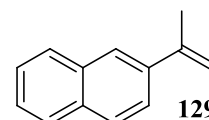
$^1\text{H}$  NMR (400 MHz,  $\text{CDCl}_3$ ):  $\delta$  5.35 (d, 1H,  $J = 10.9$  Hz,  $\text{C}=\text{CH}_2$ ), 5.89 (d, 1H,  $J = 17.6$  Hz,  $\text{C}=\text{CH}_2$ ), 6.90 (dd, 1H,  $J = 17.6, 10.9$  Hz,  $\text{CH}=\text{C}$ ), 7.43 – 7.50 (m, 2H, 2 x  $\text{ArH}$ ), 7.64 – 7.66 (m, 1H,  $\text{ArH}$ ), 7.77 (s, 1H,  $\text{ArH}$ ), 7.80 – 7.84 (m, 3H, 3 x  $\text{ArH}$ ).

$^{13}\text{C}$  NMR (100 MHz,  $\text{CDCl}_3$ ):  $\delta$  113.7, 122.8, 125.5, 125.8, 126.0, 127.3, 127.7, 127.8, 132.8, 133.2, 134.6, 136.6.

FTIR (neat): 820, 991, 1506, 3005, 3055  $\text{cm}^{-1}$ .

Preparation of 2-isopropenylphthalene **129**<sup>50,68</sup>

### Scheme 89



The following experiment was carried out according to *General Procedure I*. The data are reported as (a) amount of methyltriphenylphosphonium bromide; (b) amount of THF; (c) amount of *n*-BuLi; (d) carbonyl derivative, amount of carbonyl derivative; (e) styrene, yield.

(a) 17.57 g, 49.2 mmol, 1.2 eq; (b) 205 ml, 0.2 M; (c) 18.04 ml, 2.5 M in hexanes, 45.1 mmol, 1.1 eq; (d) 2-acetylnaphthone **130**, 7.00 g, 41 mmol, 1 eq; (e) **129**, 6.43 g, 93%, as a white gummy solid.

$^1\text{H}$  NMR (400 MHz,  $\text{CDCl}_3$ ):  $\delta$  2.45 (s, 3H,  $\text{CH}_3$ ), 5.38 (s, 1H,  $\text{C}=\text{CH}_2$ ), 5.72 (s, 1H,  $\text{C}=\text{CH}_2$ ), 7.58 – 7.64 (m, 2H, 2 x  $\text{ArH}$ ), 7.83 – 7.85 (m, 1H,  $\text{ArH}$ ), 7.92 – 7.97 (m, 3H, 3 x  $\text{ArH}$ ), 8.02 (s, 1H,  $\text{ArH}$ ).

$^{13}\text{C}$  NMR (100 MHz,  $\text{CDCl}_3$ ):  $\delta$  21.5, 112.7, 123.6, 123.9, 125.5, 125.8, 127.2, 127.4, 127.9, 132.5, 133.1, 138.0, 142.7.

FTIR (neat): 823, 883, 1504, 2972, 3053  $\text{cm}^{-1}$ .

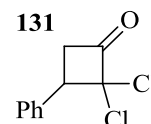


*Preparation of 2,2-dicyclobutanone intermediates*

**Scheme 90, Table 42**

The following experiments were carried out according to *General Procedure F*. The data are reported as (a) styrene derivative; (b) amount of zinc-copper couple; (c) total volume of Et<sub>2</sub>O; (d) amount of trichloroacetyl chloride; (e) amount of phosphorus(V) oxychloride; (f) cyclobutanone, <sup>1</sup>H NMR yield.

*Preparation of 2,2-dichloro-3-phenlcyclobutanone 131*<sup>52,69</sup>

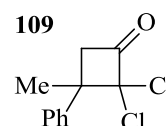


**Scheme 90, Table 42, Entry 1**

(a) styrene **131a**, 10.42 g, 100 mmol, 1 eq; (b) 19.50 g, 300 mmol, 3 eq; (c) 330 ml, 0.3 M; (d) 27.90 ml, 250 mmol, 2.5 eq; (e) 23.30 ml, 250 mmol, 2.5 eq; (f) 2,2-dichloro-3-phenlcyclobutanone **131**, 12.06 g, 56%.

<sup>1</sup>H NMR (400 MHz, CDCl<sub>3</sub>): δ 3.64 (dd, 1H, <sup>2</sup>J<sub>H-H</sub> = 17.6 Hz, J = 10.2 Hz, CH<sub>2</sub>), 3.87 (dd, 1H, <sup>2</sup>J = 17.6 Hz, J = 10.4 Hz, CH<sub>2</sub>), 4.42 (t, 1H, J = 10.2 Hz, CH), 7.72 – 7.89 (m, 5H, 5 x ArH).

*Preparation of 2,2-dichloro-3-methyl-3-phenlcyclobutanone 109*<sup>52,69</sup>



**Scheme 90, Table 42, Entry 2**

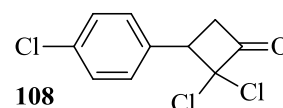
(a) α-methylstyrene **106**, 11.80 g, 100 mmol, 1 eq; (b) 19.50 g, 300 mmol, 3 eq; (c) 330 ml, 0.3 M; (d) 27.90 ml, 250 mmol, 2.5 eq; (e) 23.30 ml, 250 mmol, 2.5 eq; (f) 2,2-dichloro-3-methyl-3-phenlcyclobutanone **109**, 14.00 g, 61%.

<sup>1</sup>H NMR (400 MHz, CDCl<sub>3</sub>): δ 1.67 (s, 1H, CH<sub>3</sub>), 3.09 (d, 1H, <sup>2</sup>J<sub>H-H</sub> = 13.0 Hz, CH<sub>2</sub>), 4.01 (d, 1H, <sup>2</sup>J<sub>H-H</sub> = 13.1 Hz, CH<sub>2</sub>), 7.27 – 7.42 (m, 5H, 5 x ArH).

<sup>13</sup>C NMR (100 MHz, CDCl<sub>3</sub>): δ 29.4, 50.3, 52.5, 92.2, 126.4, 137.6, 128.6, 141.4, 191.9.

FTIR (neat): 1816 cm<sup>-1</sup>.

Preparation of 2,2,-dichloro-3-(4'-chlorophenyl)-  
cyclobutanone **108**<sup>29,52</sup>



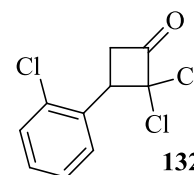
**Scheme 90, Table 42, Entry 3**

(a) 4-chlorostyrene **104**, 10.00 g, 72 mmol, 1 eq; (b) 14.04 g, 216 mmol, 3 eq; (c) 240 ml, 0.3 M; (d) 20.09 ml, 180 mmol, 2.5 eq; (e) 16.74 ml, 180 mmol, 2.5 eq; (f) 2,2,-dichloro-3-(4'-chlorophenyl)cyclobutanone **108**, 17.17 g, 96%.

<sup>1</sup>H NMR (400 MHz, CDCl<sub>3</sub>): δ 3.55 (dd, 1H, <sup>2</sup>J<sub>H-H</sub> = 17.6 Hz, J = 10.2 Hz, CH<sub>2</sub>), 3.67 (dd, 1H, <sup>2</sup>J<sub>H-H</sub> = 17.6 Hz, J = 10.4 Hz, CH<sub>2</sub>), 4.22 (t, 1H, J = 10.2 Hz, CH), 7.25 (d, 2H, J = 8.4 Hz, 2 x ArH), 7.41 (d, 2H, J = 8.4 Hz, 2 x ArH).

Preparation of 2,2,-dichloro-3-(2'-chlorophenyl)cyclobutanone **132**

**Scheme 90, Table 42, Entry 4**

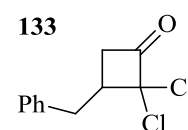


(a) 2-chlorostyrene **125**, 6.00 g, 43 mmol, 1 eq; (b) 8.39 g, 129 mmol, 3 eq; (c) 143 ml, 0.3 M; (d) 12.00 ml, 107.5 mmol, 2.5 eq; (e) 10.00 ml, 107.5 mmol, 2.5 eq; (f) 2,2,-dichloro-3-(2'-chlorophenyl)cyclobutanone **132**, 7.15 g, 67%.

<sup>1</sup>H NMR (400 MHz, CDCl<sub>3</sub>): δ 3.65 – 3.77 (m, 2H, CH<sub>2</sub>), 4.74 (t, 1H, J = 10.0 Hz, CH), 7.28 – 7.34 (m, 3H, 3 x ArH), 7.51 – 7.53 (m, 1H, ArH).

Preparation of 3-benzyl-2,2-dichlorocyclobutanone **133**<sup>69</sup>

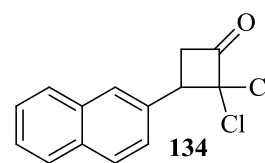
**Scheme 90, Table 42, Entry 5**



(a) allylbenzene **133a**, 5.90 g, 50 mmol, 1 eq; (b) 9.75 g, 150 mmol, 3 eq; (c) 160 ml, 0.3 M; (d) 14.00 ml, 125 mmol, 2.5 eq; (e) 11.63 ml, 125 mmol, 2.5 eq; (f) 3-benzyl-2,2,-dichloro-cyclobutanone **133**, 9.20 g, 80%.

<sup>1</sup>H NMR (400 MHz, CDCl<sub>3</sub>): δ 3.31 – 3.39 (m, 2H, CH+CH<sub>2</sub>), 3.30 (d, 2H, J = 7.5 Hz, CH<sub>2</sub>), 3.79 – 3.88 (m, 1H, CH<sub>2</sub>), 7.73 – 7.86 (m, 5H, 5 x ArH).

Preparation of 2,2-dichloro-3-(naphthalen-2-yl)-cyclobutanone **134**<sup>52,69</sup>

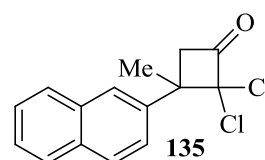


**Scheme 90, Table 42, Entry 6**

(a) 2-vinylnaphthalene **127**, 4.10 g, 26.6 mmol, 1 eq; (b) 5.20g, 80 mmol, 3 eq; (c) 90 ml, 0.3 M; (d) 7.42 ml, 66.5 mmol, 2.5 eq; (e) 6.19 ml, 66.5 mmol, 2.5 eq; (f) 2,2-dichloro-3-(naphthalen-2-yl)cyclobutanone **134**, 5.41 g, 77%.

<sup>1</sup>H NMR (400 MHz, CDCl<sub>3</sub>): δ 3.56 (dd, 1H, <sup>2</sup>J<sub>H-H</sub> = 17.6 Hz, J = 10.3 Hz, CH<sub>2</sub>), 3.73 (dd, 1H, <sup>2</sup>J<sub>H-H</sub> = 17.6 Hz, J = 10.5 Hz, CH<sub>2</sub>), 4.26 (t, 1H, J = 10.3 Hz, CH), 7.32 – 7.43 (m, 7H, 7 x ArH).

Preparation of 2,2-dichloro-3-methyl-3-(naphthalen-2-yl)cyclobutanone **135**<sup>70</sup>



**Scheme 90, Table 42, Entry 7**

(a) 2-isopropenylnaphthalene **129**, 6.43 g, 42 mmol, 1 eq; (b) 8.19 g, 126 mmol, 3 eq; (c) 140 ml, 0.3 M; (d) 11.73 ml, 105 mmol, 2.5 eq; (e) 9.77 ml, 105 mmol, 2.5 eq; (f) 2,2-dichloro-3-methyl-3-(naphthalen-2-yl)cyclobutanone **135**, 9.24 g, 79%.

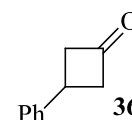
<sup>1</sup>H NMR (400 MHz, CDCl<sub>3</sub>): δ 1.75 (s, 3H, CH<sub>3</sub>), 3.20 (d, 1H, <sup>2</sup>J<sub>H-H</sub> = 16.4 Hz, CH<sub>2</sub>), 4.16 (d, 1H, <sup>2</sup>J<sub>H-H</sub> = 16.4 Hz, CH<sub>2</sub>), 7.47 – 7.55 (m, 3H, 3 x ArH), 7.66 (s, 1H, ArH), 7.82 – 7.89 (m, 3H, 3 x ArH).

Preparation of cyclobutanone substrates

**Scheme 91, Table 43**

The following experiments were carried out according to *General Procedure G*. The data are reported as (a) cyclobutanone starting material, amount; (b) amount of acetic acid; (c) amount of zinc dust; (d) cyclobutanone product, yield; (e) final purification.

*Preparation of 3-phenylcyclobutanone 36*<sup>52,69</sup>



**Scheme 91, Table 43, Entry 1**

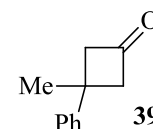
(a) 2,2-dichloro-3-phenylcyclobutanone **131**, 12.06 g, 56 mmol, 1 eq; (b) 350 ml, 0.16 M; (c) 21.84 g, 336 mmol, 6 eq; (d) 3-phenylcyclobutanone **36**, 4.90 g, 61%, yellow oil; (e) distilled under vacuum, 88 – 90 °C, 0.2 mbar.

<sup>1</sup>H NMR (400 MHz, CDCl<sub>3</sub>): δ 3.20 – 3.26 (m, 2H, CH<sub>2</sub>), 3.24 – 3.51 (m, 2H, CH<sub>2</sub>), 3.65 (dt, 1H, *J* = 8.8, 7.5 Hz, CH), 7.26 – 7.40 (m, 5H, 5 x ArH).

<sup>13</sup>C NMR (100 MHz, CDCl<sub>3</sub>): δ 28.2, 54.4 (2C), 126.3 (2C), 128.5 (2C), 143.5, 206.1.

FTIR (ν<sub>max</sub>, neat): 1778 cm<sup>-1</sup>.

*Preparation of 3-methyl-3-phenylcyclobutanone 39*<sup>52,69</sup>



**Scheme 91, Table 43, Entry 2**

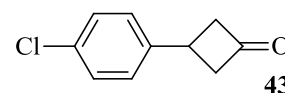
(a) 2,2-dichloro-3-methyl-3-phenylcyclobutanone **109**, 14.00 g, 61 mmol, 1 eq; (b) 380 ml, 0.16 M; (c) 23.79 g, 366 mmol, 6 eq; (d) 3-methyl-3-phenylcyclobutanone **39**, 6.21 g, 64%, colourless oil; (e) distilled under vacuum, 58 – 60 °C, 0.005 mbar.

<sup>1</sup>H NMR (400 MHz, CDCl<sub>3</sub>): δ 1.63 (s, 3H, CH<sub>3</sub>), 3.12 – 3.17 (m, 2H, CH<sub>2</sub>), 3.48 – 3.53 (m, 2H, CH<sub>2</sub>), 7.26 – 7.36 (m, 5H, 5 x ArH).

<sup>13</sup>C NMR (100 MHz, CDCl<sub>3</sub>): δ 30.9, 33.8, 59.1 (2C), 125.6 (2C), 126.1, 128.5 (2C), 148.2, 206.1.

FTIR (ν<sub>max</sub>, neat): 1778 cm<sup>-1</sup>.

Preparation of 3-(4'-chlorophenyl)cyclobutanone **43**<sup>29,52</sup>



**Scheme 91, Table 43, Entry 3**

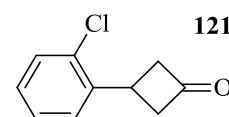
(a) 2,2-dichloro-3-(4'-chlorophenyl)cyclobutanone **108**, 17.10 g, 69 mmol, 1 eq; (b) 430 ml, 0.16 M; (c) 26.91 g, 414 mmol, 6 eq; (d) 3-(4'-chlorophenyl)cyclobutanone **43**, 4.45 g, 38%, pale yellow oil; (e) distilled under vacuum, 92 – 94 °C, 0.005 mbar.

<sup>1</sup>H NMR (400 MHz, CDCl<sub>3</sub>): δ 3.18 – 3.25 (m, 2H, CH<sub>2</sub>), 3.48 – 3.55 (m, 2H, CH<sub>2</sub>), 3.65 (dt, 1H, *J* = 8.8, 7.4 Hz, CH), 7.24 (d, 2H, *J* = 8.3 Hz, 2 x ArH), 7.33 (d, 2H, *J* = 8.5 Hz, 2 x ArH).

<sup>13</sup>C NMR (100 MHz, CDCl<sub>3</sub>): δ 27.7, 54.3 (2C), 127.8 (2C), 128.4 (2C), 131.9, 142.0, 205.3.

FTIR (ν<sub>max</sub>, neat): 1778 cm<sup>-1</sup>.

Preparation of 3-(2'-chlorophenyl)cyclobutanone **121**



**Scheme 91, Table 43, Entry 4**

(a) 2,2-dichloro-3-(2'-chlorophenyl)cyclobutanone **132**, 7.10 g, 28 mmol, 1 eq; (b) 175 ml, 0.16 M; (c) 10.92 g, 168 mmol, 6 eq; (d) 3-(2'-chlorophenyl)cyclobutanone **121**, 2.95 g, 58%, colourless oil; (e) distilled under vacuum, 88 – 90 °C, 0.02 mbar.

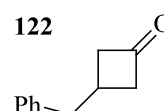
<sup>1</sup>H NMR (400 MHz, CDCl<sub>3</sub>): δ 3.22 – 3.31 (m, 2H, CH<sub>2</sub>), 3.48 – 3.58 (m, 2H, CH<sub>2</sub>), 3.97 (pent, 1H, *J* = 8.4 Hz, CH), 7.23 (dt, 1H, *J* = 7.6 Hz, <sup>4</sup>*J*<sub>H-H</sub> = 1.6 Hz, ArH), 7.30 (dt, 1H, *J* = 7.6 Hz, <sup>4</sup>*J*<sub>H-H</sub> = 1.6 Hz, ArH), 7.36 (dd, 1H, *J* = 7.6 Hz, <sup>4</sup>*J*<sub>H-H</sub> = 1.6 Hz, ArH), 7.42 (dd, 1H, *J* = 8.0 Hz, <sup>4</sup>*J*<sub>H-H</sub> = 1.6 Hz, ArH).

<sup>13</sup>C NMR (100 MHz, CDCl<sub>3</sub>): δ 26.8, 53.1 (2C), 126.7, 127.2, 128.2, 130.0, 134.5, 140.1, 206.3.

FTIR (ν<sub>max</sub>, neat): 1782 cm<sup>-1</sup>.

HMRS (ESI) *m/z* calculated for C<sub>10</sub>H<sub>10</sub>ClO [M+H]<sup>+</sup>: 181.0415. Found: 181.0414.

Preparation of 3-benzylcyclobutanone **122**<sup>69</sup>



Scheme 91, Table 43, Entry 5

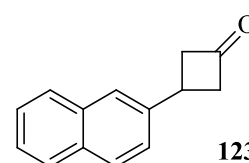
(a) 3-benzyl-2,2-dichlorocyclobutanone **133**, 9.20 g, 40 mmol, 1 eq; (b) 250 ml, 0.16 M; (c) 15.60 g, 240 mmol, 6 eq; (d) 3-benzylcyclobutanone **122**, 3.80 g, 60%, colourless oil; (e) distilled under vacuum, 74 – 76 °C, 0.005 mbar

<sup>1</sup>H NMR (400 MHz, CDCl<sub>3</sub>): δ 2.71 – 2.86 (m, 3H, CH+CH<sub>2</sub>), 2.93 (d, 2H, *J* = 7.4 Hz, CH<sub>2</sub>), 3.13 – 3.20 (m, 2H, CH<sub>2</sub>), 7.21 – 7.26 (m, 2H, 2 x ArH), 7.27 – 7.28 (m, 1H, ArH), 7.33 – 7.36 (m, 2H, 2 x ArH).

<sup>13</sup>C NMR (100 MHz, CDCl<sub>3</sub>): δ 24.6, 41.4, 51.8 (2C), 126.0 (2), 128.2 (3C), 139.8, 206.8.

FTIR (ν<sub>max</sub>, neat): 1775 cm<sup>-1</sup>.

Preparation of 3-(naphthalen-2-yl)cyclobutanone **123**<sup>52,69</sup>



Scheme 91, Table 43, Entry 6

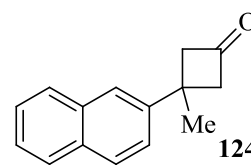
(a) 2,2-dichloro-3-(naphthalen-2-yl)cyclobutanone **134**, 5.41 g, 20 mmol, 1 eq; (b) 125 ml, 0.16 M; (c) 7.80 g, 120 mmol, 6 eq; (d) 3-(naphthalen-2-yl)cyclobutanone **123**, 2.00 g, 50%, white solid; (e) recrystallised from hexane at 4 °C.

<sup>1</sup>H NMR (400 MHz, CDCl<sub>3</sub>): δ 3.34 – 3.41 (m, 2H, CH<sub>2</sub>), 3.59 – 3.62 (m, 2H, CH<sub>2</sub>), 3.86 (pent, 1H, *J* = 8.5 Hz, CH), 7.43 – 7.53 (m, 3H, 3 x ArH), 7.74 (s, 1H, ArH), 7.82 – 7.88 (m, 3H, 3 x ArH).

<sup>13</sup>C NMR (100 MHz, CDCl<sub>3</sub>): δ 28.8, 54.8 (2C), 124.9, 125.0, 125.9, 126.6, 127.7, 127.8, 128.8, 132.4, 133.5, 141.0, 206.7.

FTIR (ν<sub>max</sub>, neat): 1776 cm<sup>-1</sup>.

Preparation of 3-methyl-3-(naphthalen-2-yl)cyclobutanone  
**124**<sup>70</sup>



**Scheme 91, Table 43, Entry 7**

(a) 2,2-dichloro-3-methyl-3-(naphthalen-2-yl)cyclobutanone **135**, 9.24 g, 33 mmol, 1 eq; (b) 206 ml, 0.16 M; (c) 12.87 g, 198 mmol, 6 eq; (d) 3-methyl-3-(naphthalen-2-yl)cyclobutanone **124**, 3.98 g, 57%, cream solid; (e) recrystallised from hexane at 4 °C.

<sup>1</sup>H NMR (400 MHz, CDCl<sub>3</sub>): δ 1.71 (s, 1H, CH<sub>3</sub>), 3.18 – 3.25 (m, 2H, CH<sub>2</sub>), 3.56 – 3.62 (m, 2H, CH<sub>2</sub>), 7.45 – 7.54 (m, 3H, 3 x ArH), 7.74 (s, 1H, ArH), 7.83 – 7.89 (m, 3H, 3 x ArH).

<sup>13</sup>C NMR (100 MHz, CDCl<sub>3</sub>): δ 31.0, 34.2, 59.3 (2C), 123.8, 124.5, 125.9, 126.5, 127.7, 127.8, 128.7, 132.0, 133.3, 145.5, 206.8,

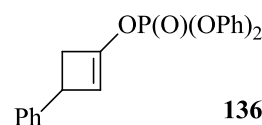
FTIR (ν<sub>max</sub>, neat): 1782 cm<sup>-1</sup>.

#### 5.6.4 Preparation of racemic enol phosphates

**Scheme 92, Table 44**

The following experiments were carried out according to *General Procedure H*. The data are reported as (a) ketone; (b) enol phosphate, yield.

Preparation of diphenyl (3-phenylcyclobut-1-en-1-yl)  
phosphate **136**



**Scheme 92, Table 44, Entry 1**

(a) 3-phenylcyclobutanone **36**, 131 mg, 0.9 mmol, 0.9 eq; (b) **136**, 194 mg, 57%.

<sup>1</sup>H NMR (400 MHz, CDCl<sub>3</sub>): δ 2.60 – 2.63 (m, 1H, CH), 3.28 – 3.32 (m, 1H, CH), 3.68 (d, 1H, J = 3.6 Hz, CH), 5.44 (s, 1H, CH=C), 7.21 – 7.27 (m, 10H, Ph x 2), 7.28 – 7.30 (m, 5H, 5 x ArH).

$^{13}\text{C}$  NMR (100 MHz,  $\text{CDCl}_3$ ):  $\delta$  37.3, 42.4 (d, 1C,  $^3J_{\text{C-P}} = 5.7$  Hz), 113.4 (d, 1C,  $^3J_{\text{C-P}} = 7.8$  Hz), 119.6 (d, 2C,  $^3J_{\text{C-P}} = 4.9$  Hz), 125.2, 126.1, 126.2, 127.9, 129.4, 141.6, 141.7 (d, 1C,  $^2J_{\text{C-P}} = 6.1$  Hz), 149.9 (d, 1C,  $^2J_{\text{C-P}} = 7.3$  Hz).

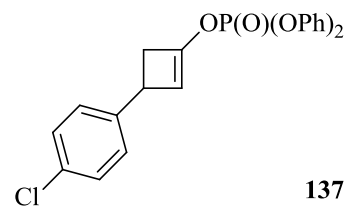
$^{31}\text{P}$  NMR (162 MHz,  $\text{CDCl}_3$ ):  $\delta$  -18.2.

FTIR (neat): 1180, 1281, 2940, 3026, 3059  $\text{cm}^{-1}$ .

HRMS (ESI)  $m/z$  calculated for  $\text{C}_{22}\text{H}_{23}\text{O}_4\text{PN}$   $[\text{M}+\text{NH}_4]^+$ : 396.1359. Found: 396.1356.

*Preparation of 3-(4'-chlorophenyl)cyclobut-1-en-1-yl  
diphenyl phosphate 137*

**Scheme 92, Table 44, Entry 2**



(a) 3-(4'-chlorophenyl)cyclobutanone **43**, 162 mg, 0.9 mmol, 0.9 eq; (b) **137**, 135 mg, 37%.

$^1\text{H}$  NMR (400 MHz,  $\text{CDCl}_3$ ):  $\delta$  2.53 – 2.57 (m, 1H, CH), 3.27 – 3.32 (m, 1H, CH), 3.65 – 3.66 (m, 1H, CH), 5.39 (s, 1H, CH=C), 7.14 – 7.16 (m, 2H, 2 x ArH), 7.22 – 7.29 (m, 8H, 8 x ArH), 7.30 – 7.39 (m, 4H, 4 x ArH).

$^{13}\text{C}$  NMR (100 MHz,  $\text{CDCl}_3$ ):  $\delta$  36.8, 42.5 (d, 1C,  $^3J_{\text{C-P}} = 5.8$  Hz), 113.0 (d, 1C,  $^3J_{\text{C-P}} = 7.8$  Hz), 119.6 (d, 2C,  $^3J_{\text{C-P}} = 4.9$  Hz), 125.3, 127.5, 128.0, 129.5, 131.8, 140.2, 141.9 (d, 1C,  $^2J_{\text{C-P}} = 9.4$  Hz), 149.8 (d, 1C,  $^2J_{\text{C-P}} = 7.3$  Hz).

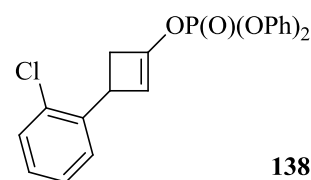
$^{31}\text{P}$  NMR (162 MHz,  $\text{CDCl}_3$ ):  $\delta$  -18.2.

FTIR (neat): 1180, 1298, 2938, 3057  $\text{cm}^{-1}$ .

HRMS (ESI)  $m/z$  calculated for  $\text{C}_{22}\text{H}_{19}\text{ClO}_4\text{P}$   $[\text{M}+\text{H}]^+$ : 413.0704. Found: 413.0696.



Preparation of 3-(2'-chlorophenyl)cyclobut-1-en-1-yl  
diphenyl phosphate **138**



**Scheme 92, Table 44, Entry 3**

(a) 3-(2'-chlorophenyl)cyclobutanone **121**, 162 mg, 0.9 mmol, 0.9 eq; (b) **138**, 221 mg, 60%.

$^1\text{H}$  NMR (400 MHz,  $\text{CDCl}_3$ ):  $\delta$  2.58 (d, 1H,  $J = 13.4$  Hz,  $\text{CH}_2$ ), 3.41 – 3.46 (m, 1H  $\text{CH}$ ), 4.04 (d, 1H,  $J = 1.8$  Hz,  $\text{CH}_2$ ), 5.52, (s, 1H,  $\text{CH}=\text{C}$ ), 7.19 – 7.40 (m, 14H, 14 x  $\text{ArH}$ ).

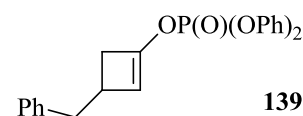
$^{13}\text{C}$  NMR (100 MHz,  $\text{CDCl}_3$ ):  $\delta$  34.9, 41.4 (d, 1C,  $^3J_{\text{C-P}} = 5.8$  Hz), 111.1 (d, 1C,  $^3J_{\text{C-P}} = 7.7$  Hz), 119.6 (d, 2C,  $^3J_{\text{C-P}} = 4.9$  Hz), 125.3, 126.3, 126.9, 127.4, 128.7, 129.5, 133.5, 139.2, 141.8 (d, 1C,  $^2J_{\text{C-P}} = 9.6$  Hz), 149.8 (d, 1C,  $^2J_{\text{C-P}} = 7.3$  Hz).

$^{31}\text{P}$  NMR (162 MHz,  $\text{CDCl}_3$ ):  $\delta$  -18.2.

FTIR (neat): 1180, 1487, 2933, 3059.

HRMS (ESI)  $m/z$  calculated for  $\text{C}_{22}\text{H}_{22}\text{ClO}_4\text{PN}$   $[\text{M}+\text{NH}_4]^+$ : 430.0969. Found: 430.0965.

Preparation of 3-benzylcyclobut-1-en-1-yl diphenyl  
phosphate **139**



**Scheme 92, Table 44, Entry 4**

(a) 3-benzylcyclobutanone **122**, 144 mg, 0.9 mmol, 0.9 eq; (b) **139**, 139 mg, 39%.

$^1\text{H}$  NMR (400 MHz,  $\text{CDCl}_3$ ):  $\delta$  2.43 (d, 1H,  $J = 13.4$ ,  $\text{CH}$ ), 2.74 (s, 3H,  $\text{CH} + \text{CH}_2$ ), 2.89 – 2.93 (m, 1H,  $\text{CH}$ ), 5.27 (s, 1H,  $\text{CH}=\text{C}$ ), 7.16 – 7.35 (m, 15H, 15 x  $\text{ArH}$ ).

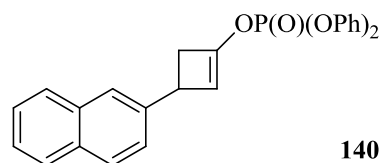
$^{13}\text{C}$  NMR (100 MHz,  $\text{CDCl}_3$ ):  $\delta$  35.1, 38.8 (d, 1C,  $^3J_{\text{C-P}} = 5.7$  Hz), 40.6, 114.6 (d, 1C,  $^3J_{\text{C-P}} = 7.8$  Hz), 120.1 (d, 2C,  $^3J_{\text{C-P}} = 5.1$  Hz), 125.7, 126.1, 128.4, 128.6, 129.9, 140.6, 141.3 (d, 1C,  $^2J_{\text{C-P}} = 9.9$  Hz), 150.4 (d, 1C,  $^2J_{\text{C-P}} = 7.3$  Hz).

$^{31}\text{P}$  NMR (162 MHz,  $\text{CDCl}_3$ ):  $\delta$  -18.1.

FTIR (neat): 1182, 1293, 2926, 3024  $\text{cm}^{-1}$ .

HRMS (ESI)  $m/z$  calculated for  $C_{23}H_{25}O_4PN$   $[M+NH_4]^+$ : 410.1516. Found: 410.1510.

*Preparation of 3-(naphthalen-2-yl)cyclobut-1-en-1-yl diphenyl phosphate 140*



**Scheme 92, Table 44, Entry 5**

(a) 3-(naphthalen-2-yl)cyclobutanone **123**, 131 mg, 0.9 mmol, 0.9 eq; (b) **140**, 250 mg, 65%.

$^1H$  NMR (400 MHz,  $CDCl_3$ ):  $\delta$  2.32 – 2.36 (m, 1H, CH), 3.38 – 3.40 (m, 1H, CH), 3.88 – 3.42 (m, 1H, CH), 5.58 (s, 1H, C=CH), 7.21 – 7.51 (m, 13H, 13 x ArH), 7.72 (s, 1H, ArH), 7.81 – 7.86 (m, 3H, 3 x ArH).

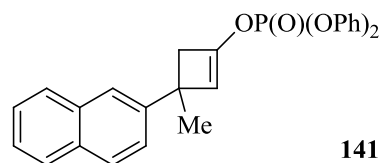
$^{13}C$  NMR (100 MHz,  $CDCl_3$ ):  $\delta$  37.5, 42.4 (d, 1C,  $^3J_{C-P} = 5.7$  Hz), 113.2 (d, 1C,  $^3J_{C-P} = 7.6$  Hz), 119.6 (d, 2C,  $^3J_{C-P} = 4.9$  Hz), 124.5, 125.0, 125.3, 125.6, 127.1, 127.7, 129.2, 129.3, 129.5, 132.1, 133.0, 139.1, 141.7 (d, 1C,  $^2J_{C-P} = 9.6$  Hz), 149.8 (d, 1C,  $^2J_{C-P} = 7.3$  Hz).

$^{31}P$  NMR (162 MHz,  $CDCl_3$ ):  $\delta$  -18.2.

FTIR (neat): 1182, 1276, 2931, 3059  $cm^{-1}$ .

HRMS (ESI)  $m/z$  calculated for  $C_{26}H_{25}O_4PN$   $[M+NH_4]^+$ : 446.1516. Found: 446.1513.

*Preparation of 3-methyl-3-(naphthalen-2-yl)cyclobut-1-en-1-yl diphenyl phosphate 141*



**Scheme 92, Table 44, Entry 6**

(a) 3-methyl-3-(naphthalen-2-yl)cyclobutanone **124**, 176 mg, 0.9 mmol, 0.9 eq; (b) **141**, 371 mg, 93%.

$^1H$  NMR (400 MHz,  $CDCl_3$ ):  $\delta$  1.66 (s, 3H,  $CH_3$ ), 2.97 (s, 2H,  $CH_2$ ), 5.72, (s, 1H,  $CH=C$ ), 7.18 – 7.25 (m, 5H, 5 x ArH), 7.32 – 7.37 (m, 5H, 5 x ArH), 7.43 – 7.48 (m, 3H, 3 x ArH), 7.70 (s, 1H, ArH), 7.79 – 7.84 (m, 3H, 3 x ArH).

$^{13}\text{C}$  NMR (100 MHz,  $\text{CDCl}_3$ ):  $\delta$  26.5, 41.7, 48.0 (d, 1C,  $^3J_{\text{C-P}} = 5.7$  Hz), 117.3 (d, 1C,  $^3J_{\text{C-P}} = 7.5$  Hz), 119.6 (d, 2C,  $^3J_{\text{C-P}} = 4.9$  Hz), 123.6, 124.2, 125.0, 125.2, 125.6, 127.0, 127.2, 127.4, 129.4, 131.5, 132.8, 141.3 (d, 1C,  $^2J_{\text{C-P}} = 9.7$  Hz), 143.1, 149.8(d, 1C,  $^2J_{\text{C-P}} = 7.0$  Hz).

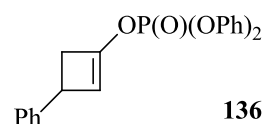
$^{31}\text{P}$  NMR (162 MHz,  $\text{CDCl}_3$ ):  $\delta$  -18.1.

FTIR (neat): 1184, 1284, 2929, 3057  $\text{cm}^{-1}$ .

HRMS (ESI)  $m/z$  calculated for  $\text{C}_{27}\text{H}_{27}\text{O}_4\text{PN}$   $[\text{M}+\text{NH}_4]^+$ : 460.1672. Found: 430.1665.

### 5.6.5 Asymmetric deprotonations to form enantioenriched enol phosphates

Preparation of diphenyl (3-phenylcyclobut-1-en-1-yl) phosphate **136**



#### Scheme 93, Table 45

Following *General Procedure A* for the formation of Mg-bisamide, data are reported as: (a) amount of  $n\text{-Bu}_2\text{Mg}$ ; (b) amine used; (c) amount of amine.

Following *General Procedure D* for the asymmetric deprotonation, data are reported as: (a) Mg-base; (b) Lewis base additive; (c) electrophile; (d) ketone; (e) temperature; (f) isolated yield; (g) er (as determined by chiral HPLC).

**Entry 1:** *General Procedure A*: (a) 1.00 ml, 1 M in THF, 1 mmol, 1 eq; (b) (*R*)-bis((*R*)-1-phenylethyl)amine **34**; (c) 0.44 ml, 2 mmol, 2 eq.

*General Procedure D*: (a) (*R,R*)-**70** (0.1 M in THF, 1 mmol, 1 eq; (b) none; (c) diphenylphosphoryl chloride, 0.42 ml, 2 mmol, 2 eq; (d) 3-phenylcyclobutanone **36**, 117 mg, 0.8 mmol, 0.8 eq; (e) -78 °C; (f) 245 mg, 81%; (g) 97:3.

**Entry 2:** *General Procedure A*: (a) 1.00 ml, 1 M in THF, 1 mmol, 1 eq; (b) (*R*)-1-phenyl-*N*-((*R*)-1-phenylethyl)-2-(piperidin-1-yl)ethanamine **115**; (c) 0.62 ml, 2 mmol, 2 eq.

*General Procedure D*: (a) (*R,R*)-**67** (0.1 M in THF, 1 mmol, 1 eq; (b) none; (c) diphenylphosphoryl chloride, 0.42 ml, 2 mmol, 2 eq; (d) 3-phenylcyclobutanone **36**, 117 mg, 0.8 mmol, 0.8 eq; (e) -78 °C; (f) 232 mg, 77%; (g) 91:9.

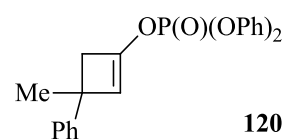
**Entry 3**: *General Procedure A*: (a) 1.00 ml, 1 M in THF, 1 mmol, 1 eq; (b) (*R*)-1-phenyl-*N*-((*R*)-1-phenylethyl)-2-(piperidin-1-yl)ethanamine **115**; (c) 0.62 ml, 2 mmol, 2 eq.

*General Procedure D*: (a) (*R,R*)-**67** (0.1 M in THF, 1 mmol, 1 eq; (b) none; (c) diphenylphosphoryl chloride, 0.42 ml, 2 mmol, 2 eq; (d) 3-phenylcyclobutanone **36**, 117 mg, 0.8 mmol, 0.8 eq; (e) -40 °C; (f) 243 mg, 80%; (i) 89:11.

Chiral HPLC analysis: Chiralcel OJ column, 10% IPA in *n*-hexane, 1.40 ml/minute flow rate, 254 nm detector,  $t_R$  (-) (minor) = 33.2 min,  $t_R$  (+) (major) = 35.7 min.

$[\alpha]_D^{20} = +4.45^\circ$  (91:9 er,  $c = 1$ ,  $\text{CHCl}_3$ ). No literature data are available for comparison.

*Preparation of 3-methyl-3-phenylcyclobut-1-en-1-yl diphenyl phosphate 120*



**Scheme 94, Table 46**

Following *General Procedure A* for the formation of Mg-bisamide, data are reported as: (a) amount of *n*-Bu<sub>2</sub>Mg; (b) amine used; (c) amount of amine.

Following *General Procedure D* for the asymmetric deprotonation, data are reported as: (a) Mg-base; (b) Lewis base additive; (c) electrophile; (d) ketone; (e) temperature; (f) isolated yield; (g) er (as determined by chiral HPLC).

**Entry 1**: *General Procedure A*: (a) 1.00 ml, 1 M in THF, 1 mmol, 1 eq; (b) (*R*)-bis((*R*)-1-phenylethyl)amine **34**; (c) 0.44 ml, 2 mmol, 2 eq.

*General Procedure D*: (a) (*R,R*)-**70** (0.1 M in THF, 1 mmol, 1 eq; (b) none; (c) diphenylphosphoryl chloride, 0.42 ml, 2 mmol, 2 eq; (d) 3-methyl-3-phenylcyclobutanone **39**, 128 mg, 0.8 mmol, 0.8 eq; (e) -78 °C; (f) 204 mg, 65%; (g) 99:1.

**Entry 2:** *General Procedure A:* (a) 1.00 ml, 1 M in THF, 1 mmol, 1 eq; (b) (*R*)-1-phenyl-*N*-((*R*)-1-phenylethyl)-2-(piperidin-1-yl)ethanamine **115**; (c) 0.62 ml, 2 mmol, 2 eq.

*General Procedure D:* (a) (*R,R*)-**67** (0.1 M in THF, 1 mmol, 1 eq; (b) none; (c) diphenylphosphoryl chloride, 0.42 ml, 2 mmol, 2 eq; (d) 3-methyl-3-phenylcyclobutanone **39**, 128 mg, 0.8 mmol, 0.8 eq; (d) -78 °C; (f) 238 mg, 76%; (g) 98:2.

**Entry 3:** *General Procedure A:* (a) 1.00 ml, 1 M in THF, 1 mmol, 1 eq; (b) (*R*)-1-phenyl-*N*-((*R*)-1-phenylethyl)-2-(piperidin-1-yl)ethanamine **115**; (c) 0.62 ml, 2 mmol, 2 eq.

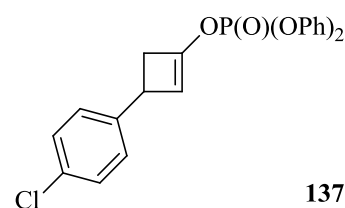
*General Procedure D:* (a) (*R,R*)-**67** (0.1 M in THF, 1 mmol, 1 eq; (b) none; (c) diphenylphosphoryl chloride, 0.42 ml, 2 mmol, 2 eq; (d) 3-methyl-3-phenylcyclobutanone **39**, 128 mg, 0.8 mmol, 0.8 eq; (f) -40 °C; (f) 213 mg, 68%; (g) 98:2.

Chiral HPLC analysis: Chiralcel OJ column, 10% IPA in *n*-hexane, 1.50 ml/min flow rate, 254 nm detector,  $t_R$  (minor) = 14.1 min,  $t_R$  (major) = 18.7 min.

$[\alpha]_D^{20} = +3.52$  °. (98:2 er,  $c = 1$ ,  $\text{CHCl}_3$ ). No literature data are available for comparison.

*Preparation of 3-(4'-Chlorophenyl)cyclobut-1-en-1-yl diphenyl phosphate 137*

**Scheme 95, Table 47**



Following *General Procedure A* for the formation of Mg-bisamide, data are reported as: (a) amount of *n*-Bu<sub>2</sub>Mg; (b) amine used; (c) amount of amine.

Following *General Procedure D* for the asymmetric deprotonation, data are reported as: (a) Mg-base; (b) Lewis base additive; (c) electrophile; (d) ketone; (e) temperature; (f) isolated yield; (g) er (as determined by chiral HPLC).

**Entry 1:** *General Procedure A:* (a) 1.00 ml, 1 M in THF, 1 mmol, 1 eq; (b) (*R*)-bis(*R*)-1-phenylethylamine **34**; (c) 0.44 ml, 2 mmol, 2 eq.

*General Procedure D:* (a) (*R,R*)-**70** (0.1 M in THF, 1 mmol, 1 eq; (b) none; (c) diphenylphosphoryl chloride, 0.42 ml, 2 mmol, 2 eq; (d) 3-(4'-chlorophenyl)cyclobutanone **43**, 144 mg, 0.8 mmol, 0.8 eq; (e) -78 °C; (f) 219 mg, 66%; (g) 90:10.

**Entry 2:** *General Procedure A:* (a) 1.00 ml, 1 M in THF, 1 mmol, 1 eq; (b) (*R*)-1-phenyl-*N*-((*R*)-1-phenylethyl)-2-(piperidin-1-yl)ethanamine **115**; (c) 0.62 ml, 2 mmol, 2 eq.

*General Procedure D:* (a) (*R,R*)-**67** (0.1 M in THF, 1 mmol, 1 eq; (b) none; (c) diphenylphosphoryl chloride, 0.42 ml, 2 mmol, 2 eq; (d) 3-(4'-chlorophenyl)cyclobutanone **43**, 144 mg, 0.8 mmol, 0.8 eq; (d) -78 °C; (f) 294 mg, 89%; (f) 87:13.

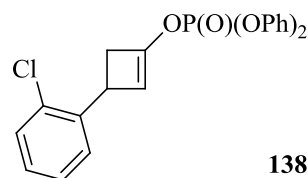
**Entry 3:** *General Procedure A:* (a) 1.00 ml, 1 M in THF, 1 mmol, 1 eq; (b) (*R*)-1-phenyl-*N*-((*R*)-1-phenylethyl)-2-(piperidin-1-yl)ethanamine **115**; (c) 0.62 ml, 2 mmol, 2 eq.

*General Procedure D:* (a) (*R,R*)-**67** (0.1 M in THF, 1 mmol, 1 eq; (b) none; (c) diphenylphosphoryl chloride, 0.42 ml, 2 mmol, 2 eq; (d) 3-(4'-chlorophenyl)cyclobutanone **43**, 144 mg, 0.8 mmol, 0.8 eq; (e) -40 °C; (f) 296 mg, 90%; (g) 53:47.

Chiral HPLC analysis: Chiralcel OJ column, 20% IPA in *n*-hexane, 1.50 ml/min flow rate, 254 nm detector,  $t_R$  (minor) = 22.1 min,  $t_R$  (major) = 29.8 min.

$[\alpha]_D^{20} = +5.64$  °. (90:10 er,  $c = 1$ ,  $\text{CHCl}_3$ ). No literature data are available for comparison.

Preparation of 3-(2'-Chlorophenyl)cyclobut-1-en-1-yl  
diphenyl phosphate **138**



**Scheme 96, Table 48**

Following *General Procedure A* for the formation of Mg-bisamide, data are reported as: (a) amount of *n*-Bu<sub>2</sub>Mg; (b) amine used; (c) amount of amine.

Following *General Procedure D* for the asymmetric deprotonation, data are reported as: (a) Mg-base; (b) Lewis base additive; (c) electrophile; (d) ketone; (e) temperature; (f) isolated yield; (g) er (as determined by chiral HPLC).

**Entry 1:** *General Procedure A*: (a) 1.00 ml, 1 M in THF, 1 mmol, 1 eq; (b) (*R*)-bis((*R*)-1-phenylethyl)amine **34**; (c) 0.44 ml, 2 mmol, 2 eq.

*General Procedure D*: (a) (*R,R*)-**70** (0.1 M in THF, 1 mmol, 1 eq; (b) none; (c) diphenylphosphoryl chloride, 0.42 ml, 2 mmol, 2 eq; (d) 3-(2'-chlorophenyl)cyclobutanone **121**, 144 mg, 0.8 mmol, 0.8 eq; (e) -78 °C; (f) 298 mg, 90%; (g) 93:7.

**Entry 2:** *General Procedure A*: (a) 1.00 ml, 1 M in THF, 1 mmol, 1 eq; (b) (*R*)-1-phenyl-*N*-((*R*)-1-phenylethyl)-2-(piperidin-1-yl)ethanamine **115**; (c) 0.62 ml, 2 mmol, 2 eq.

*General Procedure D*: (a) (*R,R*)-**67** (0.1 M in THF, 1 mmol, 1 eq; (b) none; (c) diphenylphosphoryl chloride, 0.42 ml, 2 mmol, 2 eq; (d) 3-(2'-chlorophenyl)cyclobutanone **121**, 144 mg, 0.8 mmol, 0.8 eq; (e) -78 °C; (f) 254 mg, 78%; (g) 96:4.

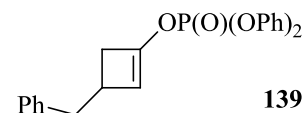
**Entry 3:** *General Procedure A*: (a) 1.00 ml, 1 M in THF, 1 mmol, 1 eq; (b) (*R*)-1-phenyl-*N*-((*R*)-1-phenylethyl)-2-(piperidin-1-yl)ethanamine **115**; (c) 0.62 ml, 2 mmol, 2 eq.

*General Procedure D*: (a) (*R,R*)-**67** (0.1 M in THF, 1 mmol, 1 eq; (b) none; (c) diphenylphosphoryl chloride, 0.42 ml, 2 mmol, 2 eq; (d) 3-(2'-chlorophenyl)cyclobutanone **121**, 144 mg, 0.8 mmol, 0.8 eq; (e) -40 °C; (f) 290 mg, 88%; (g) 96:4.

Chiral HPLC analysis: Chiralcel OJ column, 20% IPA in *n*-hexane, 1.00 ml/min flow rate, 254 nm detector,  $t_R$  (major) = 21.3 min,  $t_R$  (minor) = 22.7 min.

$[\alpha]_D^{20} = +28.58^\circ$ . (96:4 er,  $c = 1$ ,  $\text{CHCl}_3$ ). No literature data are available for comparison.

Preparation of 3-benzylcyclobut-1-en-1-yl diphenyl phosphate **139**



**Scheme 97, Table 49**

Following *General Procedure A* for the formation of Mg-bisamide, data are reported as: (a) amount of *n*-Bu<sub>2</sub>Mg; (b) amine used; (c) amount of amine.

Following *General Procedure D* for the asymmetric deprotonation, data are reported as: (a) Mg-base; (b) Lewis base additive; (c) electrophile; (d) ketone; (e) temperature; (f) isolated yield; (g) er (as determined by chiral HPLC).

**Entry 1: Entry 1:** *General Procedure A*: (a) 1.00 ml, 1 M in THF, 1 mmol, 1 eq; (b) (*R*)-bis((*R*)-1-phenylethyl)amine **34**; (c) 0.44 ml, 2 mmol, 2 eq.

*General Procedure D*: (a) (*R,R*)-**70** (0.1 M in THF, 1 mmol, 1 eq; (b) none; (c) diphenylphosphoryl chloride, 0.42 ml, 2 mmol, 2 eq; (d) 3-benzylcyclobutanone **122**, 128 mg, 0.8 mmol, 0.8 eq; (e) -78 °C; (f) 189 mg, 60%; (g) 95:5.

**Entry 2:** *General Procedure A*: (a) 1.00 ml, 1 M in THF, 1 mmol, 1 eq; (b) (*R*)-1-phenyl-*N*-((*R*)-1-phenylethyl)-2-(piperidin-1-yl)ethanamine **115**; (c) 0.62 ml, 2 mmol, 2 eq.

*General Procedure D*: (a) (*R,R*)-**67** (0.1 M in THF, 1 mmol, 1 eq; (b) none; (c) diphenylphosphoryl chloride, 0.42 ml, 2 mmol, 2 eq; (d) 3-benzylcyclobutanone **122**, 128 mg, 0.8 mmol, 0.8 eq; (e) -78 °C; (f) 171 mg, 55%; (g) 92:8.

**Entry 3:** *General Procedure A*: (a) 1.00 ml, 1 M in THF, 1 mmol, 1 eq; (b) (*R*)-1-phenyl-*N*-((*R*)-1-phenylethyl)-2-(piperidin-1-yl)ethanamine **115**; (c) 0.62 ml, 2 mmol, 2 eq.

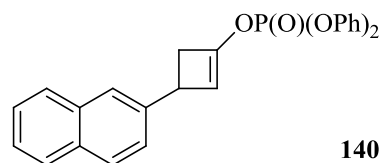


*General Procedure D:* (a) (*R,R*)-**67** (0.1 M in THF, 1 mmol, 1 eq; (b) none; (c) diphenylphosphoryl chloride, 0.42 ml, 2 mmol, 2 eq; (d) 3-benzylcyclobutanone **122**, 128 mg, 0.8 mmol, 0.8 eq; (e) -40 °C; (f) 246 mg, 79%; (g) 95:5.

Chiral HPLC analysis: Chiralcel OJ column, 20% IPA in *n*-hexane, 1.00 ml/min flow rate, 254 nm detector,  $t_R$  (minor) = 24.3 min,  $t_R$  (major) = 25.5 min.

$[\alpha]_D^{20} = +18.45^\circ$  (95:5 er,  $c = 1$ ,  $\text{CHCl}_3$ ). No literature data are available for comparison.

*Preparation of 3-(naphthalen-2-yl)cyclobut-1-en-1-yl diphenyl phosphate 140*



**Scheme 98, Table 50**

Following *General Procedure A* for the formation of Mg-bisamide, data are reported as: (a) amount of *n*-Bu<sub>2</sub>Mg; (b) amine used; (c) amount of amine.

Following *General Procedure D* for the asymmetric deprotonation, data are reported as: (a) Mg-base; (b) Lewis base additive; (c) electrophile; (d) ketone; (e) temperature; (f) isolated yield; (g) er (as determined by chiral HPLC).

**Entry 1:** *General Procedure A:* (a) 1.00 ml, 1 M in THF, 1 mmol, 1 eq; (b) (*R*)-bis((*R*)-1-phenylethyl)amine **34**; (c) 0.44 ml, 2 mmol, 2 eq.

*General Procedure D:* (a) (*R,R*)-**70** (0.1 M in THF, 1 mmol, 1 eq; (b) none; (c) diphenylphosphoryl chloride, 0.42 ml, 2 mmol, 2 eq; (d) 3-(naphthalen-2-yl)cyclobutanone **123**, 157 mg, 0.8 mmol, 0.8 eq; (e) -78 °C; (f) 181 mg, 53%; (g) 82:18.

**Entry 2:** *General Procedure A:* (a) 1.00 ml, 1 M in THF, 1 mmol, 1 eq; (b) (*R*)-1-phenyl-*N*-((*R*)-1-phenylethyl)-2-(piperidin-1-yl)ethanamine **115**; (c) 0.62 ml, 2 mmol, 2 eq.

*General Procedure D:* (a) (*R,R*)-**67** (0.1 M in THF, 1 mmol, 1 eq; (b) none; (c) diphenylphosphoryl chloride, 0.42 ml, 2 mmol, 2 eq; (d) 3-(naphthalen-2-yl)cyclobutanone **123**, 157 mg, 0.8 mmol, 0.8 eq; (e) -78 °C; (f) 239 mg, 70%; (g) 46:54.

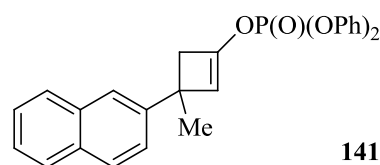
**Entry 3:** *General Procedure A:* (a) 1.00 ml, 1 M in THF, 1 mmol, 1 eq; (b) (*R*)-1-phenyl-*N*-((*R*)-1-phenylethyl)-2-(piperidin-1-yl)ethanamine **115**; (c) 0.62 ml, 2 mmol, 2 eq.

*General Procedure D:* (a) (*R,R*)-**67** (0.1 M in THF, 1 mmol, 1 eq; (b) none; (c) diphenylphosphoryl chloride, 0.42 ml, 2 mmol, 2 eq; (d) 3-(naphthalen-2-yl)cyclobutanone **123**, 157 mg, 0.8 mmol, 0.8 eq; (e) -40 °C; (f) 150 mg, 44%; (g) 48:52.

Chiral HPLC analysis: Chiralcel OJ column, 50% IPA in *n*-hexane, 1.50 ml/min flow rate, 254 nm detector,  $t_R$  (major) = 39.0 min,  $t_R$  (minor) = 50.0 min.

$[\alpha]_D^{20} = +13.68^\circ$  (82:18 er,  $c = 1$ ,  $\text{CHCl}_3$ ). No literature data are available for comparison.

*Preparation of 3-methyl-3-(naphthalen-2-yl)cyclobut-1-en-1-yl diphenyl phosphate 141*



**Scheme 99, Table 51**

Following *General Procedure A* for the formation of Mg-bisamide, data are reported as: (a) amount of *n*-Bu<sub>2</sub>Mg; (b) amine used; (c) amount of amine.

Following *General Procedure D* for the asymmetric deprotonation, data are reported as: (a) Mg-base; (b) Lewis base additive; (c) electrophile; (d) ketone; (e) temperature; (f) isolated yield; (g) er (as determined by chiral HPLC).

**Entry 1:** *General Procedure A:* (a) 1.00 ml, 1 M in THF, 1 mmol, 1 eq; (b) (*R*)-bis((*R*)-1-phenylethyl)amine **34**; (c) 0.44 ml, 2 mmol, 2 eq.

*General Procedure D:* (a) (*R,R*)-**70** (0.1 M in THF, 1 mmol, 1 eq; (b) none; (c) diphenylphosphoryl chloride, 0.42 ml, 2 mmol, 2 eq; (d) 3-methyl-3-(naphthalen-2-yl)cyclobutanone **124**, 168 mg, 0.8 mmol, 0.8 eq; (e) -78 °C; (f) 165 mg, 51%; (g) 76:24.

**Entry 2:** *General Procedure A:* (a) 1.00 ml, 1 M in THF, 1 mmol, 1 eq; (b) (*R*)-1-phenyl-*N*-((*R*)-1-phenylethyl)-2-(piperidin-1-yl)ethanamine **115**; (c) 0.62 ml, 2 mmol, 2 eq.

*General Procedure D:* (a) (*R,R*)-**67** (0.1 M in THF, 1 mmol, 1 eq; (b) none; (c) diphenylphosphoryl chloride, 0.42 ml, 2 mmol, 2 eq; (d) 3-methyl-3-(naphthalen-2-yl)cyclobutanone **141**, 168 mg, 0.8 mmol, 0.8 eq; (e) -78 °C; (f) 217 mg, 61%; (g) 61:39.

**Entry 3:** *General Procedure A:* (a) 1.00 ml, 1 M in THF, 1 mmol, 1 eq; (b) (*R*)-1-phenyl-*N*-((*R*)-1-phenylethyl)-2-(piperidin-1-yl)ethanamine **115**; (c) 0.62 ml, 2 mmol, 2 eq.

*General Procedure D:* (a) (*R,R*)-**67** (0.1 M in THF, 1 mmol, 1 eq; (b) none; (c) diphenylphosphoryl chloride, 0.42 ml, 2 mmol, 2 eq; (d) 3-methyl-3-(naphthalen-2-yl)cyclobutanone **141**, 168 mg, 0.8 mmol, 0.8 eq; (e) -40 °C; (f) (g) IQ; (h) 234 mg, 66%; (g) 53:47.

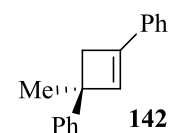
Chiral HPLC analysis: Chiralcel OJ column, 40% IPA in *n*-hexane, 1.40 ml/min flow rate, 254 nm detector,  $t_R$  (major) = 20.0 min,  $t_R$  (minor) = 38.0 min.

$[\alpha]_D^{20} = +4.77^\circ$  (76:24 er,  $c = 1$ ,  $\text{CHCl}_3$ ). No literature data are available for comparison.

## 5.7 Avenues for future work

*Preparation of (S)-(3-methylcyclobut-1-ene-1,3-diyl)dibenzene* **142**<sup>60,61</sup>

### Scheme 102



A flame-dried Schlenk flask under argon was charged with palladium(II) chloride (5 mg, 0.026 mmol, 2 mol%) and the Schlenk was evacuated and purged with argon. A solution of enol phosphate **120** (98:2 er, 513 mg, 1.31 mmol, 1 eq) in THF (2.62 ml, 0.5 M) was added to the Schlenk and stirred at rt for 5 min. Phenylmagnesium bromide solution (0.66 ml, 3M THF, 1.97 mmol, 1.5 eq) was then added over a period of 2 h *via* syringe pump and the reaction mixture was stirred for a further 16 h at rt. After this time, MeOH (80  $\mu\text{l}$ , 1.62 mmol, 2 eq) was added and the reaction mixture was transferred to a round-bottom flask and concentrated *in vacuo*. The brown residue was purified by silica gel chromatography, eluting with PE (30 – 40

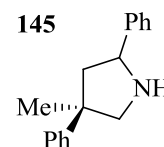
°C) to afford **142** as a colourless oil (141 mg, 49% yield <sup>1</sup>H NMR yield in a mixture with biphenyl).<sup>71</sup>

<sup>1</sup>H NMR (400 MHz, CDCl<sub>3</sub>): δ 1.66 (s, 3H, CH<sub>3</sub>), 2.94 (d, 1H, *J* = 12.5 Hz, CH<sub>2</sub>) 3.00 (d, 1H, *J* = 12.5 Hz, CH<sub>2</sub>), 6.76 (s, 1H, C=CH), 7.20 – 7.41 (m, 10H, 10 x ArH).

Diagnostic peaks for Ph-Ph: <sup>1</sup>H NMR (400 MHz, CDCl<sub>3</sub>): δ 7.41 – 7.44 (m, 2H, 2 x ArH), 7.50 – 7.52 (m, 4H, 4 x ArH), 7.65-7.67 (m, 4H 4 x ArH).

Preparation of (4*R*)-4-methyl-2,4-diphenylpyrrolidine **145**<sup>29</sup>

### Scheme 103



A flame-dried three-neck flask was charged with (*S*)-(3-methylcyclobut-1-ene-1,3-diyl)dibenzene **142** (141 mg, 0.64 mmol, 1 eq) and DCM (8 ml, 0.08 M). The reaction mixture was cooled to -78 °C and ozone gas was bubbled through the solution for 30 min. Dimethyl sulfide (0.94 ml, 12.8 mmol, 20 eq) was added at -78 °C and the reaction mixture was transferred to an argon line and warmed to rt. After stirring for 4 h at rt, the reaction mixture was concentrated *in vacuo* and the residue was re-dissolved in MeOH (8 ml, 0.08 M). Ammonium acetate (148 mg, 1.92 mmol, 3 eq) and sodium cyanoborohydride (121 mg, 1.92 mmol, 3 eq) were added and the reaction mixture was stirred at rt for 16 h. NaOH (10 ml, 1M) was added and the reaction mixture was stirred for a further 1 h before diluting with DCM (10 ml). The biphasic mixture was separated and the aqueous layer was extracted with DCM (3 x 10 ml). The combined organics were washed with water (20 ml) and saturated brine solution (20 ml) then dried over Na<sub>2</sub>SO<sub>4</sub>, filtered, and concentrated *in vacuo* to afford the substituted pyrrolidine **145** as a yellow oil (127 mg, 84% yield, tentative purity as <sup>13</sup>C NMR was unclear).

<sup>1</sup>H NMR (400 MHz, CDCl<sub>3</sub>): δ 1.27 – 1.36 (m, 2H, CH + NH), 1.47 (s, 3H, CH<sub>3</sub>), 3.19 – 3.23 (m, 1H CH<sub>2</sub>), 3.32 – 3.34 (m, 1H CH<sub>2</sub>), 4.25 – 4.31 (s, 2H, CH<sub>2</sub>), 7.22 – 7.49 (m, 10H, 10 x ArH).

## 6 References

1. (a) G. Proctor, *Asymmetric Synthesis*, **1996**, Oxford Science: Oxford; (b) R. A. Aitken, S. N. Kilényi, *Asymmetric Synthesis*, **1992**, Blackie Academic and Professional: London.
2. (a) N. S. Simpkins, *Chem. Soc. Rev.*, **1990**, *19*, 335; (b) P. J. Cox and N. S. Simpkins, *Tetrahedron: Asymm.*, **1991**, *2*, 1; (c) N. S. Simpkins, *Pure & Appl. Chem.*, **1996**, *68*, 691; (d) P. O'Brien, *J. Chem. Soc., Perkin Trans. 1*, **1998**, 1439.
3. R. P. Thummel and B. Rickborn, *J. Am. Chem. Soc.*, **1970**, *92*, 2064.
4. J. K. Whitesell and S. W. Felman, *J. Org. Chem.*, **1980**, *45*, 755.
5. (a) M. Asami, *Chem. Lett.*, **1984**, 829; (b) M. Asami, *Bull. Chem. Soc. Jpn.*, **1990**, *63*, 721.
6. (a) M. Asami, *Chem. Lett.*, **1987**, 389; (b) D. Milne and P. J. Murphy, *J. Chem. Soc., Chem. Commun.*, **1993**, 884; (c) D. M. Hodgson, J. Witherington and B. A. Moloney, *J. Chem. Soc., Perkin Trans. 1*, **1994**, 3373; (d) D. Bhuniya, A. DattaGupta and V. K. Singh, *J. Org. Chem.*, **1996**, *61*, 6086.
7. (a) M. Asami, T. Ishizaki and S. Inoue, *Tetrahedron: Asymm.*, **1994**, *5*, 793; (b) M. Asami, T. Suga, K. Honda and S. Inoue, *Tetrahedron Lett.*, **1997**, 38, 6425; (c) J. P. Tierney, A. Alexakis and P. Mangeney, *Tetrahedron: Asymm.*, **1997**, *8*, 1019.
8. M. J. Södergen, S. K. Bertilsson and P. G. Anderson, *J. Am. Chem. Soc.*, **2000**, *122*, 6610.
9. D. A. Price, N. S. Simpkins, A. M. MacLeod and A. P. Watt, *J. Org. Chem.*, **1994**, *59*, 1961.
10. (a) R. A. Ewin and N. S. Simpkins, *Synlett*, **1996**, 317; (b) R. A. Ewin, A. M. MacLeod, N. S. Simpkins and P. A. Watt, *J. Chem. Soc., Perkin Trans. 1*, **1997**, 401.

11. E. L. M. Cowton, S. E. Gibson, M. J. Schneider and M. H. Smith, *Chem. Commun.*, **1996**, 839.
12. (a) S. E. Gibson, H. Ibrahim, C. Pasquire and J. W. Steed, *Tetrahedron*, **2002**, 58, 4617; (b) S. E. Gibson, H. Ibrahim, C. Pasquite and V. M. Swamy, *Tetrahedron: Asymm.*, **2003**, 14, 1455; (c) S. E. Gibson, H. Ibrahim, C. Pasquite and V. M. Swamy, *Tetrahedron: Asymm.*, **2004**, 15, 465; (d) M. P. Castaldi, S. E. Gibson, M. Rudd and A. J. P. White, *Chem. Eur. J.*, **2006**, 12, 138; (e) S. E. Gibson, J. T. Rendell and M. Rudd, *Synthesis*, **2006**, 3631; (f) R. Felstead, S. E. Gibson, A. Rooney and E. S. Y. Tse, *Eur. J. Org. Chem.*, **2008**, 4963; (g) K. Abecassis, S. E. Gibson and M. Martin-Fontecha, *Eur. J. Org. Chem.*, **2009**, 1606.
13. (a) R. Shirai, M. Tanaka and K. Koga, *J. Am. Chem. Soc.*, **1986**, 108, 543; (b) N. S. Simpkins, *J. Chem. Soc., Chem. Commun.*, **1986**, 88.
14. R. P. C. Cousins and N. S. Simpkins, *Tetrahedron Lett.*, **1989**, 30, 7241
15. (a) D. Sato, H. Kawasaki, I. Shimada, Y. Arata, K. Okamura, T. Date and K. Koga, *J. Am. Chem. Soc.*, **1992**, 761; (b) D. Sato, H. Kawasaki, I. Shimada, Y. Arata, K. Okamura, T. Date and K. Koga, *Tetrahedron*, **1997**, 53, 7191.
16. (a) R. Shirai, D. Sato, K. Aoki, M. Tanaka, H. Kawasaki and K. Koga, *Tetrahedron*, **1997**, 53, 5963; (b) K. Koga, *Pure & Appl. Chem.*, **1994**, 66, 1487; (c) K. Aoki, K. Tomioka, H. Noguchi and K. Koga, *Tetrahedron*, **1997**, 53, 13641.
17. E. J. Corey and A. W. Cross, *Tetrahedron Lett.*, **1984**, 25, 495.
18. R. Shirai, D. Sato, K. Aoki, M. Tanaka, H. Kawasaki and K. Koga, *Tetrahedron*, **1997**, 53, 5963.
19. (a) B. J. Bunn and N. S. Simpkins, *J. Org. Chem.*, **1993**, 58, 533; (b) B. J. Bunn, N. S. Simpkins, Z. Spavold and M. J. Crimmin, *J. Chem. Soc., Perkin Trans. 1*, **1993**, 3113.
20. K. Sugasawa, M. Shindo, H. Noguchi and K. Koga, *Tetrahedron Lett.*, **1996**, 37, 7377.

21. M. Toriyama, K. Sugasawa, M. Shindo, N. Tokutake and K. Koga, *Tetrahedron Lett.*, **1997**, 38, 567.
22. (a) K Aoki, H. Noguchi, K. Tomioka and K. Koga, *Tetrahedron Lett.*, **1993**, 34, 5105; (b) K. Aoki and K. Koga, *Tetrahedron Lett.*, **1997**, 38, 2505; (c) K. Aoki and K. Koga, *Chem. Pharm. Bull.*, **2000**, 48, 571.
23. J. Busch-Peterson and E. J. Corey, *Tetrahedron Lett.*, **2000**, 41, 6941.
24. V. K. Aggarwal, P. S. Humphries and A. Fenwick, *J. Chem. Soc., Perkin Trans. 1*, **1999**, 2883.
25. C.-D. Graf, C. Malan and P. Knochel, *Angew. Chem. Int. Ed.*, **1998**, 37, 3014.
26. T. Honda and K. Endo, *J. Chem. Soc., Perkin Trans. 1*, **2001**, 2915.
27. J.-C. Poupon, E. Demont, J. Prunet and J.-P. Férézou, *J. Org. Chem.*, **2003**, 68, 4700.
28. (a) T. Honda, N. Kimura and M. Tsubuki, *Tetrahedron: Asymm.*, **1993**, 4, 1475; (b) T. Honda and N. Kimura, *J. Chem. Soc., Chem. Commun.*, **1994**, 77.
29. P. Resende, W. P. Almeida and F. Coelho, *Tetrahedron: Asymm.*, **1999**, 10, 2113.
30. M. van Gergen and H.-J. Gais, *J. Am. Chem. Soc.*, **2002**, 124, 4321.
31. T. Honda and N. Kimura, *Org. Lett.*, **2002**, 4, 4567.
32. C. M. Cain, R. P. C. Cousins, G. Coumbarides and N. S. Simpkins, *Tetrahedron*, **1990**, 46, 523.
33. V. K. Aggarwal, P. S. Humphries and A. Fenwick, *Angew. Chem. Int. Ed.*, **1999**, 38, 1985.
34. T. Hamashita, D. Sato, T. Kiyoto, A. Kumar and K. Koga, *Tetrahedron Lett.*, **1996**, 37, 8195.
35. W. Clegg, F. J. Craig, K. W. Henderson, A. R. Kennedy, R. E. Mulvey, P. A. O'Neil and D. Reed, *Inorg. Chem.*, **1997**, 36, 6238.

36. J. F. Allan, K. W. Henderson and A. R. Kennedy, *Chem. Commun.*, **1999**, 1325.
37. P. E. Eaton, C.-H. Lee and Y. Xiong, *J. Am. Chem. Soc.*, **1989**, *111*, 8016.
38. D. A. Evans and S. G. Nelson, *J. Am. Chem. Soc.*, **1997**, *119*, 6452.
39. (b) K. W. Henderson, W. J. Kerr and J. H. Moir, *Chem. Commun.*, **2000**, 479; (b) J. H. Moir, *PhD Thesis*, University of Strathclyde, **2002**; (c) K. W. Henderson, W. J. Kerr and J. H. Moir, *Tetrahedron*, **2002**, *58*, 4573.
40. J. D. Anderson, P. C. García, D. Hayes, K. W. Henderson, W. J. Kerr, J. H. Moir and K. P. Fondekar, *Tetrahedron Lett.*, **2001**, *42*, 7111.
41. (a) M. J. Bassindale, J. J. Crawford, K. W. Henderson and W. J. Kerr, *Tetrahedron Lett.*, **2004**, *45*, 4175; (b) J. J. Crawford, *PhD Thesis*, University of Strathclyde, **2004**.
42. (a) L. S. Bennie, W. J. Kerr, M. Middleditch and A. J. B. Watson, *Chem. Commun.*, **2011**, *47*, 2264; (b) L. S. Bennie, *PhD Thesis*, University of Strathclyde, **2012**; (c) M. Middleditch, *Post-Doctoral Report*, University of Strathclyde, **2007**; (d) A. J. B. Watson, *PhD Thesis*, University of Strathclyde, **2007**.
43. E. L. Carswell, D. Hayes, K. W. Henderson, W. J. Kerr and C. J. Russell, *Synlett*, **2003**, *7*, 1017.
44. (a) E. L. Carswell, *PhD Thesis*, University of Strathclyde, **2005**; (b) M. Pažický, *PhD Thesis*, University of Strathclyde, **2009**.
45. (a) H. G. Richey, Jr. and B. A. King, *J. Am. Chem. Soc.*, **1982**, *104*, 4672; (b) E. P. Squiller, R. R. Whittle and H. G. Richey, Jr., *J. Am. Chem. Soc.*, **1985**, *107*, 432; (c) H. G. Richey, Jr. and D. M. Kushlan, *J. Am. Chem. Soc.*, **1987**, *109*, 2510; (d) A. D. Pajerski, M. Parvez and H. G. Richey, Jr., *J. Am. Chem. Soc.*, **1988**, *110*, 2660.
46. K. W. Henderson, W. J. Kerr and J. H. Moir, *Chem. Commun.*, **2001**, 1722.
47. K. W. Henderson, W. J. Kerr and J. H. Moir, *Synlett*, **2001**, 1253.



48. (a) A. Alexakis, S. Gille, F. Prian, S. Rosset and K. Ditrich, *Tetrahedron Lett.*, **2004**, *45*, 1449; (b) J. A. Marshall and J. Lebreton, *J. Am. Chem. Soc.*, **1988**, *110*, 2925.
49. T. T. Tidwell, *Ketenes*, **1995**, John Wiley & Sons Inc., New York
50. C. A. Falter and M. M. Jouille, *Org. Lett.*, **2007**, *9*, 1987.
51. (a) L. R. Krepski and A. Hassner, *J. Org. Chem.*, **1978**, *43*, 2879; (b) W. T. Brady and M. O. Agho, *J. Heterocyclic Chem.*, **1983**, *20*, 501; (c) B. M. Trost and J. Xie, *J. Am. Chem. Soc.*, **2008**, *130*, 6231; (d) D. S. Radchenko, N. Koylova, O. O. Grygorenko and I. V. Komarov, *J. Org. Chem.*, **2009**, *74*, 5541.
52. A. V. Malkov, F. Friscourt, M. Bell, M. E. Swarbrick and P. Kočovský, *J. Org. Chem.*, **2008**, *73*, 3996.
53. R. Shirai, K. Aoki, D. Sato, H.-D. Kim, M. Murakata, T. Yasukata and K. Koga, *Chem. Pharm. Bull.*, **1994**, *42*, 690.
54. E. Curthbertson, P. O'Brien and T. D. Towers, *Synthesis*, **2001**, 693.
55. (a) M. Tokunaga, J. F. Larrow, F. Kakiuchi and E. N. Jacobsen, *Science*, **1997**, *277*, 936; (b) S. E. Schaus, B. D. Brandes, J. F. Larrow, M. Tokunaga, K. B. Hansen, A. E. Gould, M. E. Furrow and E. N. Jacobsen, *J. Am. Chem. Soc.*, **2002**, *124*, 1307.
56. (a) K. Takai, M. Sato, K. Oshima and H. Nozaki, *Bull. Chem. Soc. Jpn.*, **1984**, *57*, 108; (b) T. Calogeropoulou, G. B. Hammond and D. F. Wiemer, *J. Org. Chem.*, **1987**, *52*, 4185; (c) Y. Ding, W. Wang and Z. Liu, *Sulfur Silicon Relat. Elem.*, **1996**, *118*, 113.
57. M. Rajamanickam, *9 Month PhD Report*, University of Strathclyde, **2013**.
58. For reviews of the use of enol phosphates in cross-coupling reactions, see: (a) K. C. Nicolaou, P. G. Bulger and D. Sarlah, *Angew. Chem. Int. Ed.*, **2005**, *44*, 4442; (b) S. Protti and M. Fagnoni, *Chem. Commun.*, **2008**, 3611; (c) H. Fuwa, *Synlett*, **2011**, 6; (d) J. D. Sellars and P. G. Steel, *Chem. Soc. Rev.*, **2011**, *40*, 5170.

59. E. V. Anslyn and D. A. Dougherty, *Modern Physical Organic Chemistry*, **2006**, University Science Books: United States.
60. D. Gautier, S. Beckendorf, T. M. Gøgsig, A. T. Lindhardt and T. Skrydstrup, *J. Org. Chem.*, **2009**, *74*, 3536.
61. V. López-Carrillo and A. M. Echavarren, *J. Am. Chem. Soc.*, **2010**, *132*, 9292.
62. D. D. Perrin and W. L. F. Armarego, *Purification of Laboratory Chemicals*, **1998**, 3<sup>rd</sup> Edition, Pergamon Press: Oxford.
63. B. E. Love and E. G. Jones, *J. Org. Chem.*, **1999**, *64*, 3755.
64. E. Doni, S. O'Sullivan and J. A. Murphy, *Angew. Chem. Int. Ed.*, **2013**, *52*, 2239.
65. M. L. Sharma and J. Singh, *Synthetic Communications*, **2012**, *42*, 1306.
66. O. Lagerlund, M. L. H. Mantel and M. Larhed, *Tetrahedron*, **2009**, *65*, 7646.
67. C. R. Smith and T. V. RajanBabu, *Tetrahedron*, **2010**, *66*, 1102.
68. M.-Y. Lin, A. Das and R.-S. Liu, *J. Am. Chem. Soc.*, **2006**, *128*, 9640.
69. H.-J. Xu, F.-F. Zhu, Y.-Y. Shm. X. Wan, and Y.-S. Feng, *Tetrahedron*, **2012**, *68*, 4145.
70. T. Seiser and N. Cramer, *Angew. Chem. Int. Ed.*, **2008**, *47*, 9294.
71. Y. Cheng, X. Gu and P. Li, *Org. Lett.*, **2013**, *11*, 2664.

## Chapter 2

Towards the Total Synthesis of

(+)-(*S*)-Sporochnol A

## Contents

<b>1 Introduction</b> .....	178
<b>2 Proposed Work</b> .....	183
2.1 Retrosynthetic analysis .....	183
2.2 Accessing the prochiral ketone .....	184
<b>3 Results and Discussion</b> .....	186
3.1 Accessing the prochiral ketone <b>17</b> .....	186
3.2 Attempted improvements to the methyl group formation.....	192
3.3 Installing the stereogenic centre <i>via</i> a magnesium bisamide-mediated asymmetric deprotonation.....	194
3.4 Studies towards the cross-coupling of the enantioenriched enol phosphate <b>16</b> .....	197
3.5 Towards the completion of the synthesis.....	204
<b>4 Conclusions and Future Work</b> .....	208
<b>5 Experimental Procedures</b> .....	211
5.1 General Considerations .....	211
5.2 Accessing the prochiral ketone <b>17</b> .....	213
5.3 Attempted improvements to the methyl-group formation .....	223
5.4 Installing the stereogenic centre <i>via</i> a magnesium bisamide-mediated asymmetric deprotonation.....	225
5.5 Studies towards the cross-coupling of the enantioenriched enol phosphate <b>16</b> .....	227
<b>6 References</b> .....	241

# 1 Introduction

With firm foundations in the structural development of chiral magnesium amide species,<sup>1</sup> we were keen to expand these emerging protocols into the realm of total synthesis. As well as making continuous efforts to apply these systems to a broader range of cyclic and bicyclic ketones, whilst also exploring the use of alternative electrophiles, application within a target molecule synthesis was sought. The selection of an appropriate target to illustrate the applicability of such base systems would further broaden the scope of this methodology and highlight the robust nature of this chemistry. To this end, the monoterpene (+)-(*S*)-Sporochnol A **1** was chosen (**Figure 1**).

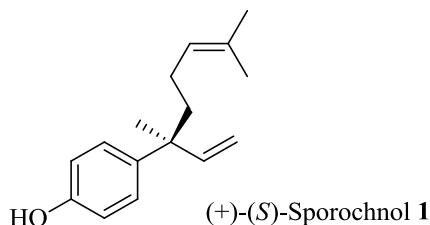


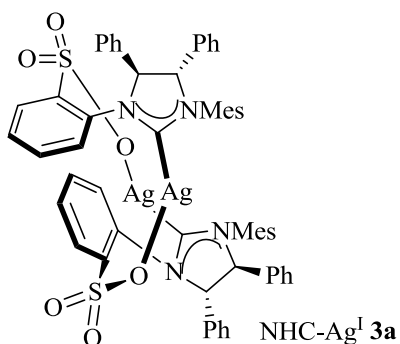
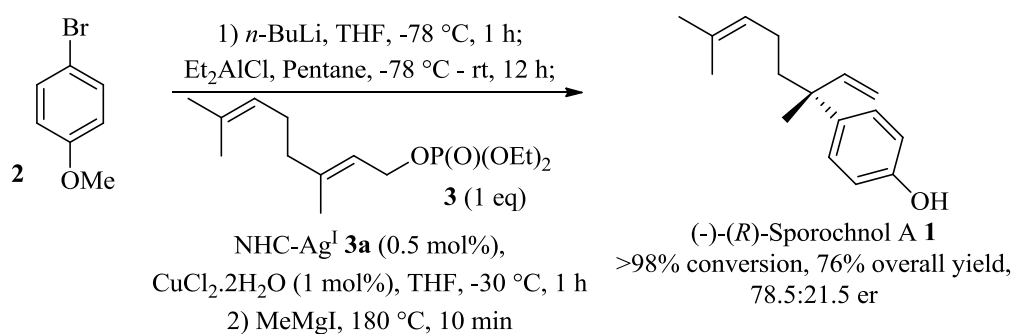
**Figure 1**

First isolated in 1993 from the Caribbean marine algae *Sporochnus Bolleanus*, (+)-(*S*)-Sporochnol A **1** has been shown to exhibit significant feeding deterrence towards herbivorous fish.<sup>2</sup> More pertinently, this natural product presents an interesting synthetic challenge. The limited number of heteroatoms within the natural product provides a lack of synthetic handles. Furthermore, the all carbon quaternary stereocentre embedded within the molecule offers a real challenge to the synthetic chemist.

Upon the initial isolation, the absolute stereochemistry of Sporochnol A **1** was uncertain. Following a relatively long linear synthetic route to this natural product starting with enantiomerically pure (*S*)-epichlorohydrin, however, Ogasawara and co-workers formed the unnatural (*R*)-Sporochnol A **1**.<sup>3</sup> This was determined through correlation to the configuration of (*S*)-epichlorohydrin and comparison with the original data, which was identical in all accounts other than the sign of the optical

rotation, leading to the conclusion that the unnatural enantiomer had been formed and (+)-(*S*)-Sporochnol A **1** is, indeed, the naturally occurring form of this product.

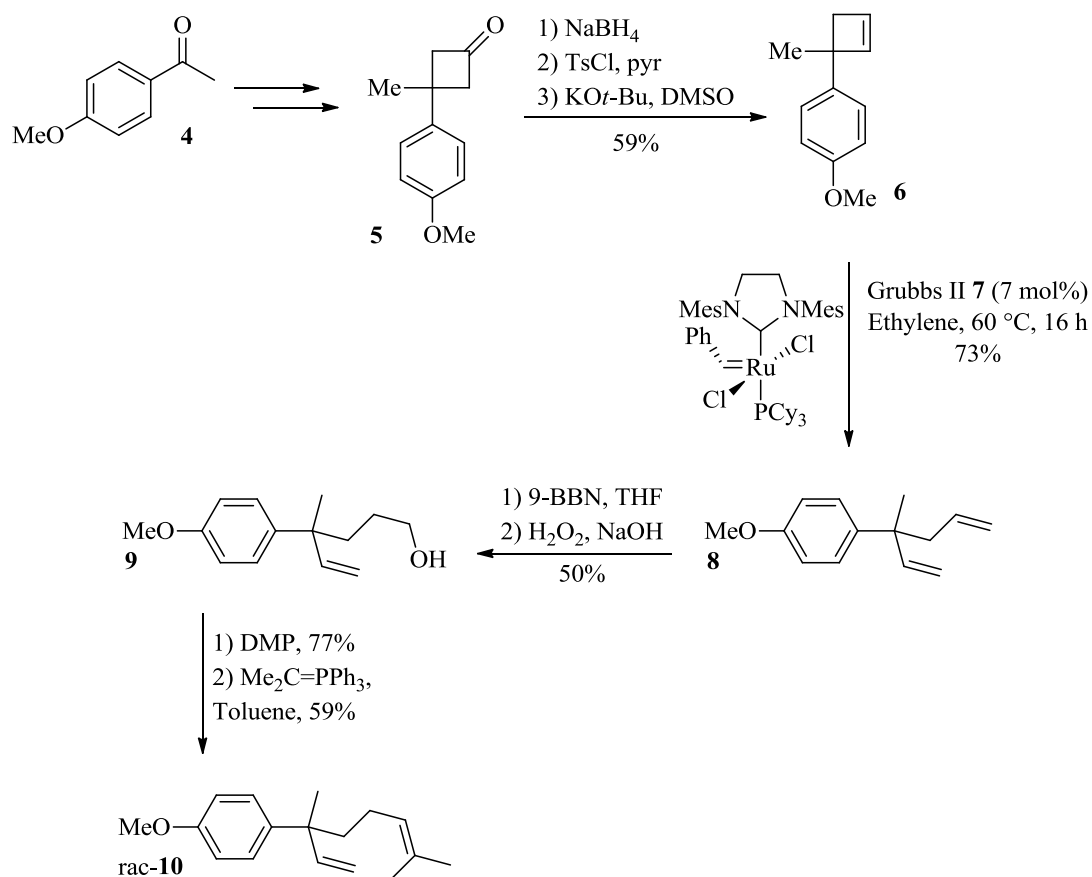
Following this clarification, a number of groups have published routes to both the natural<sup>4</sup> and unnatural enantiomers of Sporochnol A **1**.<sup>5</sup> These early synthetic pathways, however, either commence with chiral starting materials or use enzymes for a kinetic resolution of enantiomers at some stage within the synthesis. To the modern synthetic chemist, these strategies have become somewhat outdated in favour of using chiral reagents and catalysts to impart chirality within a molecule. Indeed, in this respect, Hoveyda revealed the use of a copper-catalysed allylic substitution in the formation of (-)-Sporochnol A **1**. Although a sub-stoichiometric amount of chiral ligand was used, the unnatural enantiomer was formed in just 78.5:21.5 er (**Scheme 1**).<sup>6</sup>



**Scheme 1**

In addition to the enantioselective routes published, a number of racemic routes to Sporochnol have been completed. These include, in particular, the short and efficient route developed by Li and co-workers.<sup>7</sup> For our purposes, the most significant of

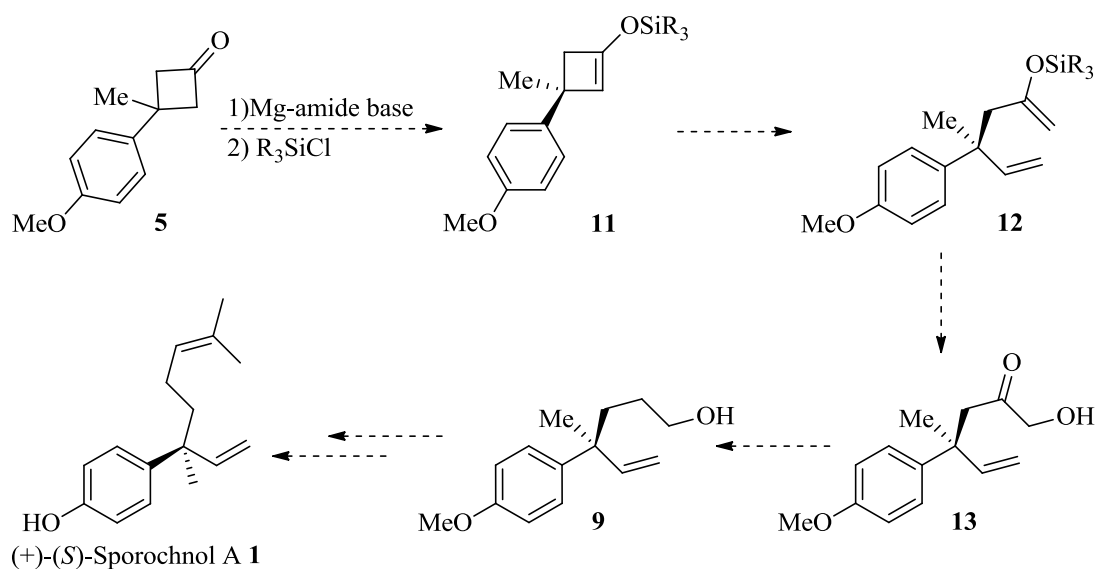
these pathways was produced by Harrity *et al.* whereby a ring opening metathesis was used as the key step in this formal synthesis.<sup>8</sup> More significantly, this route employs a prochiral ketone substrate **4** which is transformed into the cyclobutene **6** to carry out the optimised ring opening metathesis, using Grubbs second generation catalyst (Grubbs (II)) **7**, to afford the ring opened diene **8**. A hydroboration-oxidation then provided alcohol **9** which was subsequently oxidised in order to perform a Wittig reaction to access diene **10** and complete the formal synthesis (**Scheme 2**).



**Scheme 2**

Based on methods developed in our laboratory, it was envisaged that cyclobutanone **5** could be desymmetrised *via* an asymmetric deprotonation and trapped with an appropriate electrophile to impart the stereogenic centre within the molecule at an early stage. Through a series of transformations, this stereocentre could be subsequently carried through to the natural product. With this in mind, a synthetic route was devised to incorporate the use of a chiral magnesium bisamide to effect

this deprotonation and then extend the route towards the total synthesis of (+)-(*S*)-Sporochnol A **1**. The initially proposed synthetic route, therefore, began from cyclobutanone **5**.<sup>9</sup> It was envisaged that trapping with a trialkylsilane electrophile would be an effective method for the formation of the desired stereocentre, as literature precedent is available for such compounds (see also **Chapter 1**).<sup>10</sup> It was anticipated that a ring opening metathesis could be employed once again, as a potential route towards Sporochnol A, providing the ring opened product **12**. From here, a Rubottom oxidation would form the carbonyl intermediate **13** which could be, subsequently, reduced to form alcohol **9**. After this point, the completion of the synthesis would mirror that of Harrity and co-workers with, in this case, enantioenriched (+)-(*S*)-Sporochnol A **1** being accessed (**Scheme 3**).



**Scheme 3**

Previously within our laboratory, work towards the total synthesis of (+)-(*S*)-Sporochnol A had been initiated, applying the above route (**Scheme 3**). Unfortunately, early studies towards the enantioselective deprotonation were low yielding and did not afford the desired silyl enol ether **11** in an enantioenriched form. Alongside the studies towards the asymmetric deprotonations of 3-substituted and 3,3-disubstituted cyclobutanones (please refer to **Chapter 1**), it was proposed that this synthetic route could be further studied as part of this programme. Whilst these



investigations were ongoing, it was realised that the silane electrophile was producing lower than anticipated enantioselectivities for other substrates and, moreover, the better results were not always reproducible. This was overcome through the use of an alternative electrophile, diphenylphosphoryl chloride, and the formation of optically enriched enol-phosphates. Accordingly, it was proposed that an exciting new route towards (+)-(*S*)-Sporochnol A **1** could be devised to incorporate the use of this new electrophile and showcase the utility of an enantioenriched enol phosphate, in addition to the application of a magnesium bisamide. This original proposed synthetic pathway is outlined in the following section.

## 2 Proposed Work

### 2.1 Retrosynthetic analysis

As discussed, although (*S*)-(+)-Sporochnol A **1** is a seemingly simple naturally occurring terpenoid, this molecule presents an interesting synthetic challenge due to its all-carbon quaternary stereocentre. As the syntheses of this natural product described to date have used chiral auxiliaries, chiral resolutions, chiral catalysts, and chiral starting material, with varying degrees of success, it was proposed that an asymmetric deprotonation of a conformationally-locked, cyclic, prochiral ketone could be applied to induce the desired stereochemistry of the natural enantiomer of Sporochnol A. Furthermore, it is believed that using a chiral magnesium bisamide-mediated asymmetric deprotonation, developed within our laboratory and discussed further in **Chapter 1**, high levels of enantioselectivity could be achieved using readily accessed chiral bases. Trapping of the chiral enolate with an appropriate electrophile would then allow the necessary steps to the natural product to be carried out with the stereogenic centre set in place. To this end, a retrosynthetic route has been devised and is presented below (**Figure 2**).

From (*S*)-(+)-Sporochnol A **1**, the final step planned is a deprotection from the methyl-protected analogue of the natural product, **10**. This precursor could be formed *via* an elimination of the diol species **14** which, itself, could be accessed through an oxidative ring opening of alkene **15**. At this point, an important step in this synthesis would be to use a metal-mediated cross coupling to install the *iso*-propyl unit using the enantioenriched enol phosphate **16** as the coupling partner. Enol phosphate **16** is thus the product of a magnesium bisamide-mediated asymmetric deprotonation, the key step in this synthesis and that which embeds the quaternary chiral centre within the molecule. From here, the prochiral ketone **17** can be formed from cheap and readily available starting materials (**18** and **19**).

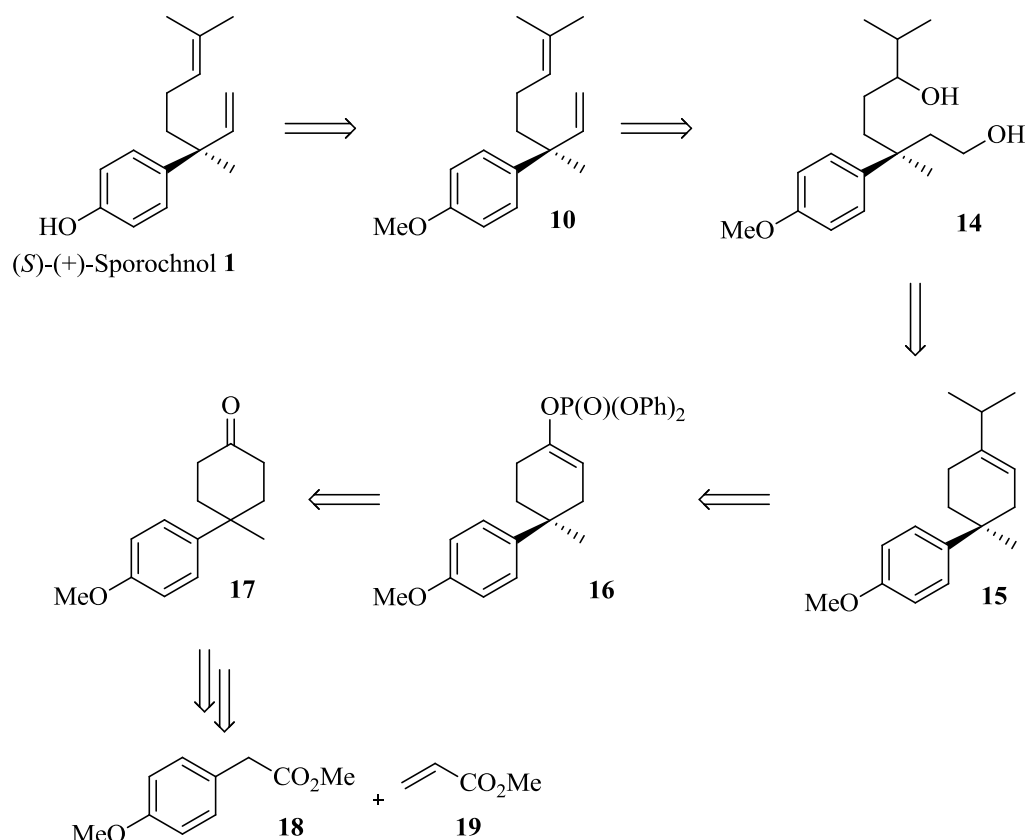


**Figure 2**

## 2.2 Accessing the prochiral ketone

As discussed, the prochiral ketone **17** is the first of two key intermediates in the proposed synthesis of (+)-(*S*)-Sporochnol A **1**. The first goal was therefore to synthesise quantities of this ketone on a large scale in order to apply the asymmetric deprotonation and continue the synthesis to the natural product. A number of routes to ketone **17** could be devised; however, one that is reliable and scalable was important for this application. As outlined in **Figure 2**, this 4,4-disubstituted cyclohexanone can be prepared from commercially available starting materials. In 2007, Julian and co-workers revealed an efficient one-pot double Michael addition-Dieckmann condensation for the formation of 4,4-disubstituted cyclohexane  $\beta$ -keto esters.<sup>11</sup> Although the  $\beta$ -keto ester was not the desired compound for this synthesis, the decarboxylation to 4,4-disubstituted cyclohexanones is also outlined in this publication. It was then envisaged that a sequence of protection, reduction, and

deprotection could be employed to access the desired ketone **17**. This proposed synthetic route to **17** is outlined below (**Figure 3**).

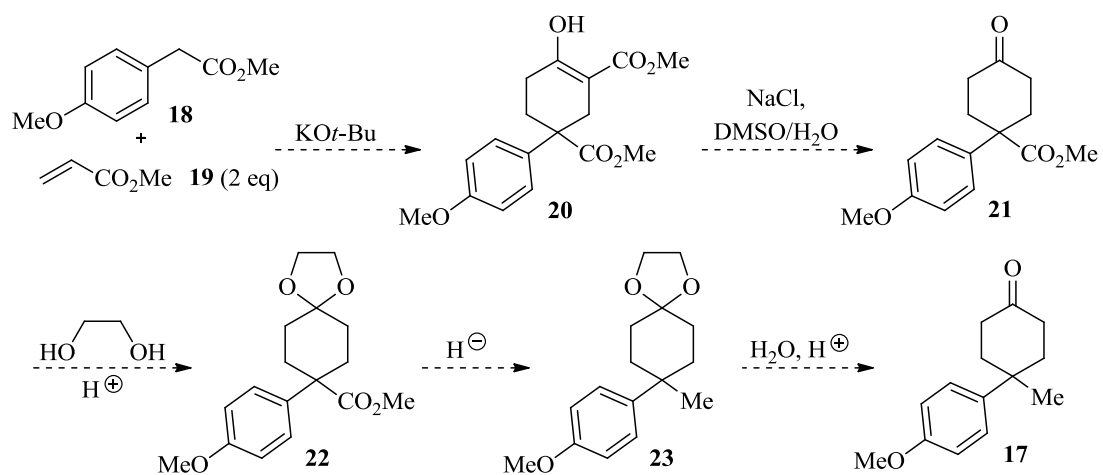
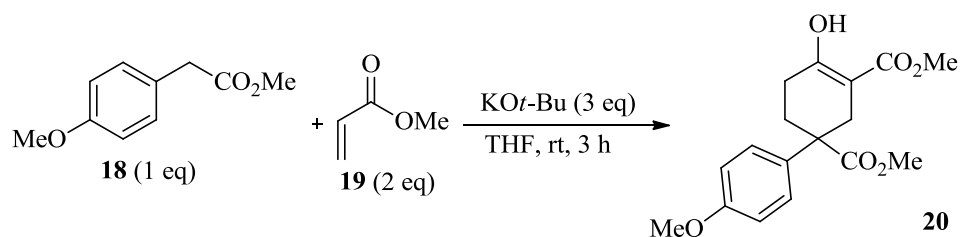


**Figure 3**

## 3 Results and Discussion

### 3.1 Accessing the prochiral ketone 17

With this proposed pathway in mind, preparation of  $\beta$ -keto ester **20** commenced, using conditions described in the literature (Scheme 4, Table 1).<sup>11</sup> Taking methyl 2-(4-methoxyphenyl)acetate **18** with two equivalents of methyl acrylate **19**, the one-pot double Michael addition-Dieckmann condensation was carried out, with the aid of potassium *tert*-butoxide. Initial attempts on a small and moderate scale (Entries 1 and 2, Table 1) were high yielding and in line with the literature precedent for the formation of **20**. In an effort to increase the overall efficiency of our proposed route to Sporochinol A **1**, this first step was scaled up to 200 mmol (Entry 3, Table 1). Pleasingly, after work-up of the reaction, a quantitative yield was obtained. It should be noted that column chromatography is not necessary for the purification of **20** and this can be used directly in the subsequent decarboxylation step.



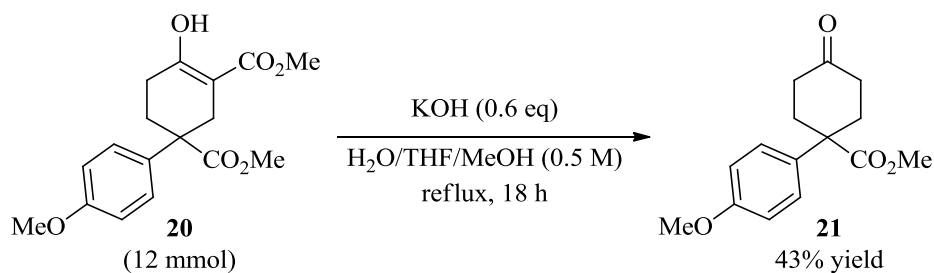
Scheme 4

Entry	Scale (mmol)	Yield (%)
1	5.5	84
2	28	87
3	200	100

Table 1

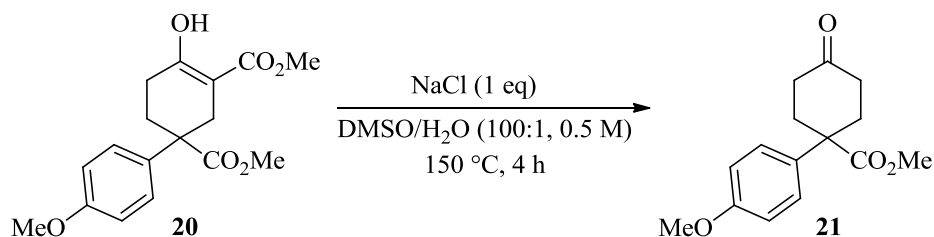
For the decarboxylation of  $\beta$ -keto ester **20**, two methods are described in the same publication as quoted above.<sup>11</sup> Either classical basic conditions using aqueous

potassium hydroxide in a THF/methanol solvent mixture, or a Krapcho method employing sodium chloride and DMSO can be utilised. Initially, classical conditions were trialled on a moderate scale (**Scheme 5**). Unfortunately, under these reaction conditions, only 43% of the desired ketone **21** was obtained. In addition, 11% of the starting material was returned but the remaining material could not be purified and it was suspected that over decarboxylation had occurred.



**Scheme 5**

In an effort to find a more efficient and higher yielding decarboxylation method, the Krapcho conditions were employed. Once again, conditions from the literature were used, and careful monitoring of the reaction was carried out to avoid over-decarboxylation. Pleasingly, this method was far more effective for the formation of **21** (**Scheme 6, Table 2**). On a moderate scale, good yields were obtained for this decarboxylation method (**Entries 1 and 2, Table 2**). When this reaction was scaled up, however, a slight drop in the yield **21** was obtained (**Entry 3, Table 2**). Having stated this, column chromatography was carried out for this step, as some unreacted starting material remained; so on such a large scale, this 59% yield was not detrimental to the amount of clean material being carried through the synthesis.

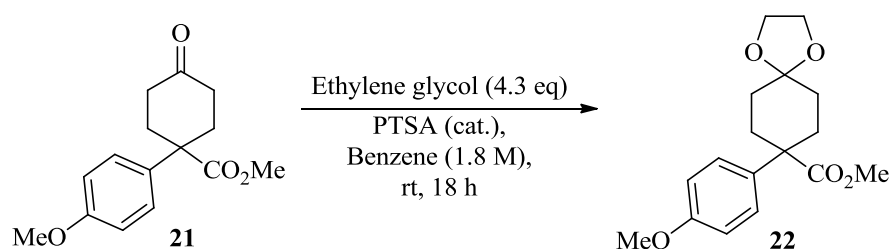


**Scheme 6**

Entry	Scale (mmol)	Yield (%)
1	12	77
2	24	73
3	200	59

**Table 2**

With the 4,4-disubstituted ketone **21** now in hand, manipulation of the second ester group could be carried out in order to obtain the required methyl group in this position. A reduction, followed by displacement with a hydride source was envisaged, so in order to prevent competing reactivity at the ketone carbonyl, this functional group was protected using ethylene glycol. Mild conditions were sought for this protection and, pleasingly, using an excess of ethylene glycol in benzene, with catalytic PTSA, was effective, high yielding, and scalable for the formation of **22** (Scheme 7, Table 3).<sup>12</sup> Furthermore, column chromatography was not required as **22** was obtained cleanly and used in the subsequent reduction step.



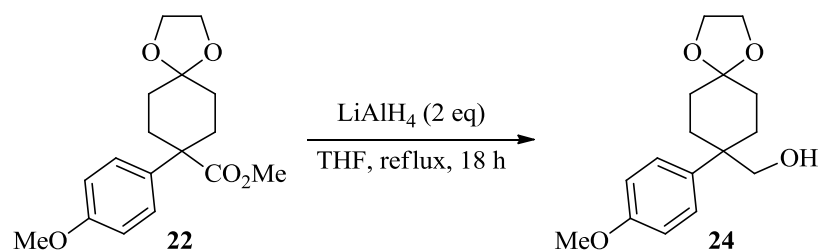
**Scheme 7**

Entry	Scale (mmol)	Yield (%)
1	5.1	94
2	28.9	93
3	117.6	90

**Table 3**

Having protected the ketone moiety, reduction of the ester commenced. Using conditions from the literature, which had shown to be compatible with an acetal

group within the molecule,  $\text{LiAlH}_4$  was utilised as the reducing agent.<sup>13</sup> Thus, taking the acetal-ester **22** in THF at 0 °C,  $\text{LiAlH}_4$  was added portionwise. The reaction mixture was then gradually heated to reflux. After stirring overnight, cooling, and working up the reaction, the alcohol **24** was obtained in excellent yield and high purity (**Scheme 8, Table 4**). As with previous steps, no purification was required.



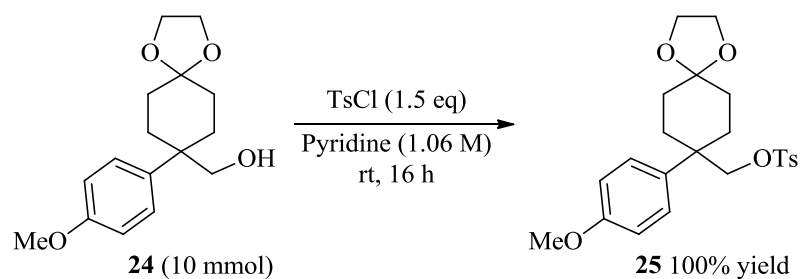
**Scheme 8**

Entry	Scale (mmol)	Yield (%)
1	2.6	100
2	13.0	98
3	106.0	96

**Table 4**

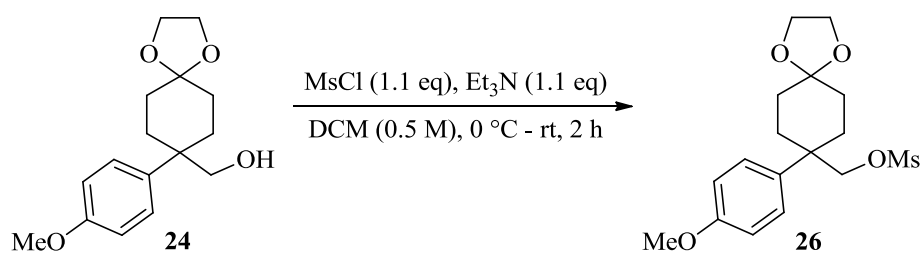
At this juncture, the final reduction of the alcohol group into a methyl group was required. It was envisaged that the newly formed alcohol could be converted to a leaving group and displaced with a hydride source. Again, evidence for this displacement in the presence of an acetal functionality was considered. Pleasingly, it has been shown that both tosylate and mesylate groups can be displaced with the highly nucleophilic lithium triethylborohydride (Super-Hydride) in the presence of an acetal.<sup>14</sup> With this precedent in hand, alcohol **24** was converted to the tosylate **25** using *p*-toluenesulfonylchloride and excess pyridine as the solvent (**Scheme 9**).





**Scheme 9**

Gratifyingly, this tosylation was quantitatively yielding and tosylate **25** was used in the Super-Hydride displacement without purification. Unfortunately, however, this resulting gum was difficult to manipulate and decomposed quickly, so full characterisation was not possible for this intermediate. Although this activated alcohol was appropriate for the subsequent displacement step, its instability was somewhat hindering, as scale-up of the Super-Hydride displacement was difficult. It was envisaged that a mesylate may be more stable and also a viable leaving group for displacement with a hydride. A mesylation of alcohol **24** was thusly carried out (**Scheme 10**).<sup>15</sup> Pleasingly, this was also an efficient preparation and mesylate **26** was formed in quantitative yield in all attempts (**Scheme 10, Table 5**). In addition, the mesylate **26** was a more stable intermediate than the tosylate **25** and could be stored for up to one month in the fridge.

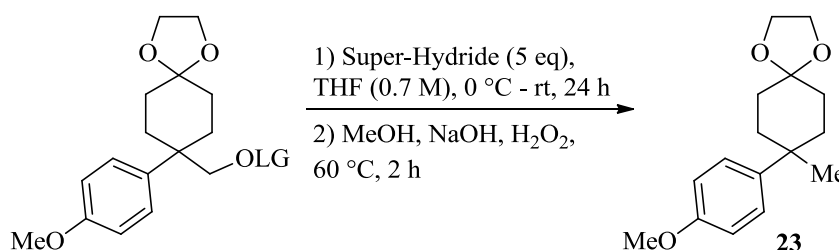


**Scheme 10**

Entry	Scale (mmol)	Yield (%)
1	3.6	100
2	19.4	100

**Table 5**

Having activated the alcohol **24** into an appropriate leaving group the displacement with Super-Hydride was attempted (**Scheme 11, Table 6**).<sup>14</sup> Initially using tosylate **25** on a small scale (**Entry 1, Table 6**), a good 65% yield was obtained after purification by column chromatography. Attempts to scale this reaction up, however, (**Entry 2, Table 6**) led to a decrease in the yield of **23**. Moreover, the tosylate gum (**25**) could not easily be separated into batches or stored for more than a day, thus, the leaving group was altered and the mesylate derivative (**26**) was employed in the Super-Hydride displacement (**Entries 3 and 4, Table 6**). Pleasingly, this substrate was easier to manipulate and store, and was, indeed, higher yielding on a larger scale than the tosylate derivative.



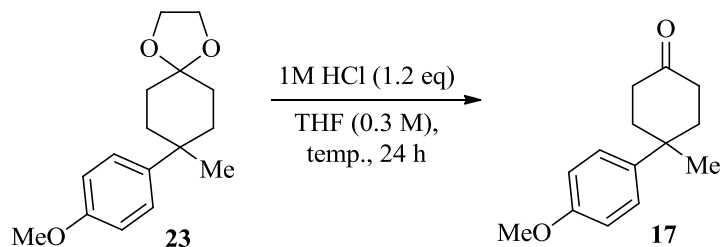
**Scheme 11**

<b>Entry</b>	<b>LG</b>	<b>Scale (mmol)</b>	<b>Yield (%)</b>
1	Ts ( <b>25</b> )	2.0	65
2	Ts ( <b>25</b> )	8.0	53
3	Ms ( <b>26</b> )	8.9	61
4	Ms ( <b>26</b> )	19.4	77

**Table 6**

With the methyl group now in place, the final step to access the desired 4,4-disubstituted cyclohexanone **17** was deprotection of the acetal **23**. Using aqueous 1M HCl and THF, the desired ketone **17** was obtained (**Scheme 12, Table 7**).<sup>16</sup> Initially, as described in the literature example, this deprotection was performed at room temperature (**Entry 1, Table 7**) but the reaction did not proceed to completion, as only a 67% yield of ketone **17** was obtained and the unreacted acetal **23** was also

recovered. Gently heating this reaction to 40 °C enhanced this yield and almost quantitative conversion was achieved, providing significant quantities of **17** (**Entry 2, Table 7**). Further preparations of ketone **17** were therefore performed at this slightly elevated temperature.



**Scheme 12**

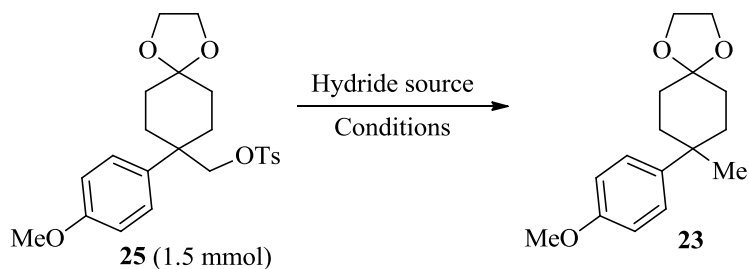
Entry	Temp.	Scale (mmol)	Yield (%)
1	rt	7.6	67
2	40 °C	12.0	99

**Table 7**

### 3.2 Attempted improvements to the methyl group formation

As some difficulties in scale up and repeatability had been an issue for the displacement of tosylate **25** with Super-Hydride for the installation of the methyl group in **23**, some alternative strategies were considered. A number of small scale trial reactions were therefore carried out to investigate alternative hydride sources for displacement of the tosylate **25**. Firstly, it should be noted that the tosylate was formed (according to **Scheme 9**) and used immediately, without purification in the following reactions. Thus, the displacement of **25** was attempted with the hydride sources and conditions outlined below (**Scheme 13, Table 8**).<sup>17,18</sup> Initially, LiAlH<sub>4</sub> was employed in diethyl ether at room temperature (**Entry 1, Table 8**),<sup>17</sup> but no reaction occurred and the tosylate **25** was recovered. Changing the solvent to THF was thought to improve the reactivity, but at both room temperature and reflux

(**Entries 2 and 3, Table 8**) no reactivity was observed. Finally, sodium borohydride was trialled, at room temperature in ethanol (**Entry 4, Table 8**)<sup>18</sup> but, again, only the starting tosylate was recovered. At this point, with improvements to the displacement having been made by using the mesylate derivative **26**, no further conditions were studied and Super-Hydride remained the hydride source of choice as good yields were obtained with this alternative intermediate.



**Scheme 13**

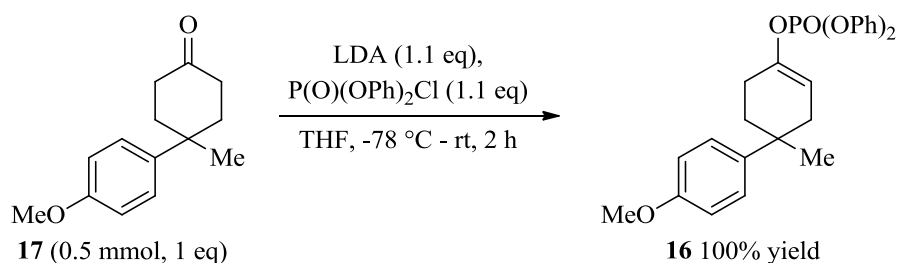
Entry	Hydride source	Conditions	Yield (%)
1	LiAlH <sub>4</sub>	Et <sub>2</sub> O, rt, 1 h	0
2	LiAlH <sub>4</sub>	THF, rt, 16 h	0
3	LiAlH <sub>4</sub>	THF, reflux, 16 h	0
4	NaBH <sub>4</sub>	EtOH, rt, 16 h	0

**Table 8**

In summary, the novel 4,4-disubstituted ketone **17** has been prepared over seven synthetic steps in up to 55% overall yield. Furthermore, only three of these steps require column chromatography and each step can be scaled up to 19 mmol or greater. Indeed, the early steps of this synthetic sequence have been performed on a 200 mmol scale and provided quantitative, or near quantitative, amounts of material.

### 3.3 Installing the stereogenic centre *via* a magnesium bisamide-mediated asymmetric deprotonation

After having devised an efficient and scalable route to the required prochiral ketone **17**, the asymmetric deprotonation to embed the stereogenic centre was carried out. In order to assess the level of enantioselectivity by chiral HPLC, a racemic mixture of the desired enol phosphate **16** was first prepared. Using the readily formed base, LDA, and trapping the resulting enolate with diphenylphosphoryl chloride, enol phosphate **16** was formed in a quantitative yield (**Scheme 14**).<sup>19</sup> This novel enol phosphate was subsequently analysed by chiral HPLC to establish an appropriate method for the determination of asymmetric induction when a chiral base is employed.

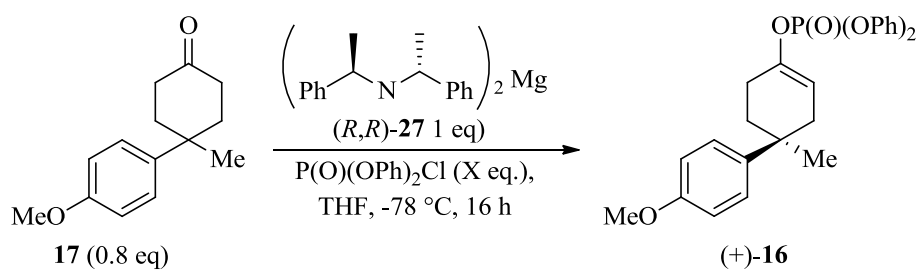


**Scheme 14**

With the prochiral ketone (**17**) in hand and a chiral HPLC method in place for the assessment of enantioselectivity of the enol phosphate **16**, optimisation of the magnesium bisamide-mediated asymmetric deprotonation commenced. Developments and applications of chiral magnesium bisamides have been ongoing within our laboratory since their first development in 2000.<sup>1a</sup> Since this seminal publication, significant advances to the magnesium bisamide structure have been made which has led to enhanced reactivity and enantioselectivity. **Chapter 1** details these advances extensively. Most notably, the recently developed *C*<sub>2</sub>-symmetric magnesium bisamide (*R,R*)-**27** has proven to be highly reactive, stable, and indeed, facilitated some of the highest levels of enantioselectivity for such a transformation to date.<sup>1d</sup> It was for these reasons that *C*<sub>2</sub>-symmetric magnesium bisamide (*R,R*)-**27** was selected for application towards the total synthesis of (+)-(*S*)-Sporochinol A **1**.

As discussed in **Chapter 1**, when the alternative electrophile, diphenylphosphoryl chloride, is employed with magnesium bisamides no additives are required within the reaction mixture in order to achieve high levels of enantioselectivity in the enol phosphate products.

Taking prochiral ketone **17** and employing  $C_2$ -symmetric magnesium bisamide (*R,R*)-**27** with diphenylphosphoryl chloride under internal quench conditions, enol phosphate **16** was formed with a good level of enantioselectivity (**Scheme 15, Table 9**). Initially, just one equivalent of the electrophile was used on a 1 mmol scale (**Entry 1, Table 9**) and a high 78% yield with 87:13 er was obtained for enol phosphate **16**. Pleasingly, when the equivalents of diphenylphosphoryl chloride were increased to two, the yield of **16** increased to 90% (**Entry 2, Table 9**). When the scale of this asymmetric deprotonation was doubled (**Entry 3, Table 9**) an outstanding quantitative yield was obtained, proving that magnesium bisamide bases are, indeed, robust and viable reagents for use within a total synthesis endeavour. Furthermore, no significant change in the enantioselectivity was observed for these subsequent deprotonations. For an all carbon quaternary stereocentre, this level of enantioinduction is very pleasing, especially considering the structural simplicity of the chiral base reagent itself. It should be noted that this is the first example of a 4,4-disubstituted cyclohexanone substrate to be desymmetrised using a chiral magnesium bisamide. This pattern of substitution makes for a more challenging desymmetrisation due to the lower barrier to ring-flipping of such a substrate. Conformational analysis of cyclohexane rings has shown that the difference in energy between a methyl- and phenyl-group is not much greater than 1 kcal/mol, whereas the difference between a proton and an alkyl or aryl substituent is at least 2 kcal/mol.<sup>20</sup> Thus, with a 4,4-disubstituted cyclohexanone substrate, such as **17**, the energy barrier for ring-flipping is expected to be lower than traditional substrates employed (see **Chapter 1** for further discussion of such desymmetrisations). It should also be highlighted that, with a chiral lithium amide base, this level of enantioselectivity can only be achieved when extremely low reaction temperatures of -100 °C are employed, albeit with a different electrophile.<sup>21</sup>



**Scheme 15**

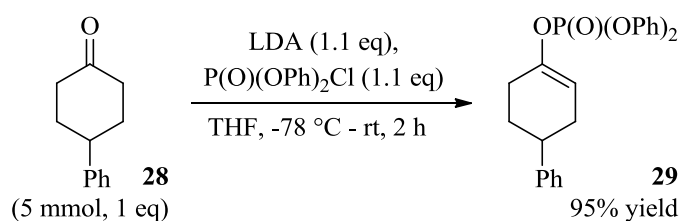
Entry	Scale (mmol)	Eq. P(O)(OPh) <sub>2</sub> Cl	Yield (%)	er ((+):(-))
1	1	1	78	87:13
2	1	2	90	88:12
3	2	2	100	86:14

**Table 9**

With high levels of enantiopurity imparted within enol phosphate **16** this enantioenriched carbon centre could be carried through the subsequent steps towards the natural product. Having formed an enol phosphate with high optical purity, it was envisaged that this could be cross coupled with an organometallic *iso*-propyl reagent and a transition metal catalyst.

### 3.4 Studies towards the cross-coupling of the enantioenriched enol phosphate **16**

Referring back to the retrosynthetic analysis (**Figure 2**), the enantioenriched enol phosphate **16** could be used as a coupling partner to install an *iso*-propyl group. There are many examples in the literature of enol phosphates being used as alternative coupling partners to triflates, due to their higher stability.<sup>22</sup> Indeed, a range of transition metal catalysts have been used alongside various different transmetallation reagents for carbon-carbon bond formation from enol phosphates. As a starting point to this cross-coupling study, the inexpensive and toxicologically benign iron catalyst Fe(acac)<sub>3</sub> was selected as this catalyst has been shown to be highly reactive towards enol phosphates for their cross-coupling with Grignard reagents.<sup>21</sup> Additionally, using a Grignard coupling agent was also favourable due to their availability, stability, and low cost, compared with other coupling agents, such as alkyl boronates. Finally, with a view to preserving the precious enol phosphate **16**, a model substrate was used for this study. Thus, deprotonating 4-phenylcyclobutanone **28** with LDA, and trapping with diphenylphosphoryl chloride, enol phosphate **29** was formed in 95% yield (**Scheme 16**).<sup>19</sup>

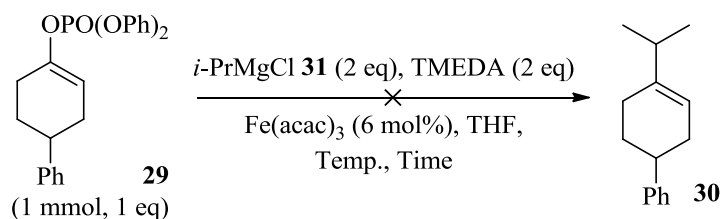


**Scheme 16**

With a model enol phosphate in hand, **29** was subjected to an iron-mediated cross-coupling reaction to form **30** with isopropylmagnesium chloride **31** (**Scheme 17**, **Table 10**).<sup>23</sup> Firstly, literature conditions were applied and the reaction was carried out at -10 °C and warmed to 0 °C over an hour (**Entry 1**, **Table 10**). Regrettably, no reaction was observed and the starting enol phosphate **29** was recovered. Attempts to improve the reactivity were made by leaving the reaction for longer (**Entry 2**, **Table**



**10)** and warming the reaction to room temperature (**Entry 3, Table 10**). Neither of these efforts was fruitful, however, and the enol phosphate **29** was returned in all cases.

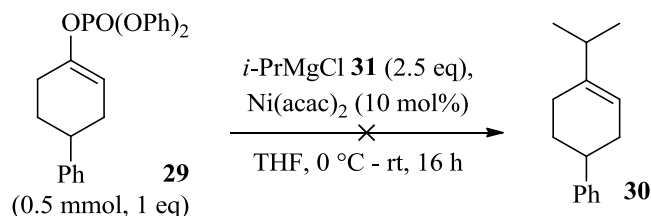


**Scheme 17**

Entry	Temp. (°C)	Time (h)	Yield (%)
1	-10 to 0	1	0
2	-10 to 0	4	0
3	-10 to rt	4	0

**Table 10**

Wishing to avoid costly transition metals and coupling agents, the nickel catalyst  $\text{Ni}(\text{acac})_2$  was considered after the lack of success achieved with the analogous iron catalyst. Again, literature conditions were employed whereby the enol phosphate **29** was added to a solution of  $\text{Ni}(\text{acac})_2$  with Grignard reagent **31** (**Scheme 18**, and **Entry 1, Table 11**).<sup>24</sup> No reaction was observed, however, so the order of addition was altered. For the procedure using  $\text{Fe}(\text{acac})_3$  (**Scheme 17**), the Grignard reagent is added last. Thus, this procedure was followed using  $\text{Ni}(\text{acac})_2$  (**Entry 2, Table 11**). Unfortunately, no reaction was observed once again and enol phosphate **29** was recovered at the end of the reaction.

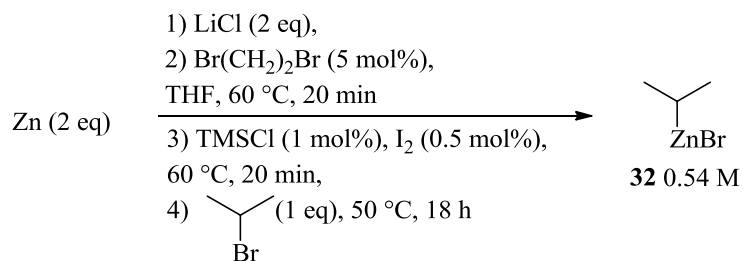


**Scheme 18**

Entry	Comments	Yield (%)
1	Enol phosphate added to Ni(acac) <sub>2</sub> + <i>i</i> -PrMgCl	0
2	<i>i</i> -PrMgCl added to Ni(acac) <sub>2</sub> + enol phosphate	0

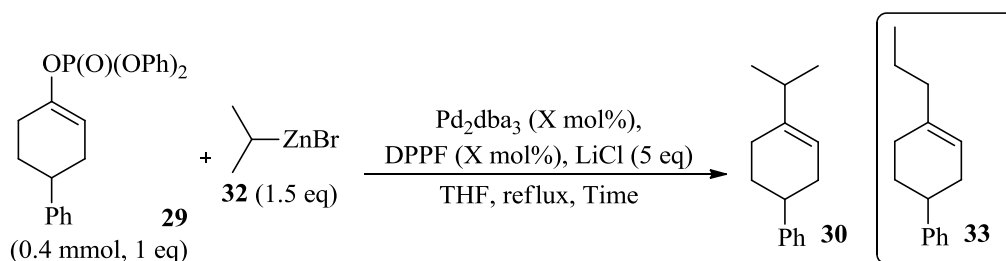
**Table 11**

Having had no success with iron or nickel catalysts, palladium was turned to as a more frequently used cross-coupling catalyst. Additionally, the coupling agent was changed from a Grignard to an alkylzinc reagent, as this coupling was also preceded in the literature. Skrydstrup has coupled a range of alkylzinc reagents with aryl and vinyl phosphates using tris(dibenzylideneacetone)dipalladium(0) (Pd<sub>2</sub>dba<sub>3</sub>) and 1,1'-bis(diphenylphosphino)ferrocene (DPPF) as a ligand to facilitate these cross-couplings, with good to excellent yields for all substrates.<sup>25</sup> With a view to using these conditions to couple the enantioenriched enol phosphate **16** and form the desired cyclohexene intermediate **15** towards the synthesis of Sporochinol A **1**, these conditions were also trialled. To this end, the required *iso*-propylzinc bromide **32** was prepared according to a method described by Knochel and co-workers (**Scheme 19**).<sup>26</sup> After activating zinc dust with lithium chloride and 1,2-dibromoethane, followed by TMSCl, 2-bromopropane was added and the suspension was heated to 50 °C in a Schlenk flask overnight. This suspension was cooled and transferred to a pear-shaped flask *via* cannula. The solution was subsequently standardised using iodine prior to use in the following Negishi cross-coupling reaction.



**Scheme 19**

With freshly prepared *iso*-propylzinc bromide **32**, the Negishi cross-coupling reaction was attempted using model enol phosphate **29** (Scheme 20).<sup>25</sup> Initially, the literature conditions were used, with the low catalyst loading of 2.5 mol% Pd<sub>2</sub>dba<sub>3</sub> and 5 mol% of the phosphine ligand, DPPF (Entry 1, Table 12). Unfortunately, none of the desired **30** was observed by <sup>1</sup>H NMR after work-up and column chromatography, but an alternative product was obtained. The *n*-propyl product **33** was thought to have formed from isomerisation of the *iso*-propylzinc bromide **32**. This product could not be cleanly isolated, however, due to large amounts of THF solvent remaining after chromatography. It was then proposed that increasing the catalyst loading may alter the reactivity of this system. So, to discover whether this prevented the observed isomerisation, the catalyst loading was doubled (Entry 2, Table 12). Under these conditions, no reactivity was observed. Finally, using the lower catalyst loading (2.5 mol%, Entry 3, Table 12) the reaction was allowed to stir at reflux for a longer time in an effort to improve the yield and establish what effect this had on the degree of isomerisation. Regrettably, no improvement to the yield was made, and the only isomer observed in the <sup>1</sup>H NMR was the *n*-propyl cyclohexene **33**. It was clear from these results that the *iso*-propylzinc bromide **32** was not an effective coupling partner for the desired reaction with an enol phosphate.



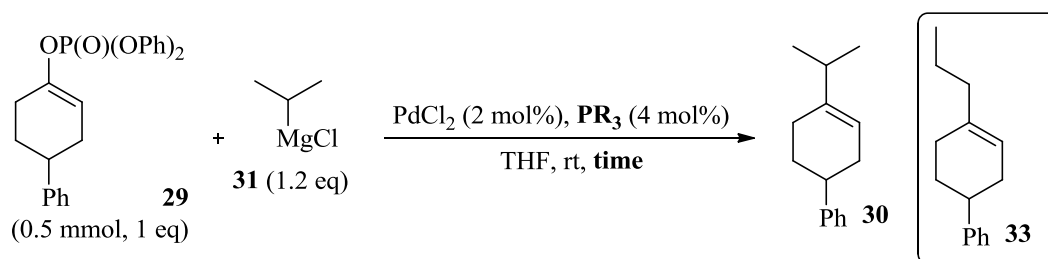
**Scheme 20**

Entry	Pd <sub>2</sub> dba <sub>3</sub> mol%	DPPF mol%	Time (h)	Yield (%) <sup>a</sup>
1	2.5	5	18	0 (66)
2	5	10	18	0 (0)
3	2.5	5	48	0 (55)

<sup>a</sup> Yield in parenthesis denotes <sup>1</sup>H NMR yield of **33**

**Table 12**

Having achieved little success with a zinc reagent, Grignard reagents were revisited as potential coupling partners with enol phosphates. Using a different palladium catalyst, palladium(II) chloride, two different phosphine ligands were investigated in an effort to overcome the isomerisation of the *iso*-propyl unit being incorporated (Scheme 21). Firstly, triphenylphosphine was employed (Entry 1, Table 13).<sup>27</sup> Although a high 86% <sup>1</sup>H NMR yield was obtained, this was the isomerised product **33** rather than the desired *iso*-propyl containing product **30**. It was deliberated that the isomerisation may be occurring after the oxidative addition step of this reaction cycle, thus, to enhance the rate of reductive elimination (to prevent the isomerisation) a bulkier phosphine ligand was used (Entry 2, Table 13).<sup>27</sup> The use of tribenzylphosphine, however, was detrimental to the yield and did not prevent the isomerisation, as **33** was the only product observed by <sup>1</sup>H NMR spectroscopy. Finally, an alternative system was considered, using ligandless conditions developed by Skrydstrup and co-workers.<sup>28</sup> A range of aryl Grignard reagents were coupled with enol phosphates in this publication, in good to excellent yields. Thus, these conditions were applied with isopropylmagnesium chloride in an effort to effect this coupling with enol phosphate **29** (Entry 3, Table 13).<sup>28</sup> Disappointingly, only 22% yield of the isomerised product was obtained once again.



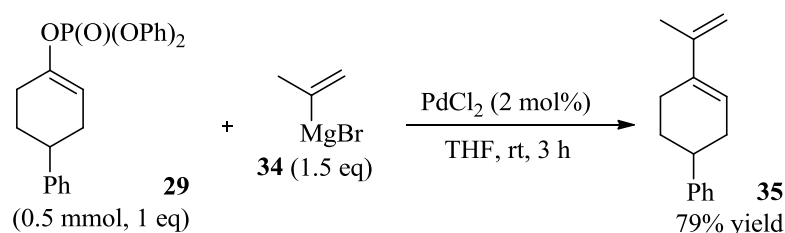
Scheme 21

Entry	PR <sub>3</sub>	Time	Yield (%) <sup>a</sup>
1	PPh <sub>3</sub>	1 h	86
2	PBn <sub>3</sub>	1 h	18
3	None	16 h	22

<sup>a</sup> Yield of **33**, <sup>1</sup>H NMR yield.

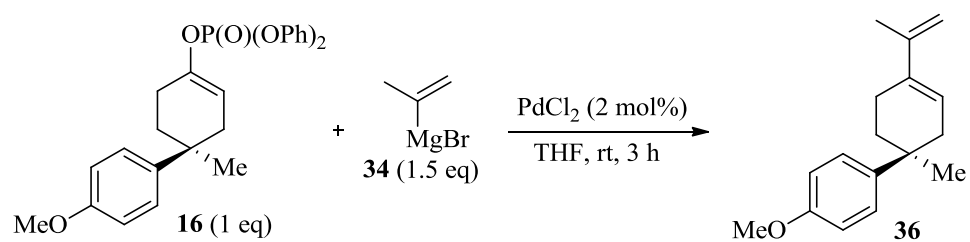
Table 13

As isomerisation had occurred in all cases we endeavoured to find an alternative coupling partner which could be converted to the required *iso*-propyl group after the coupling reaction. As Skrydstrup had used vinyl and aryl Grignard reagents it was concluded that the  $sp^2$  centre was a requirement for this type of coupling reaction. It was therefore proposed that isopropenylmagnesium bromide **34** could be employed to form a diene product (**35**). If this was to be successful and applied within the synthesis towards Sporochinol A **1**, a selective reduction of the terminal alkene, over the internal alkene, could be subsequently carried out to access the desired cyclohexene **15**. With this in mind, Skrydstrup's conditions were applied to the cross-coupling of enol phosphate **29** with isopropenylmagnesium bromide **34** (**Scheme 22**).<sup>28</sup> Delightedly, a high 79% yield of the desired diene **35** was obtained, free from solvent impurities. It should be noted that although the literature describes this reaction to be carried out in a glove box, it was found that performing this reaction in a Schlenk flask, which had been flame-dried and purged with argon before use, was sufficient for access to the desired coupled product.



**Scheme 22**

With a cross-coupling method established using a model substrate, these conditions were applied to the intermediate enol phosphate **16** in the synthesis towards Sporochinol A **1**. Pleasingly, on a small scale, excellent yields of diene **36** were obtained in all attempts at this cross coupling reaction (**Scheme 23, Table 14**).<sup>28</sup>



**Scheme 23**

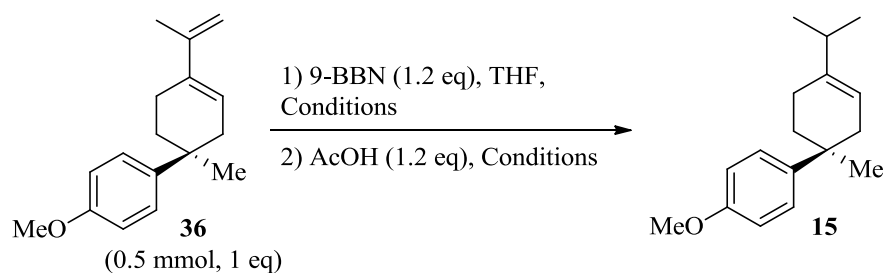
Entry	Scale (mmol)	Yield (%)
1	0.28	71
2	0.52	99
3	0.66	73
4	1.26	94

**Table 14**

After a rather extensive search through literature conditions to find an appropriate coupling method for enol phosphate **16**, the synthesis towards (+)-(*S*)-Sporochnol A **1** continued.

### 3.5 Towards the completion of the synthesis

As cyclohexene **15** had not been formed directly from the enol phosphate precursor, an additional step was required to selectively reduce the terminal alkene in the presence of the internal alkene. It was envisaged that a hydroboration – protonolysis protocol could be employed to facilitate this. 9-BBN was selected for this hydroboration due to the bulk of this borane reagent; this should only be reactive with the accessible terminal alkene. Such a protocol was not explicitly outlined within the current literature at the time, however, similar conditions allowed some trial reactions to be carried out (**Scheme 24**).<sup>29</sup> Taking diene **36** in THF at ambient temperature, 9-BBN was added and the reaction mixture was stirred over night. Following this, the reaction mixture was cooled to 0 °C and acetic acid was added to protonate the alkyl group and release the borate reagent (**Entry 1, Table 15**). Unfortunately only a 16% yield, containing a 1:1 mixture of starting material **36** and product **15**, was obtained. It was proposed that controlling the reaction temperature may aid the initial hydroboration step. The reaction was therefore repeated, but 9-BBN was added at 0 °C and held at this temperature for seven hours before allowing the reaction mixture to warm to room temperature over night. Once again, the acetic acid was added at 0 °C (**Entry 2, Table 15**). Although an improvement in the amount of material recovered from the reaction mixture was obtained (48% yield) this was also a 1:1 mixture of starting material **36** and product **15**.



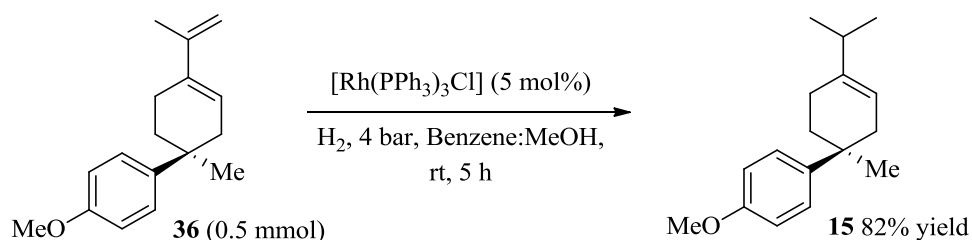
**Scheme 24**

Entry	Conditions	Yield (%) <sup>a</sup>
1	1) 9-BBN added at rt, stirred at rt for 16 h 2) AcOH added at 0 °C, warmed to rt, stirred for 1 h	16
2	1) 9-BBN added at 0 °C, warmed to rt, stirred for 16 h 2) AcOH added at 0 °C, stirred for 7 h at 0 °C	48

<sup>a</sup> Combined yield of 36:15 in a 1:1 ratio.

**Table 15**

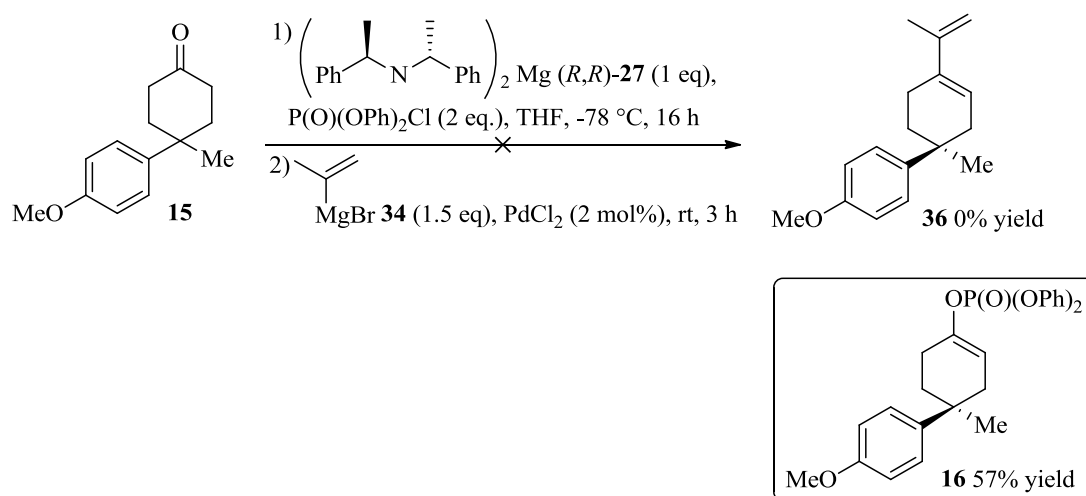
Whilst the extent of hydroboration could have been assessed through oxidation processes, it was considered more effective to try an alternative method of selective hydrogenation. Pleasingly, Wilkinson's catalyst has been shown to hydrogenate a terminal alkene in the presence of an internal alkene at a slightly elevated pressure.<sup>30</sup> In order to achieve this pressure within the laboratory, freeze-pump-thaw cycles of the reaction mixture were carried out before introducing hydrogen into the Schlenk flask (whilst frozen) to create a pressure of hydrogen (**Scheme 25**).<sup>30,31</sup> After stirring the reaction mixture for five hours, complete conversion to the alkene **15** had occurred and **15** was obtained in an excellent 82% yield.



**Scheme 25**

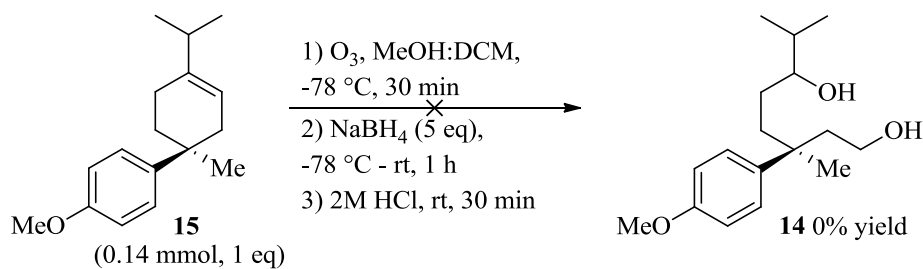


Delighted with the progress of the synthesis, but disappointed that an additional synthetic step had been introduced, an effort to combine two of the steps was made. The possibility of combining the asymmetric deprotonation and cross-coupling steps into a one-pot process was therefore proposed. A similar process has been highlighted in the literature whereby a Grignard reagent has been used to form an enol phosphate *in situ*. The palladium catalyst and another Grignard reagent are then added to the reaction vessel to facilitate the carbon-carbon bond formation.<sup>27</sup> In an attempt to replicate this under the reaction conditions developed within this synthesis the asymmetric deprotonation was carried out under the standard conditions. After leaving the reaction to stir at -78 °C for 16 hours, the reaction mixture was warmed to room temperature and palladium(II) chloride was added to the Schlenk flask in a THF solution. Finally, the Grignard **34** was added *via* syringe pump over two hours (as with the previous successful cross-coupling reactions) and the reaction mixture was stirred for a further three hours at ambient temperature. To our disappointment, however, none of the desired cross-coupled product **36** was obtained after work-up and purification of the reaction mixture. The enol phosphate **16** was the only product of this reaction, in a much reduced 57% yield (**Scheme 26**).



**Scheme 26**

Despite not being able to reduce the number of synthetic steps towards (+)-(*S*)-Sporochnol A **1**, high yields for the cross-coupling and the subsequent selective hydrogenation had been obtained. With the cyclohexene **15** finally in hand, ozonolysis of this double bond was trialed (**Scheme 27**).<sup>32</sup> Although the progress of the reaction looked promising by the blue colour appearance as ozone was bubbled through the reaction mixture, none of the desired diol **14** was obtained.



**Scheme 27**

Having been unsuccessful in the formation of diol **14**, the remaining steps of this synthesis could not be attempted at this stage. The success of the asymmetric deprotonation, however, has proved that the methodology developed within our laboratory for the desymmetrisation of prochiral ketones is a valuable technique for the induction of an all-carbon quaternary chiral centre. The following section outlines the success achieved thus far in the synthesis towards (+)-(*S*)-Sporochnol A **1** and discusses the possible routes for completion of this synthesis.

## 4 Conclusions and Future Work

Although (+)-(*S*)-Sporochnol A **1** was not obtained, a significant headway into the proposed synthetic pathway towards this natural product has been made. Moreover, the key intermediate prochiral ketone **17** has been accessed using a newly developed, scalable process. Starting from cheap and readily available starting materials, cyclohexanone **17** has been synthesised in seven synthetic steps and in up to 55% overall yield. Furthermore, only three of these seven steps require purification by column chromatography, making this an attractive and scalable route towards (+)-(*S*)-Sporochnol A. Indeed, the initial step was performed on a 200 mmol scale enabling large quantities of material to be carried through the synthesis.

Having formed the required prochiral ketone **17**, the key asymmetric deprotonation of this substrate was also highly successful. Using the  $C_2$ -symmetric magnesium bisamide (*R,R*)-**27**, this ketone (**17**) was desymmetrised and the chiral enolate trapped with a phosphorus electrophile to form enol phosphate **16** in a quantitative yield and up to 88:12 er. The all carbon quaternary stereocentre has thus been installed with excellent selectivity for a 4,4-disubstituted cyclohexanone substrate. As this first attempt for the desymmetrisation of a 4,4-disubstituted cyclohexanone, this proved our chiral magnesium bisamide-mediated method of enantioselective deprotonation to be a viable option for the formation of enantioenriched intermediates within a total synthesis.

Additionally, the subsequent cross-coupling of the enantioenriched enol phosphate **16** highlights the utility of these products as stable reagents for palladium-catalysed carbon-carbon bond formation. Specifically, after a significant amount of optimisation, a ligand-free cross-coupling of enol phosphate **16** with isopropenylmagnesium chloride **34** has been employed with palladium(II) chloride. Diene **36** was therefore obtained in almost quantitative yield, making this another robust step in the synthesis towards (+)-(*S*)-Sporochnol A.

After these two key steps in the planned synthesis, a selective hydrogenation of the diene **36** was carried out. Initial hydroboration-protonolysis attempts were unsuccessful in accessing the substituted cyclohexene **15**, however, Wilkinson's

catalyst provided a high yielding alternative. This controlled rhodium-catalysed hydrogenation provided our desired intermediate **15** in an excellent 82% yield.

An effort to oxidatively open the alkene ring in intermediate **15** was made using ozonolysis and a reductive work-up. Unfortunately, however, none of the desired diol **14** was obtained. At this point, however, significant groundwork in this total synthesis programme has been established. All steps performed thus far have been optimised and are high yielding, making this a highly efficient synthesis to this point in the pathway. From the ten steps performed to this stage, intermediate cyclohexene **15** has been accessed from commercially available starting materials in up to 45% overall yield. This is an excellent yield for an intermediate at this stage in a total synthesis. Future work, therefore, is to optimise the oxidative ring opening of **15**. From here, it is believed that our proposed route to (+)-(*S*)-Sporochnol A should be highly efficient for the completion of the synthesis as the two side chains can be derivatised in tandem. Once diol **14** has been formed, we propose that an elimination process could be employed to form diene **10** and complete the formal synthesis of (+)-(*S*)-Sporochnol A, as the final methoxy deprotection is preceded (Figure 4).

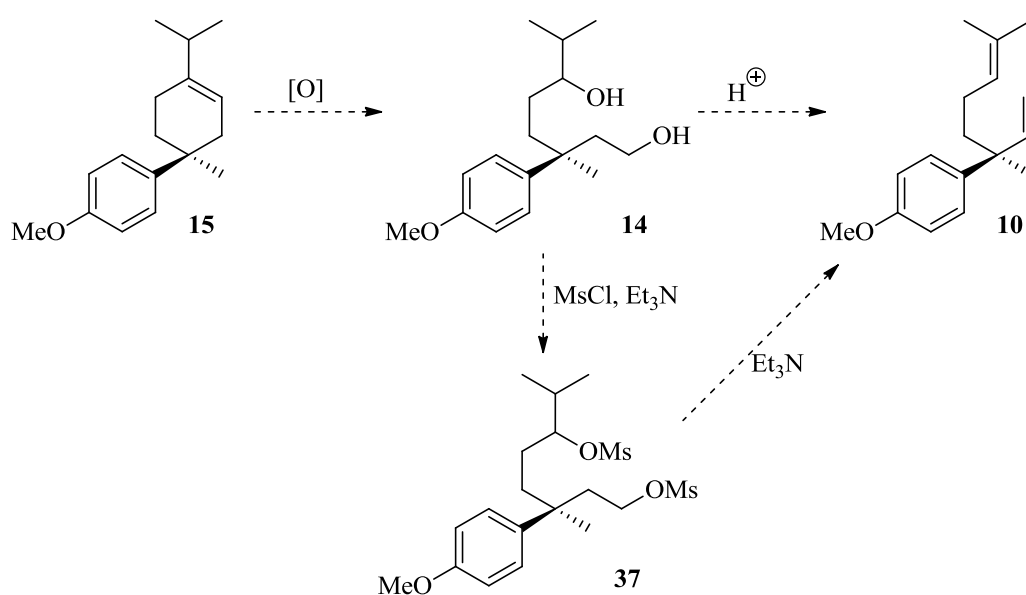


**Figure 4**

It is envisaged that the selectivity of the diol elimination step will require some optimisation, but it is suggested that this could be achieved either *via* elimination of

water to access **10** directly, or the mesylate **37** could be formed as an alternative route. This mesylate could, indeed, be isolated or simply formed *in situ* and eliminated directly to form **10**.

## 5 Experimental Procedures

### 5.1 General Considerations

All reagents were obtained from commercial suppliers and were used without further purification unless otherwise stated. Purification was carried out according to standard laboratory methods.<sup>33</sup>

- Diethyl ether, DCM, and toluene were obtained from an Innovative Technology, Pure Solv, PSP-400-5 solvent purification system.
- THF was dried by heating to reflux over sodium wire, using benzophenone ketyl as an indicator, then distilled under nitrogen.
- Methanol was dried by heating to reflux over calcium hydride then distilled under argon.
- *n*-Bu<sub>2</sub>Mg, obtained as 1 M solution in heptane and *n*-BuLi, obtained as a 2.5 M solution in hexane or THF, were standardised using salicylaldehyde phenylhydrazone as an indicator.<sup>34</sup>
- Diphenylphosphoryl chloride, TMEDA, and (*R,R*)-*bis*-(1-phenylethyl)amine were dried by heating to reflux over calcium hydride and distilled under reduced pressure, then purged with and stored under argon over 4 Å molecular sieves.
- LiCl was flame-dried under high vacuum, then purged with and stored under argon.

*Thin layer chromatography* was carried out using Camlab silica plates coated with fluorescent indicator UV<sub>254</sub>. This was analysed using a Mineralight UVGL-25 lamp and developed using potassium permanganate or vanillin solution.

*Flash chromatography* was carried out using Prolabo silica gel (230-400 mesh).

*High pressure liquid chromatography* was carried out using a Chirasil OD-H or Chirasil OJ column using a Waters 501 HPLC pump, a Waters 484 tuneable absorbance detector (set at 254 nm unless otherwise specified), and processed using a Waters 746 data module.

$^1\text{H}$  and  $^{13}\text{C}$  NMR spectra were obtained on a Bruker DPX 400 spectrometer at 400 and 100 MHz, respectively. Chemical shifts are reported in ppm, and coupling constants are reported in Hz and refer to  $^3J_{\text{H-H}}$  interactions unless otherwise specified.

FTIR spectra were obtained on a Nicolet Impact 400D machine.

High-resolution mass spectra were obtained on a Finnigan MAT900XLT instrument at the EPSRC National Mass Spectrometry Services Centre, Swansea University Swansea.

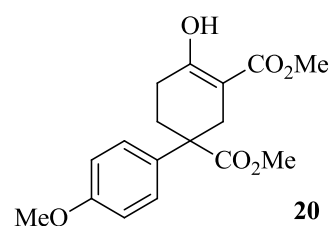
Optical rotations were obtained on Perkin Elmer 341 polarimeter using a cell with a path length of 1 dm. Concentration is expressed in g/100 cm<sup>3</sup>.

Ozone was formed using a Fischer OZ 500 ozone generator.

Air-sensitive reactions were carried out using Schlenk apparatus, which was initially evacuated and flame-dried under vacuum (0.005 mbar), then allowed to cool under an atmosphere of argon.

## 5.2 Accessing the prochiral ketone 17

Synthesis of methyl 4-hydroxy-4'-methoxy-1-(2-methoxy-2-oxoethyl)-1,2,5,6-tetrahydro-[1,1'-biphenyl]-3-carboxylate **20**<sup>11</sup>



### Scheme 4, Table 1

To a flame-dried 3-neck flask under argon was added dry THF (0.37 M), methyl 4-methoxyphenylacetate **18** (1 eq.), and methyl acrylate **19** (2 eq.), and the solution was cooled to 0 °C. Solid potassium *tert*-butoxide (3 eq.) was added portionwise and the reaction mixture was warmed to rt and stirred for 3 h. After this time, the reaction mixture was quenched with 3M HCl (0.47 M) and extracted with DCM (x 3). The combined organic layers were dried over Na<sub>2</sub>SO<sub>4</sub>, filtered, and concentrated *in vacuo* to afford **20** as an off-white solid.

**Table 1:** Data are reported as (a) volume of THF; (b) amount of methyl 4-methoxyphenylacetate **18**; (c) amount of methyl acrylate **19**; (d) amount of potassium *tert*-butoxide; (e) yield of **20**.

**Entry 1, Table 1:** (a) 15 ml, 0.37 M; (b) 0.87 ml, 5.5 mmol, 1 eq; (c) 0.99 ml, 11 mmol, 2 eq; (d) 1.85 g, 16.5 mmol, 3 eq; (e) 1.5 g, 84%.

**Entry 2, Table 1:** (a) 75 ml, 0.37 M; (b) 4.41 ml, 28 mmol, 1 eq; (c) 5.04 ml, 56 mmol, 2 eq; (d) 9.42 g, 84 mmol, 3 eq; (e) 7.8 g, 87%.

**Entry 3, Table 1:** (a) 540 ml, 0.37 M; (b) 31.80 ml, 200 mmol, 1 eq; (c) 36.00 ml, 400 mmol, 2 eq; (d) 67.27 g, 600 mmol, 3 eq; (e) 64.0 g, 100%.

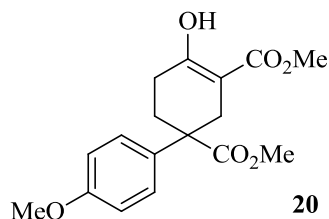
<sup>1</sup>H NMR (400 MHz, CDCl<sub>3</sub>): δ 2.16 – 2.20 (m, 2H, CH<sub>2</sub>), 2.34 – 2.46 (m, 2H, CH<sub>2</sub>), 2.70 (d, 2H, <sup>2</sup>J = 16.0 Hz, CH), 3.05 (d, 2H, <sup>2</sup>J = 16.1 Hz, CH), 3.63 (s, 3H, OCH<sub>3</sub>), 3.79 (s, 3H, OCH<sub>3</sub>), 3.81 (s, 3H, OCH<sub>3</sub>), 6.86 (d, 2H, J = 8.9 Hz, 2 x ArH), 7.27 (d, 2H, J = 8.4 Hz, 2 x ArH), 12.10 (s, 1H, OH).

<sup>13</sup>C NMR (100 MHz, CDCl<sub>3</sub>): δ 26.6, 29.5, 30.6, 48.1, 51.6, 52.4, 55.2, 95.9, 114.0, 127.1, 113.1, 158.6, 171.2, 172.5, 175.2.



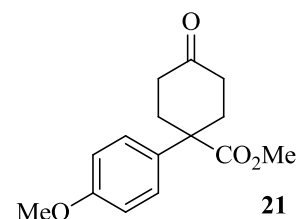
FTIR (neat): 751, 765, 1262, 1274, 1457, 1633, 2340, 2361, 3004, 3596  $\text{cm}^{-1}$ .

HRMS (ESI)  $m/z$  calculated for  $\text{C}_{17}\text{H}_{21}\text{O}_6$   $[\text{M}+\text{H}]^+$ : 321.1333. Found: 321.1335.



*Initial synthesis of methyl 1-(4-methoxyphenyl)-4-oxocyclohexanecarboxylate 21*

#### Scheme 5



To a solution of  $\beta$ -keto ester **20** (3.84 g, 12 mmol, 1 eq) in water/THF/MeOH (1:1:1, total volume 24 ml, 0.5 M) was added solid KOH (0.40 g, 7.2 mmol, 0.6 eq) and the reaction mixture was heated to reflux. After stirring for 18 h the reaction mixture was cooled to rt and diluted with water (40 ml). The aqueous layer was extracted with EtOAc (3 x 30 ml) and the combined organics were dried over  $\text{Na}_2\text{SO}_4$ , filtered, and concentrated *in vacuo*. The crude residue was purified by silica gel chromatography, eluting with a gradient of 2 – 75% EtOAc in PE (40 – 60  $^\circ\text{C}$ ) to afford ketone **21** as a yellow solid, 1.4 g, 43% yield. In addition, unreacted  $\beta$ -keto ester **20** was obtained as a white solid, 0.42 g, 11% yield.

#### Scheme 6, Table 2

A round-bottom flask fitted with a reflux condenser was charged with **20** (1 eq.), DMSO/water (100:1, 0.5 M), and sodium chloride (1 eq.). The reaction mixture was heated to 150  $^\circ\text{C}$  and stirred for 4 h. After cooling to rt, the reaction mixture was diluted with water (0.5 M) and EtOAc (0.5 M). The layers were shaken and separated

then the aqueous layer was extracted with EtOAc (x 3). The combined organic layers were washed with brine, dried over Na<sub>2</sub>SO<sub>4</sub>, filtered, and concentrated *in vacuo*. The orange residue was purified by silica gel chromatography, eluting with 2 – 80% EtOAc in PE (40 – 60 °C) to afford **21** as a yellow solid.

**Table 2:** Data are reported as (a) amount of **20**; (b) volume of DMSO/water; (c) amount of sodium chloride; (d) yield of **21**.

**Entry 1, Table 2:** (a) 3.84 g, 12 mmol, 1 eq; (b) 24 ml, 0.5 M; (c) 0.70 g, 12 mmol, 1 eq; (d) 2.4 g, 77% .

**Entry 2, Table 2:** (a) 7.68 g, 24 mmol, 1 eq; (b) 48 ml, 0.5 M; (c) 1.40 g, 24 mmol, 1 eq; (d) 2.3 g, 73%.

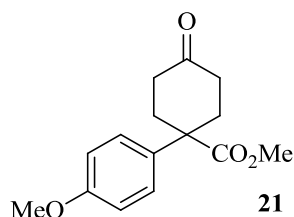
**Entry 3, Table 2:** (a) 64.00 g, 200 mmol, 1 eq; (b) 400 ml, 0.5 M; (c) 12.00 g, 200 mmol, 1 eq; (d) 30.8 g, 59%.

<sup>1</sup>H NMR (400 MHz, CDCl<sub>3</sub>): δ 2.21 – 2.25 (m, 2H, CH<sub>2</sub>), 2.27 – 2.45 (m, 2H, CH<sub>2</sub>), 2.48 – 2.56 (m, 2H, CH<sub>2</sub>), 2.71 – 2.78 (m, 2H, CH<sub>2</sub>), 3.71 (s, 3H, OCH<sub>3</sub>), 3.81 (s, 3H, OCH<sub>3</sub>), 6.90 (d, 2H, *J* = 9.0 Hz, 2 x ArH), 7.35 (d, 2H, *J* = 8.9 Hz, 2 x ArH).

<sup>13</sup>C NMR (100 MHz, CDCl<sub>3</sub>): δ 34.1, 38.5, 49.1, 52.5, 55.3, 114.2, 127.0, 132.8, 158.8, 174.8, 210.4.

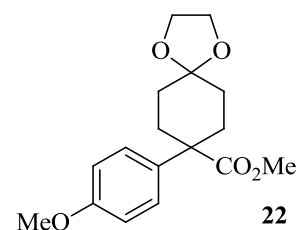
FTIR (neat): 741, 771, 1045, 1254, 1635, 1705, 2859, 2868, 2930 cm<sup>-1</sup>.

HRMS (ESI) *m/z* calculated for C<sub>15</sub>H<sub>19</sub>O<sub>4</sub> [M+H]<sup>+</sup>: 263.1278. Found: 263.1276.



Synthesis of methyl 8-(4-methoxyphenyl)-1,4-dioxaspiro[4.5]decane-8-carboxylate **22**

Scheme 7, Table 3



A round-bottom flask under argon was charged with **21** (1 eq.) and benzene (1.8 M). After stirring to dissolve **21**, ethylene glycol (4.3 eq.) and *p*-toluenesulfonic acid monohydrate (1.5 mol%) were added and the reaction mixture was stirred vigorously at rt for 18 h. The reaction mixture was poured into Et<sub>2</sub>O (0.47 M) and washed with water (x 2), saturated aqueous sodium bicarbonate solution (x 2), and saturated brine. The organic layer was dried over Na<sub>2</sub>SO<sub>4</sub>, filtered, and concentrated *in vacuo* to afford **22** as a yellow oil.

**Table 3:** Data are reported as (a) amount of **21**; (b) volume of benzene; (c) amount of ethylene glycol; (d) amount of *p*-toluenesulfonic acid; (e) yield of **22**.

**Entry 1, Table 3:** (a) 1.34 g, 5.1 mmol, 1 eq; (b) 3 ml, 1.8 M; (c) 1.22 ml, 21.9 mmol, 4.3 eq; (d) 15 mg, 0.08 mmol, 1.5 mol%; (e) 1.5 g, 94%.

**Entry 2, Table 3:** (a) 7.57 g, 28.9 mmol, 1 eq; (b) 16 ml, 1.8 M; (c) 6.92 ml, 124.3 mmol, 4.3 eq; (d) 82 mg, 0.43 mmol, 1.5 mol%; (e) 7.9 g, 93%.

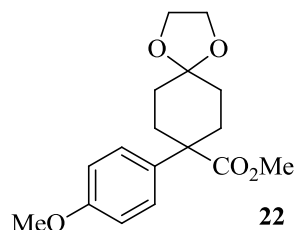
**Entry 3, Table 3:** (a) 30.82 g, 117.6 mmol, 1 eq; (b) 65 ml, 1.8 M; (c) 28.20 ml, 505.7 mmol, 4.3 eq; (d) 0.34 g, 1.79 mmol, 1.5 mol%; (e) 32.5 g, 90%.

<sup>1</sup>H NMR (400 MHz, CDCl<sub>3</sub>): δ 1.69 – 1.78 (m, 4H, 2 x CH<sub>2</sub>), 2.01 – 2.07 (m, 2H, CH<sub>2</sub>), 2.49 – 2.53 (m, 2H, CH<sub>2</sub>), 3.65 (s, 3H, OCH<sub>3</sub>), 3.79 (s, 3H, OCH<sub>3</sub>), 3.92 – 3.98 (m, 4H, 2 x OCH<sub>2</sub>), 6.86 (d, 2H, *J* = 9.0 Hz, 2 x ArH), 7.32 (d, 2H, *J* = 9.0 Hz, 2 x ArH).

<sup>13</sup>C NMR (100 MHz, CDCl<sub>3</sub>): δ 32.0, 32.4, 34.1, 38.5, 49.3, 52.1, 55.2, 64.3, 108.2, 113.8, 158.4, 175.3, 210.4.

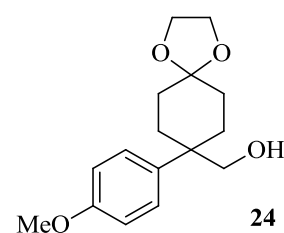
FTIR (neat): 749 765, 1264, 1274, 1634, 2345, 2360, 3002  $\text{cm}^{-1}$ .

HRMS (ESI)  $m/z$  calculated for  $\text{C}_{17}\text{H}_{23}\text{O}_5$   $[\text{M}+\text{H}]^+$ : 307.1540. Found: 307.1543.



Synthesis of (8-(4-methoxyphenyl)-1,4-dioxaspiro[4.5]decan-8-yl)methanol **24**

**Scheme 8, Table 4**



A flame-dried 3-neck flask fitted with a reflux condenser under argon was charged with **22** (1 eq.) and dry THF (0.13 M). The solution was cooled to 0 °C and  $\text{LiAlH}_4$  (2 eq.) was added portionwise. The reaction mixture was stirred at 0 °C for 20 min, then rt for 20 min before slowly heating to reflux and stirring for 18 h. After this time, the reaction mixture was cooled to 0 °C and saturated aqueous sodium carbonate solution (20% of THF volume) was slowly added until all the  $\text{LiAlH}_4$  was destroyed. The suspension was filtered through a pad a Celite and washed with plenty of  $\text{Et}_2\text{O}$ , the filtrate was subsequently concentrated *in vacuo*. The residue was dissolved in DCM (0.18 M) and washed with saturated aqueous sodium carbonate solution (x 3) then dried over  $\text{Na}_2\text{SO}_4$ , filtered, and concentrated *in vacuo* to afford **24** as a white solid.

**Table 4:** Data are reported as (a) amount of **22**; (b) volume of THF; (c) amount of  $\text{LiAlH}_4$ ; (d) yield of **24**.

**Entry 1, Table 4:** (a) 796 mg, 2.6 mmol, 1 eq; (b) 14 ml, 0.18 M; (c) 197 mg, 5.2 mmol, 2 eq; (d) 723 mg, 100%.

**Entry 2, Table 4:** (a) 3.98 g, 13 mmol, 1 eq; (b) 72 ml, 0.18 M; (c) 0.99 g, 26 mmol, 2 eq; (d) 3.5 g, 98%.

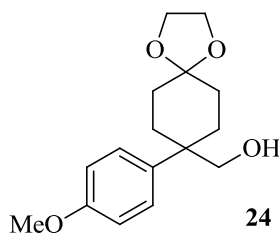
**Entry 3, Table 4:** (a) 32.45 g, 106 mmol, 1 eq; (b) 815 ml, 0.18 M; (c) 8.05 g, 212 mmol, 2 eq; (d) 28.2 g, 96%.

$^1\text{H}$  NMR (400 MHz,  $\text{CDCl}_3$ ):  $\delta$  1.51 – 1.59 (m, 2H,  $\text{CH}_2$ ), 1.64 – 1.68 (m, 2H,  $\text{CH}_2$ ), 1.76 – 1.84 (m, 2H,  $\text{CH}_2$ ), 2.24 (d, br, 2H,  $J = 13.7$  Hz,  $\text{CH}_2$ ), 3.49 (s, 2H,  $\text{CH}_2\text{OH}$ ), 3.81 (s, 3H,  $\text{OCH}_3$ ), 3.89 – 3.97 (m, 4H, 2 x  $\text{OCH}_2$ ), 6.91 (d, 2H,  $J = 8.9$  Hz, 2 x  $\text{ArH}$ ), 7.31 (d, 2H,  $J = 8.9$  Hz, 2 x  $\text{ArH}$ ).

$^{13}\text{C}$  NMR (100 MHz,  $\text{CDCl}_3$ ):  $\delta$  29.3, 30.5, 42.3, 54.8, 63.7, 72.3, 108.4, 113.6, 127.7, 133.1, 157.5.

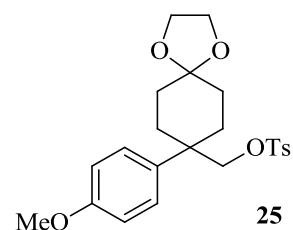
FTIR (neat): 731, 767, 891, 1140, 1514, 2878, 2931, 2953, 2993, 3493  $\text{cm}^{-1}$ .

HRMS (ESI)  $m/z$  calculated for  $\text{C}_{16}\text{H}_{22}\text{O}_4\text{Na}$  [ $\text{M}+\text{Na}$ ] $^+$ : 301.1410. Found: 301.1409.



*Synthesis of (8-(4-methoxyphenyl)-1,4-dioxaspiro[4.5]decan-8-yl)methyl 4-methylbenzenesulfonate **25***

### Scheme 9



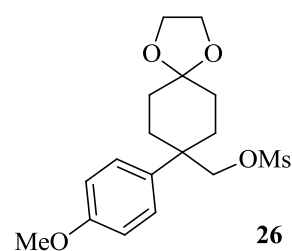
A flame-dried round bottom flask under argon was charged with the alcohol **24** (2.78 g, 10 mmol, 1 eq) and pyridine (9 ml, 1.06 M). The solution was cooled to 0 °C and tosyl chloride (2.86 g, 15 mmol, 1.5 eq) was added portionwise. The reaction mixture was stirred at 0 °C for a further 20 min then warmed to room temperature and stirred overnight. After this time, the reaction mixture was diluted with water (40 ml) and extracted with EtOAc (2 x 40 ml). The combined organics were washed with 1M

HCl (2 x 80 ml), saturated sodium bicarbonate solution (70 ml) and brine (70 ml), then dried over Na<sub>2</sub>SO<sub>4</sub>, filtered and concentrated *in vacuo* to afford **25** as an orange, gummy oil, 4.3 g, 100%

<sup>1</sup>H NMR (400 MHz, CDCl<sub>3</sub>): δ 1.48 – 1.63 (m, 4H, 2 x CH<sub>2</sub>), 1.82 – 1.89 (m, 2H, CH<sub>2</sub>), 2.15 (d, 2H, *J* = 13.6 Hz, CH<sub>2</sub>), 2.42 (s, 3H, ArCH<sub>3</sub>), 3.80 (s, 3H, OCH<sub>3</sub>), 3.83 (s, 2H, CH<sub>2</sub>OH), 3.85 – 3.95 (m, 4H, 2 x OCH<sub>2</sub>), 6.80 (d, 2H, *J* = 8.9 Hz, 2 x ArH), 7.16 (d, 2H, *J* = 8.9 Hz, 2 x ArH), 7.21 (d, 2H, *J* = 8.0 Hz, 2 x ArH), 7.52 (d, 2H, *J* = 8.3 Hz, 2 x ArH).

Synthesis of (8-(4-methoxyphenyl)-1,4-dioxaspiro[4.5]decan-8-yl)methyl methanesulfonate **26**

**Scheme 10, Table 5**



A flame dried flask under argon was charged with alcohol **24** (1 eq), triethylamine (1.1 eq), and DCM (0.5 M) and cooled to 0 °C. To this was added methanesulfonyl chloride (1.1 eq), dropwise. The reaction mixture was stirred at 0 °C for 30 min then warmed to rt and stirred for a further 90 min. After this time, 0.5 M HCl (0.4 M) was added and the layers separated. The organic layer was subsequently washed with water then brine, dried over Na<sub>2</sub>SO<sub>4</sub>, filtered, and concentrated *in vacuo* to afford **26** as a pale yellow solid.

**Table 5:** Data are reported as (a) amount of alcohol **24**; (b) amount of triethylamine; (c) volume of DCM; (d) amount of methanesulfonyl chloride; (e) yield of **26**.

**Entry 1, Table 5:** (a) 1.00 g, 3.6 mmol, 1 eq; (b) 0.55 ml, 3.9 mmol, 1.1 eq, (c) 7 ml, 0.5 M; (d) 0.31 ml, 3.9 mmol, 1.1 eq; (e) 1.2 g, 100%.

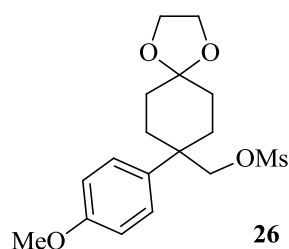
**Entry 2, Table 5:** (a) 5.40 g, 19.4 mmol, 1 eq; (b) 2.97 ml, 21.3 mmol, 1.1 eq, (c) 39 ml, 0.5 M; (d) 1.65 ml, 21.3 mmol, 1.1 eq; (e) 6.3 g, 100%.

$^1\text{H}$  NMR (400 MHz,  $\text{CDCl}_3$ ):  $\delta$  1.53 – 1.59 (m, 2H,  $\text{CH}_2$ ), 1.65 – 1.69 (m, 2H,  $\text{CH}_2$ ), 1.87 – 1.95 (m, 2H,  $\text{CH}_2$ ), 2.27 (d, br, 2H,  $J = 12.6$  Hz,  $\text{CH}_2$ ), 2.62 (s, 3H,  $\text{OSO}_2\text{CH}_3$ ), 3.81 (s, 3H,  $\text{OCH}_3$ ), 3.89 – 3.96 (m, 4H, 2 x  $\text{OCH}_2$ ), 4.07 (s, 2H,  $\text{CH}_2\text{OSO}_2\text{Me}$ ), 6.90 (d, 2H,  $J = 8.9$  Hz, 2 x  $\text{ArH}$ ), 7.32 (d, 2H,  $J = 8.9$  Hz, 2 x  $\text{ArH}$ ).

$^{13}\text{C}$  NMR (100 MHz,  $\text{CDCl}_3$ ):  $\delta$  29.4, 31.1, 42.2, 54.7, 63.5, 77.1, 108.5, 113.7, 127.6, 133.2, 157.7.

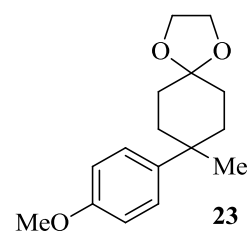
FTIR (neat): 730, 755, 1022, 1125, 1233, 1512, 2879, 2930, 2953  $\text{cm}^{-1}$ .

Unable to obtain HRMS due to the instability of this compound.



Synthesis of 8-(4-methoxyphenyl)-8-methyl-1,4-dioxaspiro[4.5]decane **23**<sup>14</sup>

**Scheme 11, Table 6**



A flame-dried 3-neck flask under an Ar atmosphere was charged with activated alcohol (**25** or **26** 1 eq) and THF (0.7 M). The solution was cooled to 0 °C and Super-Hydride solution (1M in THF, 5 eq) was added dropwise over 15 min. The resulting solution was stirred at 0 °C for 30 min before warming to rt and stirring for 24 h. After this time, the reaction mixture was cooled to 0 °C. MeOH (3 x THF volume), then NaOH (1M, 3 x THF volume) then  $\text{H}_2\text{O}_2$  (30% w/v aq, 3 x THF volume) were cautiously added. CARE: extreme fizzing! The mixture was slowly warmed to 60 °C and stirred for 2 h. After cooling to rt, the reaction mixture was quenched with 5% aqueous sodium bicarbonate solution (3 x THF volume) and extracted with DCM (x 3). The combined organics were dried over  $\text{Na}_2\text{SO}_4$ , filtered and concentrated *in*

*vacuo*. The residue was purified by silica gel chromatography, eluting with 2 – 50% Et<sub>2</sub>O in petroleum ether (40 – 60 °C), to afford **23** as a white solid.

**Table 6:** Data are reported as (a) activated alcohol; (b) amount of activated alcohol; (c) volume of THF; (d) amount of Super-Hydride solution; (e) yield of **23**.

**Entry 1, Table 6:** (a) tosylate **25**; (b) 864 mg, 2 mmol, 1 eq; (c) 3 ml, 0.7 M; (d) 10 ml, 1 M in THF, 10 mmol, 5 eq; (e) 341 mg, 65%.

**Entry 2, Table 6:** (a) tosylate **25**; (b) 3.46 mg, 8 mmol, 1 eq; (c) 11 ml, 0.7 M; (d) 40 ml, 1 M in THF, 40 mmol, 5 eq; (e) 1.1 g, 53%.

**Entry 3, Table 6:** (a) mesylate **26**; (b) 2.88 g, 8.9 mmol, 1 eq; (c) 13 ml, 0.7 M; (d) 44.5 ml, 1 M in THF, 44.5 mmol, 5 eq; (e) 1.4 g, 61%.

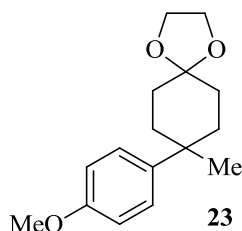
**Entry 4, Table 6:** (a) mesylate **26**; (b) 6.29 g, 19.4 mmol, 1 eq; (c) 28 ml, 0.7 M; (d) 97 ml, 1 M in THF, 97 mmol, 5 eq; (e) 3.9 g, 77%.

<sup>1</sup>H NMR (400 MHz, CDCl<sub>3</sub>): δ 1.21 (s, 3H, CH<sub>3</sub>), 1.59 – 1.63 (m, 2H, CH<sub>2</sub>), 1.67 – 1.78 (m, 4H, 2 x CH<sub>2</sub>), 2.13 – 2.17 (m, 2H, CH<sub>2</sub>), 3.80 (s, 3H, OCH<sub>3</sub>), 3.90 – 3.99 (m, 4H, 2 x OCH<sub>2</sub>), 6.86 (d, 2H, *J* = 8.9 Hz, 2 x ArH), 7.30 (d, 2H, *J* = 8.9 Hz, 2 x ArH).

<sup>13</sup>C NMR (100 MHz, CDCl<sub>3</sub>): δ 26.7, 30.7, 31.1, 34.7, 35.2, 42.2, 54.7, 63.6, 63.9, 108.5, 113.2, 126.3, 129.4, 136.7, 156.9.

FTIR (neat): 797, 889, 1183, 1244, 2867, 2898, 2960 cm<sup>-1</sup>.

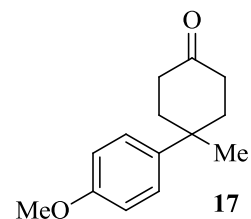
HRMS (ESI) *m/z* calculated for C<sub>16</sub>H<sub>23</sub>O<sub>3</sub> [M+H]<sup>+</sup>: 263.1642. Found: 263.1640.





Synthesis of 4-(4-methoxyphenyl)-4-methylcyclohexanone **17**

Scheme 12, Table 7



A round-bottom flask was charged with acetal **23** (1 eq), THF (0.3 M), and aqueous HCl (1M, 1.2 eq). The reaction mixture was heated at the temperature specified for 24 h. The reaction mixture was diluted with Et<sub>2</sub>O (20 ml) and quenched with saturated sodium bicarbonate (20 ml). The layers were separated and the aqueous layer was extracted with Et<sub>2</sub>O (3 x 20 ml). The combined organics were dried over Na<sub>2</sub>SO<sub>4</sub>, filtered, and concentrated *in vacuo* to afford the crude product. This cream solid was purified by silica gel chromatography, eluting with 2.5 – 75% Et<sub>2</sub>O in PE (40 – 60 °C) to afford prochiral ketone **17** was a white solid. For use in the subsequent step this solid was recrystallised from dry hexane at 4 °C and dried under vacuum for 18 h prior to use.

**Table 7:** Data are reported as (a) amount of acetal **23**; (b) volume of THF; (c) amount of HCl; (d) reaction temperature; (e) yield of prochiral ketone **17**.

**Entry 1, Table 7:** (a) 1.99 g, 7.6 mmol, 1 eq; (b) 25 ml, 0.3 M; (d) 9.1 ml, 1M, 9.1 mmol, 1.2 eq; (e) 1.11 g, 67%.

Unreacted acetal **23** was also recovered as a white solid, 0.56 g, 28% yield.

**Entry 2, Table 7:** (a) 3.10 g, 12 mmol, 1 eq; (b) 40 ml, 0.3 M; (d) 14.40 ml, 1M, 14.4 mmol, 1.2 eq; (e) 2.58 g, 99%.

<sup>1</sup>H NMR (400 MHz, CDCl<sub>3</sub>): δ 1.30 (s, 3H, CH<sub>3</sub>), 1.89 – 1.96 (m, 2H, CH<sub>2</sub>), 2.31 – 2.35 (m, 4H, 2 x CH<sub>2</sub>), 2.42 – 2.48 (m, 2H, CH<sub>2</sub>), 3.81 (s, 3H OCH<sub>3</sub>), 6.92 (d, 2H, *J* = 8.9 Hz, 2 x ArH), 7.35 (d, 2H, *J* = 8.9 Hz, 2 x ArH).

<sup>13</sup>C NMR (100 MHz, CDCl<sub>3</sub>): δ 0.52, 30.7, 36.8, 36.9, 37.9, 54.8, 113.6, 126.2, 137.5, 157.3.

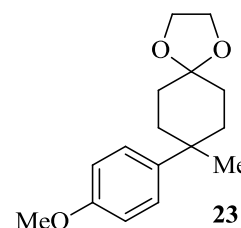
FTIR (neat): 799, 891, 1184, 1246, 1707, 2868, 2899, 2959 cm<sup>-1</sup>.

HRMS (ESI) *m/z* calculated for C<sub>14</sub>H<sub>19</sub>O<sub>2</sub> [M+H]<sup>+</sup>: 219.1380. Found: 219.1380.

### 5.3 Attempted improvements to the methyl-group formation

Attempted synthesis of of 8-(4-methoxyphenyl)-8-methyl-1,4-dioxaspiro[4.5]decane **23**

**Scheme 13, Table 8**



**Scheme 13, Entry 1, Table 8:**<sup>17</sup> A flame-dried three-neck flask under argon was charged with tosylate **25** (648 mg, 1.5 mmol, 1 eq) and Et<sub>2</sub>O (6 ml, 0.25 M) and the solution was cooled to 0 °C. To a flame-dried round-bottom flask was added LiAlH<sub>4</sub> (57 mg, 1.5 mmol, 1 eq) and Et<sub>2</sub>O (6 ml, 0.25 M). The LiAlH<sub>4</sub> solution was added to the tosylate solution, dropwise. After the addition, the reaction mixture was warmed to rt and stirred for 1 h. The reaction mixture was re-cooled to 0 °C and quenched with a saturated aqueous solution of Na<sub>2</sub>SO<sub>4</sub> (40 ml). The reaction mixture was stirred for 30 min before filtering the white precipitate and washing with Et<sub>2</sub>O. The layers were separated and the aqueous layer was extracted with Et<sub>2</sub>O (2 x 30 ml). The combined organics were subsequently washed with saturated aqueous NaHCO<sub>3</sub> (60 ml), then saturated brine (60 ml), dried over Na<sub>2</sub>SO<sub>4</sub>, filtered, and concentrated *in vacuo* to afford a cream gum. <sup>1</sup>H NMR analysis revealed only starting tosylate **25** to be present.

**Scheme 13, Entry 2, Table 8:** A flame-dried three-neck flask under argon was charged with tosylate **25** (648 mg, 1.5 mmol, 1 eq) and THF (6 ml, 0.25 M) and the solution was cooled to 0 °C. To a flame-dried round-bottom flask was added LiAlH<sub>4</sub> (57 mg, 1.5 mmol, 1 eq) and THF (6 ml, 0.25 M). The LiAlH<sub>4</sub> solution was added to the tosylate solution, dropwise. After the addition, the reaction mixture was warmed to rt and stirred for 16 h. The reaction mixture was re-cooled to 0 °C and quenched with a saturated aqueous solution of Na<sub>2</sub>SO<sub>4</sub> (40 ml). The reaction mixture was stirred for 30 min before filtering the white precipitate and washing with Et<sub>2</sub>O. The layers were separated and the aqueous layer was extracted with Et<sub>2</sub>O (2 x 30 ml). The combined organics were subsequently washed with saturated aqueous NaHCO<sub>3</sub>

(60 ml), then saturated brine (60 ml), dried over Na<sub>2</sub>SO<sub>4</sub>, filtered, and concentrated *in vacuo* to afford a cream gum. <sup>1</sup>H NMR analysis revealed only starting tosylate **25** to be present.

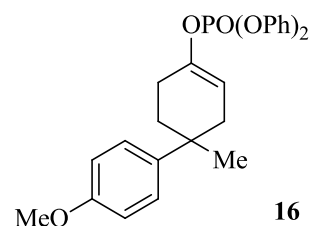
**Scheme 13, Entry 3, Table 8:** A flame-dried three-neck flask under argon was charged with tosylate **25** (648 mg, 1.5 mmol, 1 eq) and THF (6 ml, 0.25 M) and the solution was cooled to 0 °C. To a flame-dried round-bottom flask was added LiAlH<sub>4</sub> (57 mg, 1.5 mmol, 1 eq) and THF (6 ml, 0.25 M). The LiAlH<sub>4</sub> solution was added to the tosylate solution, dropwise. After the addition, the reaction mixture was slowly heated to reflux and stirred for 16 h. The reaction mixture was re-cooled to 0 °C and quenched with a saturated aqueous solution of Na<sub>2</sub>SO<sub>4</sub> (40 ml). The reaction mixture was stirred for 30 min before filtering the white precipitate and washing with Et<sub>2</sub>O. The layers were separated and the aqueous layer was extracted with Et<sub>2</sub>O (2 x 30 ml). The combined organics were subsequently washed with saturated aqueous NaHCO<sub>3</sub> (60 ml), then saturated brine (60 ml), dried over Na<sub>2</sub>SO<sub>4</sub>, filtered, and concentrated *in vacuo* to afford a cream gum. <sup>1</sup>H NMR analysis revealed only starting tosylate **25** to be present.

**Scheme 13, Entry 4, Table 8:**<sup>18</sup> A flame-dried three-neck flask under argon was charged with tosylate **25** (648 mg, 1.5 mmol, 1 eq) and EtOH (15 ml, 0.1 M). NaBH<sub>4</sub> (567 mg, 15 mmol, 10 eq) was added, portionwise, at rt and the reaction mixture was stirred at this temperature for 16 h. After this time, the reaction mixture was quenched with 1M HCl (20 ml) and extracted with DCM (3 x 15 ml). The combined organics were washed with saturated aqueous NaHCO<sub>3</sub> solution (30 ml) and saturated brine solution (30 ml), then dried over Na<sub>2</sub>SO<sub>4</sub>, filtered, and concentrated *in vacuo*. <sup>1</sup>H NMR analysis revealed only starting tosylate **25** to be present.

## 5.4 Installing the stereogenic centre *via* a magnesium bisamide-mediated asymmetric deprotonation

Synthesis of 4'-methoxy-1-methyl-1,2,3,6-tetrahydro-[1,1'-biphenyl]-4-yl diphenyl phosphate **16**

### Scheme 14



To a flame-dried, three-neck flask under argon was added diisopropylamine (0.08 ml, 0.55 mmol, 1.1 eq) and THF (2.5 ml, 0.2 M). The solution was cooled to  $-78\text{ }^{\circ}\text{C}$  and *n*-BuLi (0.22 ml, 2.5 M in hexanes, 0.55 mmol, 1.1 eq) was added, dropwise. The reaction mixture was warmed to rt over 20 min then re-cooled to  $-78\text{ }^{\circ}\text{C}$ . Ketone **17** (109 mg, 0.5 mmol, 1 eq) was dissolved in THF (2 ml, 0.25 M) in a flame-dried pear-shaped flask and the solution was added, dropwise, *via* syringe to the LDA solution. The reaction mixture was stirred for 1 h at  $-78\text{ }^{\circ}\text{C}$  then diphenylphosphoryl chloride (0.11 ml, 0.55 mmol, 1.1 eq) was added and the reaction mixture was stirred at  $-78\text{ }^{\circ}\text{C}$  for a further 30 min then at rt for 90 min. After this time, the reaction was quenched with saturated  $\text{NH}_4\text{Cl}$  (7 ml) and extracted with  $\text{Et}_2\text{O}$  (3 x 7 ml). The combined organics were dried over  $\text{Na}_2\text{SO}_4$ , filtered, and concentrated *in vacuo*. The residue was purified by silica gel chromatography, eluting with 5 – 50%  $\text{Et}_2\text{O}$  in PE ( $40 - 60\text{ }^{\circ}\text{C}$ ) to afford enol phosphate **16** as a colourless oil, 224 mg, 100% yield.

### Scheme 15, Table 9

A Schlenk flask was flame dried under vacuum and purged three times with argon. To the Schlenk was added *n*- $\text{Bu}_2\text{Mg}$  (1 M solution in heptanes, 1 eq) and the solvent removed *in vacuo* (0.005 mbar) until the appearance of a white solid. THF (0.1 M) was then added followed by (*R*)-bis((*R*)-1-phenylethyl)amine (2 eq) and the resulting mixture was heated at reflux for 90 min after which time quantitative formation of magnesium bisamide (*R,R*)-**27** was assumed. The base solution was cooled to  $-78\text{ }^{\circ}\text{C}$  and diphenylphosphoryl chloride (X eq) was added. The ketone **17** (0.8 eq) was

weighed into a flame-dried pear-shaped flask and dissolved in THF (0.5 M). The ketone solution was subsequently added to the Schlenk flask over a period of 1 h *via* syringe pump. The reaction mixture was stirred at -78 °C for 16 h before quenching with a saturated solution of NaHCO<sub>3</sub> (10 ml for 1 mmol scale, 20 ml for 2 mmol scale) and warming to rt. Et<sub>2</sub>O (15 ml) was added and the layers separated. The aqueous layer was extracted a further two times then the organics combined, dried over Na<sub>4</sub>SO<sub>4</sub>, filtered, and concentrated *in vacuo*. The resulting oil was dissolved in Et<sub>2</sub>O (15 ml) and washed with 1 M HCl (3 x 25 ml) to remove the chiral amine. The organics were dried over Na<sub>2</sub>SO<sub>4</sub>, filtered, and concentrated *in vacuo* to give an oil which was purified by silica gel chromatography, eluting with 5 – 50% Et<sub>2</sub>O in PE (40 – 60 °C), to yield enol phosphate **16** as a colourless oil.

**Table 9:** Data are reported as (a) amount of *n*-Bu<sub>2</sub>Mg; (b) volume of THF; (c) amount of (*R*)-bis((*R*)-1-phenylethyl)amine; (d) amount of diphenylphosphoryl chloride; (e) amount of ketone **17**; (f) volume of THF; (g) yield of enol phosphate **16**; (h) er of enol phosphate **16** ((+):(-)).

**Entry 1, Table 9:** (a) 1 ml, 1 M in heptanes, 1 mmol, 1 eq; (b) 10 ml, 0.1 M; (c) 0.44 ml, 2 mmol, 2 eq; (d) 0.21 ml, 1 mmol, 1 eq; (e) 174 mg, 0.8 mmol, 0.8 eq; (f) 2 ml, 0.5 M; (g) 280 mg, 78%; (h) 87:13.

**Entry 2, Table 9:** (a) 1 ml, 1 M in heptanes, 1 mmol, 1 eq; (b) 10 ml, 0.1 M; (c) 0.44 ml, 2 mmol, 2 eq; (d) 0.42 ml, 2 mmol, 2 eq; (e) 174 mg, 0.8 mmol, 0.8 eq; (f) 2 ml, 0.5 M; (g) 322 mg, 90%; (h) 88:12.

**Entry 3, Table 9:** (a) 2 ml, 1 M in heptanes, 2 mmol, 1 eq; (b) 20 ml, 0.1 M; (c) 0.88 ml, 4 mmol, 2 eq; (d) 0.83 ml, 4 mmol, 2 eq; (e) 348 mg, 1.6 mmol, 0.8 eq; (f) 4 ml, 0.5 M; (g) 725 mg, 100%; (h) 86:14.

Chiral HPLC analysis: Chiralcel OJ column, 50% IPA in *n*-hexane, 1.20 ml/min flow rate, *t*<sub>R</sub> (major) = 18.1 min, *t*<sub>R</sub> (minor) = 20.3 min.

$[\alpha]_{\text{D}}^{20} = +17.6^{\circ}$  (87:13, *c* = 1, CHCl<sub>3</sub>). No literature data are available for comparison.

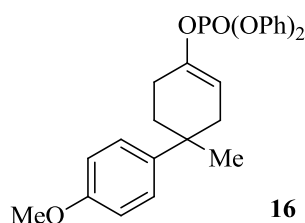
$^1\text{H}$  NMR (400 MHz,  $\text{CDCl}_3$ ):  $\delta$  1.29 (s, 3H,  $\text{CH}_3$ ), 1.81 – 1.88 (m, 1H,  $\text{CH}$ ), 2.01 – 2.07 (m, 2H,  $\text{CH}_2$ ), 2.21 – 2.26 (m, 2H,  $\text{CH}_2$ ), 2.56 – 2.60 (m, 1H,  $\text{CH}$ ), 3.80 (s, 3H,  $\text{OCH}_3$ ), 5.66 – 5.68 (m, 1H,  $\text{C}=\text{CH}$ ), 6.86 (d, 2H,  $J = 8.9$  Hz, 2 x  $\text{ArH}$ ), 7.19 – 7.22 (m, 6H, 6 x  $\text{ArH}$ ), 7.2. – 7.33 (m, 2H, 2 x  $\text{ArH}$ ), 7.43 – 7.48 (m, 4H, 4 x  $\text{ArH}$ ).

$^{13}\text{C}$  NMR (100 MHz,  $\text{CDCl}_3$ ):  $\delta$  25.7 (d, 1C,  $^3J_{\text{C-P}} = 3.9$  Hz), 28.8, 35.2, 35.6, 36.0, 55.3, 110.6 (d, 1C,  $^3J_{\text{C-P}} = 6.0$  Hz), 113.7, 120.2 (d, 2C,  $^3J_{\text{C-P}} = 5.0$  Hz), 125.5, 126.8, 129.9, 139.9, 147.3 (d, 1C,  $^2J_{\text{C-P}} = 9.5$  Hz), 150.7 (d, 1C,  $^2J_{\text{C-P}} = 7.9$  Hz), 157.7.

$^{31}\text{P}$  NMR (400 MHz,  $\text{CDCl}_3$ ):  $\delta$  -17.7.

FTIR (neat): 943, 1072, 1186, 1250, 1294, 1487, 1589, 1687, 2868, 2910, 2953, 3061  $\text{cm}^{-1}$ .

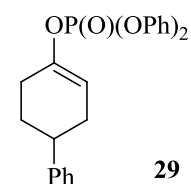
HRMS (ESI)  $m/z$  calculated for  $\text{C}_{26}\text{H}_{28}\text{O}_5\text{P}$   $[\text{M}+\text{H}]^+$ : 451.1669. Found: 451.1664.



## 5.5 Studies towards the cross-coupling of the enantioenriched enol phosphate **16**

*Synthesis of diphenyl (1,2,3,6-tetrahydro-[1,1'-biphenyl]-4-yl) phosphate **2***<sup>19</sup>

### Scheme 16



To a flame-dried, three-neck flask under argon was added diisopropylamine (0.77 ml, 5.5 mmol, 1.1 eq) and THF (5 ml, 1 M). The solution was cooled to  $-78$  °C and *n*-BuLi (2.20 ml, 2.5 M in hexanes, 5.5 mmol, 1.1 eq) was added, dropwise. The reaction mixture was warmed to rt over 20 min then re-cooled to  $-78$  °C. 4-Phenylcyclohexanone **28** (870 mg, 5.0 mmol, 1 eq) was dissolved in THF (5 ml, 1 M) in a flame-dried pear-shaped flask and the solution was added, dropwise, *via*

syringe to the LDA solution. The reaction mixture was stirred for 1 h at -78 °C then diphenylphosphoryl chloride (1.14 ml, 5.5 mmol, 1.1 eq) was added and the reaction mixture was stirred at -78 °C for a further 30 min then at rt for 90 min. After this time, the reaction was quenched with saturated NH<sub>4</sub>Cl (15 ml) and extracted with Et<sub>2</sub>O (3 x 15 ml). The combined organics were dried over Na<sub>2</sub>SO<sub>4</sub>, filtered, and concentrated *in vacuo*. The residue was purified by silica gel chromatography, eluting with 5 – 50% Et<sub>2</sub>O in PE (40 – 60 °C) to afford enol phosphate **29** as a colourless oil, 1.93 g, 95% yield.

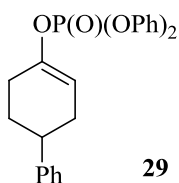
<sup>1</sup>H NMR (400 MHz, CDCl<sub>3</sub>): δ 1.85 – 1.95 (m, 1H, CH), 1.98 – 2.04 (m, 1H, CH), 2.21 – 2.50 (m, 4H, 2 x CH<sub>2</sub>), 2.87 – 2.84 (m, 1H CH), 5.66 – 5.67 (m, 1H, C=CH), 7.19 – 7.38 (m, 15H, 15 x ArH).

<sup>13</sup>C NMR (100 MHz, CDCl<sub>3</sub>): δ 27.5 (d, 1C, <sup>3</sup>J<sub>C-P</sub> = 3.7 Hz), 29.2, 31.0, 38.7, 110.9 (d, 1C, <sup>3</sup>J<sub>C-P</sub> = 5.9 Hz), 119.6 (d, 2C, <sup>3</sup>J<sub>C-P</sub> = 5.0 Hz), 124.9, 125.9, 126.3, 128.0, 129.3, 145.0, 147.1 (d, 1C, <sup>2</sup>J<sub>C-P</sub> = 9.4 Hz), 150.1 (d, 1C, <sup>2</sup>J<sub>C-P</sub> = 7.4 Hz).

<sup>31</sup>P NMR (400 MHz, CDCl<sub>3</sub>): δ -17.4.

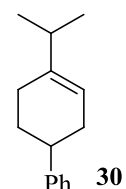
FTIR (neat): 731, 844, 1006, 1105, 1282, 1489, 1589, 2843, 2926, 3026, 3059 cm<sup>-1</sup>.

HRMS (ESI) m/z calculated for C<sub>24</sub>H<sub>24</sub>O<sub>4</sub>P [M+H]<sup>+</sup>: 407.1407. Found: 407.1405.



Attempted synthesis of 4-isopropyl-1,2,3,6-tetrahydro-1,1'-biphenyl **30**

Scheme 17, Table 10<sup>23</sup>



A flame-dried three-neck flask under argon was charged with enol phosphate **29** (406 mg, 1 mmol, 1 eq), TMEDA (0.27 ml, 2 mmol, 2 eq), Fe(acac)<sub>3</sub> (21 mg, 0.06 mmol, 6 mol%), and THF (2 ml, 0.5 M). The solution was cooled to -10 °C and *i*-PrMgCl **31** (1.00 ml, 2 M in THF, 2 mmol, 2 eq) was added, dropwise. The reaction mixture was allowed to warm to the temperature stated over the time period stated. After this time saturated aqueous NH<sub>4</sub>Cl (10 ml) was added to quench the reaction, followed by Et<sub>2</sub>O (5 ml) and the layers separated. The aqueous layer was extracted with Et<sub>2</sub>O (2 x 5 ml) and the combined organics were washed with brine (10 ml), dried over Na<sub>2</sub>SO<sub>4</sub>, filtered, and concentrated *in vacuo* to obtain a colourless oil. <sup>1</sup>H NMR analysis revealed only starting enol phosphate **29** to be present.

**Table 10:** Data are reported as (a) reaction temperature; (b) reaction time.

**Entry 1, Table 10:** (a) 0 °C; (b) 1 h.

**Entry 2, Table 10:** (a) 0 °C; (b) 4 h.

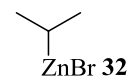
**Entry 3, Table 10:** (a) rt; (b) 4 h.

**Scheme 18,**<sup>24</sup> **Entry 1, Table 11:** A flame-dried three-neck flask was charged with Ni(acac)<sub>2</sub> (13 mg, 0.05 mmol, 10 mol%), THF (8 ml, 0.06 M), and *i*-PrMgCl **31** (0.63 ml, 2 M in THF, 1.25 mmol, 2.5 eq) and the solution was cooled to 0 °C. The solution was stirred for 10 min at 0 °C then a solution of enol phosphate **29** (203 mg, 0.5 mmol, 1 eq) in THF (8 ml, 0.06 M) was added. The reaction mixture was warmed to rt and stirred for 16 h then cooled to 0 °C and quenched with NaHCO<sub>3</sub> (10 ml). The aqueous layer was extracted with Et<sub>2</sub>O (2 x 10 ml) and the combined organics were dried over Na<sub>2</sub>SO<sub>4</sub>, filtered, and concentrated *in vacuo* to afford a colourless oil. <sup>1</sup>H NMR analysis revealed only starting enol phosphate **29** to be present.



**Scheme 18, Entry 2, Table 11:** A flame-dried three-neck flask was charged with Ni(acac)<sub>2</sub> (13 mg, 0.05 mmol, 10 mol%), THF (8 ml, 0.06 M), and enol phosphate **29** (203 mg, 0.5 mmol, 1 eq) and the solution was cooled to 0 °C. The solution was stirred for 10 min at 0 °C then *i*-PrMgCl **31** (0.63 ml, 2 M in THF, 1.25 mmol, 2.5 eq) was added. The reaction mixture was warmed to rt and stirred for 16 h then cooled to 0 °C and quenched with NaHCO<sub>3</sub> (10 ml). The aqueous layer was extracted with Et<sub>2</sub>O (2 x 10 ml) and the combined organics were dried over Na<sub>2</sub>SO<sub>4</sub>, filtered, and concentrated *in vacuo* to afford a colourless oil. <sup>1</sup>H NMR analysis revealed only starting enol phosphate **29** to be present.

*Preparation of isopropylzinc bromide 32*<sup>26</sup>



### Scheme 19

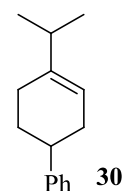
A Schlenk flask was flame-dried and purged with then cooled under argon prior to the addition of LiCl (856 mg, 20 mmol, 2 eq). The Schlenk flask with LiCl was flame-dried under vacuum (0.005 mbar) and purged with and cooled under argon. Zn dust (1.31 g, 20 mmol, 2 eq) was added and the contents of the Schlenk flask flame-dried under vacuum (0.005 mbar) once more before purging with and cooling under argon. THF (10 ml, 1 M) and 1,2-dibromoethane (43 μl, 0.5 mmol, 5 mol%) were added and the mixture was heated to 60 °C until bubbling occurred (approx. 20 min). The mixture was cooled to rt and TMSCl (13 μl, 0.1 mmol, 1 mol%) then iodine (13 mg, 0.05 mmol, 0.5 mol%) were added and the mixture was activated by heating to 60 °C for 20 min then cooling to rt. 2-Bromopropane (0.94 ml, 10 mmol, 1 eq) was added and the reaction mixture was stirred at 50 °C for 18 h. The suspension was cooled to rt and allowed to stand for 2 h. The supernatant solution was transferred to a previously flame-dried pear-shaped flask under argon *via* cannula. The colourless solution was subsequently standardised to 0.54 M using iodine in the following method.

*Standardisation:* A flame-dried Schlenk under argon was charged with iodine (254 mg, 1 mmol, 1 eq) and a saturated solution of LiCl in THF (5 ml). After the iodine is

fully dissolved the brown solution was cooled to 0 °C. *i*-PrZnBr **32** was added, dropwise, *via* a 1 ml syringe until the brown solution turned colourless.

Attempted synthesis of 4-isopropyl-1,2,3,6-tetrahydro-1,1'-biphenyl **30**<sup>35</sup>

Scheme 20, Table 12<sup>25</sup>



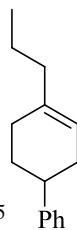
A Schlenk flask was flame-dried and purged with then cooled under argon prior to the addition of LiCl (85 mg, 2 mmol, 5 eq). The Schlenk flask with LiCl was flame-dried under vacuum (0.005 mbar) and purged with and cooled under argon. A flame-dried pear-shaped was charged with enol phosphate **29** (162 mg, 0.4 mmol, 1 eq), DPPF (5 mol% or 10 mol%) and THF (1.5 ml, 0.27 M), and the solution was transferred to the Schlenk flask *via* cannula. *i*-PrZnBr **32** (0.89 ml, 0.54 M in THF, 0.48 mmol, 1.2 eq) was subsequently added, dropwise. A flame-dried pear-shaped flask was then charged with Pd<sub>2</sub>dba<sub>3</sub> (2.5 mol% or 5 mol%) and THF (0.5 ml, 1.25 M) and this solution was transferred to the Schlenk flask *via* cannula. The reaction mixture was stirred at rt for 10 min then a cold finger was fitted to the Schlenk flask and the reaction was heated to reflux and stirred for the time specified (18 h or 48 h). After this time, the reaction mixture was cooled to rt, transferred to a round-bottom flask, and concentrated *in vacuo*. The residue was purified by silica gel chromatography, eluting with 0 – 20% Et<sub>2</sub>O in PE (30 – 40 °C). The colourless oil obtained was analysed by <sup>1</sup>H NMR which revealed the isomerised product **33** to be present with THF impurities.

**Table 12:** Data are reported as (a) amount of DPPF; (b) amount of Pd<sub>2</sub>dba<sub>3</sub>; (c) reaction time; (d) <sup>1</sup>H NMR yield of **33**.

**Entry 1, Table 12:** (a) 11 mg, 0.02 mmol, 5 mol%; (b) 9 mg, 0.01 mmol, 2.5 mol%; (c) 18 h; (d) 26 mg, 66%.

**Entry 2, Table 12:** (a) 22 mg, 0.04 mmol, 10 mol%; (b) 18 mg, 0.02 mmol, 5 mol%; (c) 18 h; (d) 0 mg, 0%.

**Entry 3, Table 12:** (a) 11 mg, 0.02 mmol, 5 mol%; (b) 9 mg, 0.01 mmol, 2.5 mol%; (c) 48 h; (d) 44 mg, 55%.



*4-Propyl-1,2,3,6-tetrahydro-1,1'-biphenyl 33*<sup>35</sup>

Diagnostic peaks from the <sup>1</sup>H NMR spectrum: <sup>1</sup>H NMR (400 MHz, CDCl<sub>3</sub>) δ: 0.92 (t, 3H, *J* = 7.4 Hz, CH<sub>3</sub>), 1.43 – 1.49 (m, 2H, CH<sub>2</sub>), 1.75 – 1.80 (m, 1H, CH), 1.94 – 2.07 (m, 4H, 4 x CH), 2.12 – 2.19 (m, 2H, CH<sub>2</sub>), 2.28 – 2.31 (m, 1H, CH), 2.73 – 2.77 (m, 1H, CH), 5.49 – 5.50 (m, 1H, C=CH), 7.12 – 7.33 (m, 5H, 5 x ArH).

**Scheme 21, Entry 1, Table 13:**<sup>27</sup> A flame-dried Schlenk under argon was charged with enol phosphate **29** (203 mg, 0.5 mmol, 1 eq), Pd(PPh<sub>3</sub>)<sub>2</sub>Cl<sub>2</sub> (7 mg, 0.01 mmol, 2 mol%), and THF (1 ml, 0.5 M). The solution was stirred for 10 min then *i*-PrMgCl **31** (0.30 ml, 2M in THF, 0.6 mmol, 1.2 eq) was added over a period of 1 h *via* syringe pump. The reaction mixture was stirred for a further 1 h at rt then quenched with PE (30 – 40 °C, 5 ml) and 2 M HCl (5 ml). The layers were separated and the aqueous layer was extracted with PE (30 – 40 °C, 2 x 5 ml). The combined organics were then washed successively with 2 M HCl (5 ml), 3 M NaOH (2 x 5 ml), and brine (5 ml) before drying over Na<sub>2</sub>SO<sub>4</sub>, filtering, and concentrating *in vacuo*. The residue was purified by silica gel chromatography, eluting with PE (30 – 40 °C) to afford a colourless oil which was analysed by <sup>1</sup>H NMR spectroscopy. Only the isomerised product **33** was obtained (85 mg, 86% yield) as a mixture with THF impurities.

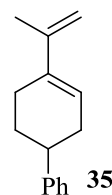
**Scheme 21, Entry 2, Table 13:**<sup>27</sup> A flame-dried Schlenk under argon was charged with PdCl<sub>2</sub> (2 mg, 0.01 mmol, 2 mol%), tribenzylphosphine (6 mg, 0.02 mmol, 4 mol%), and THF (1 ml, 0.5 M). The solution was stirred at rt for 30 min then enol phosphate **29** (203 mg, 0.5 mmol, 1 eq) was added. The solution was stirred for 10 min then *i*-PrMgCl **31** (0.30 ml, 2M in THF, 0.6 mmol, 1.2 eq) was added over a

period of 1 h *via* syringe pump. The reaction mixture was stirred for a further 1 h at rt then quenched with PE (30 – 40 °C, 5 ml) and 2 M HCl (5 ml). The layers were separated and the aqueous layer was extracted with PE (30 – 40 °C, 2 x 5 ml). The combined organics were then washed successively with 2 M HCl (5 ml), 3 M NaOH (2 x 5 ml), and brine (5 ml) before drying over Na<sub>2</sub>SO<sub>4</sub>, filtering, and concentrating *in vacuo*. The residue was purified by silica gel chromatography, eluting with PE (30 – 40 °C) to afford a colourless oil which was analysed by <sup>1</sup>H NMR spectroscopy. Only the isomerised product **33** was obtained (18 mg, 18% yield) as a mixture with THF impurities.

**Scheme 21, Entry 2, Table 13:**<sup>28</sup> A flame-dried Schlenk under argon was charged with PdCl<sub>2</sub> (2 mg, 0.01 mmol, 2 mol%), enol phosphate **29** (203 mg, 0.5 mmol, 1 eq), and THF (1 ml, 0.5 M). The solution was stirred for 10 min then *i*-PrMgCl **31** (0.30 ml, 2M in THF, 0.6 mmol, 1.2 eq) was added over a period of 1 h *via* syringe pump. The reaction mixture was stirred for a further 16 h at rt then quenched with PE (30 – 40 °C, 5 ml) and 2 M HCl (5 ml). The layers were separated and the aqueous layer was extracted with PE (30 – 40 °C, 2 x 5 ml). The combined organics were then washed successively with 2 M HCl (5 ml), 3 M NaOH (2 x 5 ml), and brine (5 ml) before drying over Na<sub>2</sub>SO<sub>4</sub>, filtering, and concentrating *in vacuo*. The residue was purified by silica gel chromatography, eluting with PE (30 – 40 °C) to afford a colourless oil which was analysed by <sup>1</sup>H NMR spectroscopy. Only the isomerised product **33** was obtained (21 mg, 22% yield) as a mixture with THF impurities.

*Synthesis of 4-(prop-1-en-2-yl)-1,2,3,6-tetrahydro-1,1'-biphenyl* **35**<sup>36</sup>

**Scheme 22**<sup>28</sup>



To a flame-dried Schlenk flask under argon was added enol phosphate **29** (203 mg, 0.5 mmol, 1 eq), PdCl<sub>2</sub> (2 mg, 0.01 mmol, 2 mol%), and THF (1 ml, 0.5 M). The mixture was stirred at rt for 10 min then isopropenylmagnesium bromide **34** (1.50 ml, 0.75 mmol, 1.5 eq) was added over a period of 2 h *via* syringe pump. The

reaction mixture was stirred for a further 3 h at rt before quenching with MeOH (1 ml), transferring to a round-bottom flask, and concentrating *in vacuo*. The residue was purified by silica gel chromatography, eluting with PE (30 – 40 °C) to afford diene **35** as a colourless oil, 78 mg, 79% yield.

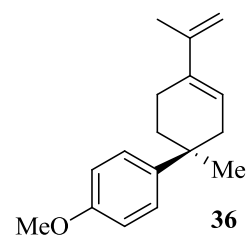
<sup>1</sup>H NMR (400 MHz, CDCl<sub>3</sub>): δ 1.80 – 1.86 (m, 1H, CH), 1.96 (s, 3H, CH<sub>3</sub>), 2.05 – 2.09 (m, 1H, CH), 2.32 – 2.40 (m, 2H, CH<sub>2</sub>), 2.44 – 2.50 (m, 2H, CH<sub>2</sub>), 2.78 – 2.81 (m, 1H, CH), 4.89 (s, 1H, C=CH), 5.01 (s, 1H, C=CH), 5.98 – 5.99 (m, 1H, C=CH), 7.21 – 7.27 (m, 3H, 3 x ArH), 7.32 – 7.34 (m, 2H, 2 x ArH).

<sup>13</sup>C NMR (100 MHz, CDCl<sub>3</sub>): δ 20.7, 26.2, 30.0, 34.1, 39.9, 110.1, 124.4, 126.1, 126.9, 128.4, 136.5, 143.4, 147.0.

FTIR (neat): 709, 777, 898, 1029, 1375, 1445, 1293, 1612, 2930, 2926, 3022, 3055 cm<sup>-1</sup>.

*Synthesis of 4'-methoxy-1-methyl-4-(prop-1-en-2-yl)-1,2,3,6-tetrahydro-1,1'-biphenyl 36*

**Scheme 23, Table 14**<sup>28</sup>



To a flame-dried Schlenk flask under argon was added enol phosphate **16** (1 eq), PdCl<sub>2</sub> (2 mol%), and THF (0.5 M). The mixture was stirred at rt for 10 min then isopropenylmagnesium bromide **34** (1.5 eq) was added over a period of 2 h *via* syringe pump. The reaction mixture was stirred for a further 3 h at rt before quenching with MeOH (1 ml), transferring to a round-bottom flask, and concentrating *in vacuo*. The residue was purified by silica gel chromatography, eluting with PE (30 – 40 °C) to afford diene **36** as a colourless oil.

**Table 14:** Data are reported as (a) amount of enol phosphate **16**; (b) amount of PdCl<sub>2</sub>; (c) volume of THF; (d) amount of isopropenylmagnesium bromide **34**; (e) yield of diene **36**.

**Entry 1, Table 14:** (a) 128 mg, 0.28 mmol, 1 eq; (b) 1 mg, 0.006 mmol, 2 mol%; (c) 0.56 ml, 0.5 M; (d) 0.84 ml, 0.5 M in THF, 0.42 mmol, 1.5 eq; (e) 48 mg, 71% yield.

**Entry 2, Table 14:** (a) 236 mg, 0.52 mmol, 1 eq; (b) 2 mg, 0.01 mmol, 2 mol%; (c) 1.04 ml, 0.5 M; (d) 1.56 ml, 0.5 M in THF, 0.78 mmol, 1.5 eq; (e) 125 mg, 99% yield.

**Entry 3, Table 14:** (a) 298 mg, 0.66 mmol, 1 eq; (b) 2 mg, 0.01 mmol, 2 mol%; (c) 1.32 ml, 0.5 M; (d) 1.98 ml, 0.5 M in THF, 0.99 mmol, 1.5 eq; (e) 116 mg, 73% yield.

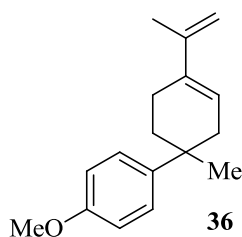
**Entry 4, Table 14:** (a) 567 mg, 1.26 mmol, 1 eq; (b) 5 mg, 0.025 mmol, 2 mol%; (c) 2.52 ml, 0.5 M; (d) 3.78 ml, 0.5 M in THF, 1.89 mmol, 1.5 eq; (e) 287 mg, 94% yield.

$^1\text{H}$  NMR (400 MHz,  $\text{CDCl}_3$ ):  $\delta$  1.26 (s, 3H,  $\text{CH}_3$ ), 1.80 – 1.88 (m, 1H,  $\text{CH}$ ), 1.93 (s, 3H,  $\text{CH}_3$ ), 1.97 – 2.08 (m, 2H, 2 x  $\text{CH}$ ), 2.26 – 2.32 (m, 2H,  $\text{CH}_2$ ), 2.59 – 2.64 (m, 1H,  $\text{CH}$ ), 3.82 (s, 3H,  $\text{OCH}_3$ ), 4.84 (s, 1H,  $\text{C}=\text{CH}$ ), 4.93 (s, 1H,  $\text{C}=\text{CH}$ ), 5.94 – 5.96 (m, 1H,  $\text{C}=\text{CH}$ ), 6.87 (d, 2H,  $J = 8.9$  Hz, 2 x  $\text{ArH}$ ), 7.29 (d, 2H,  $J = 9.1$  Hz, 2 x  $\text{ArH}$ ).

$^{13}\text{C}$  NMR (100 MHz,  $\text{CDCl}_3$ ):  $\delta$  20.1, 23.0, 28.0, 34.8, 38.0, 54.7, 109.4, 112.9, 113.1, 123.0, 126.0, 126.1, 135.7, 145.1, 156.9.

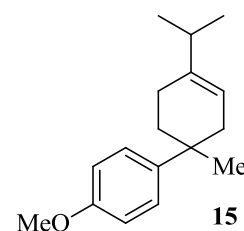
FTIR ( $\text{CHCl}_3$ ): 777, 898, 1029, 1375, 1445, 1612, 2930, 2926, 3022, 3055  $\text{cm}^{-1}$ .

*Unable to obtain accurate HRMS for compound 36.*



Attempted synthesis of 4-isopropyl-4'-methoxy-1-methyl-1,2,3,6-tetrahydro-1,1'-biphenyl **15**

Scheme 24, Table 15<sup>29</sup>

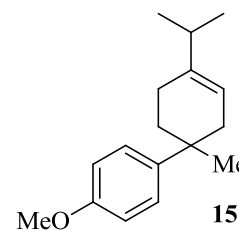


**Entry 1, Table 15:** A flame-dried three-neck flask under argon was charged with diene **36** (121 mg, 0.5 mmol, 1 eq) and THF (1.7 ml, 0.3 M). 9-BBN (1.20 ml, 0.5 M in THF, 0.6 mmol, 1.2 eq) was added and the reaction mixture was stirred at rt for 16 h. After this time the reaction mixture was cooled to 0 °C and acetic acid (30  $\mu$ l, 0.6 mmol, 1.2 eq) was added and the reaction mixture was warmed to rt and stirred for a further 1 h. The reaction was diluted with water (5 ml) and extracted with Et<sub>2</sub>O (2 x 5 ml). The combined organics were washed with water (3 x 5 ml), saturated aqueous NaHCO<sub>3</sub> (5 ml), and brine (5 ml), before drying over Na<sub>2</sub>SO<sub>4</sub>, filtered and concentrating *in vacuo* to give a colourless oil. The oil was purified by silica gel chromatography, eluting with 0 – 10% Et<sub>2</sub>O in PE (30 – 40 °C), to afford a colourless oil (20 mg, 16% combined yield) which was analysed by <sup>1</sup>H NMR spectroscopy. The spectrum revealed a mixture of starting material **36** and product **15** to be present, along with THF impurity.

**Entry 2, Table 15:** A flame-dried three-neck flask under argon was charged with diene **36** (121 mg, 0.5 mmol, 1 eq) and THF (1.7 ml, 0.3 M) then cooled to 0 °C. 9-BBN (1.20 ml, 0.5 M in THF, 0.6 mmol, 1.2 eq) was added and the reaction mixture was warmed to rt and stirred for 16 h. After this time the reaction mixture was cooled to 0 °C and acetic acid (30  $\mu$ l, 0.6 mmol, 1.2 eq) was added and the reaction mixture was stirred for a further 7 h at this temperature. The reaction was diluted with water (5 ml) and extracted with Et<sub>2</sub>O (2 x 5 ml). The combined organics were washed with water (3 x 5 ml), saturated aqueous NaHCO<sub>3</sub> (5 ml), and brine (5 ml), before drying over Na<sub>2</sub>SO<sub>4</sub>, filtered and concentrating *in vacuo* to give a colourless oil. The oil was purified by silica gel chromatography, eluting with 0 – 10% Et<sub>2</sub>O in PE (30 – 40 °C), to afford a colourless oil (58 mg, 48% combined yield) which was analysed by <sup>1</sup>H NMR spectroscopy. The spectrum revealed a mixture of starting material **36** and product **15** to be present, along with THF impurity.

Synthesis of 4-isopropyl-4'-methoxy-1-methyl-1,2,3,6-tetrahydro-1,1'-biphenyl **15**

Scheme 25<sup>30,31</sup>



A Schlenk flask was flame-dried under vacuum (0.005 mbar) then purged with and cooled under argon. Wilkinson's catalyst ( $\text{Rh}(\text{PPh}_3)_3\text{Cl}$ , 25 mg, 0.027 mmol, 5 mol%) was added to the Schlenk flask and the flask was purged three times with argon. Diene **36** (129 mg, 0.53 mmol, 1 eq) was weighed into a flame-dried pear-shaped flask and dissolved in benzene (5 ml, 0.1 M) and MeOH (5 ml, 0.1 M). The solution was transferred to the Schlenk flask *via* cannula. The reaction mixture was subsequently degassed using the following freeze-pump-thaw cycle:

1. The Schlenk stopcock was closed and the reaction vessel was lowered into a Dewar of liquid nitrogen.
2. Once the reaction mixture was frozen the stopcock was opened to the vacuum line and the atmosphere evacuated until 0.005 mbar was reached (10 – 30 min).
3. The stopcock was closed and the reaction mixture was thawed by placing into a Dewar of tepid water.
4. Cycles 1 – 3 were repeated until the evolution of gas was no longer observed when the reaction mixture was thawed.

The reaction mixture was then frozen for a final time and a hydrogen balloon fitted to the Schlenk flask arm. Hydrogen was introduced into the Schlenk at  $-196\text{ }^\circ\text{C}$  and the stopcock closed. The reaction mixture was then thawed, keeping the stopcock closed, to create a pressure of hydrogen within the Schlenk flask (approx. 4 bar). The reaction mixture was stirred at rt under this pressure of hydrogen for 5 h. After this time the solvents were removed *in vacuo* and the residue was purified by silica gel chromatography to afford cyclohexene **15** as a pink-orange oil, 106 mg, 82% yield.

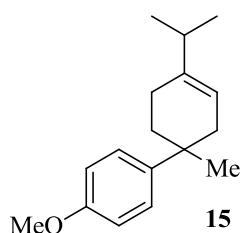


$^1\text{H}$  NMR (400 MHz,  $\text{CDCl}_3$ ):  $\delta$  0.97 (d, 6H,  $J = 6.8$  Hz,  $\text{CH}(\text{CH}_3)_2$ ), 1.25 (s, 3H,  $\text{CH}_3$ ), 1.73 – 1.77 (m, 2H, 2 x  $\text{CH}$ ), 1.85 – 1.96 (m, 2H, 2 x  $\text{CH}$ ), 2.09 – 2.19 (m, 2H, 2 x  $\text{CH}$ ), 2.42 – 2.46 (m, 1H,  $\text{CH}$ ), 3.81, (s, 3H,  $\text{OCH}_3$ ), 5.48 (s, 1H,  $\text{C}=\text{CH}$ ), 6.85 (d, 2H,  $J = 8.8$  Hz, 2 x  $\text{ArH}$ ), 7.29 (d, 2H,  $J = 8.8$  Hz, 2 x  $\text{ArH}$ ).

$^{13}\text{C}$  NMR (100 MHz,  $\text{CDCl}_3$ ):  $\delta$  13.8, 16.7, 21.9, 23.5, 25.0, 30.9, 32.2, 44.6, 113.0, 122.9, 126.1, 126.2, 135.6, 145.0, 156.8.

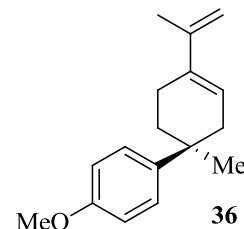
FTIR ( $\text{CHCl}_3$ ): 777, 898, 1029, 1375, 1445, 1612, 2930, 2926, 3022, 3055  $\text{cm}^{-1}$ .

Unable to obtain accurate HRMS for compound **15**.



Attempted one-pot procedure for the synthesis of 4'-methoxy-1-methyl-4-(prop-1-en-2-yl)-1,2,3,6-tetrahydro-1,1'-biphenyl **36**

**Scheme 26**<sup>27</sup>



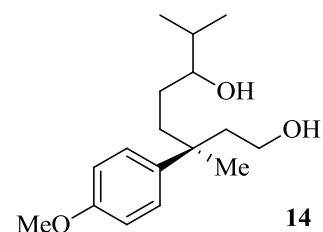
A Schlenk flask was flame dried under vacuum and purged three times with argon. To the Schlenk was added  $n\text{-Bu}_2\text{Mg}$  (1.00 ml, 1 mmol, 1 M solution in heptanes, 1 eq) and the solvent removed *in vacuo* (0.005 mbar) until the appearance of a white solid. THF (10 ml, 0.1 M) was then added followed by (*R*)-bis((*R*)-1-phenylethyl)amine (0.44 ml, 2 mmol, 2 eq) and the resulting mixture was heated at reflux for 90 min after which time quantitative formation of magnesium bisamide (*R,R*)-**27** was assumed. The base solution was cooled to  $-78$  °C and diphenylphosphoryl chloride (0.42 ml, 2 mmol, 2 eq) was added. The ketone **15** (174 mg, 0.8 mmol, 0.8 eq) was weighed into a flame-dried pear-shaped flask and

dissolved in THF (2 ml, 0.5 M). The ketone solution was subsequently added to the Schlenk flask over a period of 1 h *via* syringe pump. The reaction mixture was stirred at -78 °C for 16 h then warmed to rt. PdCl<sub>2</sub> (4 mg, 0.02 mmol, 2 mol%) was weighed into a previously flame-dried pear-shaped flask and THF added (0.5 ml, 2 M). This solution was transferred to the Schlenk flask *via* cannula. Isopropenylmagnesium bromide **34** (3.00 ml, 0.5 M in THF, 1.5 mmol, 1.5 eq) was subsequently added *via* syringe pump over a period of 2 h. The reaction mixture was stirred at rt for a further 3 h before quenching with a saturated solution of NaHCO<sub>3</sub> (10 ml for 1 mmol scale, 20 ml for 2 mmol scale). The aqueous layer was extracted with Et<sub>2</sub>O (3 x 10 ml) and the combined organics were dried over Na<sub>2</sub>SO<sub>4</sub>, filtered, and concentrated *in vacuo*. The resulting oil was purified by silica gel chromatography, eluting with 0 – 50% Et<sub>2</sub>O in PE (30 – 40 °C). The colourless oil obtained was found to be enol phosphate **16** (205 mg, 57% yield) and none of the desired diene **36** was obtained.

Data for enol phosphate **16** were in agreement with previous syntheses of this compound (please refer to **Scheme 15**).

Attempted preparation of (3*S*)-3-(4-methoxyphenyl)-3,7-dimethyloctane-1,6-diol **14**

Scheme 27<sup>32</sup>



A flame-dried three-neck flask was charged with alkene **15** (34 mg, 0.14 mmol, 1 eq), MeOH (1.40 ml, 0.1 M), and DCM (1.40 ml, 0.1 M). The solution was cooled to -78 °C and ozone was bubbled through the reaction mixture until the solution turned blue (approx. 30 min). The ozone was removed from the reaction vessel by bubbling oxygen through the reaction mixture and the three-neck flask was transferred to an argon line. NaBH<sub>4</sub> (26 mg, 0.7 mmol, 5 eq) was added at -78 °C and the reaction mixture was slowly warmed to rt and stirred for 1 h. After this time, 2 M HCl (0.35 ml, 0.7 mmol, 5 eq) was added and the reaction mixture was stirred for a further 30 min before concentrating *in vacuo*. The residue was purified by silica gel chromatography, eluting with 5 – 100% Et<sub>2</sub>O in PE (30 – 40 °C). None of the desired diol **14** was obtained.

## 6 References

1. (a) K. W. Henderson, W. J. Kerr and J. H. Moir, *Chem. Commun.*, **2000**, 479; (b) J. D. Anderson, P. C. García, D. Hayes, K. W. Henderson, W. J. Kerr, J. H. Moir and K. P. Fondekar, *Tetrahedron Lett.*, **2001**, *42*, 7111; (c) M. J. Bassindale, J. J. Crawford, K. W. Henderson and W. J. Kerr, *Tetrahedron Lett.*, **2004**, *45*, 4175; (d) L. S. Bennie, W. J. Kerr, M. Middleditch and A. J. B. Watson, *Chem. Commun.*, **2011**, *47*, 2264.
2. Y. C. Shen, P. I. Tsaim, W. Fenchal and M. E. Hay, *Phytochemistry*, **1992**, *32*, 71.
3. M. Takahashi, Y. Shioura, T. Murakami and K. Ogasawara, *Tetrahedron: Asymmetry*, **1997**, *8*, 1235.
4. (a) T. Kamikubo, M. Shimizu and K. Ogasawara, *Enantiomer*, **1997**, *2*, 297; (b) Y. Kita, A. Furukawa, J. Futamura, K. Ueda, Y. Sawama, H. Hamamoto and H. Fujioka, *J. Org. Chem.*, **2001**, *66*, 8779; (c) S. Ohira, A. Kuboki, T. Hasegawa, T. Kikuchi, T. Kutsukake and M. Nomura, *Tetrahedron Lett.*, **2002**, *43*, 4641.
5. (a) A. Fadel and L. Vabdrømme, *Tetrahedron: Asymmetry*, **1997**, *10*, 1153; (b) C. A. Luchaco-Cullis, H. Mizutani, K. E. Murphy and A. H. Hoveyda, *Angew. Chem. Int. Ed.*, **2001**, *40*, 1456.
6. F. Gao, Y. Lee, K. Mandai and A. H. Hoveyda, *Angew. Chem. Int. Ed.*, **2010**, *49*, 8370.
7. Y. Li, H. Yuan, B. Lu, Y. Li and D. Teng, *J. Chem. Res., Synop.*, **2000**, 530.
8. M. J. Bassindale, P. Hamley and J. P. A. Harrity, *Tetrahedron Lett.*, **2001**, *42*, 9055.
9. E. L. Carswell, *PhD Thesis*, University of Strathclyde, **2005**.
10. (a) T. Honda, N. Kimura and M. Tsubuki, *Tetrahedron: Asymm.*, **1993**, *4*, 1475; (b) T. Honda and N. Kimura, *J. Chem. Soc., Chem. Commun.*, **1994**,

- 77; (c) P. Resende, W. P. Almeida and F. Coelho, *Tetrahedron: Asymm.*, **1999**, *10*, 2113.
11. M. R. DeGraffenried, S. Bennett, S. Caille, F. Gonzalez-Lopez de Turiso, R. W. Hungate, L. D. Julian, J. A. Kaizerman, D. L. McMinn, Y. Rew, D. Sun, X. Yan and J. P. Powers, *J. Org. Chem.*, **2007**, *72*, 7455.
  12. A. J. Pearson and X. Fang, *J. Org. Chem.*, **1997**, *62*, 5284.
  13. R. Kitbunnadaj, M. Hoffmann, S. A. Fratantoni, G. Bongers, R. A. Bakker, K. Wieland, A. el Jilali, I. J. P. De Esch, W. M. P. B. Menge, H. Timmerman and R. Leurs, *Bioorg. Med. Chem.*, **2005**, *13*, 6309.
  14. D. A. Evans, R. L. Dow, T. L. Shih, J. M. Takacs and R. Kahler, *J. Am. Chem. Soc.*, **1990**, *112*, 5290.
  15. Y. Tang, Y. Dong and J. L. Vennerstrom, *Synthesis*, **2004**, 2540.
  16. T. Ling, C. Chowdhury, B. A. Karmer, B. G. Vong, M. A. Palladino and E. A. Theodorakis, *J. Org. Chem.*, **2001**, *66*, 8843.
  17. A. P. Kozikowski and A. Ames, *J. Org. Chem.*, **1980**, *45*, 2551.
  18. S. K. Padhi, I. A. Kaluzna, D. Buisson, R. Azerad and J. D. Stewart, *Tetrahedron: Asymmetry*, **2007**, *18*, 2133.
  19. T. Calogeropoulou, G. B. Hammond and D. F. Wiemer, *J. Org. Chem.*, **1987**, *52*, 4185.
  20. E. V. Anslyn and D. A. Dougherty, *Modern Physical Organic Chemistry*, **2006**, University Science Books: United States.
  21. T. Honda, N. Kimura and M. Tsubuki, *Tetrahedron: Asymmetry*, **1993**, *4*, 21.
  22. For reviews of the use of enol phosphates in cross-coupling reactions, see (a) K. C. Nicolaou, P. G. Bulger and D. Sarlah, *Angew. Chem. Int. Ed.*, **2005**, *44*, 4442; (b) S. Protti and M. Fagnoni, *Chem. Commun.*, **2008**, 3611; (c) H. Fuwa, *Synlett*, **2011**, 6; (d) J. D. Sellars and P. G. Steel, *Chem. Soc. Rev.*, **2011**, *40*, 5170.
  23. U. S. Larsen, L. Martiny and M. Begtrup, *Tetrahedron Lett.*, **2005**, *46*, 4261.

24. A. D. Williams and Y. Kobayashi, *J. Org. Chem.*, **2002**, *67*, 8771.
25. A. L. Hansen, J.-P. Ebran, T. M. Gøgsig and T. Skrydstrup, *J. Org. Chem.*, **2007**, *72*, 6464.
26. A. Krasovskiy, V. Malakhov, A. Gavryushin and P. Knochel, *Angew. Chem. Int. Ed.*, **2006**, *45*, 6040.
27. J. A. Miller, *Tetrahedron Lett.*, **2002**, *43*, 7111.
28. D. Gauthier, S. Beckendorf, T. M. Gøgsig, A. T. Lindhardt and T. Skrydstrup, *J. Org. Chem.*, **2009**, *74*, 3536.
29. H. C. Brown and K. J. Murray, *Tetrahedron*, **1986**, *42*, 5497.
30. G. Blay, R. Schrijvers, J. B. P. A. Wijnberg and A. de Groot, *J. Org. Chem.*, **1995**, *60*, 2188.
31. T. Mahdi, J. N. del Castillo and D. W. Stephan, *Organometallics*, **2013**, *32*, 1971.
32. T. Oishi, K. Ando, K. Inomiya, H. Sato, M. Iida and N. Chida, *Bull. Chem. Soc. Jpn.*, **2002**, *75*, 1927.
33. D. D. Perrin and W. L. F. Armarego, *Purification of Laboratory Chemicals*, **1998**, 3<sup>rd</sup> Edition, Pergamon Press: Oxford.
34. B. E. Love and E. G. Jones, *J. Org. Chem.*, **1999**, *64*, 3755.
35. R. L. Dorta and E. Suárez, *Tetrahedron Lett.*, **1994**, *35*, 5035.
36. T. Shono, R. Kurashige, R. Murkiyama, A. Tsubouchi and T. Takeda, *Chem. Eur. J.*, **2007**, *13*, 4074.

## Chapter 3

### Development of a Mild and Selective Amine Oxidation for an Improved *N*-Debenzylation Method

## Contents

<b>1 Introduction</b> .....	246
1.1 Selected oxidations of amines .....	246
1.1.1 Metal-catalysed oxidations of amines .....	249
1.1.2 Hypervalent iodine-mediated oxidation of amines .....	260
1.2 Diazodicarboxylate-mediated oxidation of amines.....	265
1.3 Deprotection of <i>N</i> -benzylamines.....	272
<b>2 Proposed Work</b> .....	274
<b>3 Results and Discussion</b> .....	275
3.1 Optimisation of reaction conditions .....	275
3.1.1 Mechanistic probes.....	281
3.1.2 Expanding the reaction scope.....	283
3.2 Development of a mild and selective <i>N</i> -debenzylation process.....	287
3.2.1 Synthesis of secondary <i>N</i> -benzylalkylamines .....	289
3.2.2 DIAD-Mediated <i>N</i> -benzyl deprotections .....	296
<b>4 Conclusions and Future Work</b> .....	302
<b>5 Experimental Procedures</b> .....	304
5.1 General Considerations .....	304
5.2 General Experimental Procedures.....	305
5.3 Optimisation of reaction conditions .....	307
5.3.1 Mechanistic probes.....	310
5.3.2 Expanding the reaction scope.....	312
5.4 Development of a mild and selective <i>N</i> -debenzylation process.....	316
5.4.1 Synthesis of secondary amines.....	317
5.4.2 Amides prepared <i>via</i> amide formation and reduction.....	320
5.4.3 DIAD-Mediated <i>N</i> -benzyl deprotections .....	326
<b>6 References</b> .....	332



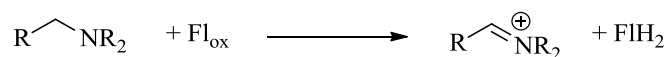
# 1 Introduction

Oxidation processes are fundamental to many aspects of organic synthesis. Furthermore, mild and selective methods are of high importance.<sup>1</sup> To this end, such protocols are continually being developed within the field of oxidation, in particular, the oxidation of heteroatoms.<sup>1</sup> Specifically, the oxidation of amines holds great importance in this field as the products can be transformed into various other functional groups which are widely used in natural and unnatural product syntheses.<sup>1</sup>

## 1.1 Selected oxidations of amines

### *Oxidation of amines by single electron transfers*

In the body, amines are metabolised by enzymes *via* oxidation processes that occur under extremely mild conditions.<sup>1c</sup> Although these metabolic pathways result in a number of different products within the body, the focus here is the oxidation to the corresponding imines and aldehydes. Mitochondrial monoamine oxidase (MAO, a flavin-dependent enzyme) catalyses this deamination of monoamines through two successive single electron transfers. The first electron transferred from the amine to flavin (Fl<sub>ox</sub>) gives an amine radical cation which then loses a proton and undergoes a second electron transfer yielding the iminium ion and reduced flavin (FlH<sub>2</sub>, **Scheme 1**).<sup>1c</sup>



**Scheme 1**

In attempts to mimic this efficient biological process, flavin and its derivatives have been used to oxidise amines to their corresponding imines, with subsequent hydrolysis giving access to the aldehyde products. Most recently, König and

Lechener have used photocatalysis with riboflavin tetraacetate (RFT) to oxidise amines to their corresponding aldehydes.<sup>2</sup> With blue-light-emitting LEDs and oxygen as the terminal oxidant, a range of benzylamines were oxidised in the presence of RFT as the photocatalyst. Through excitation of RFT by the LED, the necessary electron transfers from the amine can occur. As the reactions are carried out in an aqueous medium, hydrolysis of the imine readily occurs to yield the aldehyde and the now reduced RFT is re-oxidised by oxygen in the air. Hydrogen peroxide and ammonia are the only by-products of this reaction (**Figure 1**).<sup>2</sup>

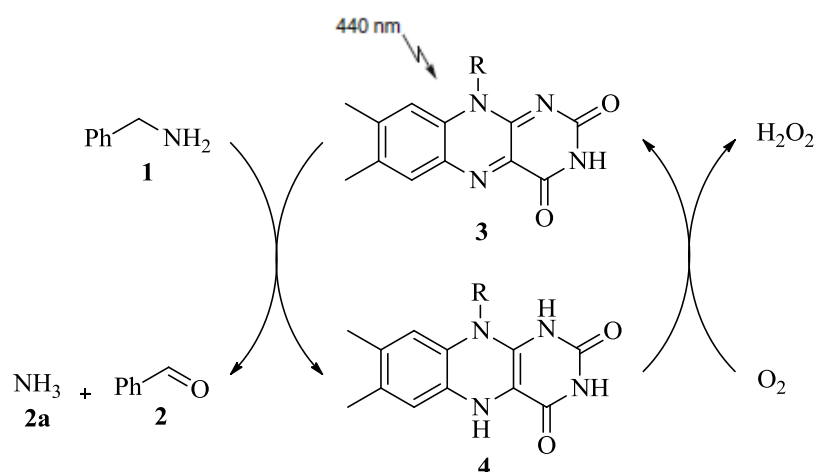
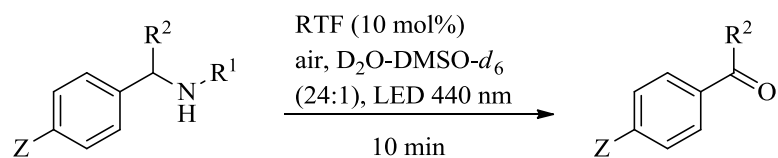


**Figure 1**

The progress of the reaction was monitored by <sup>1</sup>H NMR analysis, which showed a gradual decrease in the intensity of the benzylic protons alongside an increase in the aldehyde resonance signal. After optimisation of the reaction conditions, it was revealed that just 10 mol% RFT was sufficient for this oxidation in D<sub>2</sub>O-DMSO-*d*<sub>6</sub> (**Scheme 2**).<sup>2</sup> A wide range of substrates were subjected to the reaction conditions below, however, a large variation in the chemical yields were obtained. Alkylamines were unreactive under these conditions and low functional group tolerance was observed. The highest levels of conversion were obtained for *p*-methoxybenzylamines, which revealed this protocol to be an efficient method for the deprotection of *p*-methoxybenzylamines.



**Scheme 2**

It has been well documented that, instead of using photocatalysts and in the drive to use aerobic oxidation conditions, singlet oxygen ( $^1\text{O}_2$ ) can be used to oxidise heteroatoms, including the oxidation of amines to aldehydes.<sup>1,3</sup> Significant contributions to this field have been made by Baciocchi and Lapi who have studied the C-heteroatom cleavage of substituted dibenzylsulfides and substituted dibenzylamines.<sup>3</sup> In a similar mechanism to that of flavin,  $^1\text{O}_2$  coordinates to the heteroatom and forms a radical couple (path a, **Figure 2**). Electron transfer then generates the iminium ion (path b, **Figure 2**) which is hydrolysed *in situ* by water in the reaction mixture. In some cases, however, the coordinated  $^1\text{O}_2$  can drop to the triplet ground state through an intersystem crossing (ISC, **Figure 2**).<sup>3</sup> A small set of tertiary tertiary benzylamines were oxidised by  $^1\text{O}_2$ , generated both thermally and photochemically.

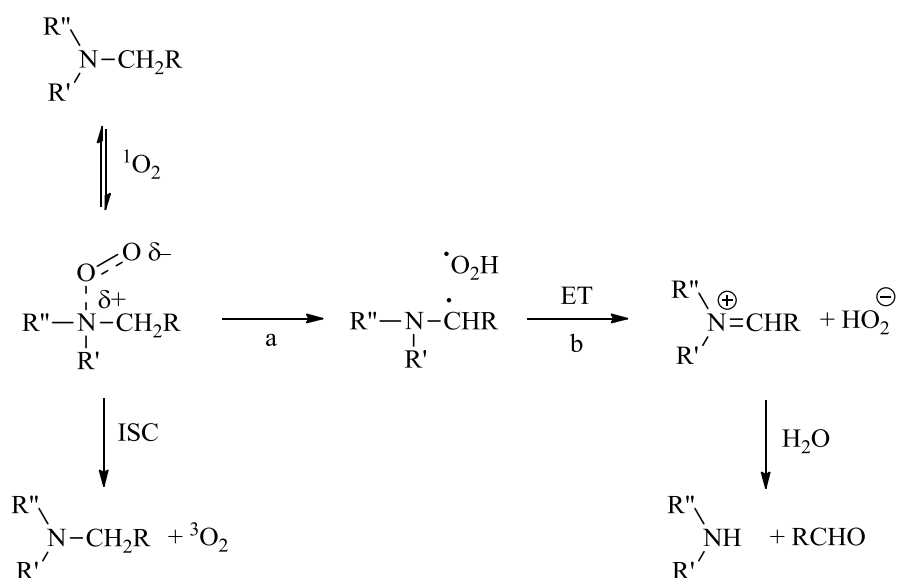


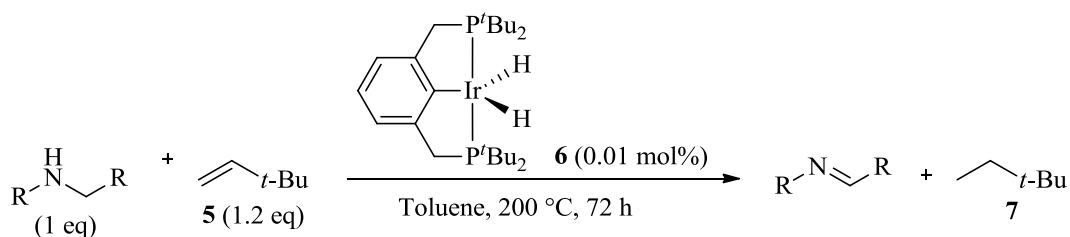
**Figure 2**

Although aerobic oxidants such as oxygen itself can facilitate the oxidation of amines there are some drawbacks to these methods. The requirement for singlet oxygen generation requires thermal energy, making such protocols unfavourable in organic synthesis. In contrast, the excited state oxygen can also be generated photochemically, however, with the use of high energy LEDs or fluorescence lamps. Such sources are not highly demanding in terms of energy, compared with thermal excitation. On the other hand, this does require the use of photosensitisers which is wasteful in terms of atom economy. The development of more efficient oxidation processes is an ever expanding field of organic synthesis. Groundwork in this area has taken advantage of the application of metal catalysis. To date, a wide range of metal catalysed methods have been developed, a selection of which are discussed herein.

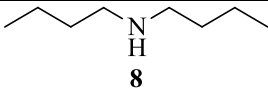
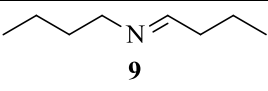
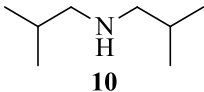
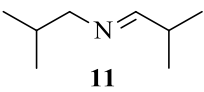
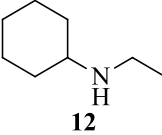
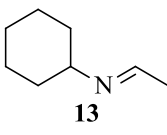
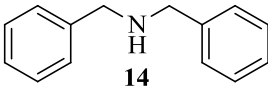
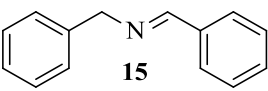
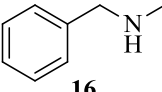
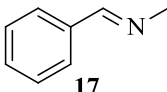
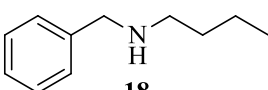
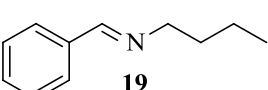
### 1.1.1 Metal-catalysed oxidations of amines

#### *Iridium-catalysed oxidations*

Iridium has been widely used in heterogeneous catalysis in the chemical industry, as well as academia, for many years. Specifically, the application of iridium complexes is becoming well preceded within transfer hydrogenation and dehydrogenation reactions.<sup>4</sup> In particular, pincer iridium complexes have been used to dehydrogenate secondary amines to imines.<sup>5</sup> In 2002, Jensen and co-workers used iridium complex **6** to catalyse the transfer dehydrogenation of a range of alkyl and benzyl secondary amines in moderate to high yields (**Scheme 3, Table 1**).<sup>5</sup> As shown, the dehydrogenation is selective for the secondary  $\alpha$ -carbon over a tertiary  $\alpha$ -carbon (**Entry 3, Table 1**). Additionally, oxidation in a benzylic position is favoured over alkyl positions (**Entries 5 and 6, Table 1**). These results also reveal that this homogeneous system is higher yielding for secondary alkylamines (**Entries 1 to 3, Table 1**) compared with secondary benzylamines (**Entries 4 to 6, Table 1**). Although a very low catalyst loading was used for this system, rather high temperatures were required with prolonged reaction times. Furthermore, only a limited scope of substrates was used as divulged in this publication.

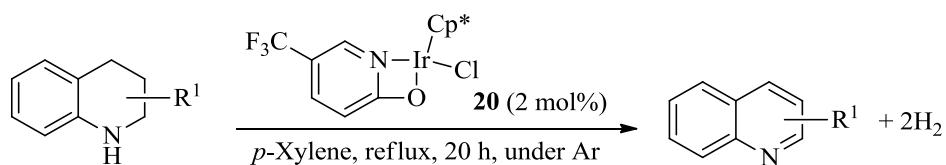


**Scheme 3**

Entry	Substrate	Product	Yield (%)
1			72
2			77
3			94
4			64
5			53
6			60

**Table 1**

Similarly, Yamaguchi has used the Cp\* iridium complex **20** for the dehydrogenation of cyclic secondary amines (**Scheme 4**, **Table 2**).<sup>6</sup> With only 2 mol% catalyst loading a small range of substituted and unsubstituted tetrahydroquinolines were oxidised by **20** under an atmosphere of argon.



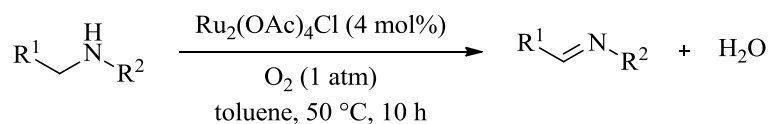
**Scheme 4**

Entry	Substrate	Conversion (%)
1	R <sup>1</sup> = H	57
2	R <sup>1</sup> = 2-Me	100
3	R <sup>1</sup> = 3-Me	86
4	R <sup>1</sup> = 4-Me	76
5	R <sup>1</sup> = 6-Me	82

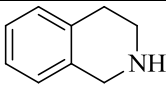
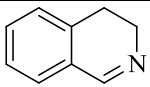
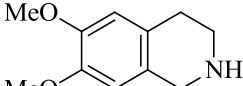
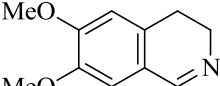
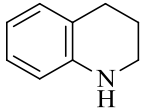
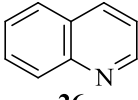
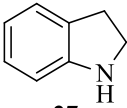
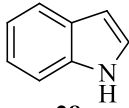
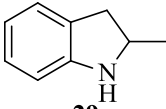
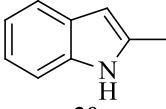
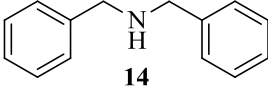
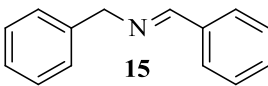
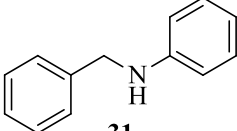
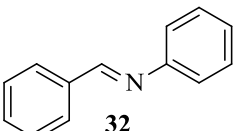
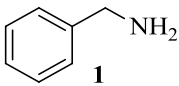
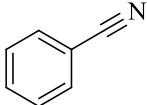
**Table 2**

#### *Ruthenium-catalysed oxidations*

In addition to iridium-catalysed methods, Murahashi and co-workers have developed the use of a dinuclear ruthenium-catalysed oxidation of amines. Using Ru<sub>2</sub>(OAc)<sub>4</sub>Cl, a range of similar secondary amines, as well as benzylamine itself (**33**), were oxidised under aerobic conditions (**Scheme 5**).<sup>7</sup> After confirmation that the dinuclear complex was, indeed, the most efficient ruthenium species for this oxidation, the following results were obtained (**Table 3**).<sup>7</sup>



**Scheme 5**

Entry	Substrate	Product	Time (h)	Conversion (%) <sup>a</sup>
1	 <b>21</b>	 <b>22</b>	3	100
2	 <b>23</b>	 <b>24</b>	12	100
3	 <b>25</b>	 <b>26</b>	72	86
4	 <b>27</b>	 <b>28</b>	1	100
5	 <b>29</b>	 <b>30</b>	485	100
6	 <b>14</b>	 <b>15</b>	18	97
7	 <b>31</b>	 <b>32</b>	48	38
8	 <b>1</b>	 <b>33</b>	7	100

<sup>a</sup> Determined by GC analysis using an internal standard.

**Table 3**

The authors propose that this oxidation of secondary amines can be rationalised through the mechanism below (**Figure 3**).<sup>7</sup> It should be noted that the oxidation states of the diruthenium core may be electronically symmetrical during the reaction,

so have been represented as  $\text{Ru}^n\text{Ru}^n$ , as opposed to  $\text{Ru(II)Ru(III)}$ . As one may predict, the initial step in this catalytic cycle is coordination of the amine to a metal centre *via* ligand exchange and subsequent  $\beta$ -hydride elimination to give the imine-ruthenium hydride species **A** (**Figure 3**). Molecular oxygen can now insert into the Ru-H bond to yield a ruthenium hydroperoxide species **B**. This intermediate then decomposes to release the imine alongside hydrogen peroxide, which breaks down further into molecular oxygen and water. For the primary amine, the nitrile is formed in a similar manner but with a second hydride transfer to the ruthenium species and subsequent oxygen insertion.

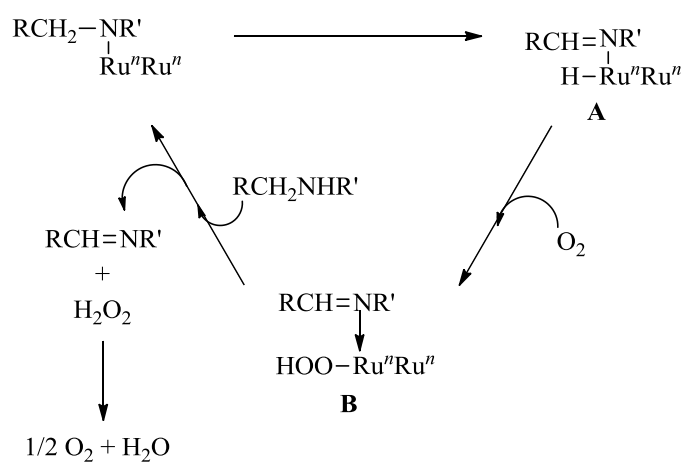


**Figure 3**

### *Copper-catalysed oxidations*

Copper complexes are known as biochemical oxidants, for example, binuclear copper complexes are key components of oxygen transport proteins hemocyanin and tyrosinase.<sup>8</sup> In attempts to mimic this activity, Komatsu and co-workers have used the binuclear copper(II) complex **34** (**Figure 4**) to catalyse the oxidation of the  $\alpha$ -carbon of ethers, as well as for amine oxidation.<sup>8</sup>



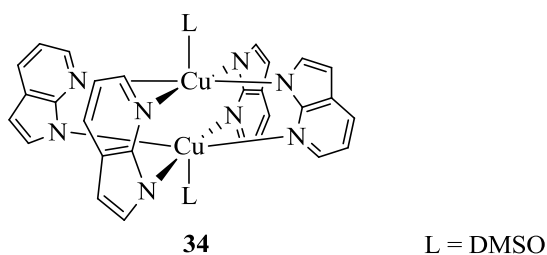
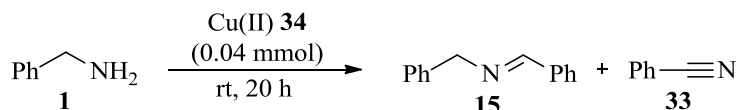


**Figure 4**

Using **34** under an atmosphere of oxygen, benzylamine **1** was oxidised to *N*-benzylidenebenzylamine (**15**) and benzonitrile (**33**) in approximately a 1:2 ratio (**Scheme 6**).<sup>8</sup> It is believed that the imine is formed from a two electron oxidation, whereas a four electron oxidation gives the nitrile.

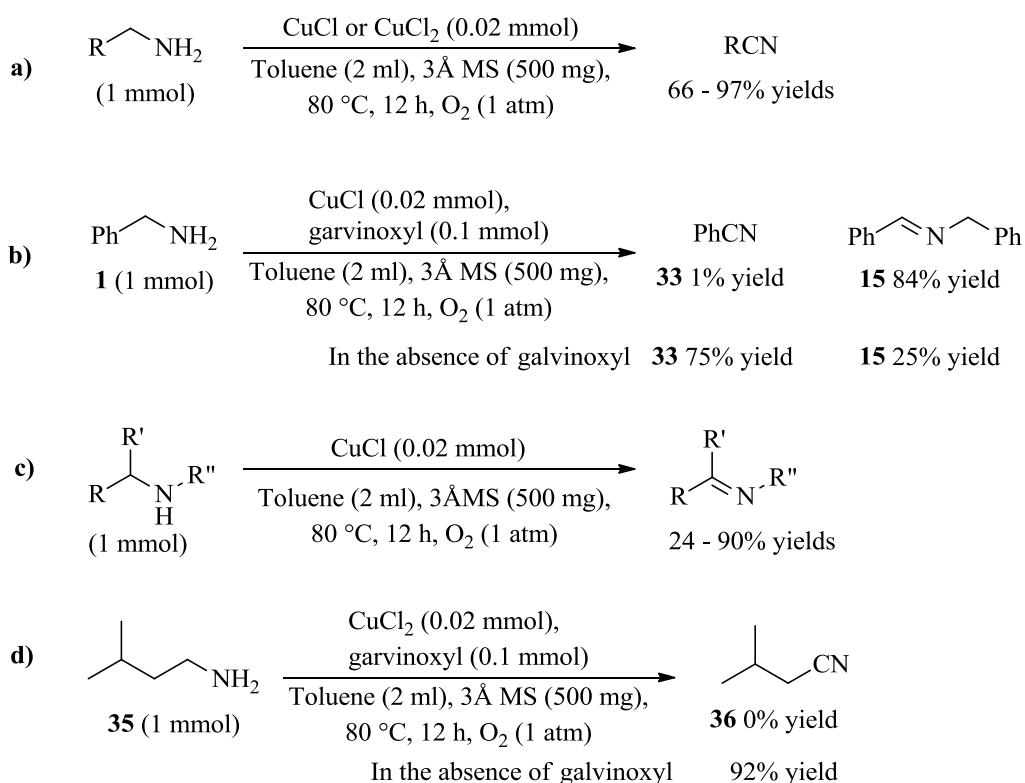


**Scheme 6**

Despite high efficiency of this procedure, however, it is extremely unselective for either of the two oxidation products. The applicability of this copper-catalysed amine oxidation is therefore extremely limited in this sense.

More recently, Uemura has disclosed an improvement to this procedure.<sup>9</sup> Using inexpensive copper(I) or copper(II) chloride in oxygen, with molecular sieves as a dehydrating agent, the successful oxidation of primary amines to nitriles (**Scheme 7a**) and secondary amines to imines was carried out (**Scheme 7c**). After optimisation of the reaction conditions, with respect to the solvent, concentration, reaction time, copper catalyst, and mass of molecular sieves required, a wide range of nitriles and imines were formed in moderate to excellent yields.<sup>9</sup> In addition to the substrate scope, a small mechanistic investigation was carried out. The addition of a radical scavenger (galvinoxyl) was employed to elucidate whether a radical process was occurring for this amine oxidation. For benzylamine **1**, when a sub-stoichiometric

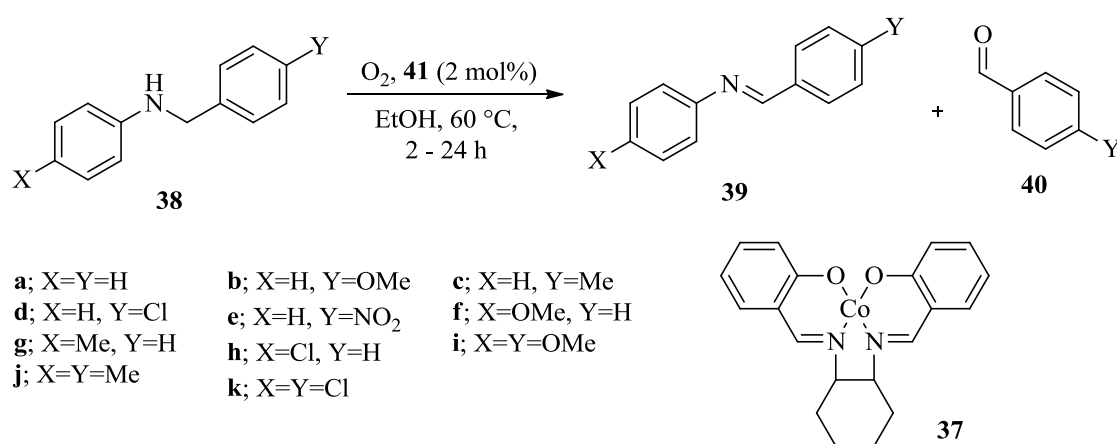
amount of galvinoxyl was employed, only the partially oxidised product **15** was obtained (**Scheme 7b**). When compared with the result for substrate **1** in the absence of this radical scavenger, this suggests that the copper-catalysed aerobic oxidation proceeds *via* a radical pathway. Complementary evidence for a radical process was observed when primary alkylamine **35** was subjected to the reaction conditions with 0.1 equivalents of galvinoxyl (**Scheme 7d**). None of the oxidised product **36** was obtained in the presence of this radical scavenger. When **35** was employed in the absence of galvinoxyl, however, a high yield of the oxidation product **36** was obtained.



**Scheme 7**

### Cobalt-catalysed oxidations

In addition to the more commonly used transition metals for oxidation processes, cobalt Schiff base complexes have also been shown to oxidise secondary aromatic amines with oxygen.<sup>10</sup> After some modifications to the structure of the Schiff base complex, the cobalt(II) complex **37** was found to be the most effective oxidation catalyst, as shown in **Scheme 8** and **Table 4**.<sup>10</sup> In ethanol, at 60 °C, the corresponding imines were obtained in high yields. This system is highly efficient for a wide range of aromatic secondary amines containing both electron-withdrawing and electron-donating groups.



**Scheme 8**

Entry	38	Reaction Time (h)	Conversion (%)	Product (%) <sup>a</sup>	
				39	40
1	38a	24	100	84	11
2	38b	24	100	80	20
3	38c	24	100	81	17
4	38d	24	100	82	18
5	38e	24	100	81	19
6	38f	2	100	94	5
7	38g	6	100	87	9
8	38h	24	100	83	16
9	38i	2	98	95	2
10	38j	24	100	88	12
11	38k	24	100	77	19

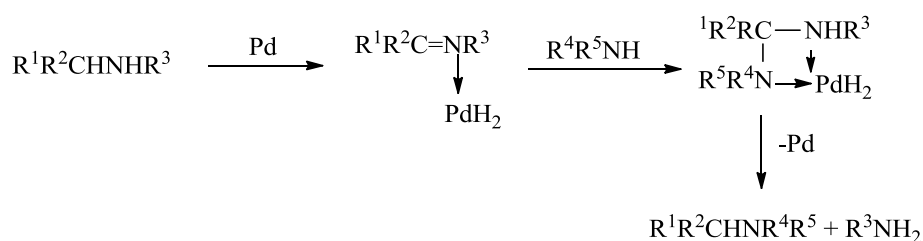
<sup>a</sup> Determined by <sup>1</sup>H NMR analysis.

**Table 4**

The authors propose that this oxidation process proceeds *via* an electron transfer mechanism. It has been hypothesised that the cobalt(II) complex **37** is rapidly oxidised to a cobalt(III)(OH) species which can readily accept an electron from the amine substrate. This would leave a radical cation on the substrate which can then be deprotonated and further oxidised to the imine. The reduced cobalt catalyst could then be reoxidised by O<sub>2</sub> to regenerate the active species. In the examples shown, the levels of oxidation were quantitative in all but one case. The drawback of this protocol, however, is that a mixture of oxidation products is obtained. Although the imine is the major product, a significant amount of aldehyde is present in each example. It is thought that the aldehydes were formed through hydrolysis by the Co(III)(OH) species that is generated.<sup>10</sup>

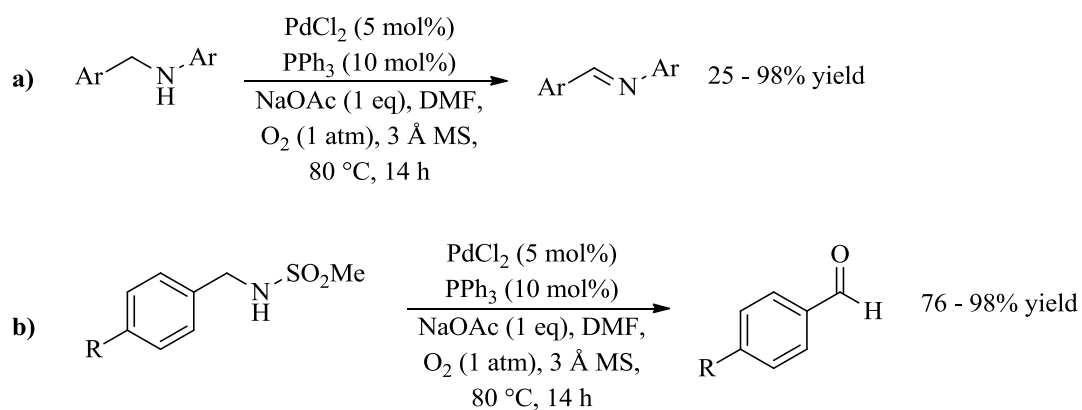
### Palladium-catalysed oxidations

Early work in relation to palladium-catalysed amine oxidations began during the studies of alkyl group exchange reactions of amines in the 1970s (**Scheme 9**).<sup>1</sup> This exchange reaction involves general steps, commencing with the oxidative addition of the palladium(0) to the N-H bond.  $\beta$ -Hydride elimination then yields an imine hydride complex which holds the highly electrophilic carbon for attack of a nucleophile (for example, another amine). Intramolecular reductive cleavage with the metal hydride then affords the amines with exchanged alkyl groups.



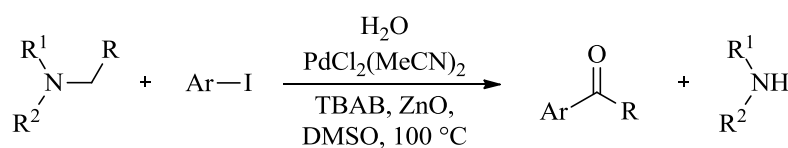
**Scheme 9**

From these preliminary studies towards the reactivity of amines with palladium, it was clear that an imine intermediate was being generated and thus an oxidation process was occurring. Indeed, palladium has been used under various aerobic oxidations, the most notable of which is the Wacker process for the oxidation of alkenes.<sup>11</sup> With these pieces of evidence in hand, Guo and Liu have developed a catalytic, aerobic oxidation of amines using a  $\text{PdCl}_2/\text{PPh}_3$  system.<sup>12</sup> After optimisation of the reaction conditions, including the palladium salt, ligand, base, and solvent, a range of secondary amines were oxidised to their corresponding imines in the benzylic position in moderate to high yields (**Scheme 10a**). In addition, three *N*-methanesulfonamides were oxidised to their corresponding aldehydes, presumably through hydrolysis of the initially formed imines by water generated during the reaction (**Scheme 10b**).



**Scheme 10**

More recently, a novel palladium-catalysed oxidative coupling reaction has been developed by Li and co-workers which takes advantage of the imine generation by palladium.<sup>13</sup> By reacting trialkylamines with aryl iodides in air and in the presence of  $\text{PdCl}_2(\text{MeCN})_2$ , TBAB, and ZnO, a range of alkyl aryl ketones were formed (**Scheme 11**).<sup>13</sup>



**Scheme 11**

As previously discussed, generation of an iminium ion can occur under the above conditions; the palladium(0) undergoes an oxidative addition into the aryl iodide bond, which can then react with the iminium ion to form a new tertiary amine. Further oxidation by the palladium then forms a second iminium ion which is hydrolysed to the desired ketone product (**Figure 5**).<sup>13</sup> A range of aryl iodides were coupled to the alkylamines in this manner, however, this process is rather low yielding for many of the substrates as divulged to this stage.

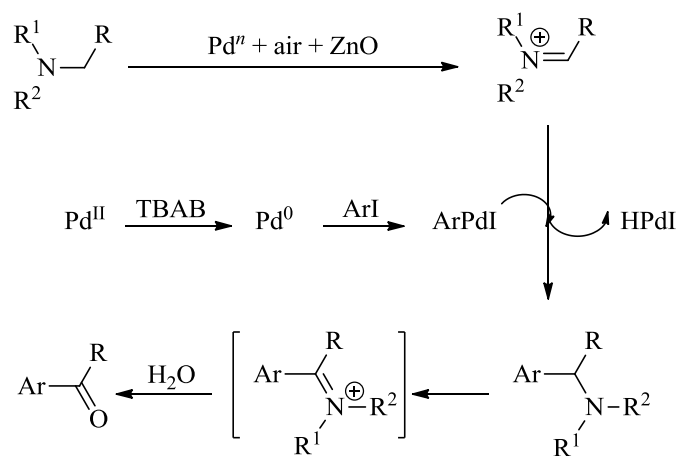


**Figure 5**

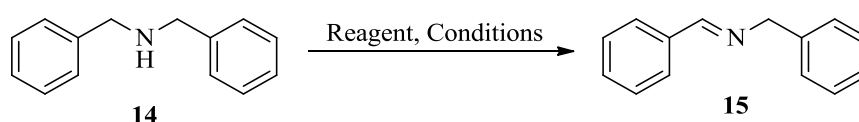
In summary, there are, indeed, many metal-catalysed oxidations of amines which subsequently afford the corresponding nitriles, imines, or aldehydes. The processes discussed thus far, however, are somewhat limited due to the lack in selectivity of oxidation products obtained. Furthermore, the use of metal catalysts can make for an expensive process. Developments of more mild and general methods for amine oxidation are, therefore, ongoing.

### 1.1.2 Hypervalent iodine-mediated oxidation of amines

Although metal-catalysed amine oxidations have proved to be versatile in terms of substrate scope, there still remain a number of shortcomings with these reagents. In particular, the metals themselves are not always cheap, nor are many of the ligands required for some of these processes. Furthermore, prolonged and occasionally rather forcing reaction conditions are required, leaving these methods as somewhat uneconomical for use in organic synthesis. These drawbacks illustrate the requirement for a milder and more general method for the oxidation of amines. A significant contribution to this field has been made by Nicolaou and co-workers, who have pioneered the use of *ortho*-iodoxybenzoic acid (IBX, **41**) for this manipulation.<sup>14</sup> Having previously shown that IBX is capable of mediating oxidation

at benzylic sites, it was envisaged that primary and secondary amines holding at least one benzyl group could undergo an IBX-mediated oxidation. This report also outlined two mechanistic possibilities for this oxidation pathway which will be discussed herein.

In order to determine the most appropriate hypervalent iodine species a number of exploratory reactions were carried out under the conditions shown below (**Scheme 12, Table 5**).<sup>14</sup> Initial results for the oxidation of dibenzylamine (**14**) to its benzylidene counterpart (**15**) using a slight excess of IBX showed encouraging results. An 83% yield of **15** was obtained with slight heating in DMSO after 30 minutes (**Entry 1, Table 5**). Pleasingly, both the reaction time and temperature could be reduced with no loss of efficiency (**Entry 2, Table 5**). An alternative oxidising agent, IBX.MPO, was then trialled under these mild reaction conditions, but this resulted in almost a 50% drop in the yield of benzylidene **15** (**Entry 3, Table 5**). Dess-Martin periodinane, to which IBX is the synthetic precursor, was also investigated but, again, with no improvement to the high yield obtained with IBX (**Entry 4, Table 5**). Diiodine pentoxide (I<sub>2</sub>O<sub>5</sub>) was also utilised in a DMSO/water medium, but with virtually no success (**Entry 5, Table 5**). Finally, the iodine(III) species IBA was trialled in addition to the iodine(V) species used thus far to determine if this compound, which forms as a by-product of the oxidation process (*vide infra*), is in fact mediating this oxidation. It was clear that this was not the case, however, as shown in **Entry 5, Table 5**.



**Scheme 12**

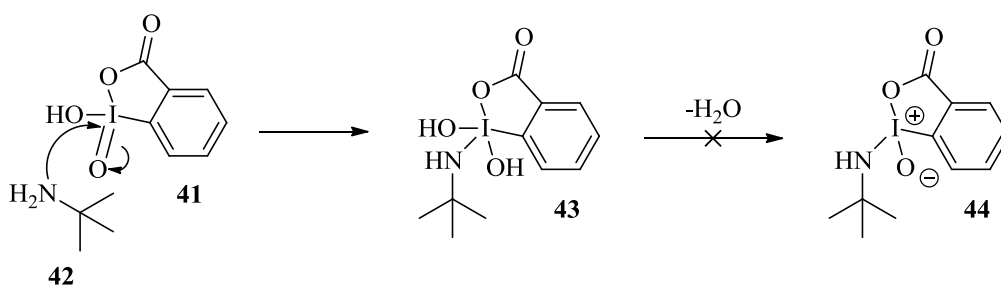


Entry	Reagent	Conditions	Yield (%)
1	IBX (1.1 eq)	DMSO (0.3 M), 45 °C, 30 min	83
2	IBX (1.1 eq)	DMSO (0.3 M), 25 °C, 10 min	83
3	IBX.MPO (1.1 eq)	DMSO (0.3 M), 25 °C, 10 min	44
4	DMP (1.1 eq)	DCM (0.3 M), 25 °C, 10 min	64
5	I <sub>2</sub> O <sub>2</sub> (1.1 eq)	DMSO/H <sub>2</sub> O (9:1), 25 °C, 90 min	1
6	IBA (1.1 eq)	DMSO (0.1 M), 25 °C, 10 min	3

**Table 5**

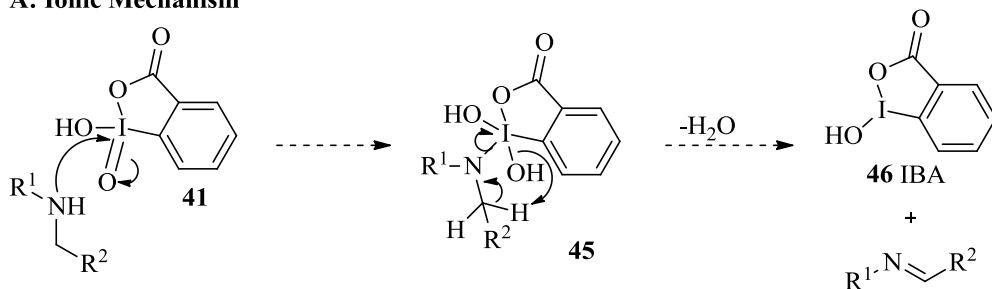
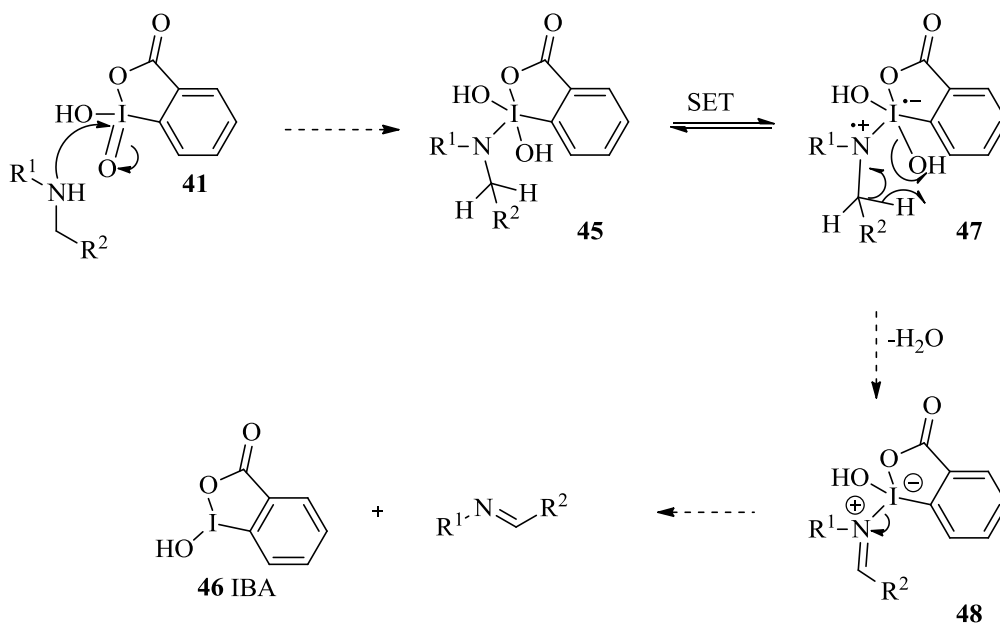
Having found these novel and mild conditions to be effective for the oxidation of dibenzylamine, the scope of this system was investigated. Pleasingly, a broad range of secondary benzylamines were oxidised by IBX with high yields of the imine products. It should be noted that free hydroxyl groups present in some substrates did not interact with IBX under these reaction conditions, and the reaction was selective for oxidation of the benzylic amine.

With these results in hand, and having studied the reactivity of IBX in alternative reactions, two possible mechanisms for this oxidation were considered.<sup>14</sup> The initial consideration of this mechanism was whether the first step involving attack of IBX by the amine substrate forms a stable reaction intermediate or if this intermediate is short lived and the loss of water is more favoured (**Scheme 13**). In the below reaction, *tert*-butylamine **42** was reacted with IBX **41** in DMSO at room temperature for 48 hours, in order to examine the reaction mixture by ESI-MS and <sup>1</sup>H NMR spectroscopy. The analysis revealed that the intermediate iodine(V) compound **43** was the only intermediate present after this time and none of the dehydrated intermediate **44** was observed (**Scheme 13**).<sup>14</sup>

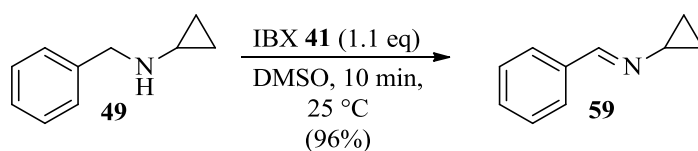


**Scheme 13**

Having shown that an iodine(V) intermediate of type **43** is likely to be present, consideration was given for whether an ionic or radical reaction mechanism was taking place for the reduction at the iodine centre. It has been postulated that if an ionic pathway is taking place, this process would involve a concerted hydrogen abstraction and loss of water to generate the imine directly from intermediate **45** (**Scheme 14A**), with formation of the IBA by-product **46**. Alternatively, if a single electron transfer occurred after addition of the amine to IBX, the nitrogen radical cation **47** would be formed; this would subsequently fragment to release the imine with the loss of water and generate IBA **46** (**Scheme 14B**).

**A: Ionic Mechanism****B: Single Electron Transfer Mechanism****Scheme 14**

In an attempt to validate either of these mechanisms, *N*-benzylcyclopropylamine **49** was reacted with IBX under the optimised conditions (**Scheme 15**).<sup>14</sup> Aminocyclopropanes have previously been shown to undergo a radical-based fragmentation after a one-electron oxidation and, therefore, have the ability to confirm the existence of nitrogen radical cations in mechanistic pathways of the enzymes cytochrome P-450 and monoamine oxidase.<sup>15</sup> During this reaction, however, the cyclopropyl group remained intact, which would support the evidence for an ionic reaction pathway;<sup>14</sup> the authors note that the possibility of a radical pathway, however, cannot be completely excluded.



**Scheme 15**

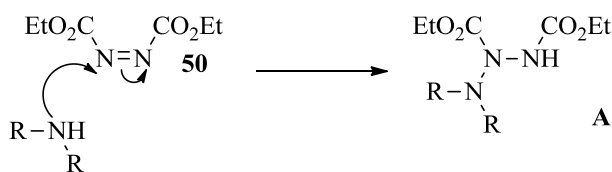
The results delineated above have successfully shown, a mild and selective oxidation of secondary amines. Using IBX, secondary benzylic amines were oxidised to the corresponding imines under ambient conditions in DMSO. A range of other heteroatoms and heterocyclic compounds were tolerated under the optimised reaction conditions and high yields were obtained across the board, making this an attractive method for amine oxidation. As previously alluded to, benzylic oxidation methods for secondary amines have the potential to fully oxidise this position to form the aldehyde and thus be utilised as a deprotection strategy. The drawback of this IBX-mediated oxidation is that the study was not applied in such a sense. Such an oxidation-deprotection strategy has been shown using diisopropyl azodicarboxylate, however, and will be discussed at length in the following section.

## 1.2 Diazodicarboxylate-mediated oxidation of amines

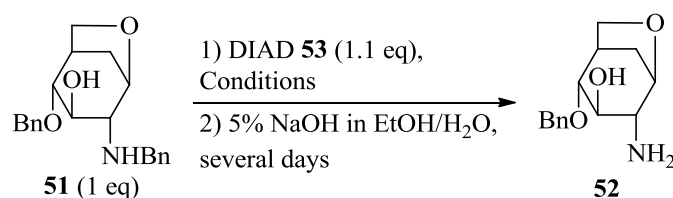
The reaction of heteroatomic nucleophiles with diazodicarboxylates has been widely studied and is most commonly used in the Mitsunobu reaction.<sup>16</sup> However, such diazodicarboxylate reagents can form interesting adducts themselves when the reaction mixture does not contain a second nucleophilic species or triphenylphosphine, as used under Mitsunobu reaction conditions.

Investigations into this interaction were initiated by Diels between 1911 and 1922.<sup>17</sup> During this time, efforts to elucidate the structure of possible adducts of the amine and diazo-ester were made. However, a full understanding was not gained at this stage. The principal evidence obtained by Diels was that of an aldehyde and a mono-dealkylated amine after acid hydrolysis.<sup>17b,17c</sup> From this, Diels proposed that triazane

structure **A** (**Figure 6**) must have been present for the reaction of secondary amines with diethyl azodicarboxylate **50**.<sup>18</sup>



Further studies attempting to confirm the existence of these adducts were carried out by Kenner and Stedman in the 1950s.<sup>18</sup> The collapse of triazane adduct **A** was proposed due to aldehyde oxidation products being observed after reacting a range of benzylamines and azodicarboxylate derivatives in ether, followed by refluxing the solution in acid. These earlier investigations were followed up by Sissman in 1973.<sup>19</sup> Work in this field, however, lay dormant until 2000 when it was revisited by Kroutil and co-workers.<sup>20</sup> Realising that this reaction of amines with dialkyl azodicarboxylates formed the corresponding imines, which were then hydrolysed to release the aldehyde and free amine, Kroutil proposed utilising this reactivity as a method of dealkylation. More specifically, it had been shown by Diels,<sup>17</sup> and Kenner *et al.*<sup>18</sup> that for secondary benzylamines the benzyl group is removed under their conditions. With a view to capitalising on this observation, Kroutil developed this reaction into a selective *N*-debenzylation of benzylamine derivatives of sugars. An example of this is highlighted below (**Scheme 16, Table 6**).<sup>20</sup> Although a high yield of deprotected amine **52** was obtained, some drawbacks to the reactions conditions are apparent. Although a short reaction time of two hours was sufficient when the reaction was performed in toluene (**Entry 1, Table 6**), a prolonged hydrolysis was carried out over several days to afford the free amine **52**. An attempted improvement was made using an acid reaction medium, however, this did not lead directly to the free amine product and the same hydrolysis procedure was employed (**Entry 2, Table 6**).



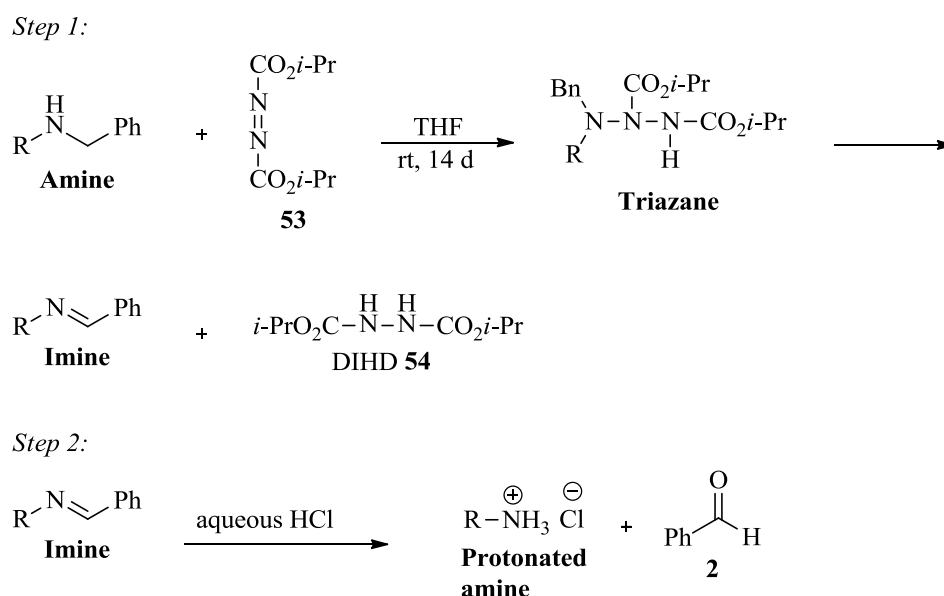
**Scheme 16**

Entry	Solvent	Temp. (°C)	Time (h)	Yield (%)
1	Toluene	Reflux	2	81
2	Pyridine/HCl (35%)	55	48	85

**Table 6**

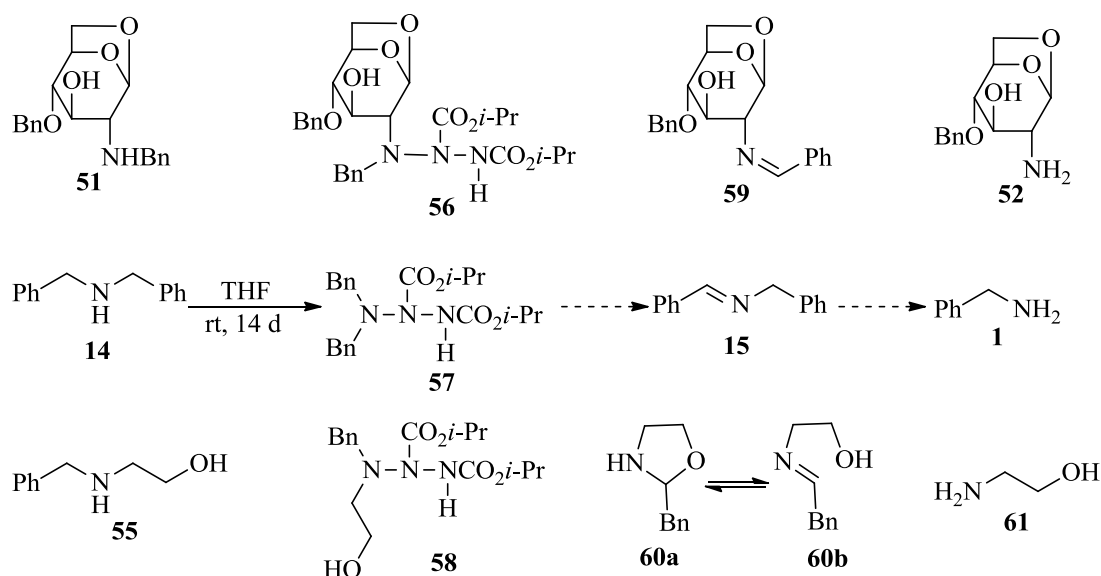
A range of sugar derivatives were employed under the above reaction conditions, however, it was revealed that the rate of reaction with DIAD is variable depending on the amine substrate used. Furthermore, the yields of free amine were not high in all instances. In general, only benzylamine sugars are reactive under the conditions used in this study, albeit at moderate levels for some of these substrates.

With these results in hand, further research was carried out by Kroutil and co-workers to determine what reaction intermediates were present and thus shed more light on the DIAD-mediated amine oxidation reaction mechanism. As discussed previously, it is believed that a triazane intermediate is formed when the secondary benzylamine substrate reacts with the central diazo nitrogen of the dialkyl azodicarboxylate.<sup>17,18</sup> The breakdown of this triazane intermediate then releases an imine and the reduced diisopropyl hydrazinodicarboxylate (DIHD). The second step of the debenzylation is hydrolysis of the imine which yields the debenzylated amine and benzaldehyde (**Scheme 17**).<sup>18,21</sup>



**Scheme 17**

In order to validate this reaction pathway a strategy was devised to react a number of amines under milder conditions.<sup>21</sup> Analysis of the reaction mixtures using various spectroscopic and chromatographic methods to elucidate the reaction intermediate structures would allow reaction intermediates to be detected. Benzylamines **51**, **14**, and **55** were consequently stirred in THF with DIAD for 14 days at room temperature. After this time, the reaction mixtures were analysed by GC-MS to determine the presence of the corresponding triazanes **56**, **57**, and **58**, respectively (**Scheme 18**).<sup>21</sup> It was revealed that the major products from each reaction were imines **59** and **15**, for **51** and **14**, respectively (**Entries 1 and 2, Table 7**).<sup>21</sup> Unfortunately, none of imine **60b** was formed from **55**, but this was thought to be due to the possibility of enamine intermediates which could be highly reactive and thus go on to form other products (**Entry 3, Table 7**). At this stage, no triazanes had been observed using GC-MS. **Table 7** summarises the molar ratios of each reaction from **Scheme 18** found by GC-MS.



**Scheme 18**

Reactant <sup>a</sup>	Product <sup>a</sup>	Imine <sup>a</sup>	DIHD Molar Ratio (%)	Benzaldehyde Molar Ratio (%)
<b>51</b> (13)	<b>52</b> (17)	<b>59</b> (43)	22	4
<b>14</b> (17)	<b>1</b> (0) <sup>b</sup>	<b>15</b> (43)	27	13
<b>55</b> <sup>c</sup> (9)	<b>61</b> <sup>d</sup> (4)	<b>60a+60b</b> <sup>e</sup> (<1)	26	18

<sup>a</sup>Numbers in parenthesis denote molar ratios. <sup>b</sup>Not detected. <sup>c</sup>In addition, three unidentified compounds were found in approx. 1:1:1 ratio (43% overall yield). <sup>d</sup>2-aminoethanol. <sup>e</sup>Both compounds were detected in low amounts.

**Table 7**

Additionally, the use of mass spectrometry and IR spectroscopy revealed the presence of triazanes **56**, **57** and **58** in the reaction mixtures. For **56**, the required mass is 544 and for **57** the mass expected is 400. **Table 8** summarises the mass ions found as well as the IR stretches observed for each intermediate. The characteristic



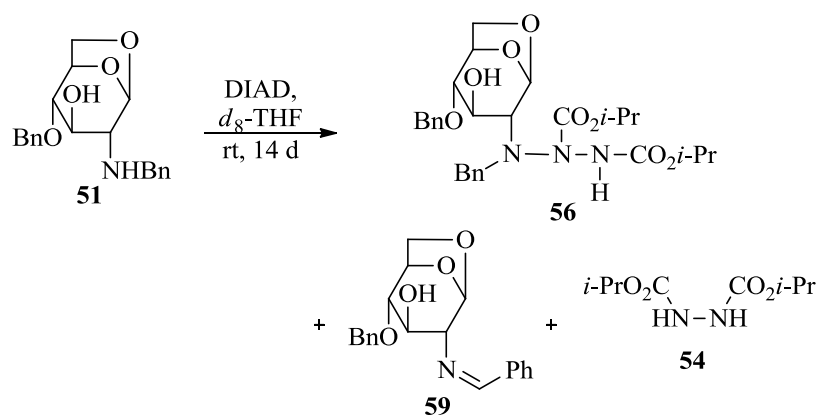
N-H, two C=O, and amide CONH bands were assigned to triazanes **56**, **57** and **58**, and are in accordance with literature values for similar structures;<sup>18,22</sup> further, these are, indeed, in agreement with the values obtained by Kenner and Steadman.<sup>18</sup>

Group	Triazane		
	56	57	58
N-H	3296	<sup>a</sup>	3309
(C=O)1	1751	1753	1753
(C=O)2	1719	1721	1722
NHCO (amide)	1515	1514	1513
Mass Ion	544 [M+H] <sup>+</sup>	400 [M+H] <sup>+</sup>	–

<sup>a</sup> Not estimated due to peak overlap.

**Table 8**

Finally, NMR spectroscopy was carried out in order to fully elucidate the structures of imines and triazanes to complement the data obtained thus far. Benzylamine **51** was reacted with DIAD **53** in perdeuterated THF for 14 days at room temperature (**Scheme 19**).<sup>21</sup> After <sup>1</sup>H NMR analysis of the reaction mixture, imine **59** was observed as the major product alongside triazane **56** and DIHD **54**. The structure of imine **59** was deduced by the presence of only one benzyl group corresponding to O–CH<sub>2</sub>–Ph at  $\delta = 4.77$  ppm and also the –CH=N– moiety at  $\delta = 8.29$  ppm. The imine group (–CH=N–) was also present in the <sup>13</sup>C NMR spectrum at  $\delta = 163.0$  ppm.



**Scheme 19**

Unfortunately, the triazane **56** could not be fully characterised using these data due to the low concentration of this component. The structure was, however, confirmed by using NOE couplings. The NOESY spectrum of the same sample showed couplings between the N-H, N-CH<sub>2</sub>-Ph, (CH<sub>3</sub>)<sub>2</sub>, H(2), and H(3) hydrogens (**Figure 7**).<sup>21</sup>

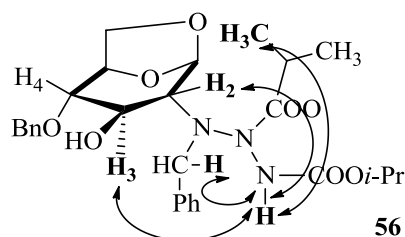


**Figure 7**

Molecular modelling also complemented these findings by outlining the proximity of the relative groups within **56**. The key distances are summarised below (**Table 9**).<sup>21</sup>

Hydrogens		Distance (Å)
N-H	(CH <sub>3</sub> ) <sub>2</sub> CH	1.69
N-H	CH <sub>2</sub> -C <sub>6</sub> H <sub>5</sub>	2.06
N-H	H(2)	2.43
N-H	H(3)	2.26

**Table 9**

This detailed study of the reaction intermediates present within the reaction of secondary *N*-benzylamines and DIAD has proved the existence of triazane intermediates. This complements the early IR studies carried out by Kenner and Steadman<sup>18</sup> and has enhanced the data available for their presence. The occurrence of imines in the <sup>1</sup>H and <sup>13</sup>C NMR spectra also provide evidence for the reaction pathway proposed (see **Scheme 17**). Although the field of DIAD-mediated amine oxidation research is small at this stage, the reaction of secondary *N*-benzylamines with dialkyl azodicarboxylates has been shown to be a useful one in organic synthesis as it could be utilised as an *N*-benzyl deprotection method. Presently, the reaction conditions employing the DIAD-mediated amine oxidation as a method for benzyl group removal are rather inefficient. The extended reaction times alongside variation in free amine yield prevent this method being used in a general sense. Furthermore, a prolonged hydrolysis procedure is required prior to isolation of the free amine products. More traditional methods for *N*-benzyl deprotection are therefore still favoured by the synthetic chemistry community.

### 1.3 Deprotection of *N*-benzylamines

As mentioned during the preceding discussion of *N*-benzylamine oxidation, some of these processes can be utilised as an *N*-benzyl deprotection. As the benzyl group is widely used in organic synthesis to protect amines, its removal is equally or, indeed, more important than its introduction into a molecule.<sup>23</sup> If deprotection is required at a

late stage within a total synthesis, care must be taken when considering this removal so as not to alter any other potentially sensitive groups in the molecule.

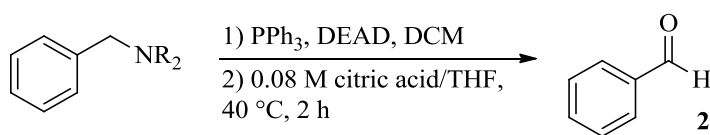
The most commonly used conditions for the removal of *N*-benzyl groups is hydrogenation with palladium on charcoal,<sup>24</sup> or palladium on charcoal under acidified conditions.<sup>25</sup> These conditions, however, are highly unselective towards this functional group alone, as other acid sensitive groups or functional groups sensitive to hydrogenation (such as unsaturated bonds within the molecule) would also be altered under these conditions. Milder oxidation methods could be used, such as metal-catalysed methods described previously, or the use of other oxidants like MCPBA<sup>26</sup> or TPAP with NMO;<sup>27</sup> again, these methods would not be exclusively selective for the *N*-benzyl position. Such methods would therefore incur further steps in a synthesis if other functional groups had to be manipulated back to their required oxidation level.

With this lack of selectivity towards *N*-benzyl groups alone, and the requirement for harsh reaction conditions, there remains a need for a mild and selective deprotection method for these groups. With the selective reactivity of *N*-benzyl groups over *O*-benzyl groups observed by Kroutil for the reaction of such substrates with DIAD,<sup>20</sup> this has proved to be a large step forward in terms of selectivity in *N*-debenzylation chemistry. At this stage, however, the conditions developed are not yet economical as reaction times are long, high temperatures are required for some substrates, and the product cannot be isolated from the reaction until a long hydrolysis of the crude reaction mixture has been performed. Additionally, the scope of this reaction has not been expanded past the sugars divulged in this publication.<sup>20</sup> Although a few other substrates have been used in the later work by this research group, these were only employed for mechanistic probing and thus a true expansion of the scope is still required.<sup>21</sup> With this in mind we have attempted to improve upon these reaction conditions and make this oxidation and deprotection system more widely utilisable.

## 2 Proposed Work

As investigative groundwork regarding the mechanism of DIAD-mediated amine oxidations has been put in place, it was felt that exploiting this mild reaction would be advantageous for the oxidation of a wider range of amine substrates. To date, only a range of sugar derivatives have been employed, preventing this methodology from being general. Furthermore, for certain sugar substrates, extended reaction times and harsh conditions are required.

From work within the laboratory of Professor André B. Charette, at the Université de Montréal, a similar oxidation process was observed as a side reaction from an alternative study. Under a Mitsunobu-type reaction (containing DEAD, PPh<sub>3</sub>, and a substituted benzylamine) benzaldehyde **2** was observed as a by-product (**Scheme 20**).<sup>29</sup> Due to confidentiality agreements, other products and details from the reaction have been eliminated from this scheme, but the isolation of benzaldehyde **2** was believed to have been formed *via* attack of DEAD on the substituted benzylamine, to generate an imine, which was hydrolysed to benzaldehyde **2** during the second step.



**Scheme 20**

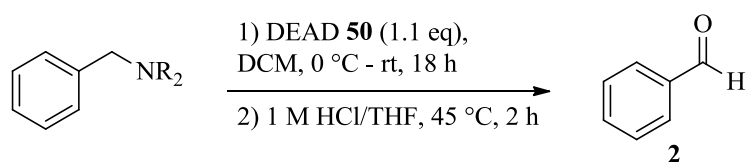
Thus, during a four month placement within the Charette Laboratory, and subsequent completion of studies at Strathclyde, optimisation of this amine oxidation was proposed as an improved method for the oxidation of benzylamines. Additionally, making the substrate scope of this oxidation more general, it was proposed that this method could be applied as an alternative deprotection strategy.

## 3 Results and Discussion

With a view to broadening the scope of the reaction of *N*-benzylamines with dialkyl azodicarboxylates, and in order to investigate this reactivity ourselves, improvements to the conditions for this reaction have been made and have shown some interesting reactivity within this emerging system.

### 3.1 Optimisation of reaction conditions

As a starting point for this study, to investigate the reactivity of benzylamines with DEAD **50**, all other reaction components were removed. The reactivity of primary, secondary, and tertiary benzylamines were therefore assessed under the reaction conditions previously optimised in the Charette laboratory.<sup>29</sup> Thus, benzylamine **1**, dibenzylamine **14**, and tribenzylamine **62** were reacted with DEAD **50** in DCM for 18 hours at room temperature, followed by an acidic hydrolysis using 1 M HCl and THF at 45 °C for 2 hours (**Scheme 21**). After extraction of the acidic phase with DCM, triphenylmethane was added for use as an internal standard to obtain <sup>1</sup>H NMR yields for these reactions. A distinct difference in reactivity was apparent between primary, secondary, and tertiary amines in that only the secondary amine **14** (**Entry 2, Table 10**) was even moderately reactive under these conditions. Indeed, benzylamine **1** and tribenzylamine **62** showed no or very little reactivity to form benzaldehyde **2** (**Entries 1 and 3, Table 10**).



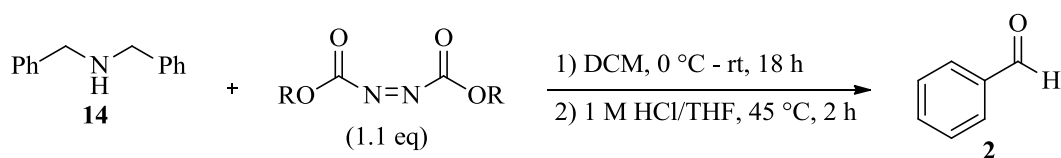
**Scheme 21**

Entry	Amine	<sup>1</sup> H NMR Yield (%) <sup>a</sup>
1	Benzylamine <b>1</b>	0
2	Dibenzylamine <b>14</b>	55
3	Tribenzylamine <b>62</b>	7

<sup>a</sup> Calculated using Ph<sub>3</sub>CH as an internal standard.

**Table 10**

Having found that dibenzylamine **14** was the most reactive amine towards DEAD, an investigation into establishing the most effective dialkyl azodicarboxylate reagent for this oxidation reaction commenced. The more commonly-used DIAD **53** was compared in addition to the dibenzyl derivative **63** (**Scheme 22**, **Table 11**). It should be noted that all optimisation reactions from this point onwards were run in parallel. Thus, a reference reaction, keeping the previous reaction's conditions the same, was carried out in each case (**Entry 1**, **Table 11**). As the remaining results revealed, there was little difference in reactivity between the DEAD and DIAD reagents (**50** and **53**), however, the dibenzyl derivative **63** was not sufficiently activated for this procedure. At this stage, as DIAD has become more commonly used in recent years due to its slightly elevated stability and lower toxicity,<sup>28</sup> this reagent was selected for further studies in the optimisation of the oxidation of benzylamines with dialkyl azodicarboxylates.



**Scheme 22**

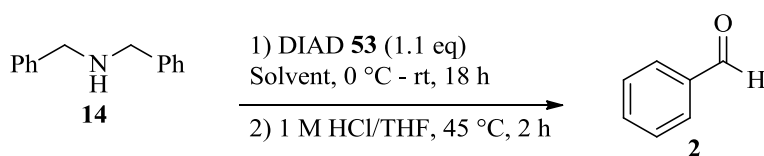
Entry	R	<sup>1</sup> H NMR Yield (%) <sup>a</sup>
1	Et ( <b>50</b> )	56
2	<i>i</i> -Pr ( <b>53</b> )	61
3	Bn ( <b>63</b> )	4

<sup>a</sup> Calculated using Ph<sub>3</sub>CH as an internal standard.

**Table 11**

With an appropriate amine and dialkyl azodicarboxylate in hand, a full optimisation of this oxidation protocol was carried out. Attention was initially turned to the reaction solvent; it was postulated that DCM may not be the most appropriate solvent for this reaction. As such, a solvent study was first performed, as previous accounts of this type of reaction have used coordinating solvents such as THF.<sup>20,21</sup> Indeed, the results of this solvent study (**Scheme 23, Table 12**) are in line with other literature examples. The more coordinating solvents THF, MeCN, and dioxane (**Entries 2, 5, and 6, Table 12**) showed at least a 22% increase in the <sup>1</sup>H NMR yield compared with DCM (**Entry 1, Table 12**). Diethyl ether and toluene (**Entries 3 and 4, Table 12**) were not effective, yielding only 53% and 57% of benzaldehyde, respectively, as calculated by <sup>1</sup>H NMR spectroscopy. Finally, DMF proved to be significantly detrimental to the yield of this oxidation process (**Entry 7, Table 12**). Taking these results into accord, THF was chosen as the solvent for use in further investigations.





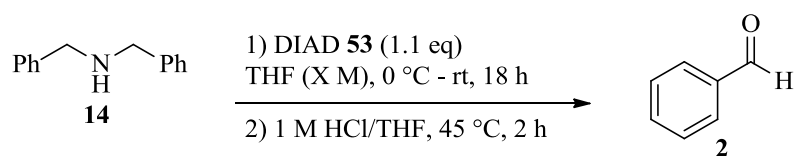
**Scheme 23**

Entry	Solvent	<sup>1</sup> H NMR Yield (%) <sup>a</sup>
1	DCM	60
2	THF	87
3	Et <sub>2</sub> O	53
4	Toluene	57
5	MeCN	82
6	Dioxane	82
7	DMF	16

<sup>a</sup> Calculated using Ph<sub>3</sub>CH as an internal standard.

**Table 12**

With an improved yield at this early stage, the reaction concentration was also investigated in an effort to further enhance the formation of benzaldehyde. Concentrations from 0.05 M to 1.0 M were, subsequently, studied for the reaction of dibenzylamine **14** and DIAD **53** (**Scheme 24**, **Table 13**). A general trend showed an increase in yield from 56 to 83% with an increase in concentration from 0.05 M to 0.8 M (**Entries 1 to 5**, **Table 13**). A slight drop in yield, to 72%, was observed when the reaction mixture was further concentrated to 1.0 M (**Entry 6**, **Table 13**). As such, a concentration of 0.8 M was therefore deemed to be the most appropriate for this oxidation method.



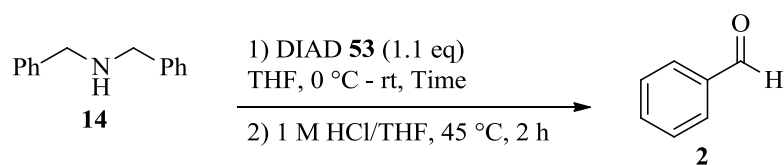
**Scheme 24**

Entry	Concentration (M)	<sup>1</sup> H NMR Yield (%) <sup>a</sup>
1	0.05	56
2	0.1	60
3	0.3	71
4	0.5	82
5	0.8	83
6	1.0	72

<sup>a</sup> Calculated using Ph<sub>3</sub>CH as an internal standard.

**Table 13**

Having made improvements to the dialkyl azodicarboxylate reagent, solvent, and reaction concentration, the reaction time was subsequently investigated to establish whether this oxidation required the extended reaction time of 18 hours. The new benchmark reaction was therefore repeated for reaction times of one, two, three, four, six, and 18 hours to investigate the extent of reaction after these times (**Scheme 25, Table 14**). Following this study, the results clearly show a gradual increase in the yield of benzaldehyde **2** over time and confirm that this oxidation reaction does require the more extended reaction time.



**Scheme 25**

Entry	Time (h)	<sup>1</sup> H NMR Yield (%) <sup>a</sup>
1	1	45
2	2	59
3	3	70
4	4	71
5	6	69
6	18	81

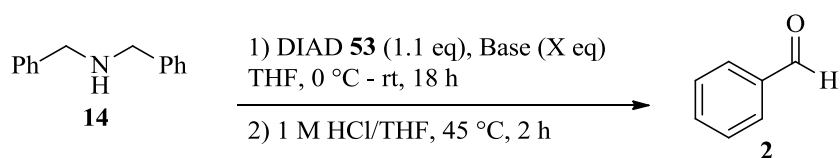
<sup>a</sup> Calculated using Ph<sub>3</sub>CH as an internal standard.

**Table 14**

After initially only forming benzaldehyde in 55% <sup>1</sup>H NMR yield with DEAD, and DCM as the reaction solvent, an iterative optimisation process has enhanced this yield. By using a coordinating solvent (THF) in a more concentrated reaction mixture, 81% of benzaldehyde has been observed by <sup>1</sup>H NMR. As shown by Kroutil, this reaction was believed to be proceeding through a triazane intermediate. It was therefore proposed that the breakdown of this reaction intermediate may be enhanced by external factors. Thus, some mechanistic investigations were carried out to support this proposal.

### 3.1.1 Mechanistic probes

As discussed in **Section 1.2**, the mechanism of the reaction of secondary benzylamines with DIAD **53** is thought to proceed *via* an attack on one of the central DIAD **53** nitrogen atoms by the benzylamine substrate, followed by loss of a proton to form an imine. The imine is then hydrolysed to the aldehyde during an acidic hydrolysis (see **Scheme 17**). With this mechanism in mind, it was hypothesised that the addition of an external base could aid the imine formation, thus increasing the rate of reaction and yield. A study of external bases was therefore carried out (**Scheme 26, Table 15**). Initially, inorganic bases, potassium *tert*-butoxide and sodium hydride, were trialled (**Entries 1 and 2, Table 15**), however, somewhat surprisingly, this resulted in an extremely detrimental effect on the chemical yield. In the case of potassium *tert*-butoxide, no reaction occurred at all and just 10% yield of benzaldehyde was observed when employing sodium hydride. Despite these disappointing initial results, attention was turned to organic bases including DBU, DIPEA, and pyridine. As carried out previously, control reactions were carried out alongside these parallel reactions (**Entries 6 and 10, Table 15**). The use of DBU and DIPEA (**Entries 3 and 4, Table 15**) however, resulted in a large decrease in the <sup>1</sup>H NMR yield of benzaldehyde, to 31% and 44%, respectively. In contrast, pyridine showed no reduction in benzaldehyde yield (**Entry 5, Table 15**). From these findings it was envisaged that the base itself could be reacting with DIAD and thus preventing the desired reaction from occurring. In this regard, the result observed when employing pyridine could be attributed to the reduced basicity of this particular base. With these findings in mind and in an attempt to overcome the competing reaction of the amine base with DIAD, it was thought that a catalytic amount of base may still be helpful for improving the reaction conditions. As such, this study was repeated using 5 mol% of DBU, DIPEA, and pyridine (**Entries 7, 8, and 9, Table 15**). The decrease in yield observed when DBU and DIPEA were employed (**Entries 7 and 8, Table 15**) implied that an undesired interaction of the base species itself with the DIAD electrophile was occurring once more. Again, pyridine showed no appreciable reduction in the yield of benzaldehyde (**Entry 9, Table 15**) compared with the reactions containing no external base (**Entries 6 and 10, Table 15**).



**Scheme 26**

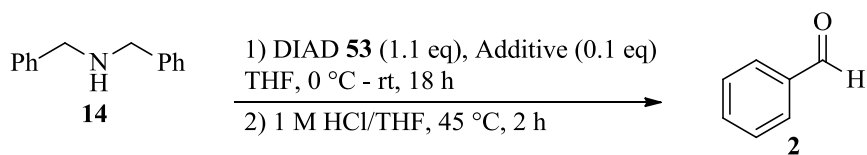
Entry	Base	Equivalents	<sup>1</sup> H NMR Yield (%) <sup>a</sup>
1	KO <i>t</i> -Bu	1.1	0
2	NaH	1.1	10
3	DBU	1.1	31
4	DIPEA	1.1	44
5	Pyridine	1.1	80
6	None	–	83
7	DBU	5 mol%	69
8	DIPEA	5 mol%	66
9	Pyridine	5 mol%	85
10	None	–	89

<sup>a</sup> Calculated using Ph<sub>3</sub>CH as an internal standard.

**Table 15**

From this short additive study, it was decided that the addition of an external base was, indeed, detrimental for the formation of benzaldehyde in these reactions. With a view to confirming whether our reactions were proceeding *via* the mechanism proposed by Kroutil (**Scheme 17**) the application of radical scavengers was considered. It is known that oxidation of amines can, in some cases, proceed through this type of pathway as opposed to the more common ionic pathway (*vide supra*).<sup>14</sup> With this in mind, the radical scavengers TEMPO and galvinoxyl were added to the benchmark reaction of dibenzylamine **14** with DIAD **53** in THF (**Scheme 27**, **Table 16**). As shown in **Table 16**, the addition of such radical scavengers did not decrease the yield of benzaldehyde **2** by a significant amount. It can be interpreted from these

results that a radical process is not underway in these reactions, as one would expect the yield to be greatly reduced if this was the case.



**Scheme 27**

Entry	Additive	<sup>1</sup> H NMR Yield (%) <sup>a</sup>
1	TEMPO	77
2	Galvinoxyl	77

<sup>a</sup> Calculated using Ph<sub>3</sub>CH as an internal standard.

**Table 16**

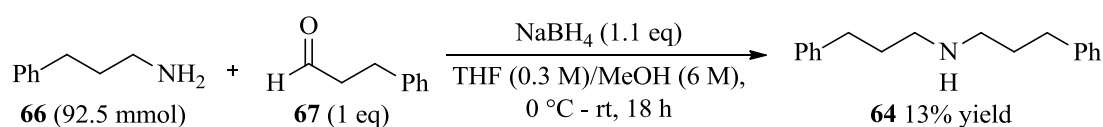
With some clarification that an ionic process is taking place, expansion of these studies, with regards to the scope of this oxidation reaction, was undertaken. Indeed, a high yielding and efficient process had been developed at this point and it was envisaged that these improved reaction conditions could be applied to a wider range of substrates, making this a more general method for the oxidation of amines.

### 3.1.2 Expanding the reaction scope

Having greatly improved the yield of benzaldehyde from 55% to between 81% and 89% the scope of this oxidation procedure was studied. It was postulated that this emerging method for the oxidation of secondary benzylamines could be applied to a broader range of benzylamines and, indeed, alkylamines. As the reaction was initially trialled with primary and tertiary benzylamines (benzylamine **1** and tribenzylamine **62**) it was decided that these substrates should be reconsidered. In addition, to probe whether the benzyl groups are necessarily required for this

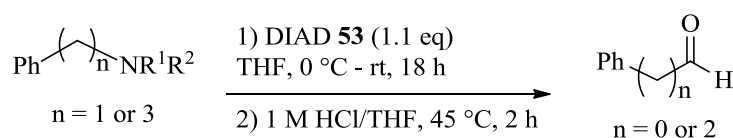
reaction, a secondary alkyl amine, bis(3-phenylpropyl)amine **64** was synthesised and used under these new conditions. Furthermore, it was proposed that the low reactivity of tribenzylamine **62** was due to the steric bulk of this substrate, so an alternative tertiary benzylamine (**65**) was also investigated. Unlike the other substrates, the secondary alkyl amine bis(3-phenylpropyl)amine **64** first had to be synthesised.

Using conditions from within the Charette laboratory,<sup>29</sup> a reductive amination of 3-phenylpropanal **67** with 3-phenylpropan-1-amine **66** was carried out (**Scheme 28**). After purification of this reaction mixture, the desired secondary amine **64** was obtained in 13% yield. Although this yield is low, sufficient material was available for the subsequent studies.



**Scheme 28**

With the requisite amines in hand, these were applied to the DIAD-mediated oxidation conditions, the findings of which are summarised in **Scheme 29** and **Table 17**. Unfortunately, under the conditions optimised for dibenzylamine **14**, benzylamine **1** and tribenzylamine **62** did not show an improved reactivity. Benzylamine **1** (**Entry 1, Table 17**) only showed a 3% yield of benzaldehyde **2** and tribenzylamine **62** (**Entry 2, Table 17**) did not react at all under these conditions. The secondary alkyl amine **64** unfortunately showed only a 15% yield of the corresponding 3-phenylpropanal **67** (**Entry 3, Table 17**) and the alternative tertiary amine **79** only yielded 21% of benzaldehyde **2** (**Entry 4, Table 17**).



**Scheme 29**

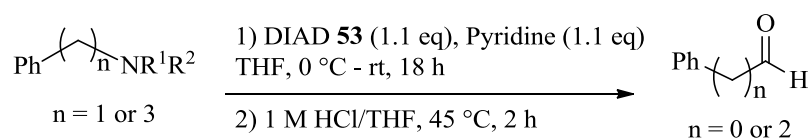
Entry	Amine	n	R <sup>1</sup>	R <sup>2</sup>	Aldehyde	n	<sup>1</sup> H NMR Yield (%) <sup>a</sup>
1	Benzylamine <b>1</b>	1	H	H	<b>2</b>	0	3
2	Dibenzylamine <b>14</b>	1	H	Bn	<b>2</b>	0	81
3	Tribenzylamine <b>62</b>	1	Bn	Bn	<b>2</b>	0	0
4	Bis(3-phenyl-propyl)amine <b>64</b>	3	H	(CH <sub>2</sub> ) <sub>3</sub> Ph	<b>67</b>	2	15 <sup>b</sup>
5	<i>N,N</i> -dimethyl-1-phenylmethanamine <b>65</b>	1	Me	Me	<b>2</b>	2	21

<sup>a</sup> Calculated using Ph<sub>3</sub>CH as an internal standard. <sup>b</sup> 3-Phenylpropanal **67** <sup>1</sup>H NMR yield.

**Table 17**

Disappointed with the above results in relation to alternative amine substrates, the use of additives was reconsidered in an attempt to enhance the reactivity of this system. Considering whether the amine substrates were sufficiently reactive for the initial attack of the DIAD, it was thought that the limiting step may be the collapse of the resulting triazane intermediate. Accordingly, pyridine was trialled as an external base for these substrates as this had proved to be the only external base compatible with these reaction conditions (see **Scheme 26** and **Table 15**). As outlined below (**Scheme 30**, **Table 18**) the addition of pyridine did not enhance the yields of the desired products any further, as approximately the same <sup>1</sup>H NMR yields were obtained.





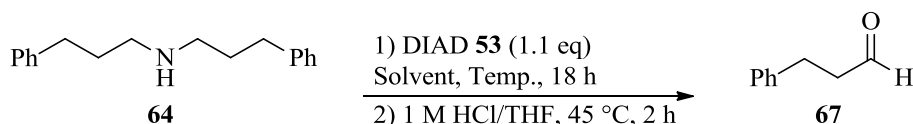
**Scheme 30**

Entry	Amine	n	R <sup>1</sup>	R <sup>2</sup>	Aldehyde	n	<sup>1</sup> H NMR Yield (%) <sup>a</sup>
1	Benzylamine <b>1</b>	1	H	H	<b>2</b>	0	3
2	Dibenzylamine <b>14</b>	1	H	Bn	<b>2</b>	0	80
3	Tribenzylamine <b>62</b>	1	Bn	Bn	<b>2</b>	0	Trace
4	Bis(3-phenylpropyl)amine <b>64</b>	3	H	(CH <sub>2</sub> ) <sub>3</sub> Ph	<b>67</b>	2	19 <sup>b</sup>

<sup>a</sup> Calculated using Ph<sub>3</sub>CH as an internal standard. <sup>b</sup> 3-Phenylpropanal **67** <sup>1</sup>H NMR yield.

**Table 18**

Despite the results to date in relation to substrate **64**, further probes to establish whether the benzyl moiety was crucial for the imine formation were carried out. By increasing the reaction temperature it was hoped that this low reactivity would be overcome (**Scheme 31**, **Table 19**). However, carrying out the reaction at 70 °C in THF (**Entry 1**, **Table 19**) resulted in a poor 11% yield of aldehyde **67** as observed by <sup>1</sup>H NMR analysis. Subsequently, as 1,4-dioxane had proved to be an effective solvent in our initial solvent study, this solvent was also trialled with bis(3-phenylpropyl)amine **64** at both room temperature (**Entry 2**, **Table 19**) and the more elevated temperature of 70 °C (**Entry 3**, **Table 19**). Disappointingly, the two reactions only resulted in <sup>1</sup>H NMR yields of 18% and 13%, respectively.



**Scheme 31**

Solvent	Temperature (°C)	<sup>1</sup> H NMR Yield (%) <sup>a</sup>
THF	0 °C – 70 °C	11
1,4-Dioxane	0 °C – r.t.	18
1,4-Dioxane	0 °C - 70 °C	13

<sup>a</sup> Calculated using Ph<sub>3</sub>CH as an internal standard.

**Table 19**

With no improvements made to the yield of 3-phenylpropanal **67**, it was believed that the benzyl groups were necessary for this oxidation protocol. Realising this apparent limitation within this developing oxidation protocol, it was proposed that this could be used to an advantage. Benzyl groups are commonly used as protecting groups in organic synthesis and their removal can require rather harsh and forcing conditions. It was envisioned that this tandem DIAD-mediated oxidation/hydrolysis protocol could be used as a mild and selective method for the deprotection of *N*-benzylamines.

### 3.2 Development of a mild and selective *N*-debenzylation process

Having established that these mild amine oxidation conditions could be used as a means to selectively deprotect benzylamines, we proposed to obtain a range of secondary *N*-benzylamines for subjection to our reaction conditions (**Figure 8**). Given the selectivity for oxidation at the benzylic position, it was hoped that the amines would be fragmented into benzaldehyde and the respective free amine. As commonly used methods to remove benzyl groups involve the use of metal catalysts, it was envisaged that our selective and mild deprotection strategy would be a viable alternative. More specifically, metal-catalysed methods can be somewhat unselective towards other functional groups within the molecule. For example, hydrogenation conditions will reduce other regions of unsaturation and heteroatoms may impede the level of reactivity required for removal of the benzyl group. It is believed that this

improved method of *N*-benzylamine oxidation/hydrolysis will overcome these issues due to the selectivity observed for this reaction thus far.

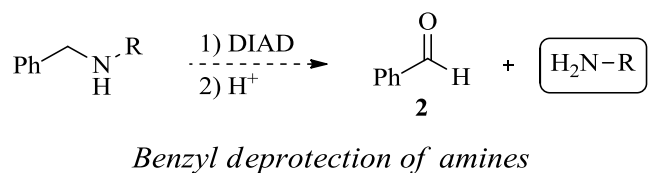
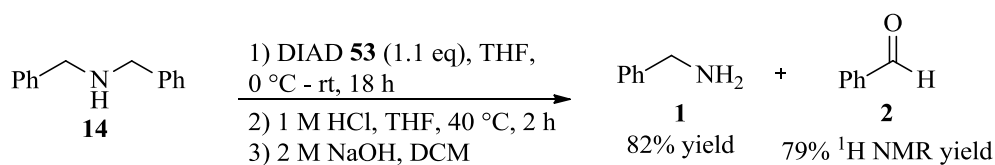


**Figure 8**

To fully capitalise on this methodology as a deprotection strategy, it was important that the free amine was fully recovered from the reaction mixture. In this respect, in a benzyl deprotection strategy the amine is the product of value. To this end, a slight modification to the work-up of this reaction was required in order to provide the deprotected amine and make this a viable deprotection method. Thus, dibenzylamine **14** was employed to the newly optimised conditions in an effort to isolate benzylamine **1** from the reaction mixture (**Scheme 32**). After performing the reaction in the usual manner, the DCM extractions from the acidic aqueous layer were concentrated and analysed by  $^1\text{H}$  NMR spectroscopy to reveal 79% benzaldehyde to be present (when compared to the triphenylmethane internal standard), which is in line with our previous results for these newly optimised conditions. The acidic aqueous layer remaining from the hydrolysis step contained the protonated primary amine. In order to extract this as the free amine product, to prove this to be a viable method for amine deprotection, a further portion of DCM was added to the aqueous phase in a separating funnel. 2 M sodium hydroxide was then added until the aqueous layer reached pH10. The layers were shaken and separated, and, after three more extractions with DCM, benzylamine **1** was obtained in 82% yield.



**Scheme 32**

Satisfied that these conditions would provide high yields of deprotected primary amines, a range of *N*-benzylalkylamines were synthesised and subjected to these mild deprotection conditions.

### 3.2.1 Synthesis of secondary *N*-benzylalkylamines

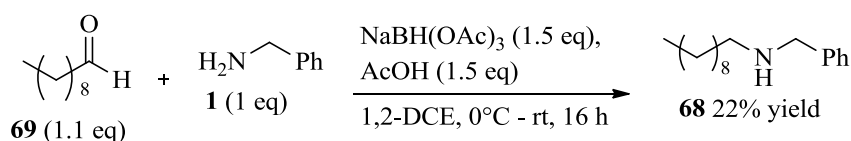
In order to explore a range of compatible substituents within the substrate scope, other heteroatoms, substitution, and hybridisation were incorporated into the range of secondary benzylamine. The outcomes of these deprotections will be discussed in the following subsection, however, the substrates themselves first had to be synthesised. Depending on the available starting materials, these secondary *N*-benzylalkylamines were synthesised *via* a reductive amination or *via* amide synthesis and subsequent reduction using LiAlH<sub>4</sub>.

#### *Amines prepared via reductive amination*

Reductive amination is a well established procedure for the controlled formation of a wide range of secondary amines. This method was therefore selected as a preferred route into the desired *N*-benzylalkylamines for this deprotection study. Using sodium triacetoxyborohydride as the reducing agent under literature conditions, the first set of *N*-benzylalkylamines was synthesised.<sup>30</sup> It should be noted that for each of the following reductive aminations, the reactions were performed on a 10 mmol scale, the sodium triacetoxyborohydride was formed *in situ* from acetic acid and sodium

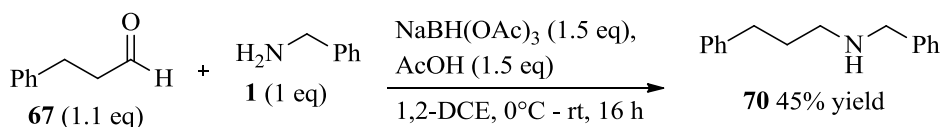
borohydride, and the *N*-benzylalkylamines were purified by an acid/base wash in order to avoid the use of column chromatography.<sup>31</sup>

Firstly, the relatively simple structured *N*-benzylalkylamines were synthesised using these literature conditions. In this instance, *N*-benzyldecan-1-amine **68** was formed from decanal **69** and benzylamine **1** in a low 22% yield (**Scheme 33**). Although the yield for this amine is rather disappointing, it should be noted that column chromatography was avoided and an acid/base extraction was used as an alternative method of purification.



**Scheme 33**

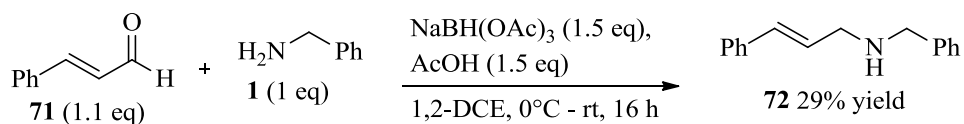
In the same manner, *N*-benzyl-3-phenylpropan-1-amine **70** was formed in 45%, after purification, from 3-phenylpropanal **67** and benzylamine **1** (**Scheme 34**). It was envisaged that amines **68** and **70** would be applicable examples of *N*-benzylalkylamines containing neutral alkyl groups.



**Scheme 34**

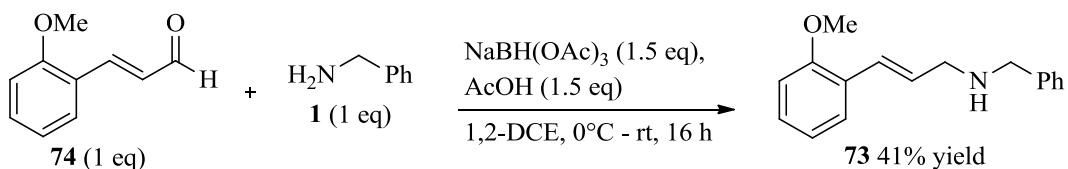
In an attempt to introduce some variety in the substrate scope for this deprotection strategy, the tolerance of double bonds was thought to be a valuable functional group to study. As debenzilation conditions usually require hydrogenation techniques, alkenes are also reduced and are therefore incompatible with these deprotection conditions. Due to the mild nature of this DIAD-mediated deprotection strategy it

was believed that double bonds would survive these reaction conditions. Thus, aldehydes containing at least one unsaturated portion were synthesised under the standard reductive amination conditions. For a direct comparison with **70**, *trans*-cinnamaldehyde **71** was reacted with benzylamine **1** to form (*E*)-*N*-benzyl-3-phenylprop-2-en-1-amine **72** in a 29% yield (**Scheme 35**).



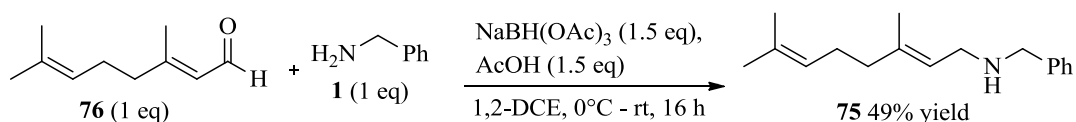
**Scheme 35**

To investigate the impact of substitution and other heteroatoms in the DIAD-mediated deprotection (*E*)-*N*-benzyl-3-(2-methoxyphenyl)prop-2-en-1-amine **73** was synthesised from benzylamine **1** and the required aldehyde **74** under the same conditions as described previously. The desired *N*-benzylalkylamine **73** was formed in a moderate 41% yield (**Scheme 36**).



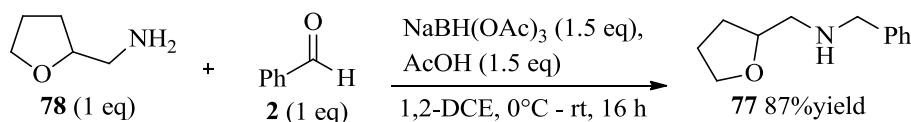
**Scheme 36**

A final substrate containing unsaturation was **75**. Containing another, more remote, alkene moiety, aldehyde **76** was employed with benzylamine **1** in the reductive amination (**Scheme 37**). After purification using an acid/base extraction, **75** was obtained in a 49% yield.



**Scheme 37**

In an effort to prove the compatibility of more complex functional groups and heteroatoms, (tetrahydrofuran-2-yl)methanamine **77** was reacted with benzaldehyde **2** to provide *N*-benzyl-1-(tetrahydrofuran-2-yl)methanamine **78** in a good 87% yield (Scheme 38).

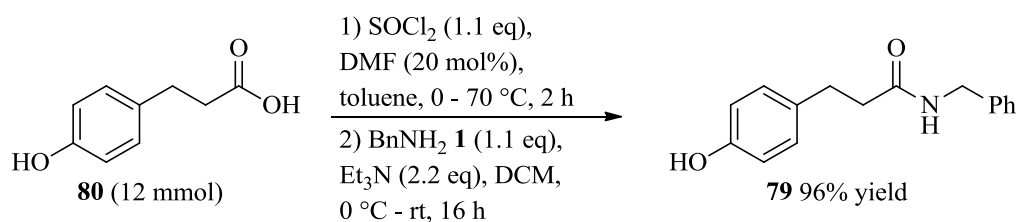


**Scheme 38**

Although the yields of these reductive aminations are somewhat variable and in some cases low, a straight-forward synthesis was used to avoid the use of column chromatography. Furthermore, these reactions were performed on a large enough scale so as to provide ample material for application of these substrates in the DIAD-mediated deprotection reactions. With a view to incorporating a wider variety of functionality within the amine substrates, but with a lack of availability with regards to the starting aldehydes and amines required, an alternative strategy was sought for access to the remaining substrates required for this study.

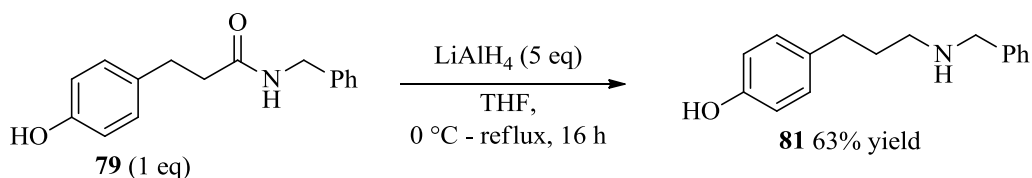
### Amines prepared via amide formation and reduction

An alternative route to access the desired secondary *N*-benzylalkylamines was *via* a LiAlH<sub>4</sub>-mediated reduction of secondary amides. Although this involves an additional synthetic step, to form the amide, the requisite carboxylic acids or acid chlorides were readily available. Thus, *N*-benzyl-3-(4-hydroxyphenyl)propanamide **79** was formed from 3-(4-hydroxyphenyl)propanoic acid **80** which was converted into the acid chloride *in situ* before the addition of benzylamine **1** (Scheme 39).<sup>31</sup> The required amide **79** was formed in a 96% yield and was used without purification in the subsequent reduction to form the secondary amine.



Scheme 39

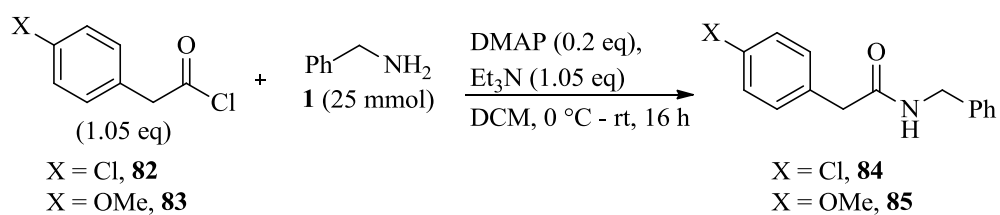
With the secondary amide **79** in hand, a LiAlH<sub>4</sub> reduction was performed in order to access the secondary amine **81** bearing a free hydroxyl group, following a literature procedure (Scheme 40).<sup>32</sup> Once again, to avoid column chromatography, the crude amine **81** was subjected to an acid/base wash to provide a 63% yield of **81** for use in the DIAD-mediated deprotection.



Scheme 40



Having successfully formed a secondary benzylamine *via* an amide and reduction method this protocol was applied for the remaining substrates required. Acid chlorides **82** and **83** were commercially available for the formation of the chloro-substituted secondary amide **84** and methoxy-substituted secondary amide **85**, thus, slightly different conditions were employed to form these amides (**Scheme 41**, **Table 20**).<sup>31</sup> Reacting the acid chloride with benzylamine **1** with catalytic DMAP, amides **84** and **85** were formed in 40% and 26% yield, respectively (**Entries 1 and 2**, **Table 20**).

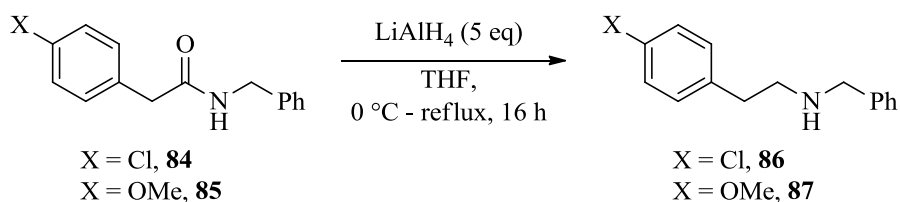


**Scheme 41**

Entry	Acid chloride	Amide	Yield (%)
1	<b>82</b>	<b>84</b>	40
2	<b>83</b>	<b>85</b>	26

**Table 20**

As with the previous amide (**79**) the chloro- and methoxy-derivatives (**84** and **85**) were subjected to the same reduction conditions, followed by an acid/base wash for purification (**Scheme 42**, **Table 21**). Although only moderate yields were achieved for both substrates, column chromatography was avoided and the reactions were performed on a large enough scale to provide sufficient material for the application of secondary amines **86** and **87** in the selective deprotection protocol.



**Scheme 42**

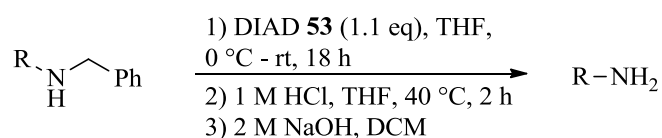
Entry	Amide	Amine	Yield (%)
1	<b>84</b>	<b>86</b>	18
2	<b>85</b>	<b>87</b>	37

**Table 21**

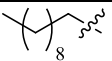
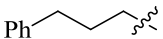
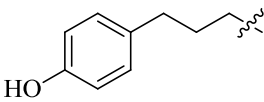
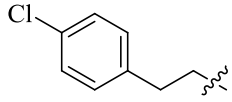
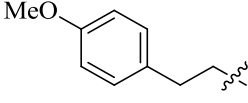
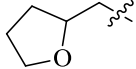
These final three examples containing heteroatom substituents from the aromatic ring were hoped to provide further evidence of heteroatom compatibility within the newly developed mild and selective *N*-debenzylation process. With a range of secondary amines now in hand, containing a variety of functionality, a study of this methodology commenced. It was envisaged that by using the newly developed mild oxidation/hydrolysis conditions, these secondary benzylamines could be efficiently deprotected to afford free amines, thus proving this methodology to be a viable alternative to traditional deprotection methods.

### 3.2.2 DIAD-Mediated *N*-benzyl deprotections

To present the findings of the deprotection study in terms of the success and limitations of our developed *N*-debenzylation protocol, the protected secondary amines have been categorised. Firstly, a number of secondary *N*-benzylalkylamines containing neutral alkyl groups and heteroatom incorporation further from the core nitrogen atom were subjected to the DIAD-mediated *N*-debenzylation conditions in order to obtain the deprotected primary amines (**Scheme 43, Table 22**). Considering the neutral *N*-benzyldecan-1-amine **68**, the yield of decan-1-amine **88** was far lower than expected at 20% (**Entry 1, Table 22**), especially when compared with the yield of 3-phenylpropan-1-amine **66** (63%, **Entry 2, Table 22**). The low yield of decan-1-amine **88** was thusly attributed to isolation problems on account of the volatility of this product. The good yield for the formation of 3-phenylpropan-1-amine **66** confirms this developed protocol to be an effective deprotection strategy for the removal of *N*-benzyl protecting groups. The inclusion of heteroatoms has proved that this improved deprotection protocol is general and that other functionality can be tolerated under these reaction conditions, as the deprotected amines were all obtained in high yields (**Entries 3 to 6, Table 22**). Of particular note is the free hydroxyl group present in benzylamine **81** (**Entry 3, Table 22**). This group could have potentially reacted with the DIAD and prevented the amine oxidation and subsequent benzyl removal occurring. The high yield of primary amine **91**, however, proves that this reaction is selective towards the nitrogen nucleophile.



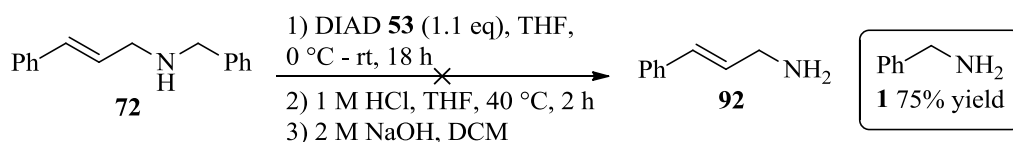
**Scheme 43**

Entry	R	<i>N</i> -benzyl-alkylamine	Amine product	Yield (%)
1		<b>68</b>	<b>88</b>	20
2		<b>70</b>	<b>66</b>	63
3		<b>81</b>	<b>89</b>	81
4		<b>86</b>	<b>90</b>	85
5		<b>87</b>	<b>91</b>	96
6		<b>77</b>	<b>78</b>	73

**Table 22**

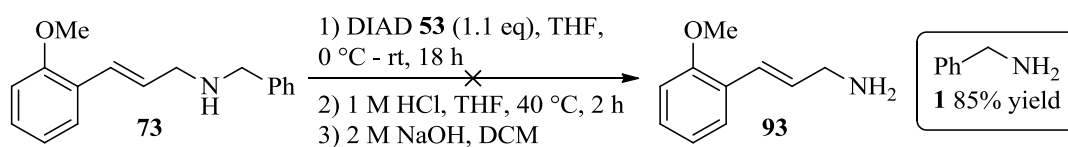
This preliminary study has established that our mild amine oxidation protocol has been improved and is becoming more generalised, compared with the original conditions used by Kroutil (for the effective removal of *N*-benzyl protecting groups).<sup>20</sup> In an effort to expand the variety of compatible substrates and provide free alkylamines bearing heteroatoms in other parts of the molecule, further expansion of the functional group compatibility was carried out to prove that these conditions are a viable alternative to traditional *N*-benzyl deprotection strategies. As alluded to previously, reductive conditions using palladium on charcoal under a hydrogen atmosphere are often used to remove a benzyl protecting group. Under such harsh

reaction conditions, however, sensitive groups such as alkenes can undergo a reduction. For larger or more complex molecules, for example, intermediates in a total synthesis, the preservation of key functionalities is paramount when removing protecting groups. Thus, it is believed that the DIAD-mediated deprotection conditions may be applicable to such substrates and therefore make this protocol a useful alternative when sensitive functional groups must remain intact. Accordingly, the secondary *N*-benzylalkylamines containing unsaturated portions were subjected to the DIAD-mediated deprotection conditions. Firstly, the deprotection of (*E*)-*N*-benzyl-3-phenylprop-2-en-1-amine **72** was attempted (**Scheme 44**). Surprisingly, none of the expected (*E*)-3-phenylprop-2-en-1-amine **92** was obtained, but instead the reaction gave 75% yield of benzylamine **1**. Oxidation had occurred at the position adjacent to the alkene rather than the benzylic position, as predicted.



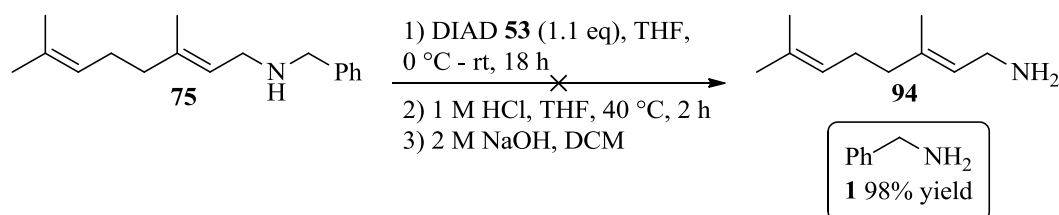
**Scheme 44**

In order to confirm whether the above example was an outlier in terms of the position of oxidation, an alternative *N*-benzylalkylamine containing substitution in the phenyl ring was subjected to the reaction conditions. Thus, secondary benzylamine **73** was subjected to the developed reaction conditions to discover which site oxidation would occur at and therefore which primary amine would be obtained (**Scheme 45**). As with the previous example, none of the desired primary amine **93** was obtained but 85% of benzylamine **1** was yielded instead. Again, oxidation had occurred at the conjugated alkenyl site of the secondary benzylamine **73** as opposed to the benzylic site.



**Scheme 45**

It was postulated that the outcomes depicted in **Scheme 44** and **Scheme 45**, above, could be due to the conjugation of the alkene portions of these two amine compounds with the aryl rings. This could mean that the initial imine formation at this position is lower in energy and, therefore, more favoured than the imine formation in the benzyl position. A final example of an *N*-benzylalkylamine containing double bonds (**75**) was trialled to determine whether this was the case (**Scheme 46**). Once again, only benzylamine **1** was obtained (in a 98% yield) and none of the predicted amine **94**.

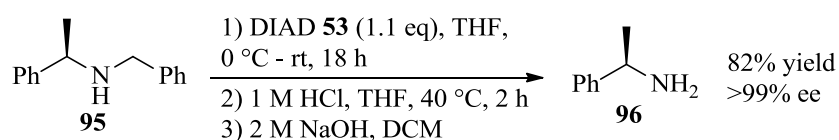


**Scheme 46**

These unanticipated results revealed some interesting characteristics of the DIAD-mediated amine oxidation protocol. They have shown that even if a benzylic position is not present, a *pseudo*-benzylic position (i.e. that containing an sp<sup>2</sup> centre other than that within an aryl ring) can also be oxidised. This was observed for amines **72**, **73**, and **75**. For the first two examples, with amines **72** and **73**, the oxidation at this alternative site was thought to be due to the increased conjugation and implicit stability of this position for imine formation. This may also be true for amine **75** as the imine formed in this position is also in conjugation with an alkene (although there is no further conjugation with an aryl ring) which may be more readily formed

under the reaction conditions used that the benzylic imine. Thus, the conjugated aldehydes are formed during the hydrolysis step and benzylamine is obtained at the end of the reaction.

A final substrate to study the limitations of this newly optimised deprotection protocol was a commercially available amine containing a stereogenic centre. If the chirality remains intact under the reaction conditions, this provides more evidence for this methodology to be relatively general, mild, and, therefore, a viable deprotection strategy for use in synthetic chemistry. To this end, (*R*)-*N*-benzyl-1-phenylethanamine **95** was subjected to the DIAD-mediated deprotection conditions (**Scheme 47**). Pleasingly, this particular substrate highlighted two further parameters of selectivity for this deprotection strategy. Firstly, oxidation (and thus hydrolysis and subsequent removal) occurred at the least hindered benzylic position, revealing the initial oxidation process to be strongly influenced by steric hindrance. The chiral primary amine (*R*)-1-phenylethanamine **96** was therefore the only product of this reaction, obtained in a good 82% yield. Furthermore, the optical rotation measurement of **96** showed comparable ee to the commercial source of the single enantiomer, showing that the stereocentre had not been corrupted under the reaction conditions. This proves our deprotection protocol to be selective for secondary amines and mild enough not to interfere with other functionality and chirality within the molecule.



**Scheme 47**

After having subjected a wider range of secondary *N*-benzylamines to the mild deprotection protocol developed within the Charette laboratory, a more general approach to the DIAD-mediated deprotection of *N*-benzylamines has been realised. Originally developed by Kroutil and co-workers,<sup>20</sup> this DIAD-mediated

oxidation/hydrolysis procedure had only been applied to a range of sugar derivatives. Using the thorough mechanistic information, also presented by Kroutil,<sup>21</sup> we have improved this deprotection method by using milder reaction conditions (in particular for the hydrolysis step) and developing a chromatography-free extraction method for obtaining the free amine products. Moreover, our newly improved protocol has proved to be general for secondary alkyl-*N*-benzylamines containing a variety of other heteroatoms and functionality. It is, therefore, anticipated that this mild and selective strategy can be applied across a wider range of synthetic endeavours to overcome problems with selectivity compared with traditional deprotection methods.



## 4 Conclusions and Future Work

After observing the formation of benzaldehyde from an alternative project within the Charette laboratory, an optimisation of the reaction conditions was carried out to access this oxidation product. With an initial  $^1\text{H}$  NMR yield of 55% for the oxidation of dibenzylamine **14** in DCM, optimisation of the reaction conditions provided a large improvement to between 80% and 89%  $^1\text{H}$  NMR yield of benzaldehyde **2** from this oxidation reaction. This was achieved by changing the solvent to THF, with a higher reaction concentration, and using moderately more forcing hydrolysis conditions of 1 M HCl instead of 0.08 M citric acid (which had been employed in the original Charette project).

Further investigations and attempted improvements were made after achieving these early improvements. Employing external bases in an effort to enhance the collapse of the triazane intermediate, however, was met with no success. Indeed, it was thought that the nitrogen bases may have been undergoing competing reactions with DIAD, which could account for the great decrease in yields for these reactions. Further studies in relation to the reaction mechanism concluded that the oxidation process taking place is occurring *via* an ionic pathway, as no significant drop in benzaldehyde formation was observed when the radical scavengers TEMPO or galvinoxyl were added to the reaction mixtures.

An initial attempt to expand the scope of this reaction to secondary alkyl amines was subsequently trialled using bis(3-phenylpropyl)amine **64**. Unfortunately, after several modifications to the reaction conditions including reaction solvent, reaction temperature, and the addition of external additives no improvement on the maximum 15% yield of aldehyde **67** was ever attained. With these results in mind, and in order to capitalise on the observed selectivity of this reaction for oxidation of the secondary benzylic amine, it was realised that this could be used as a mild *N*-benzyl deprotection method. A range of secondary alkyl benzyl amines were synthesised in good yields and subjected to our novel deprotection conditions.

For all examples containing an alkyl group, high yields of the deprotected amines were obtained, proving this to be a mild and selective benzyl-group removal protocol. Heteroatoms were generally well tolerated and selectivity of this oxidation/deprotection was highlighted, once again, by the lack of reactivity of a free hydroxyl group. Furthermore, for amines containing a stereogenic centre, this remained intact during the reaction, with no erosion of ee. A limitation of this deprotection strategy was observed, however, when a competing oxidation site was present within the secondary *N*-benzylamine substrate. For substrates **72**, **73**, and **75** which contained an allylic moiety in place of a phenyl ring, oxidation occurred preferentially in the *pseudo*-benzylic position (adjacent to the alkene rather than the phenyl ring). Further improvements towards the tolerance of alkene components are therefore required in order to assess whether a more remote double bond is tolerated under our developed reaction conditions. It is believed that such functionality will be compatible, but that the lack of selectivity with the substrates used in this study was due to the more favoured formation of a potentially more stable imine when substrates **72**, **73**, and **75** were employed.

## 5 Experimental Procedures

### 5.1 General Considerations

All reagents were obtained from commercial suppliers and were used without further purification unless otherwise stated. Purification was carried out according to standard laboratory methods.<sup>33</sup>

Diethyl ether, THF, DCM, and toluene were obtained from an Innovative Technology, Pure Solv, PSP-400-5 solvent purification system.

*Thin layer chromatography* was carried out using Camlab silica plates coated with fluorescent indicator UV<sub>254</sub>. This was analysed using a Mineralight UVGL-25 lamp and developed using potassium permanganate or vanillin solution.

*Flash chromatography* was carried out using Prolabo silica gel (230-400 mesh).

<sup>1</sup>H and <sup>13</sup>C NMR spectra were obtained on a Bruker DPX 400 spectrometer at 400 and 100 MHz, respectively. Chemical shifts are reported in ppm, and coupling constants are reported in Hz and refer to <sup>3</sup>J<sub>H-H</sub> interactions unless otherwise specified.

*FTIR spectra* were obtained on a Nicolet Impact 400D machine.

*High-resolution mass spectra* were obtained on a Finnigan MAT900XLT instrument at the EPSRC National Mass Spectrometry Services Centre, Swansea University, Swansea.

*Optical rotations* were obtained on Perkin Elmer 341 polarimeter using a cell with a path length of 1 dm. Concentration is expressed in g/100 cm<sup>3</sup>. ee was calculated using: %ee = ([α]<sub>obs</sub>/[α]<sub>max</sub>)x100.

## 5.2 General Experimental Procedures

*General Procedure A for the reaction of amines with dialkyl azodicarboxylate reagents to obtain the aldehyde*

A flame-dried flask under argon was charged with the amine (1.5 mmol, 1 eq) and the solvent, and the solution was then cooled to 0 °C in an ice bath. The dialkyl azodicarboxylate reagent (1.65 mmol, 1.1 eq) was added dropwise to this solution and the now orange reaction mixture was left to stir at this temperature for 10 min before warming to rt and stirred for 18 h (unless otherwise specified). After this time, the reaction was quenched with 1M HCl (5 ml) and THF (5 ml) then heated to 45 °C for 2 h. The biphasic mixture was subsequently cooled to rt, separated, and the aqueous acidic layer was extracted with DCM (2 x 10 ml). The organic extractions were combined, dried with anhydrous Na<sub>2</sub>SO<sub>4</sub>, and filtered. Triphenylmethane (366 mg, 1.5 mmol, 1 eq) was added to the yellow solution, to be used as an internal standard for <sup>1</sup>H NMR analysis, before concentrating the solution *in vacuo*. The residue was dissolved in CDCl<sub>3</sub> and a sample was analysed by <sup>1</sup>H NMR spectroscopy.

Unless otherwise stated, the <sup>1</sup>H NMR signals used to determine NMR yield are:

<sup>1</sup>H NMR (400 MHz, CDCl<sub>3</sub>): δ 5.71 (s, 1H, Ph<sub>3</sub>CH) and 10.12 (s, 1H, PhC(O)H).

*General Procedure B for the reaction of amines with dialkyl azodicarboxylate reagents to obtain the primary amine*

A flame-dried flask under argon was charged with the amine (1.5 mmol, 1 eq) and the appropriate solvent before cooling to 0 °C in an ice bath. The dialkyl azodicarboxylate reagent (1.65 mmol, 1.1 eq) was added dropwise to this solution and the now orange reaction mixture was left to stir at this temperature for 10 min before warming to rt and stirring for 18 h. After this time, the reaction was quenched with the 1 M HCl (5 ml) and THF (5 ml) then heated to 40 °C for 2 h. The biphasic

mixture was subsequently cooled to rt, separated, and the aqueous acidic layer was extracted with DCM (2 x 10 ml). The organic extractions were discarded and the remaining acidic layer was partitioned with DCM. 2 M NaOH was added until pH 10 – 11 was reached. The layers were shaken and separated and the now basic aqueous layer was extracted with DCM (x 3). The combined organics were dried over Na<sub>2</sub>SO<sub>4</sub>, filtered, and concentrated *in vacuo* to afford the deprotected primary amine.

*General Procedure C for the synthesis of secondary benzylamines.*

A flame-dried flask under argon, equipped with an outlet needle, was charged with sodium borohydride (0.57 g, 15 mmol, 1.5 eq) and 1,2-dichloroethane (30 ml) and cooled to 0 °C. Glacial acetic acid (2.58 ml, 45 mmol, 4.5 eq) was added dropwise over a period of 10 minutes and the suspension was left to stir at 0 °C for 45 minutes to ensure complete formation of sodium triacetoxyborohydride. The reaction mixture was warmed to rt over a 30 minute period before the addition of the amine (10 mmol, 1 eq) and glacial acetic acid (0.86 ml, 15 mmol, 1.5 eq). The reaction mixture was stirred for a further 5 minutes then the carbonyl derivative (11 mmol, 1.1 eq; or 10 mmol, 1 eq) was added dropwise and the reaction was left to stir for 16 hours. After this time, saturated aqueous NaHCO<sub>3</sub> (30 ml) was added slowly to quench the reaction. The amine product was extracted with EtOAc (4 x 50 ml) and the combined organic extracts were concentrated *in vacuo*. The crude yellow oil was then purified by dissolving in EtOAc (80 ml) and washing with citric acid (0.08 M, 3 x 80 ml). The combined acidic washings were subsequently extracted once with EtOAc (100 ml) before being added to DCM (100 ml). The aqueous layer was basified by the slow addition of saturated aqueous NaOH until pH 10-11 was reached. The biphasic mixture was shaken and separated before extracting the now basic layer with DCM (3 x 150 ml). The combined DCM layers were dried with anhydrous Na<sub>2</sub>SO<sub>4</sub>, filtered, and concentrated *in vacuo* to afford the amine product as a pale yellow oil.

### 5.3 Optimisation of reaction conditions

#### *Studies to Determine the Reactivity of Benzylamines with DEAD*

##### **Scheme 21, Table 10**

Following *General Procedure A*, data are reported as (a) amine; (b) solvent; (c) dialkyl azodicarboxylate reagent; (d) aldehyde product; (e) <sup>1</sup>H NMR yield.

**Entry 1:** (a) benzylamine **1**, 0.16 ml, 1.5 mmol, 1 eq; (b) DCM, 5 ml, 0.3 M; (c) DEAD **50**, 0.26 ml, 1.65 mmol, 1.1 eq; (d) benzaldehyde **2**; (e) 0%.

**Entry 2:** (a) dibenzylamine **14**, 0.29 ml, 1.5 mmol, 1 eq; (b) DCM, 5 ml, 0.3 M; (c) DEAD **50**, 0.26 ml, 1.65 mmol, 1.1 eq; (d) benzaldehyde **2**; (e) 55%.

**Entry 3:** (a) tribenzylamine **62**, 431 mg, 1.5 mmol, 1 eq; (b) DCM, 5 ml, 0.3 M; (c) DEAD **50**, 0.26 ml, 1.65 mmol, 1.1 eq; (d) benzaldehyde **2**; (e) 7%.

#### *Optimisation of Diazo Reagent*

##### **Scheme 22, Table 11**

Following *General Procedure A*, data are reported as (a) amine; (b) solvent; (c) dialkyl azodicarboxylate reagent; (d) aldehyde product; (e) <sup>1</sup>H NMR yield.

**Entry 1:** (a) dibenzylamine **14**, 0.29 ml, 1.5 mmol, 1 eq; (b) DCM, 5 ml, 0.3 M; (c) diethyl azodicarboxylate **50**, 0.26 ml, 1.65 mmol, 1.1 eq; (d) benzaldehyde **2**; (e) 56%.

**Entry 2:** (a) dibenzylamine **14**, 0.29 ml, 1.5 mmol, 1 eq; (b) DCM, 5 ml, 0.3 M; (c) diisopropyl azodicarboxylate **53**, 0.33 ml, 1.65 mmol, 1.1 eq; (d) benzaldehyde **2**; (e) 61%.

**Entry 3:** (a) dibenzylamine **14**, 0.29 ml, 1.5 mmol, 1 eq; (b) DCM, 5 ml, 0.3 M; (c) dibenzyl azodicarboxylate **63**, 492 mg, 1.65 mmol, 1.1 eq; (d) benzaldehyde **2**; (e) 4%.

*Optimisation of Reaction Solvent*

**Scheme 23, Table 12**

Following *General Procedure A*, data are reported as (a) amine; (b) solvent; (c) dialkyl azodicarboxylate reagent; (d) aldehyde product; (e) <sup>1</sup>H NMR yield.

**Entry 1:** (a) dibenzylamine **14**, 0.29 ml, 1.5 mmol, 1 eq; (b) DCM, 5 ml, 0.3 M; (c) DIAD **53**, 0.33 ml, 1.65 mmol, 1.1 eq; (d) benzaldehyde **2**; (e) 60%.

**Entry 2:** (a) dibenzylamine **14**, 0.29 ml, 1.5 mmol, 1 eq; (b) THF, 5 ml, 0.3 M; (c) DIAD **92**, 0.33 ml, 1.65 mmol, 1.1 eq; (d) benzaldehyde **2**; (e) 87%.

**Entry 3:** (a) dibenzylamine **14**, 0.29 ml, 1.5 mmol, 1 eq; (b) Et<sub>2</sub>O, 5 ml, 0.3 M; (c) DIAD **53**, 0.33 ml, 1.65 mmol, 1.1 eq; (d) benzaldehyde **2**; (e) 53%.

**Entry 4:** (a) dibenzylamine **14**, 0.29 ml, 1.5 mmol, 1 eq; (b) Toluene, 5 ml, 0.3 M; (c) DIAD **53**, 0.33 ml, 1.65 mmol, 1.1 eq; (d) benzaldehyde **2**; (e) 57%.

**Entry 5:** (a) dibenzylamine **14**, 0.29 ml, 1.5 mmol, 1 eq; (b) MeCN, 5 ml, 0.3 M; (c) DIAD **53**, 0.33 ml, 1.65 mmol, 1.1 eq; (d) benzaldehyde **2**; (e) 82%.

**Entry 6:** (a) dibenzylamine **14**, 0.29 ml, 1.5 mmol, 1 eq; (b) 1,4-Dioxane, 5 ml, 0.3 M; (c) DIAD **53**, 0.33 ml, 1.65 mmol, 1.1 eq; (d) benzaldehyde **2**; (e) 82%.

**Entry 7:** (a) dibenzylamine **14**, 0.29 ml, 1.5 mmol, 1 eq; (b) DMF, 5 ml, 0.3 M; (c) DIAD **53**, 0.33 ml, 1.65 mmol, 1.1 eq; (d) benzaldehyde **2**; (e) 16%.

### *Optimisation of Reaction Concentration*

#### **Scheme 24, Table 13**

Following *General Procedure A*, data are reported as (a) amine; (b) solvent; (c) dialkyl azodicarboxylate reagent; (d) aldehyde product; (e)  $^1\text{H}$  NMR yield.

**Entry 1:** (a) dibenzylamine **14**, 0.29 ml, 1.5 mmol, 1 eq; (b) THF, 30 ml, 0.05 M; (c) DIAD **53**, 0.33 ml, 1.65 mmol, 1.1 eq; (d) benzaldehyde **2**; (e) 56%.

**Entry 2:** (a) dibenzylamine **14**, 0.29 ml, 1.5 mmol, 1 eq; (b) THF, 15 ml, 0.1 M; (c) DIAD **53**, 0.33 ml, 1.65 mmol, 1.1 eq; (d) benzaldehyde **2**; (e) 60%.

**Entry 3:** (a) dibenzylamine **14**, 0.29 ml, 1.5 mmol, 1 eq; (b) THF, 5 ml, 0.3 M; (c) DIAD **53**, 0.33 ml, 1.65 mmol, 1.1 eq; (d) benzaldehyde **2**; (e) 71%.

**Entry 4:** (a) dibenzylamine **14**, 0.29 ml, 1.5 mmol, 1 eq; (b) THF, 3 ml, 0.5 M; (c) DIAD **53**, 0.33 ml, 1.65 mmol, 1.1 eq; (d) benzaldehyde **2**; (e) 82%.

**Entry 5:** (a) dibenzylamine **14**, 0.29 ml, 1.5 mmol, 1 eq; (b) THF, 1.9 ml, 0.8 M; (c) DIAD **53**, 0.33 ml, 1.65 mmol, 1.1 eq; (d) benzaldehyde **2**; (e) 83%.

**Entry 6:** (a) dibenzylamine **14**, 0.29 ml, 1.5 mmol, 1 eq; (b) THF, 1.5 ml, 1.0 M; (c) DIAD **53**, 0.33 ml, 1.65 mmol, 1.1 eq; (d) benzaldehyde **2**; (e) 72%.

### *Optimisation of Reaction Time*

#### **Scheme 25, Table 14**

Following *General Procedure A*, data are reported as (a) amine; (b) solvent; (c) dialkyl azodicarboxylate reagent; (d) reaction time; (e) aldehyde product; (f)  $^1\text{H}$  NMR yield.



**Entry 1:** (a) dibenzylamine **14**, 0.29 ml, 1.5 mmol, 1 eq; (b) THF, 1.9 ml, 0.8 M; (c) DIAD **53**, 0.33 ml, 1.65 mmol, 1.1 eq; (d) 1 h; (e) benzaldehyde **2**; (f) 45%.

**Entry 2:** (a) dibenzylamine **14**, 0.29 ml, 1.5 mmol, 1 eq; (b) THF, 1.9 ml, 0.8 M; (c) DIAD **53**, 0.33 ml, 1.65 mmol, 1.1 eq; (d) 2 h; (e) benzaldehyde **2**; (f) 59%.

**Entry 3:** (a) dibenzylamine **14**, 0.29 ml, 1.5 mmol, 1 eq; (b) THF, 1.9 ml, 0.8 M; (c) DIAD **53**, 0.33 ml, 1.65 mmol, 1.1 eq; (d) 3 h; (e) benzaldehyde **2**; (f) 70%.

**Entry 4:** (a) dibenzylamine **14**, 0.29 ml, 1.5 mmol, 1 eq; (b) THF, 1.9 ml, 0.8 M; (c) DIAD **53**, 0.33 ml, 1.65 mmol, 1.1 eq; (d) 4 h; (e) benzaldehyde **2**; (f) 71%.

**Entry 5:** (a) dibenzylamine **14**, 0.29 ml, 1.5 mmol, 1 eq; (b) THF, 1.9 ml, 0.8 M; (c) DIAD **53**, 0.33 ml, 1.65 mmol, 1.1 eq; (d) 6 h; (e) benzaldehyde **2**; (f) 69%.

**Entry 6:** (a) dibenzylamine **14**, 0.29 ml, 1.5 mmol, 1 eq; (b) THF, 1.9 ml, 0.8 M; (c) DIAD **53**, 0.33 ml, 1.65 mmol, 1.1 eq; (d) 18 h; (e) benzaldehyde **2**; (f) 81%.

### 5.3.1 Mechanistic probes

#### *Studies to Determine the Effectiveness of an External Base*

#### **Scheme 26, Table 15**

To a flame-dried flask under argon was added dibenzylamine **14** (0.29 ml, 1.5 mmol, 1 eq), THF (1.9 ml, 0.8 M) and base. The resulting solution was cooled to 0 °C in an ice bath. DIAD **53** (0.33 ml, 1.65 mmol, 1.1 eq) was added dropwise to this solution and the now orange reaction mixture was left to stir at this temperature for 10 min before being warmed to rt and stirred for 18 h. After this time, the reaction was quenched with HCl (1 M, 5 ml) and THF (5 ml) and heated to 45 °C for 2 h. The biphasic mixture was then cooled to rt, separated and the aqueous acidic layer was extracted with DCM (2 x 10 ml). The organic extractions were combined, dried with anhydrous Na<sub>2</sub>SO<sub>4</sub>, and filtered. Triphenylmethane (366 mg, 1.5 mmol, 1 eq) was added to the yellow solution, to be used as an internal standard for <sup>1</sup>H NMR analysis,

before concentrating the solution *in vacuo*. The residue was dissolved in CDCl<sub>3</sub> and a sample was analysed by <sup>1</sup>H NMR spectroscopy.

**Table 19:** Following the above procedure, data are reported as (a) base; (b) amount of base; (c) <sup>1</sup>H NMR yield of **2**.

**Entry 1:** (a) KO<sup>t</sup>-Bu; (b) 185 mg, 1.65 mmol, 1 eq; (c) 0%.

**Entry 2:** (a) NaH; (b) 40 mg, 1.65 mmol, 1 eq; (c) 10%.

**Entry 3:** (a) DBU; (b) 0.25 ml, 1.65 mmol, 1 eq; (c) 31%.

**Entry 4:** (a) DIPEA; (b) 0.29 ml, 1.65 mmol, 1 eq; (c) 44%.

**Entry 5:** (a) pyridine; (b) 0.13 ml, 1.65 mmol, 1 eq; (c) 80%.

**Entry 6:** (a) none; (b) - ; (c) 83%.

**Entry 7:** (a) DBU; (b) 11 μl, 0.075 mmol, 5 mol%; (c) 69%.

**Entry 8:** (a) DIPEA; (b) 13 μl, 0.075 mmol, 5 mol%; (c) 66%.

**Entry 9:** (a) pyridine; (b) 6 μl, 0.075 mmol, 5 mol%; (c) 85%.

**Entry 10:** (a) none; (b) - ; (c) 89%.

#### *The use of Radical Scavengers*

#### **Scheme 27, Table 16**

To a flame-dried flask under argon was added dibenzylamine **14** (0.29 ml, 1.5 mmol, 1 eq) and THF (1.9 ml, 0.8 M). To this was added the radical scavenger (0.1 mmol, 0.1 eq) and the solution was cooled to 0 °C in an ice bath. DIAD **53** (0.33 ml, 1.65 mmol, 1.1 eq) was added dropwise to this solution and the now orange reaction mixture was left to stir at this temperature for 10 min before warming to rt and stirred

for 18 h. After this time, the reaction was quenched with HCl (1 M, 2 ml) and THF (2 ml) and heated to 45 °C for 2 h. The biphasic mixture was then cooled to rt, separated and the aqueous acidic layer was extracted with DCM (2 x 10 ml). The organic extractions were combined, dried with anhydrous Na<sub>2</sub>SO<sub>4</sub>, and filtered. Triphenylmethane (366 mg, 1.5 mmol, 1 eq) was added to the yellow solution, to be used as an internal standard for <sup>1</sup>H NMR analysis, before concentrating the solution *in vacuo*. The residue was dissolved in CDCl<sub>3</sub> and a sample was analysed by <sup>1</sup>H NMR spectroscopy.

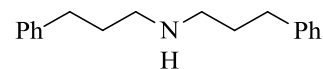
**Table 16:** Following the above procedure, data are recorded as (a) additive; (b) amount of additive; (c) <sup>1</sup>H NMR yield of **2**.

**Entry 1:** (a) TEMPO; (b) 16 mg, 0.1 mmol, 0.1 eq; (c) 77%.

**Entry 2:** (a) galvinoxyl; (b) 42 mg, 0.1 mmol, 0.1 eq; 77%.

### 5.3.2 Expanding the reaction scope

Preparation of bis(3-phenylpropyl)amine **64**<sup>34</sup>



#### Scheme 28

A flame-dried flask under an atmosphere of nitrogen was charged with 3-phenylpropan-1-amine **66** (13.1 ml, 92.5 mmol, 1 eq) and a mixture of THF/methanol (308 ml: 15 ml). The solution was cooled in an ice bath and 3-phenylpropanal **67** (12.2 ml, 92.5 mmol, 1 eq) was added dropwise, followed by the portionwise addition of sodium borohydride (3.8 g, 101.75 mmol, 1.1 eq). The reaction mixture was stirred at 0 °C for 10 minutes after which time the ice bath was removed and the reaction was left to stir at rt for a further 18 h. Saturated Na<sub>2</sub>CO<sub>3</sub> solution (300 ml) was slowly added to quench the reaction, followed by DCM (200 ml). The biphasic mixture was shaken and the layers were separated. The aqueous portion was extracted a further 3 times with DCM (200 ml) and the combined organic extracts were dried over Na<sub>2</sub>SO<sub>4</sub>, filtered, and concentrated *in vacuo* to

afford the crude amine **64**, which also contained a large amount of undesired tertiary amine. Purification of the crude mixture by silica gel chromatography, eluting with 40 – 80% EtOAc in hexanes provided 3.04 g (13% yield) of the desired amine **64**.

$^1\text{H}$  NMR (400 MHz,  $\text{CDCl}_3$ ):  $\delta$  1.88 – 1.99 (m, 4H, 2 x  $\text{CH}_2$ ), 2.61 – 2.72 (m, 8H, 4 x  $\text{CH}_2$ ), 7.16 – 7.21 (m, 5H, 5 x ArH), 7.26 – 7.31 (m, 5H, 5 x ArH).

$^{13}\text{C}$  NMR (100 MHz,  $\text{CDCl}_3$ ):  $\delta$  32.2, 34.2, 49.9, 126.3, 128.8, 128.9, 142.6.

FTIR ( $\text{cm}^{-1}$ , neat): 695, 1032, 1453, 1602, 2923, 3680.

### *Reactivity of Alternative Amines*

#### **Scheme 29, Table 17**

Following *General Procedure A*, data are reported as (a) amine; (b) solvent; (c) dialkyl azodicarboxylate reagent; (d) aldehyde product; (e)  $^1\text{H}$  NMR yield.

**Entry 1:** (a) benzylamine **1**, 0.16 ml, 1.5 mmol, 1 eq; (b) THF, 1.9 ml, 0.8 M; (c) DIAD **53**, 0.33 ml, 1.65 mmol, 1.1 eq; (d) benzaldehyde **2**; (e) 3%.

**Entry 2:** (a) dibenzylamine **14**, 0.29 ml, 1.5 mmol, 1 eq; (b) THF, 1.9 ml, 0.8 M; (c) DIAD **53**, 0.33 ml, 1.65 mmol, 1.1 eq; (d) benzaldehyde **2**; (e) 81%.

**Entry 3:** (a) tribenzylamine **62**, 431 mg, 1.5 mmol, 1 eq; (b) THF, 1.9 ml, 0.8 M; (c) DIAD **53**, 0.33 ml, 1.65 mmol, 1.1 eq; (d) benzaldehyde **2**; (e) 0%.

**Entry 4:** (a) bis(3-phenylpropyl)amine **64**, 418 mg, 1.5 mmol, 1 eq; (b) THF, 1.9 ml, 0.8 M; (c) DIAD **53**, 0.33 ml, 1.65 mmol, 1.1 eq; (d) 3-phenylpropanal **122**; (e) 15%.

$^1\text{H}$  NMR signals used to determine the  $^1\text{H}$  NMR yield of 3-phenylpropanal **122** (400 MHz,  $\text{CDCl}_3$ ):  $\delta$  5.71 (s, 1H,  $\text{Ph}_3\text{CH}$ ), 9.84 (s, 1H,  $\text{C}(\text{O})\text{H}$ ).

**Entry 5:** (a) *N,N*-dimethyl-1-phenylmethanamine **65**, 0.23 ml, 1.5 mmol, 1 eq; (b) THF, 1.9 ml, 0.8 M; (c) DIAD **53**, 0.33 ml, 1.65 mmol, 1.1 eq; (d) benzaldehyde **2**; (e) 21%.

*Reactivity of Alternative Amines with an External Base*

**Scheme 30, Table 18**

To a flame-dried flask under argon was added the amine (1.5 mmol, 1 eq) and THF (1.9 ml, 0.8 M). To this was added pyridine (0.13 ml, 1.65 mmol, 1.1 eq) and the solution was cooled to 0 °C in an ice bath. DIAD **53** (0.33 ml, 1.65 mmol, 1.1 eq) was added dropwise to this solution and the now orange reaction mixture was left to stir at this temperature for 10 min before being warmed to rt and stirred for 18 h. After this time, the reaction was quenched with HCl (1 M, 2 ml) and THF (2 ml) and heated to 45 °C for 2 h. The biphasic mixture was then cooled to rt, separated and the aqueous acidic layer was extracted with DCM (2 x 10 ml). The organic extractions were combined, dried with anhydrous Na<sub>2</sub>SO<sub>4</sub>, and filtered. Triphenylmethane (366 mg, 1.5 mmol, 1 eq) was added to the yellow solution, to be used as an internal standard for <sup>1</sup>H NMR analysis, before concentrating the solution *in vacuo*. The residue was dissolved in CDCl<sub>3</sub> and a sample was analysed by <sup>1</sup>H NMR spectroscopy.

**Table 18:** Following the above procedure, data are reported as (a) amine; (b) amount of amine; (c) aldehyde product; (d) <sup>1</sup>H NMR yield of aldehyde.

**Entry 1:** (a) benzylamine **1**; (b) 0.16 ml; (c) **2**; (d) 3%.

**Entry 2:** (a) dibenzylamine **14**; (b) 0.29 ml; (c) **2**; (d) 80%.

**Entry 3:** (a) tribenzylamine **62**; (b) 431 mg; (c) **2**; (d) Trace.

**Entry 4:** (a) bis(3-phenylpropyl)amine **64**; (b) 418 mg; (c) **122**; (d) 19%.

$^1\text{H}$  NMR signals used to determine the  $^1\text{H}$  NMR yield of 3-phenylpropanal **122** (400 MHz,  $\text{CDCl}_3$ ):  $\delta$  5.71 (s, 1H,  $\text{Ph}_3\text{CH}$ ), 9.84 (s, 1H,  $\text{C(O)H}$ ).

*Studies to Enhance the Reactivity with Bis(3-phenylpropyl)amine 64*

**Scheme 31, Table 19**

To a flame-dried flask under argon was added bis(3-phenylpropyl)amine **64** (418 mg, 1.5 mmol, 1 eq) which was dissolved in the specified solvent (1.9 ml, 0.8 M) and the solution was cooled to 0 °C in an ice bath. DIAD **53** (0.33 ml, 1.65 mmol, 1.1 eq) was added dropwise to this solution and the now orange reaction mixture was left to stir at this temperature for 10 min before being warmed to the specified temperature and stirred for 18 h. After this time, the reaction was quenched with HCl (1 M, 2 ml) and THF (2 ml) and heated to 45 °C for 2 h. The biphasic mixture was then cooled to rt, separated, and the aqueous acidic layer was extracted with DCM (2 x 10 ml). The organic extractions were combined, dried with anhydrous  $\text{Na}_2\text{SO}_4$ , and filtered. Triphenylmethane (366 mg, 1.5 mmol, 1 eq) was added to the yellow solution, to be used as an internal standard for  $^1\text{H}$  NMR analysis, before concentrating the solution *in vacuo*. The residue was dissolved in  $\text{CDCl}_3$  and a sample was analysed by  $^1\text{H}$  NMR spectroscopy.

**Table 19:** Following the above procedure, data are reported as (a) solvent; (b) reaction temperature; (c)  $^1\text{H}$  NMR yield of **67**.

$^1\text{H}$  NMR signals used to determine the  $^1\text{H}$  NMR yield (400 MHz,  $\text{CDCl}_3$ ):  $\delta$  5.71 (s, 1H,  $\text{Ph}_3\text{CH}$ ), 9.84 (s, 1H,  $\text{C(O)H}$ ).

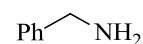
**Table 23, Entry 1:** (a) THF; (b) 70 °C; (c) 11%.

**Table 23, Entry 2:** (a) 1,4-Dioxane; (b) rt; (c) 18%.

**Table 23, Entry 3:** (a) 1,4-Dioxane; (b) 70 °C; (c) 13%.

## 5.4 Development of a mild and selective *N*-debenzylation process

Preparation of benzylamine **1**<sup>35</sup>



### Scheme 32

A flame-dried flask under argon was charged with dibenzylamine **14** (0.29 ml, 1.5 mmol, 1 eq) and THF (1.9 ml, 0.8 M). The solution was then cooled to 0 °C in an ice bath. DIAD **53** (0.33 ml, 1.65 mmol, 1.1 eq) was added dropwise to this solution and the now orange reaction mixture was left to stir at this temperature for 10 min before warming to rt and stirring for 18 h. After this time, the reaction was quenched with 1 M HCl (5 ml) and THF (5 ml) then heated to 40 °C for 2 h. The biphasic mixture was subsequently cooled to rt, separated, and the aqueous acidic layer was extracted with DCM (2 x 10 ml). The organic extractions were combined, dried with anhydrous Na<sub>2</sub>SO<sub>4</sub>, and filtered. Triphenylmethane (366 mg, 1.5 mmol, 1 eq) was added to the yellow solution, to be used as an internal standard for <sup>1</sup>H NMR analysis, before concentrating the solution *in vacuo*. The residue was dissolved in CDCl<sub>3</sub> and a sample was analysed by <sup>1</sup>H NMR spectroscopy to reveal 79% of benzaldehyde product. The remaining acidic layer was partitioned with DCM and 2 M NaOH was added until pH 10 was reached. The layers were shaken and separated and the now basic aqueous layer was extracted with DCM (x 3). The combined organics were dried over Na<sub>2</sub>SO<sub>4</sub>, filtered, and concentrated *in vacuo* to afford the deprotected benzylamine **1** (130 mg, 82% yield) as a colourless oil.

<sup>1</sup>H NMR signals used to determine the <sup>1</sup>H NMR yield of benzaldehyde **2** (400 MHz, CDCl<sub>3</sub>): δ 5.71 (s, 1H, Ph<sub>3</sub>CH), 10.12 (s, 1H, PhC(O)H).

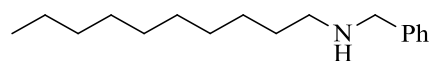
<sup>1</sup>H NMR (400 MHz, CDCl<sub>3</sub>): δ 1.68 (bs, 2H, NH<sub>2</sub>), 3.85 (s, 2H, CH<sub>2</sub>), 7.17 – 7.36 (m, 5H, 5 x ArH).

<sup>13</sup>C NMR (100 MHz, CDCl<sub>3</sub>): δ 48.9, 123.4, 127.1, 129.2, 144.5.

FTIR (neat): 817, 1611, 3310, 3398 cm<sup>-1</sup>.

### 5.4.1 Synthesis of secondary amines

Preparation of *N*-benzyldecan-1-amine **6**<sup>36</sup>



#### Scheme 33

Following *General Procedure C*, data are reported as (a) amine derivative; (b) carbonyl derivative; (c) amine product; (d) yield.

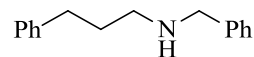
(a) benzylamine **1**, 1.09 ml, 10 mmol, 1 eq; (b) decanal **69**, 2.07 ml, 11 mmol, 1.1 eq; (c) *N*-benzyldecan-1-amine **68**; (d) 0.53 g, 22%.

<sup>1</sup>H NMR (400 MHz, CDCl<sub>3</sub>): δ 0.84 -0.95 (m, 3H, CH<sub>3</sub>), 1.21 – 1.49 (m, 16H, 16 x CH), 2.45 (t, 2H, *J* = 6.8 Hz, CH<sub>2</sub>), 3.91 (s, 2H, CH<sub>2</sub>), 7.13 – 7.18 (m, 3H, 3 x ArH), 7.23 (d, 2H, *J* = 9.8 Hz, 2 x ArH).

<sup>13</sup>C NMR (100 MHz, CDCl<sub>3</sub>): δ 14.4, 24.7, 29.3, 31.0, 31.1, 32.7, 33.8, 50.9, 55.8, 127.2, 130.5, 130.9, 138.6.

FTIR: 1016, 1606, 2895, 3370 cm<sup>-1</sup>.

Preparation of *N*-benzyl-3-phenylpropan-1-amine **70**<sup>37</sup>



#### Scheme 34

Following *General Procedure C*, data are reported as (a) amine derivative; (b) carbonyl derivative; (c) amine product; (d) yield.

(a) benzylamine **1**, 1.09 ml, 10 mmol, 1 eq; (b) 3-phenylpropanal **67**, 1.32 ml, 11 mmol, 1.1 eq; (c) *N*-benzyl-3-phenylpropan-1-amine **70**; (d) 1.01 g, 45%.

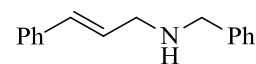
<sup>1</sup>H NMR (400 MHz, CDCl<sub>3</sub>): δ 1.84 (s, 1H, NH), 1.97 – 2.02 (m, 2H, CH<sub>2</sub>), 2.81 – 2.84 (m, 4H, 2 x CH<sub>2</sub>), 3.93 (s, 2H, CH<sub>2</sub>), 7.36 – 7.49 (m, 10H, 10 x ArH).

<sup>13</sup>C NMR (100 MHz, CDCl<sub>3</sub>): δ 31.4, 33.3, 48.5, 53.7, 125.5, 126.6, 127.8, 128.02, 128.06, 128.09, 140.2, 141.9.



FTIR (neat): 1028, 1119, 1452, 2812, 2857, 2928, 3024  $\text{cm}^{-1}$ .

Preparation of (*E*)-*N*-benzyl-3-phenylprop-2-en-1-amine **72**<sup>38,39</sup>



### Scheme 35

Following *General Procedure C*, data are reported as (a) amine derivative; (b) carbonyl derivative; (c) amine product; (d) yield.

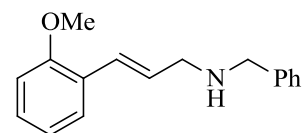
(a) benzylamine **1**, 1.09 ml, 10 mmol, 1 eq; (b) cinnamaldehyde **71**, 1.38 ml, 11 mmol, 1.1 eq; (c) (*E*)-*N*-benzyl-3-phenylprop-2-en-1-amine **72**; (d) 0.64 g, 29%.

<sup>1</sup>H NMR (400 MHz, CDCl<sub>3</sub>):  $\delta$  1.55 (s, 1H, NH), 3.46 (dd, 2H,  $J = 6.3$  Hz,  $^4J = 1.4$  Hz, CH<sub>2</sub>), 3.87 (s, 2H, CH<sub>2</sub>), 6.35 (dt, 1H,  $J = 6.3, 15.9$  Hz, C=CH), 6.57 (d, 1H,  $J = 15.9$  Hz, C=CH), 7.22 – 7.30 (m, 10H, 10 x ArH).

<sup>13</sup>C NMR (100 MHz, CDCl<sub>3</sub>):  $\delta$  51.0, 53.4, 126.6, 127.1, 127.5, 128.1, 128.2, 128.4, 128.5, 131.7, 137.2, 140.0.

FTIR (neat): 2816, 2915, 3025, 3061, 3080, 3311  $\text{cm}^{-1}$ .

Preparation of (*E*)-*N*-benzyl-3-(2-methoxyphenyl)prop-2-en-1-amine **73**<sup>39,40</sup>



### Scheme 36

Following *General Procedure C*, data are reported as (a) amine derivative; (b) carbonyl derivative; (c) amine product; (d) yield.

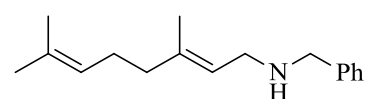
(a) benzylamine **1**, 1.09 ml, 10 mmol, 1 eq; (b) (*E*)-3-(2-methoxyphenyl)acrylaldehyde **74**, 1.62 g, 10 mmol, 1 eq; (c) (*E*)-*N*-benzyl-3-(2-methoxyphenyl)prop-2-en-1-amine **73**; (d) 1.04 g, 41%.

$^1\text{H}$  NMR (400 MHz,  $\text{CDCl}_3$ ):  $\delta$  1.96 (s, 1H, NH), 3.54 (d, 2H,  $J = 6.4$  Hz,  $\text{CH}_2$ ), 3.89 (s, 3H,  $\text{OCH}_3$ ), 3.92 (s, 2H,  $\text{CH}_2$ ), 6.39 – 6.47 (m, 1H,  $\text{C}=\text{CH}$ ), 6.92 – 6.99 (m, 2H,  $\text{C}=\text{CH} + \text{ArH}$ ), 7.01 – 7.03 (m, 2H, 2 x  $\text{ArH}$ ), 7.27 – 7.36 (m, 5H, 5 x  $\text{ArH}$ ), 7.52 – 7.59 (m, 1H,  $\text{ArH}$ ).

$^{13}\text{C}$  NMR (100 MHz,  $\text{CDCl}_3$ ):  $\delta$  51.3, 52.9, 55.0, 110.4, 120.3, 125.8, 125.9, 126.4, 126.5, 127.9, 128.0, 128.6, 128.8, 139.9, 156.2.

FTIR (neat): 1026, 1240, 1487, 2883, 2933, 3026  $\text{cm}^{-1}$ .

Preparation of (*E*)-*N*-benzyl-3,7-dimethylocta-2,6-dien-1-amine **75**<sup>41</sup>



### Scheme 37

Following *General Procedure C*, data are reported as (a) amine derivative; (b) carbonyl derivative; (c) amine product; (d) yield.

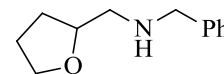
(a) benzylamine **1**, 1.09 ml, 10 mmol, 1 eq; (b) citral **76**, 1.71 ml, 10 mmol, 1 eq; (c) (*E*)-*N*-benzyl-3,7-dimethylocta-2,6-dien-1-amine **75**; (d) 1.19 g, 49%.

$^1\text{H}$  NMR (400 MHz,  $\text{CDCl}_3$ ):  $\delta$  1.62 – 1.76 (m, 9H, aliphatic  $\text{CH}_2 + \text{CH}_3$ ), 2.03 – 2.14 (m, 4H, aliphatic  $\text{CH}_2 + \text{CH}_3$ ), 3.25 – 3.29 (m, 2H,  $\text{CH}_2$ ), 3.81 (s, 2H,  $\text{CH}_2$ ), 5.11 – 5.14 (m, 1H,  $\text{C}=\text{CH}$ ), 5.31 – 5.35 (m, 1H,  $\text{C}=\text{CH}$ ), 7.26 – 7.38 (m, 5H, 5 x  $\text{ArH}$ ).

$^{13}\text{C}$  NMR (100 MHz,  $\text{CDCl}_3$ ):  $\delta$  15.8, 17.1, 25.2, 26.1, 39.3, 46.0, 52.9, 122.2, 123.6, 126.4, 127.6, 127.9, 131.1, 137.5, 139.9.

FTIR (neat): 1028, 1105, 1452, 2854, 2914, 3026, 3300  $\text{cm}^{-1}$ .

Preparation of *N*-benzyl-1-(tetrahydrofuran-2-yl)methanamine  
**77**<sup>42,43</sup>



### Scheme 38

Following *General Procedure C*, data are reported as (a) amine derivative; (b) carbonyl derivative; (c) amine product; (d) yield.

(a) (tetrahydrofuran-2-yl)methanamine **78**, 1.13 ml, 10 mmol, 1 eq; (b) benzaldehyde **2**, 1.02 ml, 10 mmol, 1 eq; (c) (tetrahydrofuran-2-yl)methanamine **77**; (d) 1.66 g, 87%.

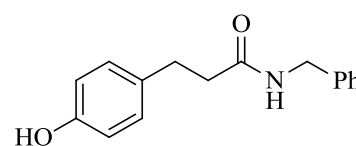
<sup>1</sup>H NMR (400 MHz, CDCl<sub>3</sub>): δ 1.50 – 1.56 (m, 1H, CH), 1.75 – 2.02 (m, 4H, 2 x CH<sub>2</sub>), 2.62 – 2.73 (m, 2H, CH<sub>2</sub>), 3.21 (s, 1H, NH), 3.67 – 3.84 (m, 2H, CH<sub>2</sub>), 4.01 – 4.12 (m, 2H, 2 x CH), 7.21 – 7.38 (m, 5H, 5 x ArH).

<sup>13</sup>C NMR (100 MHz, CDCl<sub>3</sub>): δ 25.8, 29.3, 53.4, 53.7, 67.9, 78.1, 127.0, 128.3, 128.9, 139.8.

FTIR (neat): 1030, 1109, 1489, 2532, 2862, 2930, 3258 cm<sup>-1</sup>.

### 4.4.2 Amides prepared *via* amide formation and reduction

Preparation of *N*-benzyl-3-(4-hydroxyphenyl)propanamide **79**<sup>31</sup>



### Scheme 39

A flame-dried round-bottom flask, equipped with a condenser, was charged with 3-(4-hydroxyphenyl)propanoic acid **80** (2.00 g, 12 mmol, 1 eq). The acid was diluted with dry toluene (40 ml, 0.3 M) and dry DMF (0.19 ml, 2.4 mmol, 20 mol%). The solution was cooled to 0 °C and thionyl chloride (1.53 ml, 13.2 mmol, 1.1 eq) was added dropwise *via* syringe. Upon completion of the addition, the reaction mixture was heated to 70 °C for 2 h then cooled to 0 °C. The reaction mixture was diluted

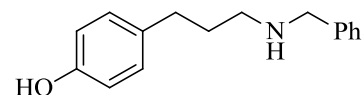
with DCM (60 ml, 0.2 M) and benzylamine **1** (1.44 ml, 13.2 mmol, 1.1 eq) was added followed by triethylamine (3.68 ml, 26.4 mmol, 2.2 eq). The reaction was slowly warmed to rt and stirred for 16 h. After this time, it was quenched by the slow addition of saturated aqueous Na<sub>2</sub>CO<sub>3</sub> solution until pH 10 – 11 was reached. The biphasic mixture was diluted with DCM, shaken, and the layer separated. The aqueous layers was extracted with DCM (x 2) and the combined organic extracts were dried over Na<sub>2</sub>SO<sub>4</sub>, filtered, and concentrated *in vacuo* to afford *N*-benzyl-3-(4-hydroxyphenyl)propanamide **79**, 2.94 g, 96% yield.

<sup>1</sup>H NMR (400 MHz, CDCl<sub>3</sub>): δ 2.47 – 2.51 (m, 2H, CH<sub>2</sub>), 2.85 – 3.01 (m, 2H, CH<sub>2</sub>), 4.39 (d, 2H, *J* = 5.6 Hz, CH<sub>2</sub>), 5.83 – 5.91 (m, 1H, NH), 6.47 – 6.76 (m, 1H, ArH), 6.82 – 6.89 (m, 1H, ArH), 6.95 – 6.97 (m, 1H, ArH), 7.01 – 7.03 (m, 1H, ArH), 7.13 – 7.33 (m, 5H, 5 x ArH).

<sup>13</sup>C NMR (100 MHz, CDCl<sub>3</sub>): δ 30.4, 37.9, 43.1, 115.0, 121.1, 127.0, 127.3, 128.5, 128.9, 131.1, 131.6, 137.4, 137.7, 148.6, 154.2, 172.1.

FTIR (neat): 1635, 3150, 3340 cm<sup>-1</sup>.

*Preparation of 4-(3-(benzylamino)propyl)phenol 81*<sup>32</sup>



#### Scheme 40

A flame-dried three-neck flask, purged with argon and equipped with a reflux condenser, was charged with dry THF (46 ml, 0.25 M) and cooled to 0 °C. LiAlH<sub>4</sub> (2.18 g, 57.5 mmol, 5 eq) was added, portionwise. *N*-Benzyl-3-(4-hydroxyphenyl)propanamide **79** (2.94 g, 11.5 mmol, 1 eq) was dissolved in THF (23 ml, 0.5 M) and the solution was added, dropwise, to the suspension of LiAlH<sub>4</sub> in THF. The reaction mixture was warmed to rt then slowly heated to reflux and stirred for 16 h. After this time, the reaction mixture was cooled to 0 °C and water (32 ml) was added extremely slowly. CAUTION! This process results in vigorous H<sub>2</sub> evolution. The mixture was then acidified with 4 M HCl until pH 8 was reached. The organic layer was separated and the aqueous phase was extracted with EtOAc (3 x 30

ml). The organics were dried over Na<sub>2</sub>SO<sub>4</sub>, filtered, and concentrated *in vacuo* to afford the crude amine. The residue was dissolved in EtOAc (50 ml) and washed with citric acid (0.08 M, 3 x 50 ml). The combined acidic washings were subsequently extracted once with EtOAc (60 ml) before being added to DCM (80 ml). The aqueous layer was basified by the slow addition of saturated aqueous NaOH until pH 10-11 was reached. The biphasic mixture was then shaken and separated before extracting the now basic layer with DCM (3 x 150 ml). The combined DCM layers were dried with anhydrous Na<sub>2</sub>SO<sub>4</sub>, filtered, and concentrated *in vacuo* to afford the 4-(3-(benzylamino)propyl)phenol **81** as a dark yellow oil, 1.75 g, 63% yield.

<sup>1</sup>H NMR (400 MHz, CDCl<sub>3</sub>): δ 1.84 (t, 2H, *J* = 7.5 Hz, CH<sub>2</sub>), 2.56 (t, 2H, *J* = 7.5 Hz, CH<sub>2</sub>), 2.69 (t, 2H, *J* = 7.5 Hz, CH<sub>2</sub>), 3.80 (s, 2H, CH<sub>2</sub>), 4.28 (s, 1H, NH), 6.63 (d, 2H, *J* = 8.0 Hz, 2 x ArH), 6.95 (d, 2H, *J* = 7.5 Hz, 2 x ArH), 7.26 – 7.36 (m, 5H, 5 x ArH).

<sup>13</sup>C NMR (100 MHz, CDCl<sub>3</sub>): δ 31.2, 32.6, 48.5, 53.8, 115.5, 127.3, 128.4, 128.6, 129.3, 132.8, 139.3, 154.7.

FTIR (neat): 3300 cm<sup>-1</sup>.

*Preparation of N-benzyl-2-(4-chlorophenyl)acetamide 84 and N-benzyl-2-(4-methoxyphenyl)acetamide 85*

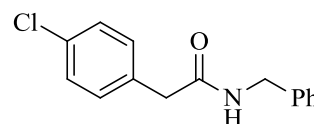
#### **Scheme 41, Table 20**

To a flame-dried round-bottom flask equipped with a septum and under argon was added benzylamine **1** (2.73 ml, 25 mmol, 1 eq). This was dissolved with DCM (43 ml, 0.58 M) and cooled to 0 °C. Triethylamine (3.66 ml, 26.25 mmol, 1.05 eq) was added followed by the dropwise addition of the acid chloride (26.25 mmol, 1.05 eq). The reaction mixture was warmed to rt and stirred for 16 h. After this time, the reaction mixture was quenched with saturated aqueous Na<sub>2</sub>CO<sub>3</sub> solution until pH 10 – 11 was reached and then diluted with DCM. The biphasic mixture was shaken and

separated then the aqueous layer was extracted with DCM (x 2). The organics were dried over Na<sub>2</sub>SO<sub>4</sub>, filtered, and concentrated *in vacuo* to afford the secondary amide.

**Table 20:** Following the above procedure, data are reported as (a) acid chloride; (b) amide; (c) yield.

*Preparation of N-benzyl-2-(4-chlorophenyl)acetamide*  
**84**<sup>43</sup>



### Entry 1

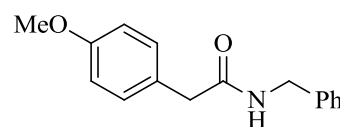
(a) 2-(4-chlorophenyl)acetyl chloride **82**, 3.84 ml, 26.25 mmol, 1.05 eq; (b) *N*-benzyl-2-(4-chlorophenyl)acetamide **84**; (c) 2.62 g, 40%.

<sup>1</sup>H NMR (400 MHz, CDCl<sub>3</sub>): δ 3.61 (s, 2H, CH<sub>2</sub>), 4.44 (d, 2H, CH<sub>2</sub>), 5.66 (s, 1H, NH), 7.21 – 7.25 (m, 4H, 4 x ArH), 7.29 – 7.34 (m, 5H, 5 x ArH).

<sup>13</sup>C NMR (100 MHz, CDCl<sub>3</sub>): δ 43.1, 43.8, 127.69, 127.74, 128.9, 129.3, 130.9, 133.3, 133.4, 138.1, 170.4.

FTIR (neat): 690, 1608, 2833, 2932, 2999, 3306 cm<sup>-1</sup>.

*Preparation of N-benzyl-2-(4-methoxyphenyl)acetamide*  
**85**<sup>43</sup>



### Entry 2

(a) 2-(4-methoxyphenyl)acetyl chloride **83**, 4.01 ml, 26.25 mmol, 1.05 eq; (b) *N*-benzyl-2-(4-methoxyphenyl)acetamide **85**; (c) 1.62 g, 26%.

<sup>1</sup>H NMR (400 MHz, CDCl<sub>3</sub>): δ 3.60 (s, 2H, CH<sub>2</sub>), 3.82 (s, 3H, OCH<sub>3</sub>), 4.43 (d, 2H, *J* = 5.6 Hz, CH<sub>2</sub>), 5.72 (s, 1H, NH), 6.90 (d, 2H, *J* = 8.8 Hz, 2 x ArH), 7.19 – 7.22 (m, 3H, 3 x ArH), 7.25 – 7.34 (m, 4H, 4 x ArH).

$^{13}\text{C}$  NMR (100 MHz,  $\text{CDCl}_3$ ):  $\delta$  42.4, 43.1, 54.8, 114.0, 126.2, 126.9, 127.0, 128.2, 130.1, 137.7, 158.4, 170.8.

FTIR (neat): 1633, 2837, 2968, 3032, 3063, 3289  $\text{cm}^{-1}$ .

*Preparation of N-benzyl-2-(4-chlorophenyl)ethanamine 86 and N-benzyl-2-(4-methoxyphenyl)ethanamine 87*

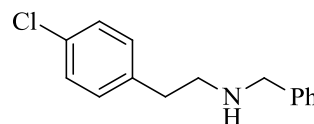
#### **Scheme 42, Table 21**

A flame-dried three-neck flask was purged with argon and equipped with a reflux condenser before being charged with dry THF (0.25 M) and cooled to 0 °C.  $\text{LiAlH}_4$  (5 eq) was added, portionwise. The amide (1 eq) was dissolved in THF (0.5 M) and the solution was added, dropwise, to the suspension of  $\text{LiAlH}_4$  in THF. The reaction mixture was warmed to rt then slowly heated to reflux and stirred for 16 h. After this time, the reaction mixture was cooled to 0 °C and water (40 ml) was added extremely slowly. CAUTION! This process results in vigorous  $\text{H}_2$  evolution. The mixture was then acidified with 4M HCl until pH 8 was reached. The organic layer was separated and the aqueous phase was extracted with EtOAc (3 x 30 ml). The organics were dried over  $\text{Na}_2\text{SO}_4$ , filtered, and concentrated *in vacuo* to afford the crude amine. The residue was dissolved in EtOAc (40 ml) and washed with citric acid (0.08 M, 3 x 40 ml). The combined acidic washings were subsequently extracted once with EtOAc (50 ml) before being added to DCM (70 ml). The aqueous layer was basified by the slow addition of saturated aqueous NaOH until pH 10-11 was reached. The biphasic mixture was then shaken and separated before extracting the now basic layer with DCM (3 x 150 ml). The combined DCM layers were dried with anhydrous  $\text{Na}_2\text{SO}_4$ , filtered, and concentrated *in vacuo* to afford the amine.

**Table 21:** Following the above procedure, data are reported as (a) volume of THF; (b) amount of  $\text{LiAlH}_4$ ; (c) amide, amount of amide; (d) volume of THF; (e) amine; (f) yield.

Preparation of *N*-benzyl-2-(4-chlorophenyl)ethanamine

**86**<sup>44,45</sup>



**Entry 1**

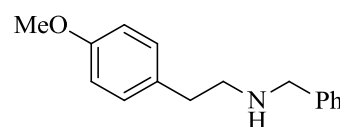
(a) 40 ml, 0.25 M; (b) 1.90 g, 50 mmol, 5 eq; (c) *N*-benzyl-2-(4-chlorophenyl)acetamide **84**, 2.61 g, 10 mmol, 1 eq; (d) 20 ml, 0.5 M; (e) *N*-benzyl-2-(4-chlorophenyl)ethanamine **86**; (f) 0.44 g, 18%.

<sup>1</sup>H NMR (400 MHz, CDCl<sub>3</sub>): δ 2.79 – 2.85 (m, 2H, CH<sub>2</sub>), 2.87 – 2.92 (m, 2H, CH<sub>2</sub>), 3.79 (s, 2H, CH<sub>2</sub>), 7.13 (d, 2H, *J* = 8.4 Hz, 2 x ArH), 7.21 – 7.36 (m, 7H, 7 x ArH).

<sup>13</sup>C NMR (100 MHz, CDCl<sub>3</sub>): δ 35.2, 49.9, 55.3, 113.9, 127.1, 128.3, 128.5, 128.6, 130.1, 132.0, 138.4, 139.9.

FTIR (neat): 665, 1244, 1510, 2833, 2932, 2999, 3306 cm<sup>-1</sup>.

Preparation of *N*-benzyl-2-(4-methoxyphenyl)ethanamine **87**<sup>44,45</sup>



**Entry 2**

(a) 26 ml, 0.25 M; (b) 1.20 g, 31.5 mmol, 5 eq; (c) *N*-benzyl-2-(4-methoxyphenyl)acetamide **85**, 1.60 g, 6.3 mmol, 1 eq; (d) 13 ml, 0.5 M; (e) *N*-benzyl-2-(4-methoxyphenyl)ethanamine **87**; (f) 0.55 g, 37%.

<sup>1</sup>H NMR (400 MHz, CDCl<sub>3</sub>): δ 2.80 (t, 2H, *J* = 6.8 Hz, CH<sub>2</sub>), 2.88 – 2.92 (t, 2H, *J* = 6.8 Hz, CH<sub>2</sub>), 3.81 (s, 3H, OCH<sub>3</sub>), 3.83 (s, 2H, CH<sub>2</sub>), 6.86 (d, 2H, *J* = 8.7 Hz, ArH), 7.15 (d, 2H, *J* = 8.6 Hz, 2 x ArH), 7.26 – 7.34 (m, 5H, 5 x ArH).

<sup>13</sup>C NMR (100 MHz, CDCl<sub>3</sub>): δ 34.7, 50.0, 53.2, 54.8, 113.4, 126.9, 127.7, 128.1, 129.2, 131.5, 139.2, 157.6.

FTIR (neat): 1031, 1510, 2833, 2931, 3028, 3061, 3310 cm<sup>-1</sup>.



### 5.4.3 DIAD-Mediated *N*-benzyl deprotections

*Preparation of primary amines*

#### Scheme 43, Table 22

Following *General Procedure B*, data are reported as (a) amine; (b) solvent; (c) dialkyl azodicarboxylate reagent; (d) amine product; (e) yield.

*Preparation of decan-1-amine 88*<sup>46</sup>

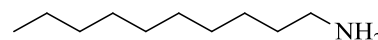


#### Table 22, Entry 1

(a) *N*-benzyl-3-phenylpropan-1-amine **68**, 371 mg, 1.5 mmol, 1 eq; (b) THF, 1.9 ml, 0.8 M; (c) DIAD, 0.33 ml, 1.65 mmol, 1.1 eq; (d) decan-1-amine **88**; (e) 56 mg, 20%.

<sup>1</sup>H NMR (400 MHz, CDCl<sub>3</sub>): δ 0.89 – 0.92 (m, 3H, CH<sub>3</sub>), 1.26 – 1.48 (m, 16H, aliphatic CH<sub>2</sub>), 1.92 – 2.72 (bs, 2H, NH<sub>2</sub>), 2.70 (t, 2H, *J* = 7.0 Hz, CH<sub>2</sub>).

<sup>13</sup>C NMR (100 MHz, CDCl<sub>3</sub>): δ 14.4, 23.1, 27.3, 27.4, 29.8, 29.9, 30.1, 32.4, 34.6, 42.7.

FTIR (neat): 1070, 1611, 3328, 3400 cm<sup>-1</sup>.

Preparation of 3-phenylpropan-1-amine **66**<sup>37</sup>

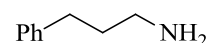


**Table 22, Entry 2**

(a) *N*-benzyl-3-phenylpropan-1-amine **70**, 338 mg, 1.5 mmol, 1 eq; (b) THF, 1.9 ml, 0.8 M; (c) DIAD, 0.33 ml, 1.65 mmol, 1.1 eq; (d) 3-phenylpropan-1-amine **66**; (e) 127 mg, 63%.

<sup>1</sup>H NMR (400 MHz, CDCl<sub>3</sub>): δ 1.82 – 1.89 (m, 2H, CH<sub>2</sub>), 2.65 (t, 2H, *J* = 7.6 Hz, CH<sub>2</sub>), 2.76 (t, 2H, *J* = 7.3 Hz, CH<sub>2</sub>), 4.17 (bs, 2H, NH<sub>2</sub>), 7.17 – 7.29 (m, 5H, 5 x ArH).

<sup>13</sup>C NMR (100 MHz, CDCl<sub>3</sub>): δ 32.6, 35.3, 40.1, 125.4, 127.7, 128.1, 141.0.

FTIR (neat): 696, 1452, 1643, 2928, 3026, 3337 cm<sup>-1</sup>.

Preparation of 4-(3-aminopropyl)phenol **89**<sup>47</sup>

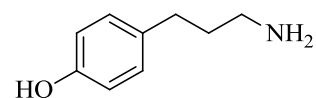


**Table 22, Entry 3**

(a) 4-(3-(benzylamino)propyl)phenol **81**, 362 mg, 1.5 mmol, 1 eq; (b) THF, 1.9 ml, 0.8 M; (c) DIAD, 0.33 ml, 1.65 mmol, 1.1 eq; (d) 4-(3-aminopropyl)phenol **89**; (e) 183 mg, 81%.

<sup>1</sup>H NMR (400 MHz, CDCl<sub>3</sub>): δ 1.25 – 1.34 (m, 2H, CH<sub>2</sub>), 2.50 – 2.73 (m, 4H, 2 x CH<sub>2</sub>), 3.88 (bs, 2H, NH<sub>2</sub>), 6.73 (d, 2H, *J* = 8.4 Hz, 2 x CH(Ar)), 6.95 (d, 2H, *J* = 8.4 Hz, 2 x CH(Ar)).

<sup>13</sup>C NMR (100 MHz, CDCl<sub>3</sub>): δ 22.1, 33.2, 65.0, 115.5, 127.3, 129.3, 139.2, 162.1.

FTIR (neat): 1030, 1339, 1645, 2679, 2860, 3059, 3281 cm<sup>-1</sup>.

Preparation of 2-(4'-chlorophenyl)ethanamine **90**<sup>48</sup>

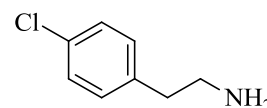


**Table 22, Entry 4**

(a) *N*-benzyl-2-(4-chlorophenyl)ethanamine **86**, 368 mg, 1.5 mmol, 1 eq; (b) THF, 1.9 ml, 0.8 M; (c) DIAD, 0.33 ml, 1.65 mmol, 1.1 eq; (d) 2-(4-chlorophenyl)ethanamine **90**; (e) 197 mg, 85%.

<sup>1</sup>H NMR (400 MHz, CDCl<sub>3</sub>): δ 1.95 (br s, 2H, NH<sub>2</sub>), 2.73 (t, 2H, *J* = 7.0 Hz, CH<sub>2</sub>), 2.96 (t, 2H, *J* = 6.8 Hz, CH<sub>2</sub>), 7.16 (d, 2H, *J* = 8.5 Hz, 2 x ArH), 7.27 (d, 2H, *J* = 8.5 Hz, 2 x ArH).

<sup>13</sup>C NMR (100 MHz, CDCl<sub>3</sub>): δ 39.1, 43.3, 114.0, 128.6, 130.2, 138.2.

FTIR (neat): 682, 1087, 1383, 1645, 2529, 2930, 3252 cm<sup>-1</sup>.

Preparation of 2-(4-methoxyphenyl)ethanamine **91**<sup>48</sup>

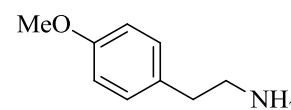


**Table 22, Entry 5**

(a) *N*-benzyl-2-(4-methoxyphenyl)ethanamine **87**, 362 mg, 1.5 mmol, 1 eq; (b) THF, 1.9 ml, 0.8 M; (c) DIAD, 0.33 ml, 1.65 mmol, 1.1 eq; (d) 2-(4-methoxyphenyl)ethanamine **91**; (e) 218 mg, 96%.

<sup>1</sup>H NMR (400 MHz, CDCl<sub>3</sub>): δ 1.78 (br s, 2H, NH<sub>2</sub>), 2.71 (t, 2H, *J* = 7.0 Hz, CH<sub>2</sub>), 2.95 (t, 2H, *J* = 6.8 Hz, CH<sub>2</sub>), 3.81 (s, 3H, OCH<sub>3</sub>), 6.87 (d, 2H, *J* = 8.8 Hz, 2 x ArH), 7.14 (d, 2H, *J* = 8.4 Hz, 2 x ArH).

<sup>13</sup>C NMR (100 MHz, CDCl<sub>3</sub>): δ 38.5, 43.1, 54.8, 113.4, 129.2, 131.3, 157.6.

FTIR (neat): 1030, 1323, 1510, 2594, 2860, 3030, 3254 cm<sup>-1</sup>.

Preparation of (tetrahydrofuran-2-yl)methanamine **78**<sup>49,50</sup>

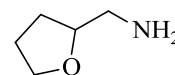


**Table 22, Entry 6**

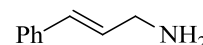
(a) *N*-benzyl-1-(tetrahydrofuran-2-yl)methanamine **77**, 287 mg, 1.5 mmol, 1 eq; (b) THF, 1.9 ml, 0.8 M; (c) DIAD, 0.33 ml, 1.65 mmol, 1.1 eq; (d) (tetrahydrofuran-2-yl)methanamine **78**; (e) 111 mg, 73%.

<sup>1</sup>H NMR (400 MHz, CDCl<sub>3</sub>): δ 1.21 (br s, 2H, NH<sub>2</sub>), 1.48 – 1.56 (m, 1H, CH), 1.89 – 2.00 (m, 2H, CH<sub>2</sub>), 2.74 – 2.83 (m, 4H, 2 x CH<sub>2</sub>), 3.76 – 3.87 (m, 2H, 2 x CH).

<sup>13</sup>C NMR (100 MHz, CDCl<sub>3</sub>): δ 26.6, 28.1, 47.5, 64.3, 81.0.

FTIR (neat): 1103, 1615, 3330, 3404 cm<sup>-1</sup>.

Attempted preparation of (*E*)-3-phenylprop-2-en-1-amine **92**



**Scheme 44**

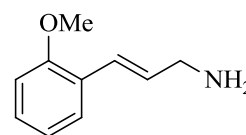
Following *General Procedure B*, data are reported as (a) amine; (b) solvent; (c) dialkyl azodicarboxylate reagent; (d) amine product; (e) yield.

(a) (*E*)-*N*-benzyl-3-phenylprop-2-en-1-amine **72**, 335 mg, 1.5 mmol, 1 eq; (b) THF, 1.9 ml, 0.8 M; (c) DIAD, 0.33 ml, 1.65 mmol, 1.1 eq; (d) benzylamine **1**; (e) 121 mg, 75%.

Benzylamine **1**<sup>35</sup>

Data are in agreement with previous preparations of this amine.

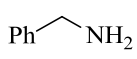
Attempted preparation of (*E*)-3-(2-methoxyphenyl)prop-2-en-1-amine **93**



#### Scheme 45

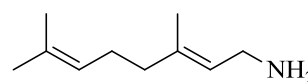
Following *General Procedure B*, data are reported as (a) amine; (b) solvent; (c) dialkyl azodicarboxylate reagent; (d) amine product; (e) yield.

(a) (*E*)-*N*-benzyl-3-(2-methoxyphenyl)prop-2-en-1-amine **73**, 387 mg, 1.5 mmol, 1 eq; (b) THF, 1.9 ml, 0.8 M; (c) DIAD, 0.33 ml, 1.65 mmol, 1.1 eq; (d) benzylamine **1**; (e) 136 mg, 85%.

Benzylamine **1**<sup>35</sup> 

Data are in agreement with previous preparations of this amine.


Attempted preparation of (*E*)-3,7-dimethylocta-2,6-dien-1-amine **95**



#### Scheme 46

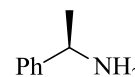
Following *General Procedure B*, data are reported as (a) amine; (b) solvent; (c) dialkyl azodicarboxylate reagent; (d) amine product; (e) yield.

(a) (*E*)-*N*-benzyl-3,7-dimethylocta-2,6-dien-1-amine **75**, 364 mg, 1.5 mmol, 1 eq; (b) THF, 1.9 ml, 0.8 M; (c) DIAD, 0.33 ml, 1.65 mmol, 1.1 eq; (d) benzylamine **1**; (e) 157 mg, 98%.

Benzylamine **1**<sup>35</sup> 

Data are in agreement with previous preparations of this amine.

Preparation of (*R*)-1-phenylethanamine **96**<sup>51,52</sup>



**Scheme 47**

Following *General Procedure B*, data are reported as (a) amine; (b) solvent; (c) dialkyl azodicarboxylate reagent; (d) amine product; (e) yield.

(a) (*R*)-*N*-benzyl-1-phenylethanamine **95**, 317 mg, 1.5 mmol, 1 eq; (b) THF, 1.9 ml, 0.8 M; (c) DIAD, 0.33 ml, 1.65 mmol, 1.1 eq; (d) (*R*)-1-phenylethanamine **96**; (e) 149 mg, 82%.

$[\alpha]_{\text{D}}^{20} = +34.5^{\circ}$  ( $c = 1.0$ ,  $\text{CHCl}_3$ ) [lit.  $[\alpha]_{\text{D}}^{20} + 32.0^{\circ}$  ( $c = 0.3$ ,  $\text{CHCl}_3$ )]<sup>51</sup>

<sup>1</sup>H NMR (400 MHz,  $\text{CDCl}_3$ ):  $\delta$  1.42 (d, 3H,  $J = 6.6$  Hz,  $\text{CH}_3$ ), 1.67 (br s, 2H  $\text{NH}_2$ ), 4.14 (q, 1H,  $J = 6.6$  Hz,  $\text{CH}$ ), 7.26 – 7.28 (m, 1H,  $\text{ArH}$ ), 7.33 – 7.35 (m, 4H, 4 x  $\text{ArH}$ ).

<sup>13</sup>C NMR (100 MHz,  $\text{CDCl}_3$ ):  $\delta$  25.9, 51.5, 128.7, 126.9, 128.7, 148.1.

FTIR (neat): 1454, 1630, 3441  $\text{cm}^{-1}$ .

## 6 References

1. (a) T. J. Donohoe, *Oxidation and Reduction in Organic Synthesis*, **2000**, Oxford University Press: Oxford; (b) S.-I. Murahashi, *Angew. Chem. Int. Ed.*, **1995**, *34*, 2443; (c) S.-I. Murahashi, *Pure & Appl. Chem.*, **1992**, *64*, 403.
2. R. Lechner and B. König, *Synthesis*, **2010**, 1712.
3. E. Baciocchi, T. D. Giacco, O. Lanzalunga and A. Lapi, *J. Org. Chem.*, **2007**, *72*, 9582.
4. Y. Obora and Y. Ishii, *Synlett*, **2011**, 30.
5. X.-Q. Gu, W. Chen, D. Morales-Morales and C. M. Jensen, *J. Mol. Catal. A: Chem.*, **2002**, *189*, 119.
6. R. Yamaguchi, C. Ikeda, Y. Takahashi and K. Fujita, *J. Am. Chem. Soc.*, **2009**, *131*, 8410.
7. S.-I. Murahashi, Y. Okano, H. Sato, T. Nakae and N. Komiya, *Synlett*, **2007**, 1675.
8. S. Minakata, Y. Ohshima, A. Takemiya, I. Ryu, M. Komatsu and Y. Ohshiro, *Chem. Lett.*, **1997**, 311.
9. Y. Maeda, T. Nishimura and S. Uemura, *Bull. Chem. Soc. Jpn.*, **2003**, *76*, 2399.
10. A. Nishinaga, S. Yamazaki and T. Matsuura, *Tetrahedron Lett.*, **1988**, *29*, 4115.
11. J. A. Keith and P. M. Henry, *Angew. Chem. Int. Ed.*, **2009**, *48*, 9038.
12. J.-R. Wang, Y. Fu, B.-B. Zhang, X. Cui and Q.-X. Guo, *Tetrahedron Lett.*, **2006**, *47*, 8293.
13. Y. Liu, B. Yao, C.-L. Deng, R.-Y. Tang, X.-G. Zhang and J.-H. Li, *Org. Lett.*, **2011**, *13*, 2184.
14. K. C. Nicolaou, C. J. N. Mathison and T. Montagnon, *J. Am. Chem. Soc.*, **2004**, *126*, 5192.

15. (a) J. Lee, J. S. U, S. C. Blackstock and J. K. Chan, *J. Am. Chem. Soc.*, **1997**, *119*, 10241; (b) T. Itoh, K. Kaneda and S. Teranishi, *Tetrahedron Lett.*, **1975**, 2801; (c) S. Mabic and N. Castagnoli, *J. Med. Chem.*, **1996**, *39*, 3694; (d) T. L. Macdonald, K. Zirvi, L. T. Burka, P. Peyman and F. P. Guengerich, *J. Am. Chem. Soc.*, **1982**, *104*, 2050.
16. (a) O. Mitsunobu and Y. Yamada, *Bull. Chem. Soc. Jpn.*, **1967**, *40*, 2380; (b) O. Mitsunobu, *Synthesis*, **1981**, 1; (c) J. Reynolds and M. Kassiou, *Curr. Org. Chem.*, **2009**, *13*, 1610.
17. (a) O. Diels, *Liebigs Ann. Chem.*, **1922**, *429*, 1; (b) O. Diels and E. Fischer, *Chem. Ber.*, **1914**, *47*, 2043; (c) O. Diels and M. Paquin, *Chem. Ber.*, **1913**, *46*, 2000; (d) O. Diels and P. Fritzsche, *Chem. Ber.*, **1911**, *44*, 3018.
18. G. W. Kenner and R. J. Steadman, *J. Chem. Soc.*, **1952**, 2089.
19. E. E. Sissman and A. Makriyannis, *J. Org. Chem.*, **1973**, *38*, 1652.
20. J. Kroutil, T. Trnka and M. Černý, *Org. Lett.*, **2000**, *2*, 1681.
21. J. Kroutil, T. Trnka and M. Černý, *Synthesis*, **2004**, 446.
22. (a) N. Egger, L. Hoesch and A. S. Dreiding, *Helv. Chim. Acta.*, **1983**, *66*; (b) K. H. Linke and H. J. Göhausen, *Chem. Ber.*, **1971**, *104*, 301.
23. (a) T. W. Greene and P. G. M. Wuts, *Protective Groups in Organic Synthesis*, *3<sup>rd</sup> Edition*, **1999**, John Wiley & Sons: New York; (b) P. J. Kocienski, *Protecting Groups*, **1994**, Thieme: Stuttgart.
24. W. H. Hartung and R. Simonoff, *Org. React.*, **1953**, 263.
25. (a) B. D. Gray and P. W. Jeffs, *J. Chem. Soc., Chem. Commun.*, **1987**, 1329; (b) B. ElAmin, G. M. Anantharamaiah, G. P. Royer and G. E. Means, *J. Org. Chem.*, **1979**, *44*, 3442; (c) S. Ram and L. D. Spicer, *Tetrahedron Lett.*, **1987**,



- 28, 515; (d) B. M. Adger, C. O'Farrell, N. J. Lewis and M. B. Mitchell, *Synthesis*, **1987**, 53.
26. T. Monkovic, H. Wong and C. Bachand, *Synthesis*, **1985**, 770.
27. A. Goti and M. Romani, *Tetrahedron Lett.*, **1994**, 35, 6567.
28. N. Rabjohn, *Organic Syntheses*, **1948**, 48, 58.
29. G. Pelletier, W. S. Bechara, A. Aubé and A. B. Charette, *Unpublished Results*, Université de Montréal.
30. C. R. Smith and T. V. RajanBabu, *Org. Lett.*, **2008**, 10, 1657.
31. G. Pelletier, W. S. Bechara and A. B. Charette, *J. Am. Chem. Soc.*, **2010**, 132, 12817.
32. N. A. Braun, M. Ousmer, J. Bray, D. Bouchu, K. Peters, E.-M. Peters and M. A. Ciufolini, *J. Org. Chem.*, **2000**, 65, 4397.
33. D. D. Perrin and W. L. F. Armarego, *Purification of Laboratory Chemicals*, **1998**, 3<sup>rd</sup> Edition, Permagon Press: Oxford.
34. B. Miriyala, S. Bhattacharyya and J. S. Williamson, *Tetrahedron*, **2004**, 60, 1463.
35. J. Z. Saavedra, A. Resendez, A. Rovira, S. Eagon, D. Haddenham and B. Singaram, *J. Org. Chem.*, **2012**, 77, 221.
36. P. R. Likhari, R. Arundhathi, M. L. Kantam and P. S. Prathima, *Eur. J. Org. Chem.*, **2009**, 5383.
37. T. Nishikata and H. Nagashima, *Angew. Chem. Int. Ed.*, **2012**, 51, 5363.
38. D. Krishnan, M. Wu, M. Chiang, Y. Li, P.-H. Leung and S. A. Pullarkat, *Organometallics*, **2013**, 32, 2389.
39. J. Blid, P. Brandt and P. Somfai, *J. Org. Chem.*, **2004**, 69, 3043.

40. T. Ohmura and J. F. Hartwig, *J. Am. Chem. Soc.*, **2002**, *124*, 15164.
41. B. C. Ranu, A. Majee and A. Sarkar, *J. Org. Chem.*, **1998**, *63*, 370.
42. C. A. Gentle and T. D. H. Bugg, *J. Chem. Soc., Perkin Trans. 1*, **1999**, 1279.
43. R. M. Lanigan, P. Starkov and T. D. Sheppard, *J. Org. Chem.*, **2013**, *78*, 4512.
44. C. Brinkmann, A. G. M. Barrett, M. S. Hill and P. A. Procopiou, *J. Am. Chem. Soc.*, **2012**, *134*, 2193.
45. Z. Zhang, D. C. Leitch, M. Lu, B. O. Patrick and L. L. Schafer, *Chem. Eur. J.*, **2007**, *13*, 2012.
46. G. Bartoli, G. D. Antonio, R. Giovannini, S. Giuli, S. Lanari, M. Paoletti and E. Marcantoni, *J. Org. Chem.*, **2008**, *73*, 1919.
47. J. Apelt, X. Ligneau, H. H. Pertz, J.-M. Arrang, C. R. Ganellin, J.-C. Schwartz, W. Schunack and H. Startk, *J. Med. Chem.*, **2002**, *45*, 1128.
48. H. Kurouchi, K. Kawamoto, H. Sugimoto, S. Nakamura, Y. Otani and T. Ohwada, *J. Org. Chem.*, **2012**, *77*, 9313.
49. D. Haddenham, L. Pasumansky, J. DeSoto, S. Eagon and B. Singaram, *J. Org. Chem.*, **2009**, *74*, 1964.
50. G. C. Hirst, P. Rafferty, K. Ritter, D. Calderwood, N. Wishart, L. D. Arnold and M. M. Friedman, *US Pat.*, US 6 921 763, B2, **2005**.
51. M. Atobe, N. Yamazaki and C. Kibayashi, *J. Org. Chem.*, **2004**, *69*, 5595.
52. Y. Xie, H. Pan, X. Xiao, S. Li and Y. Shi, *Org. Biomol. Chem.*, **2012**, *10*, 8960.